Thèse de doctorat de l'Université de Versailles Saint-Quentin-en-Yvelines

Spécialité : Biologie

présentée par

Carine Laurent

le 7 Octobre 2005

pour obtenir le grade de Docteur de l'Université de Versailles Saint-Quentin-en-Yvelines

Rôle du stress oxydatif dans le développement des effets cellulaires radio-induits au niveau cutané : application aux irradiations localisées accidentelles

JURY :

Monsieur B. Mignotte	Président
Monsieur J. Cadet	Rapporteur
Monsieur J.-L. Lefaix	Rapporteur
Monsieur E. Lartigau	Examinateur
Monsieur P. Voisin	Examinateur
Monsieur J.-P. Pouget	Examinateur

A mes parents,

« L'inspiration ne vient normalement qu'après un travail acharné. »

Max Weber

Le savant et le politique

Remerciements

Je tiens tout d'abord à remercier Jean-Pierre Pouget qui m'a appris comment travailler et qui a mis en place toute cette étude. Je le remercie aussi pour toute sa confiance, son soutien et sa disponibilité.

Je remercie également Philippe Voisin, mon directeur de thèse, qui m'a accueillie dans son laboratoire et dans son service.

J'adresse mes plus vifs remerciements à Jean Cadet et Jean-Louis Lefaix d'avoir accepté d'être rapporteurs de ce travail, ainsi qu'à Bernard Mignotte, président du jury, et Eric Lartigau.

Je remercie beaucoup Sylvie Delanian et Jean-Louis Lefaix pour les précieuses discussions concernant l'association pentoxifylline et α-tocophérol, leur gentillesse et leur disponibilité.

Je remercie particulièrement Pascale Voisin et Martine Delbos pour leur aide pour mes dernières manips et pour les discussions qu'on a eues, surtout dans notre nouveau bureau.

Je remercie tout le personnel de l'ancien Laboratoire de Dosimétrie Biologique Multiparamétrique et du nouveau Laboratoire de Dosimétrie Biologique.

Je remercie également tout le personnel du SRBE, anciennement SARAM, tout particulièrement les étudiants : Céline, Muriel, Sabine, Fabien, Frédéric, Olivier, Marie et les autres.

Enfin, pour leur patience et leur compréhension, je remercie ma famille et mes amis. C'est promis, d'ici quelques temps, mes week-ends leur seront entièrement consacrés. Je remercie particulièrement mes parents qui m'ont permis de faire cette thèse grâce à leur soutien de tout point de vue. Je remercie aussi mon frère pour son écoute (un jour peut-être tu auras une vraie moto ! DUCATI DUCATI DUCATIIIII !). Je remercie Sophie, Laurence et Caro pour nos conversations, nos sorties, nos randos etc. Enfin, je suis très reconnaissante envers mon espagnol qui fait à peu près tout pour moi (dès demain, j'apprends à me servir de la serpillière). Tu es trop gentil mais je t'assure que ça en vaut le coup.

SOMMAIRE

ABREVIATIONS

ADN : acide désoxyribonucléique

ARN : acide ribonucléique

αT : alpha-tocophérol

ATM : protéine "*ataxia telangiectasia* mutated"

ATR : ATM and Rad3- related

CDB : cassures double-brins

CSB : cassures simple-brins

DNA-PK : DNA-activated protein kinase

ERO : espèces réactives de l'oxygène

GPx : glutathion peroxydase

Gy : Gray

γ-H2AX : forme phosphorylée de l'histone H2AX

HMVEC-d : human microvascular endothelial cells from dermis

4-HNE : 4-hydroxynonénal

MDA : malonedialdéhyde

NHEJ : non-homologous end joining

NHF-d : normal human fibroblasts from dermis

PARP : poly-(ADP ribose) polymérase

PTX : pentoxifylline

REB : réparation par excision de base et resynthèse

RH : recombinaison homologue

SAI : syndrome aigu d'irradiation

SCRI : syndrome cutané radio-induit

SIPS : stress-induced premature senescence

SOD : superoxyde dismutase

SVF : sérum de veau fœtal

TEL : transfert d'énergie linéique

Tx : Trolox

ETUDE BIBLIOGRAPHIQUE

I- Accidents d'irradiation et syndrome cutané radio-induit

1. Sources d'exposition

Les sources d'exposition aux rayonnements ionisants (Figure 1) sont d'origine naturelle pour 58% ou artificielle pour 41% (exposition médicale). Il en résulte une exposition annuelle moyenne de 4 mSv, sachant que le Sievert (Sv) est une unité de grandeur qui évalue les effets biologiques sur les tissus vivants et est fonction de la dose absorbée (en Gray, Gy), de l'organe et de la nature du rayonnement.

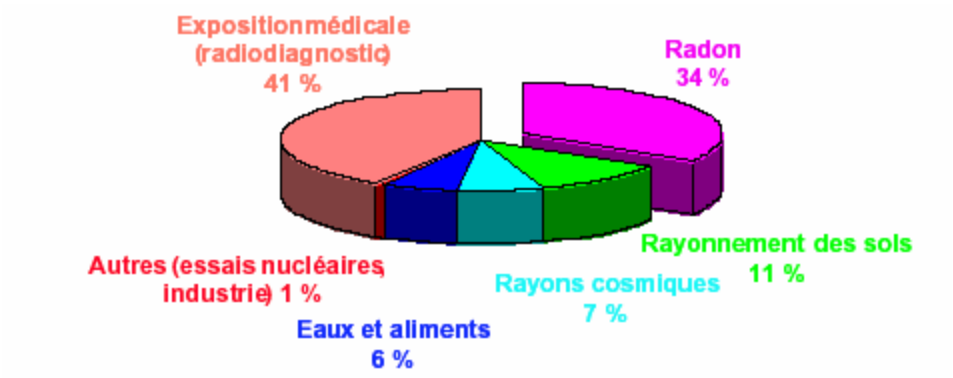

Figure 1. Exposition moyenne de la population française : contribution des diverses sources (IRSN, 2001).

2. Accidents d'irradiation

La plupart des surexpositions accidentelles aux rayonnements survenues dans les dernières décennies (Tableau 1) se sont produites dans le secteur de l'industrie.

date	location	type of accident/event	highest dose (rem)	deaths	injuries
29 Mar 1990	USA	fluoroscopy accident	L	0	1
21 Jun 1990	Soreq, Israel	accident at commerical irradiation facility	1,5	1	0
Jun 1990	Shanghai, PRC	irradiator accident	1,2	2	5
10-20 Dec 1990	Zarragosa, Spain	radiotherapy accident	L	18	9
1990	Sasolburg, South Africa	orphaned source	L	0	4
Aug 1991	Forbach, France	irradiator accident	L	0	1
26 Oct 1991	Nesvizh, Belarus	irradiator accident	1,1	1	0
11 Dec 1991	Maryland, USA	irradiator accident	L	0	1
1977?-1991	United Kingdom	radiography accident	L	1	0
16-21 Nov 1992	City of Indiana, Pennsylvania, USA	radiotherapy accident	L	1	0
19 Nov 1992	Jilin, Xinzhou, PRC	lost industrial source	800	3	5
17 Nov 1992	Hanoi, Vietnam	irradiation accident	L	0	1
Nov 1992	PRC	irradiator accident	?	0	4
1992	San Antonio, Texas, USA	radiotherapy accident	L	0	1
1993	Russia	homocide using radioactive source	?	1	0
28 Apr 1994	Tokyo, Japan	irradiator accident	L	0	1
21 Oct-18 Nov 1994	Tammiku, Estonia	lost source	400	1	4
1994	Texas City, Texas, USA	irradiator accident	L	0	1
1995	France	radiography accident	L	0	1
1995	France	orphaned source	L	0	1
1995	Tyler, Texas, USA	radiotherapy accident	L	0	1
Jun 1996-9 Oct 1997	Lilo Training Center, Tbilisi, Georgia	lost sources	590	0	11
24 Jul 1996	Gilan, Iran	lost industrial radiography source	450	0	1
22 Aug-27 Sept 1996	San Jose, Costa Rica	radiotherapy accident	L	7	81
17 Jun 1997	Arzamas-16, Russia	criticality accident with uranium assembly	4,85	1	0
1997	Georgia	lost source	?	1	?
1998	Houston, Texas, USA	irradiator accident	L	0	1
10 Dec 1998-8 Jan 1999	Istanbul, Turkey	lost radiograpy sources	310	0	10
20 Feb 1999	Yanango, Peru	lost source	150	0	1
13 Sep 1999	Grozny, Russia	attempted theft of sources	high	3	3
30 Sep-1 Oct 1999	Toki-mura, Japan	criticality accident with uranium solution	1,8	2	1
1999	Houston, Texas, USA	radiotherapy accident	L	0	1
1999	Kingisepp, Russia	orphaned source	?	3	
24 Jan-20 Feb 2000	Samut Prakarn, Thailand	lost radiography source	200	3	7
5 Jun-3 Jul 2000	Mit Halfa, Egypt	lost radiography source	?	2	5
Aug 2000-24 Mar 2001	Panama City, Panama	radiotherapy accident	L	17	11
27 Feb 2001	Bialystok Oncology Center, Poland	radiotherapy accident	L	0	5
~2001	Samara, Russia	lost radiography source	275	0	3
summer 2001	Kandalaksha, Russia	orphaned source	?	0	4
early Dec 2001-Feb 2002	Liya, Georgia	lost radioisotope source	?	0	3
2003-13 Nov 2003	Kola Harbor, Russia	orphaned sources	?	?	1+?

Tableau 1. Liste des accidents d'irradiation impliquant les rayonnements ionisants depuis 1990 (compilé par Robert Johnston, 8 Avril 2005). L=localisé, 100 rem = 1 Sv.

a) irradiation globale aiguë

L'irradiation globale aiguë accidentelle représente 16% des accidents d’irradiation (Figure 2).

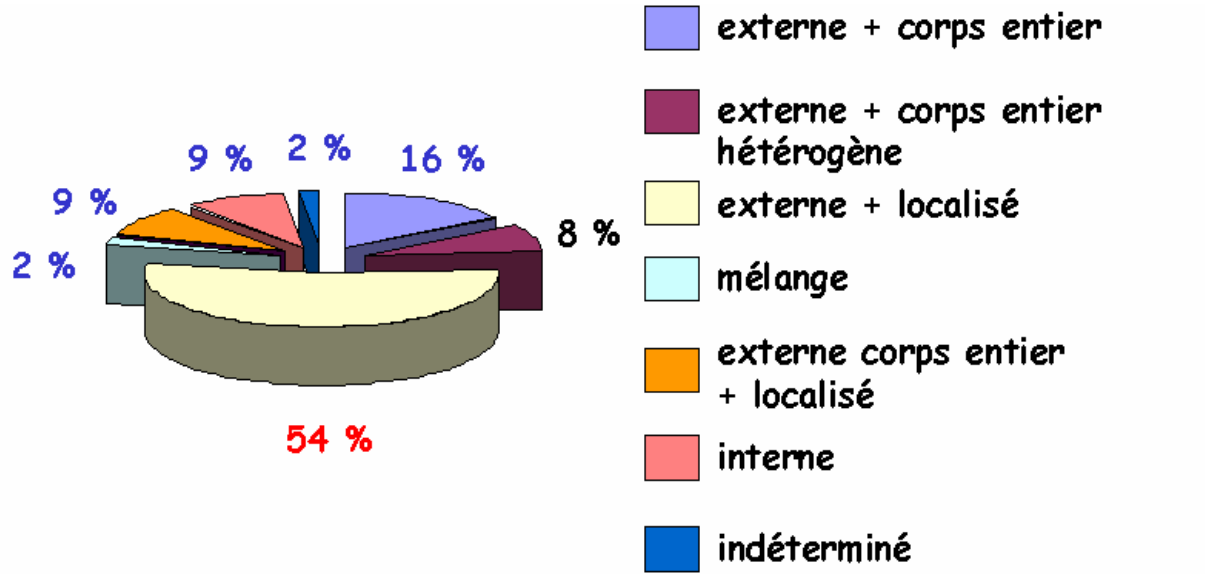

Figure 2. Représentation des différents types d’irradiation lors des accidents radiologiques (IRSN, 2001).

Dans le cas d’une irradiation forte à fort débit, le syndrome aiguë d'irradiation globale (SAI) évolue selon les descriptions habituelles en 4 phases :

- phase initiale ou prodromique,
- phase de latence ou de rémission clinique,
- phase d'état ou critique,
- phase de restauration.

La chronologie du SAI peut être représentée par la figure suivante (Figure 3) donnant, en abscisse, la gravité des lésions et, en ordonnée, le temps après l’irradiation. Les effets apparaissent à partir de quelques minutes à plusieurs semaines après irradiation, le délai d’apparition des lésions étant d’autant plus faible que la dose d’irradiation est élevée.

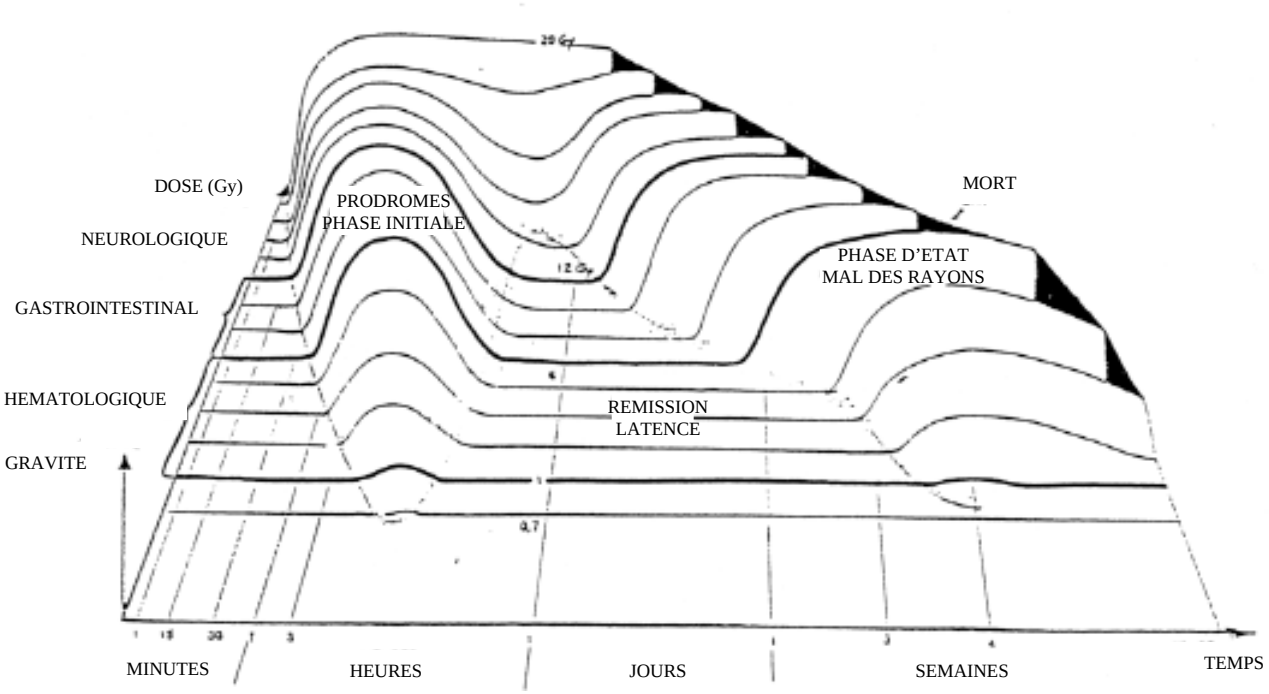

Figure 3. Schéma représentant les différentes phases du syndrome aiguë d'irradiation (tiré de http://laennec.univ-lyon1.fr).

On distingue trois syndromes qui apparaissent au-delà de doses-seuils (Tableau 2) :

* 1 à 6-7 Gy :	Syndrome hématopoïétique. C'est le syndrome habituellement décrit comme « mal des rayons » type,
* 6-7 à 12 Gy :	Syndrome digestif dominant,
* >12 Gy :	Syndrome nerveux central avec décès rapide

Tableau 2. Le syndrome aiguë d'irradiation (tiré de http://laennec.univ-lyon1.fr).

Le syndrome hématopoïétique est prédominant entre 1 et 6-7 Gy, le syndrome digestif apparaît entre 6-7 Gy et 12 Gy et le syndrome nerveux central au-dessus de 12 Gy.

D'importantes variations sont observées en fonction des paramètres de l'irradiation : dose moyenne, répartition topographique (hétérogénéité), répartition chronologique. Ces variations touchent à la fois la gravité, la nature des lésions et la chronologie.

La plupart des accidents d'irradiation aiguë externe sont en fait des irradiations localisées ou, au moins, hétérogènes. Hormis quelques accidents très particuliers (irradiation céphalique...), l'organe cible commun est la peau, pour plusieurs raisons:

- la topographie (la peau est la couche la plus superficielle anatomiquement),
- la forte radiosensibilité de la peau (l'épiderme est un tissu à renouvellement très rapide),
- la distribution de dose en fonction de la profondeur.

b) irradiations localisées

Parmi les accidents d'irradiation, 54% sont des irradiations externes et localisées (Lefaix et Daburon, 1998). Ces irradiations localisées aiguës peuvent aussi provenir de surdosage thérapeutique. Elles conduisent, dans bien des cas, à une irradiation sévère du tissu cutané qui nécessite, par le corps médical, une prise en charge spécialisée. Elles restent un problème délicat à traiter car la peau et les tissus sous-jacents sont composés de nombreux types cellulaires différents qui peuvent répondre différemment à l'irradiation. De plus, la dose délivrée est souvent difficile à déterminer ainsi que l'étendue et la limite du territoire irradié. Outre la dose, de nombreux autres paramètres peuvent moduler cette réponse tels que la nature et l'énergie du rayonnement. Après une irradiation externe, les lésions cutanées sont les plus patentes et peuvent permettre de préjuger de la meilleure approche thérapeutique possible pour les équipes médicales. Les irradiations β sont les plus délétères car la dose est délivrée en surface avec une faible énergie.

3. Syndrome cutané radiologique

Les effets des rayonnements ionisants sur la peau sont très variables du fait de la grande diversité des types cellulaires impliqués (kératinocytes, fibroblastes, cellules endothéliales…). Ces effets seront fonction de la radiosensibilité, des cinétiques de renouvellement, de disparition et de restauration de ces cellules. Des fortes doses de rayonnements ionisants conduisent à la mort des cellules qui composent le tissu cutané. Elles se traduisent par l'apparition des lésions précoces, considérées comme provenant de l'atteinte de la couche

basale proliférante de l'épiderme, et tardives, reliées aux atteintes du derme et des tissus sous-jacents. Les lésions précoces et tardives constituent le syndrome cutané radiologique (Tableau 3).

Dose unique (Gy)	Dose fractionnée (2 Gy/j)	Lésion majeure	Délai d'apparition des lésions	Lésion fonctionnelle	Lésion histologique
5-7	≤ 20	Dépilation	≃ 18 j		Follicule vide
10-20	20-40	Érythème	12-17 j	Hyperémie	Aucune
20-30	-	-	2-6 j	-	-
10-20	≃ 45	Pigmentation		Aucune	Augmentation de la mélanine
10-20	≃ 45	Desquamation sèche	30-70 j		Hyperplasie
20-24	45-50	Desquamation humide avec guérison	30-50 j	Exsudation de serum	Diminution de la densité cellulaire
				Restauration de la barrière fonctionnelle	Régénération cellulaire
> 24	> 50 > 60	Desquamation humide sans guérison			
17-24	45-50	Télangiectasie	6 mois - 1 an	Aucune	Perte de cellules et de vaisseaux, dilatation vasc.
> 27	> 60	Nécrose sans guérison	Quelques mois ou années	Perte de la barrière protectrice	Nécrose

Tableau 3. Syndrome cutané radiologique (d'après Archambeau *et al*., 1995).

a) effets précoces des rayonnements ionisants sur la peau

Avant même l'apparition des effets dits précoces, c'est-à-dire se produisant dans les jours et semaines suivant l'irradiation, des effets immédiats peuvent avoir lieu dans les premières heures. Le premier symptôme ainsi observable est la **radiodermite**, définie comme une réaction inflammatoire de la peau équivalente à une brûlure du premier degré (Archambeau *et al*., 1995). Apparaît ensuite l'**érythème aigu** dans les 24 heures suivant une irradiation d'au moins 15 Gy. Il est dû à la dilatation des capillaires dans le derme. Différentes lésions sont ensuite observées (pour revue, Daburon, 1997) :

- l'**érythème secondaire** : il apparaît entre la 3ème et la 4ème semaine post-irradiation (5 Gy) et est associé à une thrombose des artérioles (Rubin et Casarett, 1968).

- la **dépilation** : elle se produit pour des doses de 2 ou 3 Gy, les follicules pileux étant très radiosensibles, et a lieu aux environs des 14ème et 18ème jour.

- la **desquamation sèche** : elle apparaît quelques jours après le développement de l'érythème précoce consécutivement à une exposition à une dose de 10 à 15 Gy et se caractérise par un gonflement et une prolifération de l'endothélium vasculaire tandis qu'une perte de cellules épidermiques est observée mais celle-ci est compensée puisqu'elle n'aboutit pas à l'exsudation de sérum.

- la **desquamation humide** (ou radiodermite exsudative) : elle a lieu environ 3 à 4 semaines après une irradiation de plus de 16 Gy et est due à une perte suffisante de cellules de la couche basale de l'épiderme pour conduire à l'exsudation de sérum. Elle est associée à une réponse inflammatoire forte du derme.

- la **nécrose dermique** : elle se produit, environ 70 jours après irradiation, lorsque la desquamation humide est intense et durable. Elle serait due à la perte des cellules endothéliales, à la réduction de la densité des capillaires et à la diminution du flux sanguin dans le derme (Moustafa et Hopewell, 1979; Archambeau *et al*., 1984).

b) effets tardifs des rayonnements ionisants sur la peau

Les effets tardifs cutanés radio-induits apparaissent des semaines, des mois ou des années après irradiation et ne sont pas obligatoirement précédés des effets précoces. Ainsi, l'observation des lésions précoces ne peut servir à prédire les lésions tardives. Les lésions tardives observées sont les suivantes (pour revue, Daburon, 1997) :

- l'**atrophie**, la **télangiectasie** et la **pigmentation** : une atrophie de l'épiderme due à des atteintes progressives du tissu conjonctivo-vasculaire et à l'ischémie peut apparaître longtemps après une irradiation à forte dose. Elle est caractérisée par un amincissement, un assèchement et une dépilation de l'épiderme. En parallèle, les petits vaisseaux du derme se dilatent, on les appelle alors capillaires télangiectasiques. Selon la dose reçue, on observe également une hyper- ou une hypopigmentation. L'hypopigmentation a lieu dans le cas de doses plus faibles et est liée à la destruction des mélanocytes alors que l'hyperpigmentation, pour des doses d'irradiation plus fortes, est due à une augmentation de la synthèse de mélanine.

- l'**ischémie** : elle apparaîtrait à cause de la prolifération des cellules endothéliales survivantes, se multipliant pour combler les morts cellulaires survenant dans les cellules qui tentent de se diviser, provoquant l'occlusion localisée ou partielle des artérioles (Hopewell, 1974, 1980). Ces hyperplasies focales n'apparaissent pas dans les capillaires (Archambeau *et al*., 1984, 1985). Le très faible taux de renouvellement de ces cellules expliquerait le délai d'apparition de cette lésion. L'ischémie est très toxique pour les cellules car elle est liée à la formation excessive d'espèces réactives de l'oxygène (ERO) par les polynucléaires neutrophiles et aussi via la xanthine déshydrogénase. Par ailleurs, dans le cas où l'on aurait un rétablissement de la circulation sanguine (ou reperfusion), l'afflux brutal d'oxygène conduit lui aussi à la formation d'ERO endommageant le tissu.

- la **nécrose** : elle constitue le stade ultime de la réponse tissulaire à l'irradiation et apparaît selon la dose et le fractionnement (Archambeau, 1987). Elle peut se développer en quelques semaines ou quelques mois ou s'étendre sur plusieurs années par des poussées successives suivant celles d'apparition des lésions vasculaires (Gongora et Magdelenat, 1986).

- la **fibrose** (Peter, 1996; Lefaix *et al*., 1997) : elle correspond à une formation pathologique de tissu fibreux essentiellement composé de fibres de collagène. Elle se développe le plus souvent comme un processus cicatriciel en remplacement d'un parenchyme détruit. Elle apparaît de manière progressive sur plusieurs années et est constituée de trois phases : la phase de constitution (de 6 à 24 mois post-irradiation) asymptomatique ou liée à une inflammation aiguë ou chronique ; la phase de séquelle organisée avec disparition des signes inflammatoires, épaississement du derme et des tissus sous-cutanés, élargissement des capillaires dermiques et amincissement ou hypertrophie de l'épiderme ; la phase très tardive avec une atrophie sous-cutanée associée à une rétractation des tissus (sclérose) qui reste soumise à des poussées inflammatoires en cas de traumatismes.

- les **cancers cutanés** : des lésions cancéreuses peuvent apparaître avec un temps moyen de latence de 24,5 années après l'irradiation (Dutreix, 1986). Peu d'informations sont disponibles à propos de ces cancers. On sait que deux types prédominent : les carcinomes basocellulaires qui sont peu agressifs, assez fréquents et se développent à partir de la couche basale de l'épiderme et qui prédominent sur les carcinomes spinocellulaires qui sont des tumeurs invasives des couches supérieures de l'épiderme.

4. Traitement du syndrome cutané radiologique

Les accidents d'irradiation aiguë localisée nécessitent un traitement dans lequel la prise en charge des lésions du tissu cutané est bien souvent la priorité médicale. Même lors des traitements par radiothérapie et malgré l'amélioration des techniques, des séquelles peuvent encore se produire de manière imprévisible du fait de la grande variabilité de la radiosensibilité individuelle. Deux sortes de traitement sont proposés.

Le **traitement chirurgical** consiste en l'exérèse suivie de greffes ou de lambeaux pédiculés provenant d'une zone peu ou pas irradiée (Moussard, 1963). Il est utilisé dans les cas où le tissu est destiné à la nécrose, c'est-à-dire lorsqu'il a été exposé à une dose de plus de 20 à 25 Gy selon la superficie exposée. L'exérèse intervient assez précocement après l'irradiation afin que la greffe puisse bénéficier d'une perfusion sanguine encore satisfaisante (Patterson et Wiernik, 1976). Chez le porc, Daburon *et al.* ont montré : (i) qu'une exérèse précoce limitée à la peau irradiée à 30-40 Gy diminue la réaction inflammatoire locale précoce, empêche l'atteinte septique profonde, accélère la cicatrisation et limite l'extension de la fibrose (Daburon *et al*., 1986) et (ii) qu'une greffe cutanée transitoire après des irradiations plus étendues ou à des doses plus élevées (64 Gy) permet la prolifération d'un tissu de bourgeonnement comblant la dépression provoquée par la nécrose profonde avant de nécroser par manque d'irrigation sanguine et d'être remplacée par une deuxième greffe qui fonctionne car le tissu de bourgeonnement est en croissance (Daburon *et al*., 1986).

Le **traitement pharmacologique** est l'autre solution. L'apparition des lésions tardives cutanées radio-induites a longtemps été considérée comme irréversible. De plus, les traitements testés se sont souvent montrés décevants ou fastidieux. Pourtant, une action thérapeutique semble possible sur les évènements conduisant à la mort cellulaire cutanée décalée dans le temps observée après exposition du tissu aux rayonnements ionisants (pour revue, Hendry, 1994). De nombreux traitements ont ainsi été testés : anti-inflammatoires stéroïdiens et non-stéroïdiens, protecteurs de la membrane vasculaire, vasodilatateurs, anticoagulants, antiagrégants plaquettaires, thrombolytiques, anti-ischémiques, facteurs de croissance, cytokines etc.

a) les anti-inflammatoires, les inhibiteurs de l'ACE, les anti-fibrosants, l'oxygène hyperbarique

Les anti-inflammatoires (pour revue, Delanian *et al*., 1993) stéroïdiens agissent de manière transitoire sur les poussées inflammatoires observées après irradiation mais ne permettent pas de réverser les lésions établies. Les anti-inflammatoires non-stéroïdiens se sont montrés assez efficaces chez le lapin mais seule l'association avec un antiagrégant plaquettaire a permis de limiter très significativement et très durablement la radionécrose musculaire précoce et tardive (Lefaix *et al*., 1992).

Le captopril, inhibiteur de l'ACE (angiotensin-converting enzyme), s'est montré efficace pour éviter les effets tardifs de l'irradiation dans le poumon, le cœur et les reins chez le rongeur (Ward *et al*., 1993; Yarom *et al*., 1993; Molteni *et al*., 2001; Moulder *et al*., 2002).

Des agents anti-fibrosants ont également été testés tels que l'IL-1β (Zang *et al*., 1997), l'interféron γ (Moulin *et al*., 1998), les antagonistes du TGF-β1 (pour revue, Border et Noble, 1994), la pentoxifylline et des agents inhibant la synthèse de matrice extracellulaire ou la dégradant (colchicine, cytochalasine B, vinblastine, D-penicillamine, β-aminopropionitrile, les analogues de la proline, les cytostatiques) (Lorenzen, 1981; Uitto *et al*., 1982; Ward *et al*., 1983). Certains de ces agents pourraient toutefois être toxiques (Fuller, 1981).

Les résultats du traitement par HBO (oxygène hyperbarique) sont assez variables. Ce traitement conduit à une guérison de l'ostéoradionécrose dans 15 à 43% des cas (Tibbles et Edelsberg, 1996; Pasquier *et al*., 2004). Une autre étude de phase III randomisée n'a pas montré de différences avec le placébo (Annane *et al.*, 2004).

b) les anti-oxydants

L'approche par les anti-oxydants, ou par les composés modulant le stress oxydatif, s'est révélée être la plus convaincante. Parmi ces substances, il faut citer la SOD, la pentoxifylline (PTX), l'α-tocophérol, la catalase, les chélateurs du fer et l'allopurinol.

Le traitement SOD

Dès 1983, la Cu/Zn SOD sous forme liposomale s'est révélée très efficace dans le traitement de la fibronécrose radio-induite pour réduire l'inflammation et la fibrose (Emerit *et al*., 1983).
La forme bovine liposomale de la Cu/Zn SOD a également montré son efficacité pour traiter la fibrose radio-induite (Baillet *et al*., 1986; Delanian *et al*., 1994). En effet, après 6 semaines de traitement chez 34 patients souffrant de fibrose consécutive à la radiothérapie, la fibrose avait régressé en moyenne de 57% (Delanian *et al*., 1994). Ceci a été confirmé dans un modèle de porc, exposé localement à 160 Gy et développant une fibrose 6 mois après irradiation, avec 75% de régression à 12 semaines (Lefaix *et al*., 1996). Dans un modèle de co-culture tridimensionnel de peau, les critères de la fibrose étaient également diminués par le traitement SOD (Vozenin-Brotons *et al*., 2001).
Cependant, la SOD sous forme bovine ne peut être produite pour un traitement clinique car on ne peut garantir l'absence de problèmes infectieux.
D'autres études se sont intéressées au traitement SOD par thérapie génique *in vitro* et *in vivo* (Epperly *et al*., 1998; Guo *et al*., 2003).

Le traitement PTX

La PTX est un dérivé de méthylxanthine connue pour le traitement des maladies vasculaires grâce à sa capacité à augmenter l'oxygénation des tissus. *In vivo*, l'administration de la PTX réduit les lésions tardives radio-induites cutanées chez la souris (Dion *et al*., 1989) et au niveau du poumon chez le rat (Koh *et al*., 1995). Cependant, d'autres études effectuées chez le même animal n'ont pas montré d'effet bénéfique de la PTX sur les lésions cutanées radio-induites précoces (Dion *et al*., 1989; Ward *et al*., 1992) et tardives (Koh *et al*., 1995) ainsi que chez le porc (Lefaix *et al*., 1999). Chez des patients souffrant de nécrose ou de fibrose tardive radio-induite, la PTX a permis la guérison ou l'amélioration de l'état des tissus mous (Dion *et al*., 1990; Okunieff *et al*., 2004). Un effet protecteur significatif contre la radiotoxicité pulmonaire précoce et tardive a été montré chez des patients sous radiothérapie (Ozturk *et al*., 2004). Mais la PTX n'a pas réduit la fibrose radio-induite chez des patients sous radiothérapie (Delanian *et al*., 2003).

Le traitement α-tocophérol

Peu d'études se sont intéressées aux effets de l'αT, connu pour ses propriétés anti-oxydantes, sur les lésions macroscopiques radio-induites *in vivo*. Un traitement par une vitamine E hydrosoluble a permis de diminuer le nombre de métaphases aberrantes et le niveau de micronoyaux dans la moelle osseuse de souris irradiées (Sarma et Kesavan, 1993; Satyamitra *et al*., 2003). L'administration d'αT a conduit à une amélioration de la mucite orale observée après radiothérapie lors d'essais cliniques (Worthington *et al*., 2002). Toutefois, aucune régression de la fibrose cutanée radio-induite n'a pu être observée (Delanian *et al*., 2003).

Le traitement PTX/α-tocophérol

Le traitement associant PTX et αT s'est révélé aussi efficace que le traitement SOD avec une période de traitement plus longue. Il a permis la réduction des lésions tardives radio-induites de la peau. En effet, l'association a provoqué la régression de la fibrose cutanée radio-induite chez le porc irradié alors que la PTX seule n'avait pas d'effet (Tableau 4) (Lefaix *et al*., 1999).

Time from start of dosing	Control pigs	Pigs dosed with PTX	Pigs dosed with PTX+ α-tocopherol
6 weeks			
L	1 ± 4%	0 ± 4%	−6 ± 9%
W	−4 ± 3%	1 ± 6%	−14 ± 7%*
D	0 ± 6%	2 ± 4%	−12 ± 8%
13 weeks			
L	3 ± 5%	2 ± 8%	−21 ± 10%*
W	−10 ± 8%	−4 ± 9%	−31 ± 6%‡
D	−5 ± 11%	1 ± 10%	−35 ± 16%†
26 weeks			
L	1 ± 10%	3 ± 7%	28 ± 7%*
W	−7 ± 2%	−6 ± 10%	−48 ± 7%‡
D	2 ± 10%	−2 ± 10%	−52 ± 7%‡

Abbreviations: PTX = pentoxifylline; L and W = linear length and width; D = depth measured by ultrasound scans.
Means comparison of the linear dimensions, Student *t*-test:
* $p < 0.05$;
† $p < 0.01$;
‡ $p < 0.001$.

Tableau 4. Pourcentage moyen de régression de la fibrose après 6, 13 et 26 semaines de traitement PTX ou PTX/αT chez le porc (Lefaix *et al*., 1999).

Chez des patients ayant subi une radiothérapie, ce traitement a conduit à une régression continue des lésions chroniques (Delanian *et al*., 1999; Delanian *et al*., 2003) et à une réduction des lésions fibroatrophiques utérines radio-induites (Letur-Konirsch *et al*., 2002). D'autre part, lorsque l'association est administrée avec du clodronate, une réversion complète de l'osteoradionécrose et de la fibrose radio-induite a pu être observée (Delanian *et al*., 2005; Delanian et Lefaix, 2002).

II- La radiobiologie du tissu cutané

La peau est l'organe le plus externe du corps des animaux vertébrés. Sa principale fonction est d'établir une barrière de protection contre les agressions extérieures tout en permettant certains échanges. Elle est le siège de nombreux processus métaboliques qui sont modulés par les conditions physiologiques de l'organisme et les conditions de l'environnement. La peau (Figure 4) est constituée de l'extérieur vers l'intérieur, de trois zones distinctes d'origines embryologiques différentes : l'épiderme (d'origine ectodermique), le derme et l'hypoderme (d'origine mésodermique).

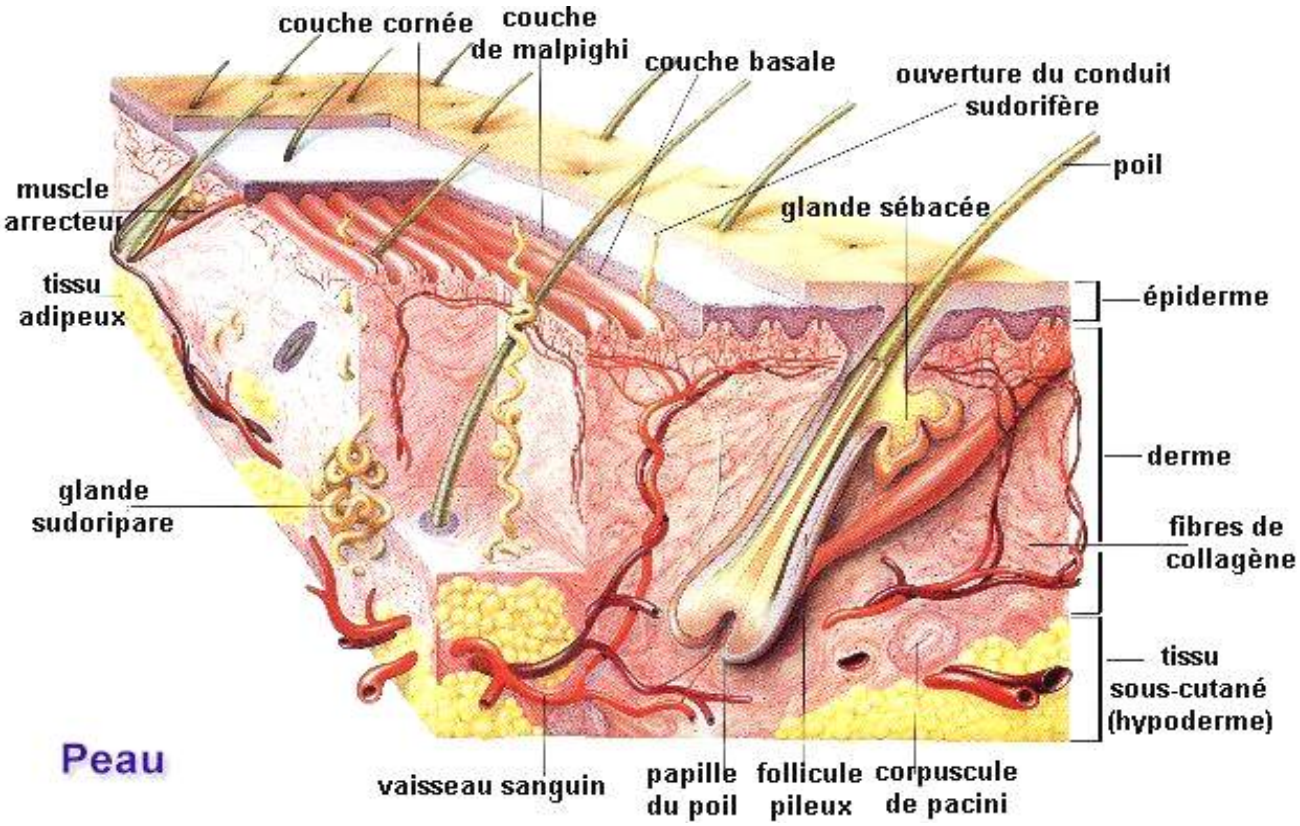

Figure 4. Morphologie détaillée de la peau humaine.

1. L'épiderme, la théorie épithéliale

L'épiderme constitue la couche la plus superficielle de la peau. C'est un épithélium pluristratifié, kératinisé. La face superficielle est criblée de nombreux petits orifices correspondants aux ostiums pilaires et aux pores sudoraux qui sont des structures épithéliales spécialisées d'annexes épidermiques (respectivement les follicules pilo-sébacés et les glandes sudorales) logées en grande partie dans le derme et l'hypoderme (Grosshans, 1997).

Si différents types cellulaires coexistent dans l'épiderme, les **kératinocytes** sont largement majoritaires (90%). Ce sont des cellules épithéliales différenciées pour la synthèse des kératines qui représentent 95% des protéines totales de l'épiderme. Ces kératines sont des protéines fibreuses organisées en tonofilaments qui forment, avec les microfilaments d'actine et les microtubules, le cytosquelette des kératinocytes. La différenciation des kératinocytes

s'accompagne d'un ensemble de transformations morphologiques et biochimiques qui aboutit à la formation de cellules anucléées et aplaties qui se desquament à la surface de la peau, les cornéocytes. Ainsi, au cours de leur maturation cornée, les kératinocytes migrent de la profondeur vers la surface de l'épiderme (en environ 30 jours chez l'homme) et se répartissent en 4 couches (Figure 5) :

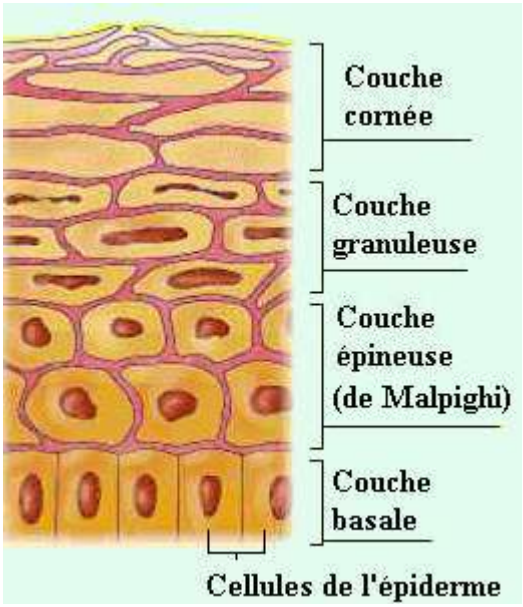

Figure 5. Schéma de l'épiderme.

- la couche basale constituée d'une rangée unique de cellules cylindriques ou cubiques, qui jouent un rôle important dans la régénération épidermique,

- la couche malpighienne (ou stratum spinosum) constituée de 5 à 10 couches cellulaires superposées qui s'aplatissent au fur et à mesure de leur ascension,

- la couche granuleuse (ou stratum granulosum) formée de 1 à 3 couches cellulaires disposées parallèlement à la surface cutanée. Le caractère essentiel des cellules de cette couche est la présence des grains de kératohyaline, principalement formés d'une protéine riche en histidine : la profilaggrine. Les dernières couches possèdent des kératinosomes qui interviennent dans la desquamation et la formation d'un manteau lipidique pericellulaire,

- la couche cornée (ou stratum corneum) formée de 5 à 10 assises de cornéocytes, cellules lamelleuses aux limites cytoplasmiques indistinctes qui desquament à la surface de la peau, assurant un rôle de barrière.

Des doses assez faibles (0,5 à 1 Gy) suffisent à diminuer la production de cellules épidermiques (Barton *et al*., 1985). Au delà de 1 Gy, une réduction du taux de desquamation des cornéocytes et une modification de l'activité estérase non-spécifique dans la couche granuleuse ont été observées. La réaction épithéliale aiguë peut s'expliquer facilement par les lésions des cellules souches et la perte des cellules les plus superficielles (Devik, 1955; Epstein et Maibach, 1965; Withers, 1967). Après irradiation, la destruction ou l'altération réversible des cellules souches de la basale de l'épiderme conduit à l'apparition d'une épithéliite exsudative dans un délai proportionnel au temps de transit des cellules de l'épiderme ou temps de renouvellement de la peau (Von Essen, 1972). Par ailleurs, les potentialités de régénération sont fortes puisque 1 cellule par cm^2, résultant d'une irradiation de 20 Gy, suffit pour la réépithélialisation.

Récemment, les lésions de l'épiderme, considérées comme à l'origine des effets précoces, ont été mises en avant pour leur possible rôle sur les lésions tardives radio-induites (Dorr et Hendry, 2001). Cette théorie, appelée « Consequential Late Effect », se base sur des données cliniques montrant que les réactions aiguës peuvent moduler les lésions tardives radio-induites (Figure 6). Elle s'oppose à celle du « Primary Late Effect » qui ne donne aucune corrélation entre effets précoces et tardifs radio-induits.

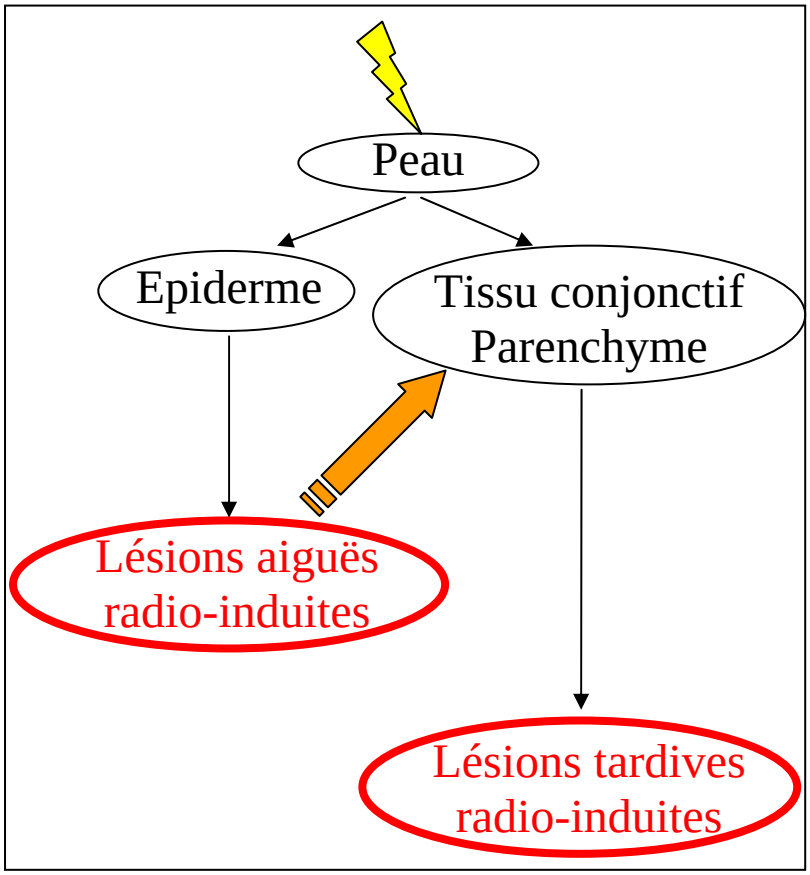

Figure 6. Théorie du « Consequential Late Effect ».

D’autres types cellulaires s’organisent au sein de l’épiderme avec les kératinocytes (Kanatinakis, 1995) : les **mélanocytes**, responsables de la synthèse et de la maturation de la mélanine ; les **cellules de Langerhans**, chargées de présenter les antigènes exogènes déposés sur la peau aux lymphocytes ; les **cellules de Merckel**, considérées comme des mécanorécepteurs et participant à la formation du plexus nerveux superficiel et au positionnement des muscles pilo-érecteurs ; les **fibres nerveuses**, très résistantes à l’irradiation, pouvant moduler la fonction de présentation antigénique.

L’épiderme possède ou est parcouru par différentes **annexes épidermiques** comme les canaux excréteurs des glandes sudorales assurant un rôle fondamental dans la thermorégulation ; les tiges des poils dont les follicules pileux sont localisés dans la partie profonde de l’hypoderme ; les ongles, constitués de cornéocytes compacts.

2. La jonction dermo-épidermique

La jonction dermo-épidermique appelée aussi membrane basale épidermique est une structure complexe séparant l’épiderme du derme (Briggaman, 1982; Stanley *et al*., 1982), élaborée à la fois par les kératinocytes basaux et les fibroblastes dermiques. Elle peut être divisée en 4 zones allant de l’épiderme vers le derme, (i) la **membrane plasmique des kératinocytes basaux** avec leur structure d’attache : les hémidesmosomes, (ii) la **lamina lucida** traversée par des filaments d’ancrage, (iii) la **lamina densa** formant la zone d’ancrage des filaments et des fibres issus de l’épiderme et de la zone fibrillaire, (iiii) la **zone fibrillaire** qui contient des fibres d'ancrages reliant la lamina densa de la membrane basale à des plaques d'ancrage dans le derme papillaire (Uitto et Pulkkinen, 1996).

La jonction dermo-épidermique assure dans la peau des fonctions fondamentales : elle possède un rôle de support mécanique pour l’adhésion de l’épiderme au derme et un rôle de barrière sélective permettant le contrôle des échanges moléculaires et cellulaires entre les deux compartiments. Elle est également, à travers les glycoprotéines qui la constituent - en particulier les laminines - le support de l’adhésion et de la migration des kératinocytes lors de

la restauration de l'intégrité épidermique (Zhang et Kramer, 1996), étape fondamentale de la cicatrisation cutanée.

3. Le derme

Le derme, d'épaisseur très variable selon les régions du corps, est un tissu conjonctif fibro-élastique composé de cellules et de fibres baignant dans une substance amorphe appelée substance fondamentale. L'ensemble fibres et substance fondamentale est regroupé sous le nom de matrice extracellulaire.

Histologiquement, le derme est divisé en deux zones : une zone superficielle papillaire et une zone profonde réticulaire (Grosshans, 1997) :

- Le **derme papillaire** est un tissu conjonctif lâche qui s'insinue entre les crêtes de l'épiderme, formant ainsi les papilles dermiques. Il est composé d'un réseau de faisceaux de collagène relativement fins et orientés perpendiculairement à la membrane basale épidermique. Ces faisceaux baignent dans une substance interfibrillaire abondante constituée de protéoglycannes, de glycosaminoglycannes et de fibres élastiques. Cette partie du derme est riche en vaisseaux sanguins et en cellules, principalement des fibroblastes.

- Le **derme réticulaire profond** se différencie du derme papillaire par un tissu conjonctif dense constitué de faisceaux de fibres de collagènes entremêlées à des fibres élastiques qui suivent généralement l'orientation des faisceaux de collagènes, de plus en plus épais vers la profondeur du derme. Le derme réticulaire contient peu de substance fondamentale et peu de cellules conjonctives.

La **matrice extracellulaire du tissu conjonctif dermique** est constituée de quatre types de macromolécules : les collagènes, l'élastine, les glycoprotéines de structure et les protéoglycannes. La nature et la quantité de ces composants régissent les propriétés mécaniques de la peau normale. Les collagènes représentent les protéines les plus abondantes

du derme (70 à 80%) (Van der Rest, 1993). L'élastine est le constituant majeur (90%) des fibres élastiques du derme adulte. Elle est toujours associée à des structures microfibrillaires. L'ensemble représente 2 à 4 % du volume du derme et confère à la peau ses propriétés d'élasticité et de souplesse. Les glycoprotéines de structure sont composées de motifs structuraux répétés formant ensemble des domaines qui confèrent à ces molécules leurs différentes fonctions (Johansson, 1996). Ces molécules jouent un rôle dans les interactions cellules-matrice, en particulier dans les phénomènes d'adhésion et de migration cellulaire. Il est important de noter que la fibronectine est une composante essentielle de la matrice provisoire qui est mise en place lors des phénomènes de réparation tissulaire (O'Keefe *et al*., 1985; Gailit *et al*., 1993). Les protéoglycannes sont des macromolécules complexes de grande taille dont l'hydratation assure en grande partie la tonicité de la peau. Ils sont dispersés entre les fibres du tissu conjonctif dermique. Certains des protéoglycannes sont capables de s'agréger entre eux et/ou avec d'autres molécules de la matrice extracellulaire pouvant ainsi intervenir dans les interactions cellule-matrice. Ils peuvent également se lier à des facteurs de croissance ou se comporter en co-récepteurs de ces derniers. En étant ainsi capables d'interagir avec les facteurs de croissance, les protéoglycannes sont capables d'intervenir dans la modulation des comportements cellulaires, comme la prolifération, la différenciation, la migration etc. (Gallo *et al*., 1996).

Les rayonnements ionisants conduisent à des altérations structurales des différents constituants de la matrice et agiront sur leur métabolisme.

a) les fibroblastes, la théorie stromale

Les cellules majoritairement représentées dans le derme sont les **fibroblastes**, cellules-clés du tissu conjonctif.

Elles sont généralement décrites comme des grandes cellules (100 µm) fusiformes ou étoilées possèdant de longs prolongements cytoplasmiques. En fait, leur morphologie varie selon leur localisation tissulaire et leur état de différenciation (pour revue, Delanian et Lefaix, 2004).

Lorsqu'il est quiescent dans le tissu conjonctif mature, on l'appelle **fibrocyte**. Pauvre en organites cytoplasmiques au repos, le **fibroblaste** en activité sous l'effet de divers stimuli tels que l'irradiation possède à l'inverse de nombreux organites cellulaires témoignant d'une grande activité de synthèse. Les fibroblastes produisent et sécrètent en effet la majorité des

molécules constituant la matrice extracellulaire notamment les collagènes, l'élastine, les glycoprotéines de structure et les protéoglycannes mais aussi des protéinases capables de dégrader et de remodeler cette matrice, telles les métalloprotéinases matricielles (MMPs). Outre leurs fonctions dans l'équilibre dynamique entre la synthèse et la dégradation de la matrice extracellulaire, ils permettent également la régulation par la sécrétion de facteurs de croissance tels que l'interféron-β, le PDGF, l'EGF, le TGF-β1, les interleukines et les prostaglandines (Rubin *et al*., 1995; Taipale et Keski-Oja, 1997). Les fibroblastes communiquent ainsi avec les cellules mésenchymateuses et épithéliales. Après irradiation, un phénomène de sénescence prématurée (SIPS, stress-induced premature senescence) a été observé dans les fibroblastes (Toussaint *et al*., 2002) et la sécrétion des constituants de la MEC est diminuée. Par ailleurs, les fibroblastes irradiés perdent leur capacité de division (Delanian *et al*., 1998; Delanian *et al*., 2001). La mort cellulaire se produit ensuite par apoptose ou nécrose (Rudolph *et al*., 1988; Burger *et al*., 1998).
Gabbiani *et al*. (Gabbiani *et al*., 1971) ont décrit une autre forme de fibroblastes, les **myofibroblastes**, ayant des propriétés contractiles, sécrétoires et macrophagiques, retrouvés dans le tissu de granulation qui se forme lors de la réparation dermique et impliqués dans la fibrose post-radique (Martin, 1991). Ces myofibroblastes, décrits par Maximov dès 1923 et qui apparaissent au cours de la phase inflammatoire initiale, sont présents lors de la fibrogenèse et de la fibrose constitutive. Ils présentent une réduction de la sécrétion des MMPs et une augmentation de l'expression des anti-collagénases.

Par ailleurs, les fibroblastes présentent une activité en enzymes antioxydantes supérieure à celle des kératinocytes *in vitro* (Yohn *et al*., 1991).

Comme dans l'épiderme, on note l'apparition après irradiation d'un processus dynamique de multiplication-migration, nécessaire à la réparation du tissu (von Essen, 1969). Mais les fibroblastes accumulent les lésions (Pouget *et al*., 2004) du fait de leur faible renouvellement, la plupart étant en phase G0 du cycle cellulaire. Il a ainsi été montré que les dommages résiduels de l'ADN étaient corrélés à la survie cellulaire (Wurm *et al*., 1994). Rudolph *et al*. (Rudolph *et al*., 1988) considèrent ainsi que les dommages causés par l'irradiation aux fibroblastes et à leurs cellules souches sont permanents et responsables des lésions cutanées tardives radio-induites. Cette **hypothèse stromale**, aussi supportée par Withers *et al*. (Withers *et al*., 1980), pour expliquer l'apparition des lésions tardives après irradiation de la peau s'oppose ainsi à la théorie épithéliale de Dörr et Hendry (cf II.1 et Figure 5). Elle propose que

les lésions tardives sont dues à la déplétion des cellules du parenchyme et/ou du stroma qui sont des cellules se renouvelant lentement expliquant l'apparition tardive des lésions.
Par ailleurs, la théorie stromale repose sur l'importance des espèces réactives de l'oxygène (ERO). En effet, l'existence d'une production continuelle d'ERO, ainsi qu'une dérégulation de la prolifération et du métabolisme des fibroblastes, ont été montrées dans des cas de fibrose des poumons ou de cirrhose du foie (Fubini et Hubbard, 2003; Poli, 2000).

b) les cellules endothéliales, la théorie vasculaire

Le système vasculaire présent au niveau du derme (Figure 7) intervient dans la thermorégulation, la régulation de la pression artérielle et la défense immunitaire de l'organisme. Il est formé d'artères sous-cutanées qui cheminent dans les fascias et envoient des collatérales qui traversent l'hypoderme et atteignent le derme profond où elles s'anastomosent pour former le plexus artériel profond, disposé horizontalement : celui-ci envoie des artères "en candélabre" qui remontent verticalement dans le derme et forment, dans la zone sous papillaire, le plexus artériel superficiel. De ce plexus, se détachent des artérioles précapillaires qui donnent naissance aux anses capillaires comportant un bras ascendant et un bras descendant (veinule postcapillaire). Le réseau veineux comporte également un plexus veineux sous papillaire et un plexus veineux profond.

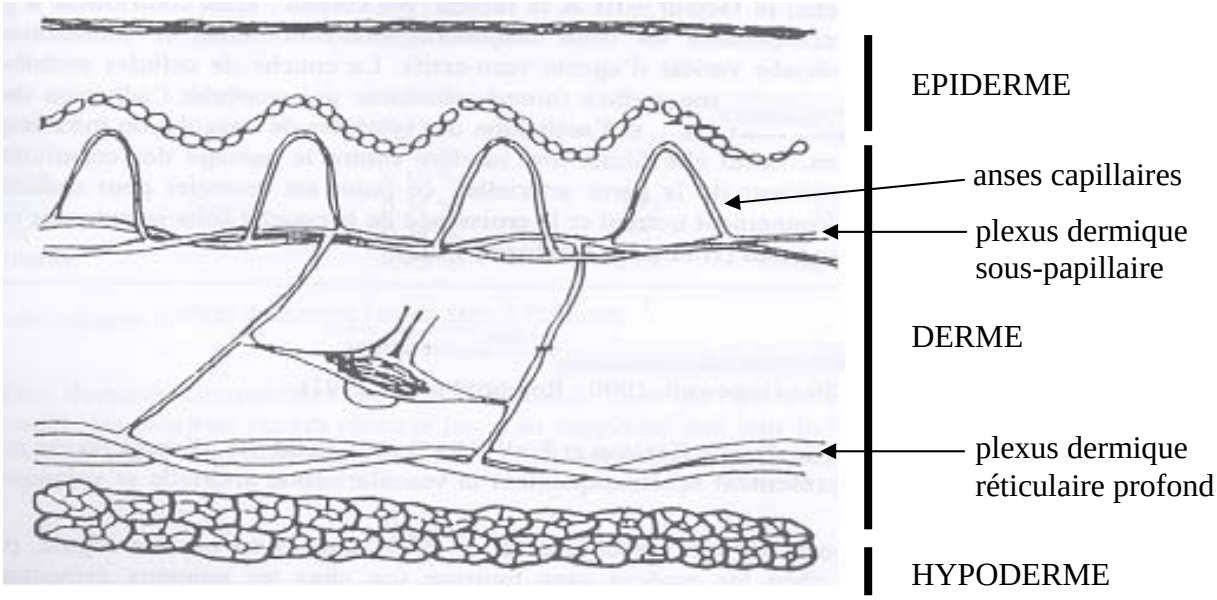

Figure 7. Schéma de la vascularisation cutanée (Swain et Grant, 1989).

Le derme contient également des **cellules endothéliales** qui participent à la formation des vaisseaux en formant un revêtement contitué d'une monocouche de cellules. Cette couche de cellules endothéliales présente une surface thromborésistante empêchant l'adhésion des plaquettes et des leucocytes et l'activation des systèmes de coagulation. D'autre part, elle forme une barrière essentielle au maintien du micro-environnement pour les cellules adjacentes (Huttner et Gabbiani, 1982).
Comme dans le cas des fibroblastes, la morphologie des cellules endothéliales, qui présentent un lent temps de renouvellement, est très variée. Leurs propriétés sont également diverses. Elles synthétisent la prostacycline (PGI2), le facteur VIII et le facteur von Willebrand. Elles représentent aussi un élément important dans l'inflammation cutanée car elles synthétisent et sécrètent des cytokines pro-inflammatoires (IL-1, IL-8) et des facteurs de croissance (M-CSF, G-CSF, GM-CSF, MCP). Elles expriment aussi des molécules d'adhésion.

Lors de la phase précoce après irradiation, la dégénérescence des cellules endothéliales initie les phénomènes inflammatoires par un défaut de la paroi vasculaire entraînant l'extravasation des protéines sériques et la formation d'œdème. Avant les deux hypothèses, épithéliale de Dörr et Hendry (2001) et stromale de Withers *et al*. (1980), la pathogénie des effets tardifs a aussi été expliquée par une **théorie vasculaire**. Pour Rubin et Casarett (Casarett, 1964; Rubin, 1984; Rubin et Casarett, 1968), des effets vasculaires jouent un rôle primordial dans l'apparition des lésions tardives par la constitution d'une fibrose artériolaire et interstitielle progressive contribuant à l'hypoplasie retardée du parenchyme. Les principales lésions radio-induites de l'endothélium apparaissent sur les petits vaisseaux : les cellules endothéliales gonflent entraînant la formation de thromboses. De même, les cellules endothéliales survivantes à l'irradiation se divisent le long de la lumière des vaisseaux formant des grappes contribuant aux thromboses (Hopewell, 1974, 1980). Denham considère qu'une hypoxie graduelle se produit après irradiation mais l'on a pas établi si elle était la cause ou la conséquence des lésions tardives dues à l'irradiation (Denham et Hauer-Jensen, 2002).

Le derme contient également des **dendrocytes dermiques**, qui représentent une population hétérogène de cellules mésenchymateuses dendritiques précédemment confondues avec des fibroblastes. On les trouve dans le derme papillaire en position périvasculaire et dans le derme profond autour des annexes épidermiques.

A côté de ces cellules spécifiques, on trouve des cellules d'origine sanguine telles que les **mastocytes**, cellules intervenant dans les réactions allergiques, retrouvées en petit nombre autour des capillaires dermiques ; les **macrophages** qui possèdent un rôle crucial dans l'inflammation, la détersion du tissu et l'activation de l'immunité.

L'**innervation cutanée** est riche et complexe. La voie afférente, constituée d'un nerf sensitif du système cérébro-spinal, est impliquée dans la perception des variations et agressions extérieures comme le toucher, les vibrations, la pression, la température, la douleur etc. Cette fonction est assurée par un réseau composé de fibres, de terminaisons nerveuses et de corpuscules tactiles (corpuscules de Wagner-Meissner et de Vater-Pacini). La voie efférente comporte des fibres qui régulent la vasomotricité, la sécrétion sudorale et la pilo-arrection (Kanatinakis, 1995).

4. L'hypoderme

L'hypoderme est un tissu adipeux séparant le derme et les plans aponévrotiques et musculaires sous-jacents. Il est constitué de septa conjonctifs qui cloisonnent les lobes adipeux. Les cellules adipeuses qui le constituent sont des cellules mésenchymateuses différenciées, rondes ou polygonales, possédant un noyau triangulaire périphérique et un cytoplasme riche en triglycérides et en acides gras. Outre son rôle énergétique dû à la réserve de graisse qui le constitue, l'hypoderme possède également un rôle de protection mécanique et thermique.

III- Phénomènes radio-induits au niveau cellulaire et moléculaire

Les rayonnements ionisants sont définis comme ayant une énergie cinétique suffisante (au moins 4,3 eV, correspondant à l'énergie d'ionisation du potassium) pour arracher des électrons à la matière. Entrent dans cette catégorie les rayonnements γ, X, β, α, etc. Ceux-ci vont produire des ionisations et des excitations des atomes constituant le milieu traversé. Le nombre et la distribution spatiale des évènements produits vont conditionner les effets biologiques. Deux paramètres à l'échelle macroscopique décrivent ces interactions : la dose et le TEL (transfert d'énergie linéique). La dose est définie comme la quantité d'énergie absorbée par unité de masse du milieu et est exprimée en Gray (Gy). Le TEL est défini comme la quantité d'énergie libérée par unité de longueur, il s'exprime en keV/µm. Ionisations et excitations résultent de deux types d'effets : les effets directs et les effets indirects.

1. Effets direct et indirect du rayonnement gamma du ^{137}Cs

a) effet direct

Il résulte d'un dépôt d'énergie directement sur le substrat qui peut conduire à son ionisation, si l'énergie transmise par les rayonnements est suffisante pour que l'électron quitte l'atome, ou à une excitation dans le cas contraire.

b) effet indirect

Les rayonnements ionisants interagissent avec la molécule d'eau conduisant à sa radiolyse (Figure 8) :

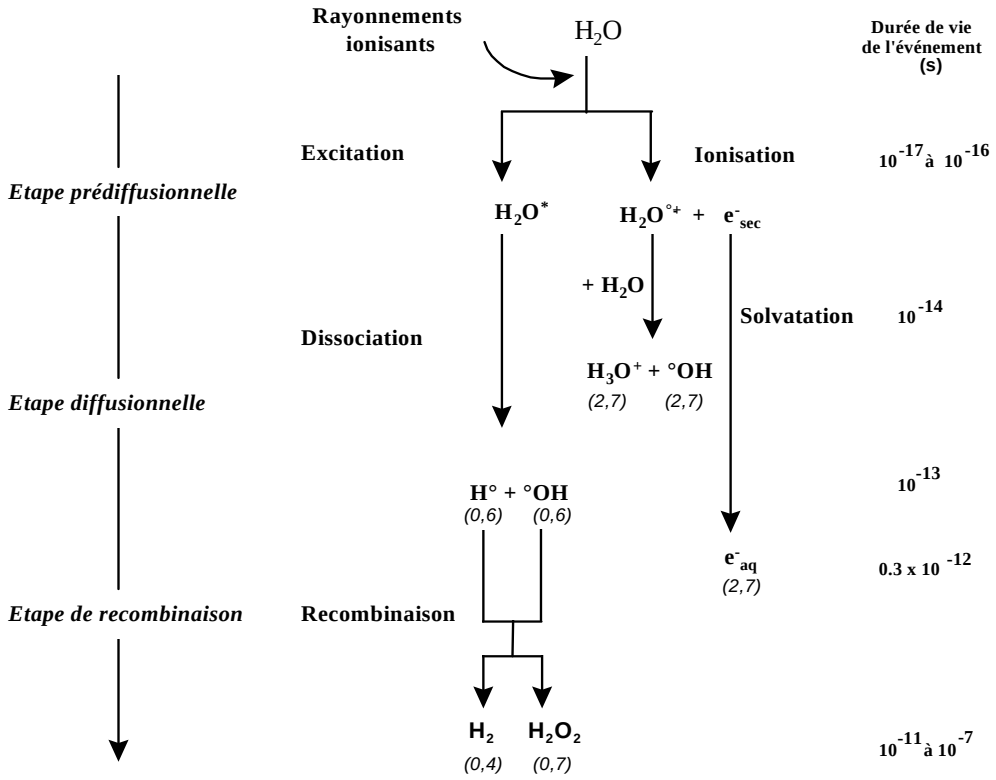

( ) : rendements radiolytiques des espèces exprimés en nombre de molécules/100 eV

Figure 8. Radiolyse de l'eau (Bensasson *et al*., 1993).

Ce type d'interaction est prépondérant avec les rayonnements de faible TEL, tels que les rayonnements γ et X. On estime ainsi qu'environ 75% des interactions des rayonnements gamma avec la matière se font par cette voie (Ward, 1988). L'eau, constituant majeur des organismes vivants, est ainsi ionisée et excitée générant des espèces, telles que °OH et H°, e^-_{aq} et H^+, selon les processus décrits ci-dessus. Les radicaux produits peuvent se recombiner et produire des espèces moléculaires (H_2O_2 et H_2) ou diffuser dans le milieu. En présence d'oxygène, la formation de nouvelles espèces radicalaires plus stables ayant un potentiel de diffusion plus important est favorisée. Peuvent ainsi être formés l'anion superoxyde $O_2^{\circ -}$ et le radical hydroxyle HO_2°.

Ces espèces radicalaires, caractérisées par la présence d'un ou plusieurs électrons célibataires dans une orbitale externe, sont également produites *in vivo* (Fridovich, 1975; Kehrer, 1993) (Figure 9).

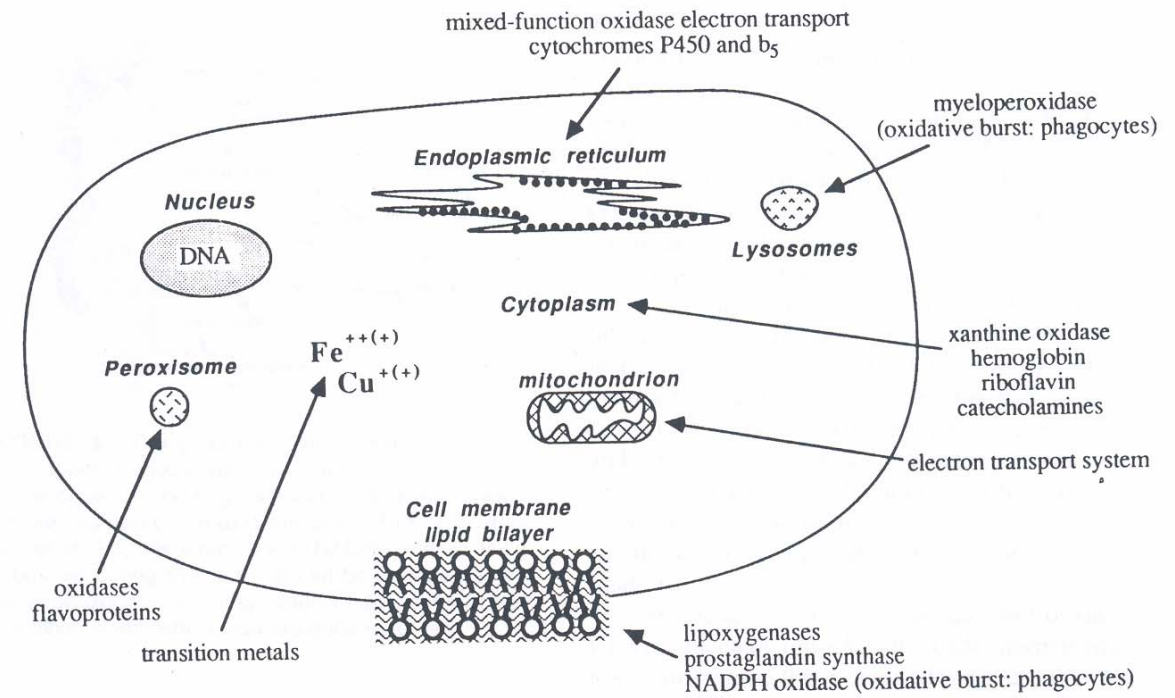

Figure 9. Sources cellulaires de radicaux libres (d'après Kehrer, 1993).

Elles ont une très grande réactivité chimique et donc une durée de vie courte pour la plupart. Les trois principales formes de radicaux libres oxygénés générés en permanence dans les mitochondries, les péroxysomes, le réticulum endoplasmique, la membrane plasmique et le cytoplasme sont :

- l'anion superoxyde $O_2^{\circ -}$ (O_2 + 1 e- → $O_2^{\circ -}$), non-réactif, produit dans la mitochondrie par des fuites électroniques au niveau des complexes I et III, ou par le coenzyme Q semi-réduit produit au niveau du complexe II de la chaîne respiratoire, ou par des réactions enzymatiques (NADPH oxydase membranaire, NADPH cytochrome P450 réductase, xanthine oxydase, aldéhyde oxydase),

- le peroxyde d'hydrogène H_2O_2, non-réactif, provenant de la dismutation de l'anion superoxyde par les superoxydes dismutases (2 $O^{\circ}{}_2^-$ + 2 H^+ → H_2O_2 + O_2), l'anion superoxyde étant non-diffusible alors que le peroxyde d'hydrogène l'est et a une durée de vie longue,

- le radical hydroxyle °OH, le plus réactif des radicaux car sans moyen de défense directe, produit essentiellement par la réaction d'Haber-Weiss (1) et de Fenton (2 et 3), catalysée par les métaux de transition tel que le fer :

$$(1) \qquad O°_2^- + H_2O_2 \rightarrow O_2 + OH^- + °OH$$

$$(2) \qquad O°_2^- + Fe^{3+} \rightarrow O_2 + Fe^{2+}$$

$$(3) \qquad Fe^{2+} + H_2O_2 \rightarrow Fe^{3+} + OH^- + °OH$$

Contrairement aux espèces produites physiologiquement, la distribution de ces espèces après l'irradiation n'est pas homogène dans le milieu. Des excitations et ionisations sont produites tout au long du parcours du rayonnement. La production d'ionisations, présentes à l'extrémité des trajectoires des électrons secondaires, se fait en grappes (Figure 10). Les rayonnements à fort TEL produisent des ionisations moins dispersées et en plus grande densité (Goodhead, 1989, 1994; Prise *et al*., 1994; Holley et Chatterjee, 1996).

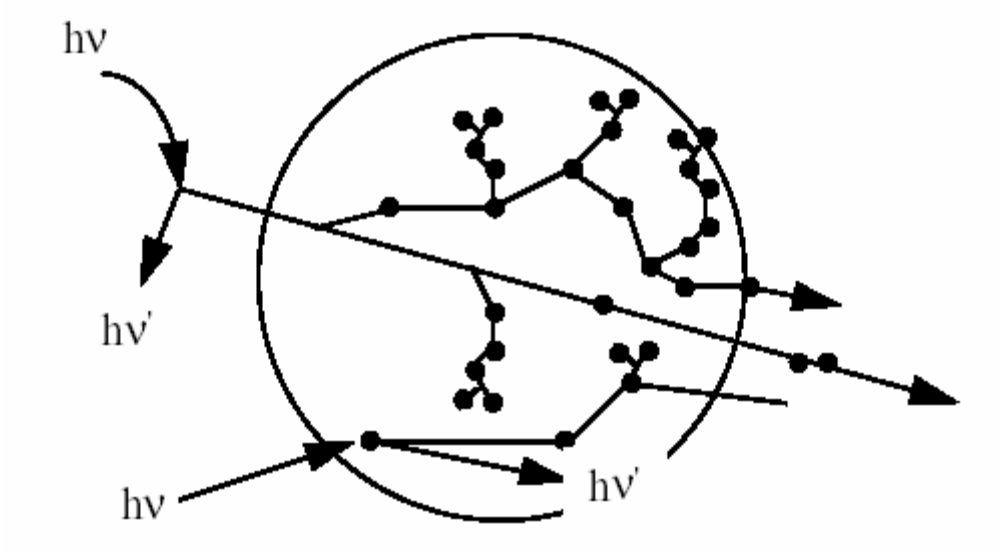

Figure 10. Trace d'un rayonnement de faible TEL dans le noyau cellulaire (tiré de Pouget, 2000).

2. Effets sur les macromolécules biologiques

Dans le cas où les systèmes de défense ont été dépassés, les radicaux s'attaquent aux macromolécules biologiques dans l'environnement direct de leur lieu de production. Les

radicaux étant très réactifs et ayant donc une durée de vie courte, toutes les molécules biologiques possédant des doubles liaisons sont susceptibles d'être touchées et des produits de dégradation sont engendrés (bases oxydées et coupures de l'ADN nucléaire et mitochondrial, produits de péroxydations lipidiques, protéines oxydées, cholestérol oxydé). Ces produits de dégradation ont une durée de vie plus longue et certains d'entre eux peuvent entraîner l'activation ou la répression de gènes (ATM, NFκB, AP1, c-jun, c-fos…).

a) les dommages lipidiques

Les radicaux libres générés lors de la radiolyse de l'eau, en particulier les radicaux hydroxyle, sont susceptibles d'interagir au niveau des doubles liaisons C=C avec les chaînes d'acides gras polyinsaturés qui constituent le double feuillet phospholipidique des membranes (Bonnefont-Rousselot, 1994). Ils entraînent alors la peroxydation des acides gras polyinsaturés (Gutteridge et Halliwell, 1990) provoquant une désorganisation membranaire (perturbation des propriétés physicochimiques des membranes, des communications intercellulaires et du fonctionnement des enzymes membranaires) pouvant aboutir à la lyse cellulaire à de fortes doses d'irradiation. Cette attaque radicalaire se déroule en trois phases : initiation, propagation et terminaison (Figure 11). Les hydroperoxydes lipidiques formés sont dégradés principalement en malonedialdéhyde (MDA) (Chaudhary *et al*., 1996) et 4-hydroxynonénal (4-HNE) (Chen et Chung, 1996) qui réagissent de manière covalente avec les protéines et les inactivent. Ce sont des produits très toxiques (mutagènes) puisqu'ils peuvent également modifier l'ADN et sont impliqués dans les mécanismes apoptotiques (Ramakrishnan *et al*., 1993).

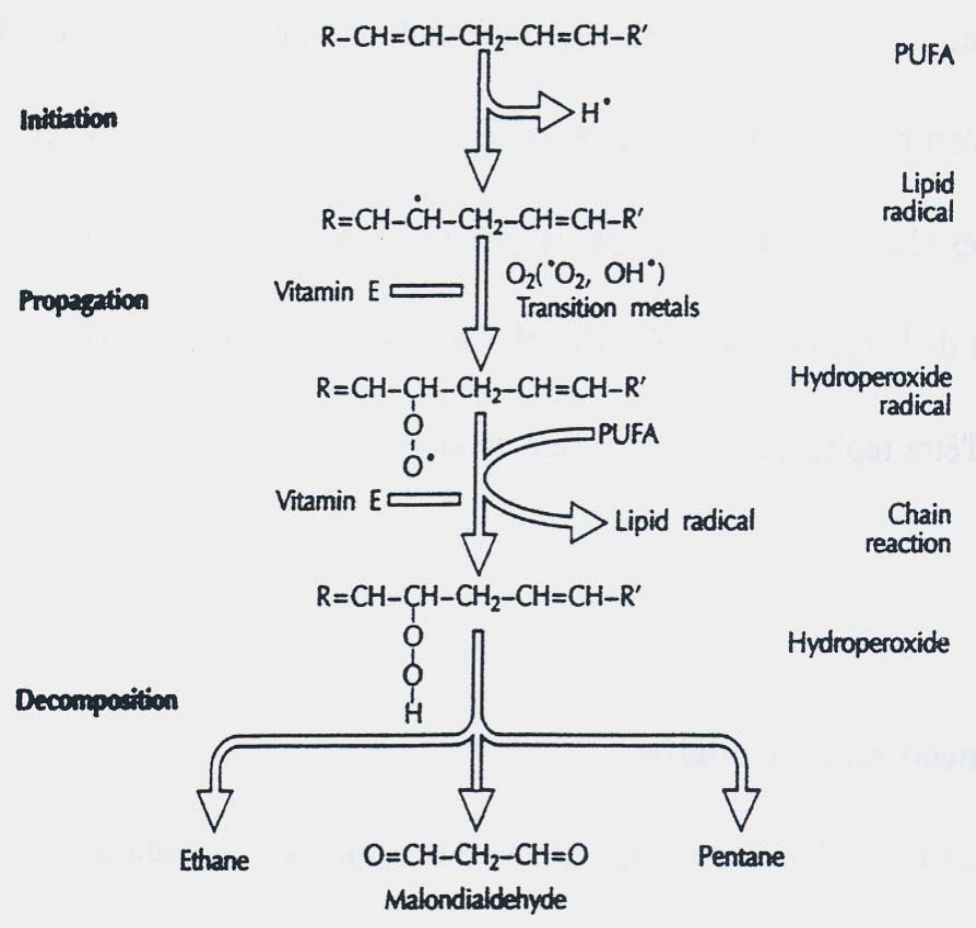

Figure 11. Peroxydation des acides gras polyinsaturés.

b) l'oxydation des protéines

Les protéines sont clivées et les acides aminés sont oxydés, il y a nitrosylation des tyrosines (entraînant l'altération des voies de signalisation) et carbonylation (Davies *et al*., 1991). La dénaturation des enzymes et protéines membranaires entraîne une perturbation du fonctionnement cellulaire.

c) les atteintes de l'ADN

Le spectre des lésions de l'ADN est large (von Sonntag, 1987; Cadet *et al*., 1997; Cadet *et al*., 2003) : modifications des bases puriques et pyrimidiques, perte de bases (« sites abasiques »),

cassures simple- ou double-brins, altérations des sucres (2-désoxyriboses) et aussi pontages ADN-protéines (Figure 12).

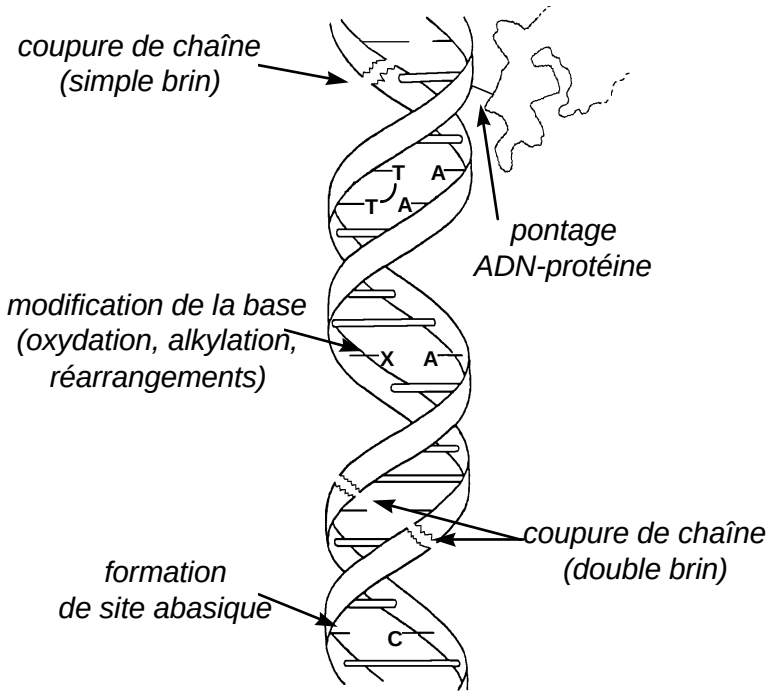

Figure 12. Lésions radio-induites de l'ADN (www-dsv.cea.fr).

Les coupures simple-brins

Pour un rayonnement de faible TEL, on dénombre environ 1000 cassures simple-brins (CSB) produites par cellule de mammifère par Gy (Ahnström et Erixon, 1981; Goodhead, 1994). Elles proviennent de l'arrachement d'un atome d'hydrogène du sucre par le radical °OH conduisant à la rupture des liaisons phosphate-sucre (Tubiana *et al*., 1986; von Sonntag, 1987). La relation dose-effet est linéaire, c'est-à-dire que la formation de CSB augmente avec la dose d'irradiation. Le niveau de CSB est moindre avec des TEL plus élevés. Les CSB sont vite réparées, dans l'heure qui suit l'exposition aux rayonnements, et elles auraient peu d'impact en matière de létalité des cellules.

Les coupures double-brins

Ces cassures sont beaucoup plus délétères. On en dénombre, pour un rayonnement de faible TEL, 40 à 100 par cellule de mammifère par Gy (Goodhead, 1994). Elles se produisent à la suite d'une rupture des deux chaînes en des sites assez proches l'un de l'autre. Deux mécanismes peuvent expliquer leur formation : un radical °OH agit sur le 2-désoxyribose (Siddiqi et Bothe, 1987) puis le radical est transféré au deuxième brin ou plusieurs radicaux °OH agissent sur la molécule d'ADN en des sites proches (Ward, 1985). La réparation de ces cassures peut être lente expliquant la radiosensibilité (Radford, 1986; Frankenberg-Schwager et Frankenberg, 1990; Iliakis, 1991; Ross *et al*., 1995).

Les bases modifiées

Une trentaine de produits de modification des bases a été mise en évidence par chromatographie gazeuse ou liquide couplée à la spectrométrie de masse ou par résonance magnétique nucléaire (Cadet et Téoule, 1978; Téoule, 1987; von Sonntag, 1987; Dizdaroglu, 1992; Cadet *et al*., 1999; Cadet *et al*., 2004). Le nombre de bases modifiées par cellule eucaryote par Gy est estimé à 2000 à faible TEL. On distingue les bases pyrimidiques et les bases puriques modifiées. Elles résultent principalement de l'attaque des radicaux hydroxyle sur le cycle aromatique mais sont également produites par ionisation directe. La figure 13 présente l'oxydation de la guanine.

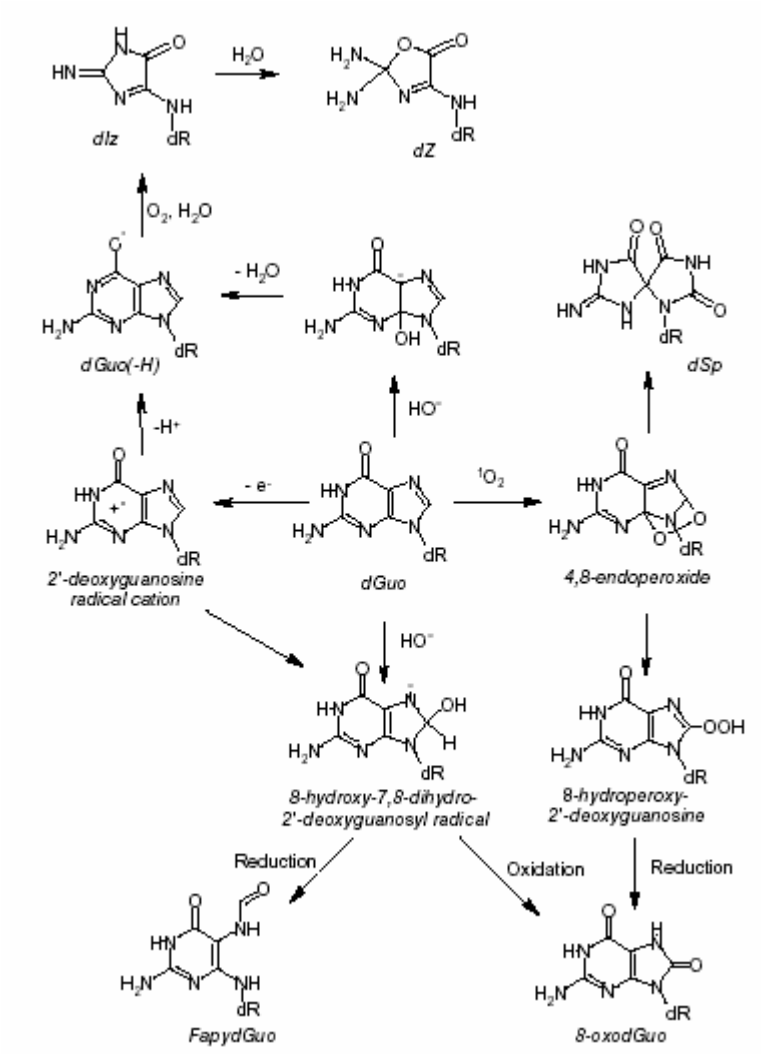

Figure 13. Schéma d'oxydation de la guanine (Cadet *et al.*, 2003).

Les pontages ADN-protéines

Après exposition aux rayonnements gamma, des pontages, dans lesquels le radical °OH peut être impliqué, peuvent se produire entre l'ADN et des protéines environnantes (30 par cellule par Gy), entre les deux brins ou à l'intérieur d'un même brin (Oleinick *et al*., 1987). Ainsi, des pontages tyrosine-thymine ou entre différents acides aminés et la thymine ou la cytosine ont été identifiés (Gajewski *et al*., 1988; Dizdaroglu et Gajewski, 1989; Nackerdien *et al*., 1991).

Les altérations des sucres

Les radicaux °OH peuvent conduire, via l'arrachement d'un atome d'hydrogène, à la formation d'une coupure de brin par libération du 2-désoxyribose ou par l'altération du sucre qui reste relié à l'extrémité 3' ou 5' du squelette phosphodiester, ou à la formation d'un site abasique, c'est-à-dire un sucre altéré mais relié par l'extrémité 3' et 5' au squelette phosphodiester. Différents sucres altérés ont été identifiés (Beesk *et al*., 1979; von Sonntag, 1987).

Par ailleurs, l'effet direct conduit également à la formation de bases modifiées de même nature mais dans des proportions différentes (Decarroz *et al*., 1986). On peut ainsi obtenir :

- une coupure de l'ADN à la suite de la formation d'un cation radical à partir du 2-désoxyribose,
- l'oxazolone, la 8-oxodGuo ou la FapyGua après formation d'un cation radical à partir de la 2'-désoxyguanosine,
- la 8-oxodAdo ou la FapydAdo après formation d'un cation radical à partir de la 2'-désoxyadénosine,
- le 5-HmdUrd, le 5-FordUrd ou la (6-hydroxy)5-hydroperoxy-5,6-dihydrothymidine après formation d'un cation radical à partir de la 2'-désoxythymidine.

En dehors de toute irradiation, des lésions spontanées de l'ADN ont lieu : des cassures simple- et double-brins (5000 par heure), des dépurinations (1500 par heure), des pertes de bases (1250 par heure). Des modifications de bases (2000 à 1000 par jour) se produisent également. Toutefois, aucune mutation n'apparaît pour autant car la plupart des dommages est réparée. L'atteinte de l'ADN peut toutefois avoir de graves conséquences somatiques ou héréditaires en altérant la synthèse de protéines fondamentales au fonctionnement de la cellule.

D'autre part, l'ADN mitochondrial est également une cible des rayonnements ionisants. Il est plus facilement touché de par sa localisation cytoplasmique, et ses dommages sont très inefficacement corrigés. Ils peuvent provoquer des mutations induisant une diminution de l'activité cytochrome oxydase ou l'altération de la chaîne respiratoire engendrant une production accrue d'espèces réactives oxygénées.

La molécule d'ARN, elle aussi cytoplasmique, est plus facilement oxydée et altérée. Toutefois, sa durée de vie est courte mais ces dommages entraîneront tout de même des erreurs lors de la traduction en protéines.

Ces molécules endommagées sont souvent impliquées dans des voies de signalisation conduisant à l'apoptose. Elles sont à l'origine, au niveau physiologique, de modifications de la croissance cellulaire et de phénomènes liés à l'inflammation, c'est l'« oxidative paradox » puisque des concentrations physiologiques d'espèces réactives de l'oxygène ont un effet bénéfique sur la croissance cellulaire tandis que des taux élevés sont destructeurs (Remacle *et al*., 1995).

3. Réponses des cellules

La réponse des cellules aux rayonnements ionisants, mais aussi au stress oxydatif, est constituée par : une première ligne correspondant aux systèmes de défenses anti-oxydantes avec les systèmes non-enzymatiques et les systèmes enzymatiques et une deuxième ligne de réponse formée par les systèmes de dégradation et de réparation de l'ADN, des lipides et des protéines. Enfin, la dernière ligne de réponse est un processus conduisant à la mort cellulaire.

a) les défenses anti-oxydantes

Face aux espèces réactives de l'oxygène, les cellules s'adaptent et se défendent (Burton *et al*., 1985; Kehrer, 1993). Les systèmes de défenses anti-oxydantes agissent à différents niveaux de la cascade d'activation de l'oxygène (Figure 14) et sont de plusieurs natures.

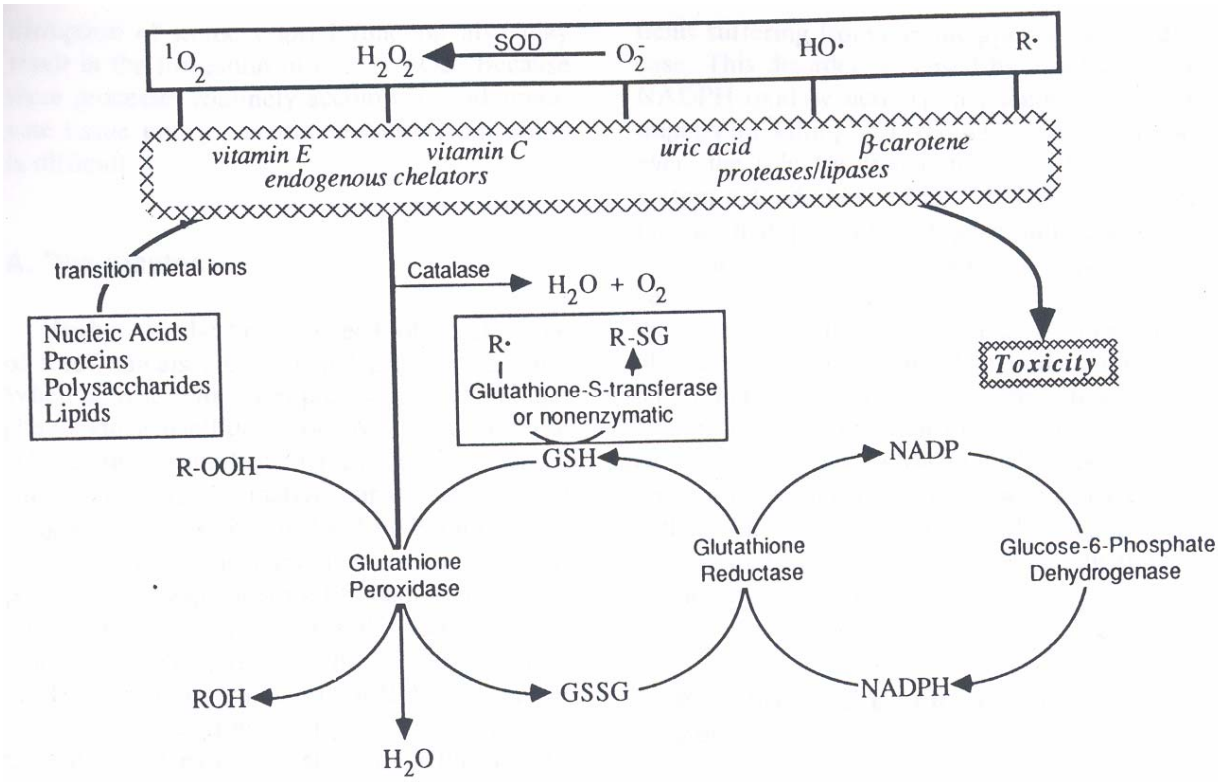

Figure 14. Systèmes biologiques de défenses anti-oxydantes. Les cellules contiennent un spectre d'anti-oxydants chimiques et enzymatiques qui travaillent de concert pour minimiser les réactions oxydatives dans la cellule (d'après Kehrer, 1993).

Les systèmes de défenses non-enzymatiques

Les systèmes non-enzymatiques sont représentés par une série de petites molécules (vitamine E, vitamine C…). Selon leur concentration, les piégeurs de radicaux libres ont des effets protecteurs ou pathologiques. Ces molécules doivent être capables de réaliser cette fonction à très faibles concentrations (Halliwell et Gutteridge, 1995). Elles constituent la première ligne de défense, on ne peut pas encore vraiment parler de stress oxydatif car des radicaux libres sont produits en permanence dans l'organisme, c'est l'« homéostasie d'oxydoréduction ».

La **vitamine E**, tout comme la vitamine A, est lipophile. Elle est située dans toutes les membranes cellulaires (Valk et Hornstra, 2000). Elle est apportée par l'alimentation sous 8 formes stériques différentes et est trouvée dans l'organisme essentiellement sous la forme α-tocophérol. C'est la plus efficace de ces petites molécules. Elle s'oxyde en piégeant O_2, $O_2^{\circ-}$, OH° ou un radical peroxyle lipidique produit dans la membrane plasmique ou peut donner un

H° qui va neutraliser les radicaux libres. Elle peut ensuite être réduite par le glutathion réduit (GSH) ou par la **vitamine C**. *In vivo*, la vitamine C retrouve sa forme réduite sous l'action de la déshydroascorbate réductase qui utilise le GSH comme cofacteur, elle n'est pas synthétisée dans les organismes humains et primates et doit donc aussi être apportée par l'alimentation. Le **glutathion** et la **thioredoxine** sont des piégeurs de radicaux hydroxyle et d'oxygène singulet, ils permettent de générer des espèces réduites pour les enzymes anti-oxydantes. On peut également citer l'**ubiquinone** (ou coenzyme Q), **l'acide urique**, la **transferrine**, l'**apotransferrine**, la **métallothionéine** et certains acides gras monoinsaturés tel l'**acide oléique**.

Les systèmes de défenses enzymatiques

En deuxième ligne de défense, on trouve les enzymes anti-oxydantes (Diplock, 1993; Pugliese, 1998) : les glutathion peroxydases (GPx), les superoxyde dismutases (SOD) et la catalase.

Les **SOD** transforment les radicaux $O_2^{\circ -}$ en H_2O_2 selon la réaction suivante (Deby, 1991) :

$$2\ O^{\circ}{}_2^{-} + 2\ H^{+} \rightarrow H_2O_2 + O_2$$

On distingue trois types de SOD selon le métal agissant comme cofacteur métallique catalysant toutes la même réaction : la Cu/Zn SOD (cytoplasmique constitutive et extracellulaire), la Mn SOD (mitochondriale, inductible) et la Fe SOD (exclusivement chez les procaryotes).

La **catalase** catalyse la décomposition de H_2O_2 en H_2O et O_2 selon la réaction suivante :

$$2\ H_2O_2 \rightarrow 2\ H_2O + O_2$$

Elle se situe dans les péroxysomes où les réactions d'oxydations produisent H_2O_2 : la catalase le détruit au fur et à mesure de sa formation.

Les **GPx** réduisent les hydroperoxydes en alcool, la GPx à sélénium réduit le peroxyde d'hydrogène mais ses substrats principaux sont les hydroperoxydes provenant de la

péroxydation des acides gras polyinsaturés. Elle nécessite, pour son fonctionnement, la présence de glutathion réduit. Celui-ci est régénéré par la glutathion réductase (GR) :

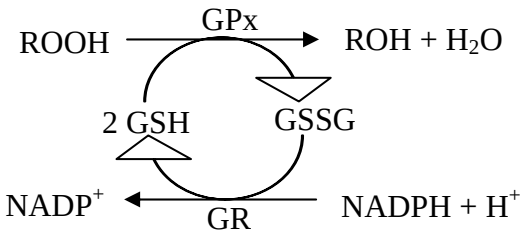

b) les arrêts dans le cycle cellulaire

L'exposition aux rayonnements ionisants des cellules conduit à un arrêt en phase G2 dans toutes les lignées (d'environ une heure par Gy), à un arrêt en phase S ou à un arrêt en G1 dans les lignées exprimant une protéine p53 normale (pour revue, Favaudon, 2000). Ces arrêts au niveau des points de contrôle du cycle cellulaire proviennent de l'activation de signaux cellulaires provoquée par la reconnaissance des dommages radio-induits de l'ADN. Ils permettent la mise en œuvre des mécanismes de réparation pour éviter les erreurs de réplication (transition G1-S) et les aberrations chromosomiques pendant la mitose (transition G2-M).

Signalisation des cassures de l'ADN

Les protéines PARP, DNA-PKcs et ATM peuvent être activées par les lésions de l'ADN engendrées dans les cellules normales irradiées. Elles entraînent alors la modification d'autres protéines.

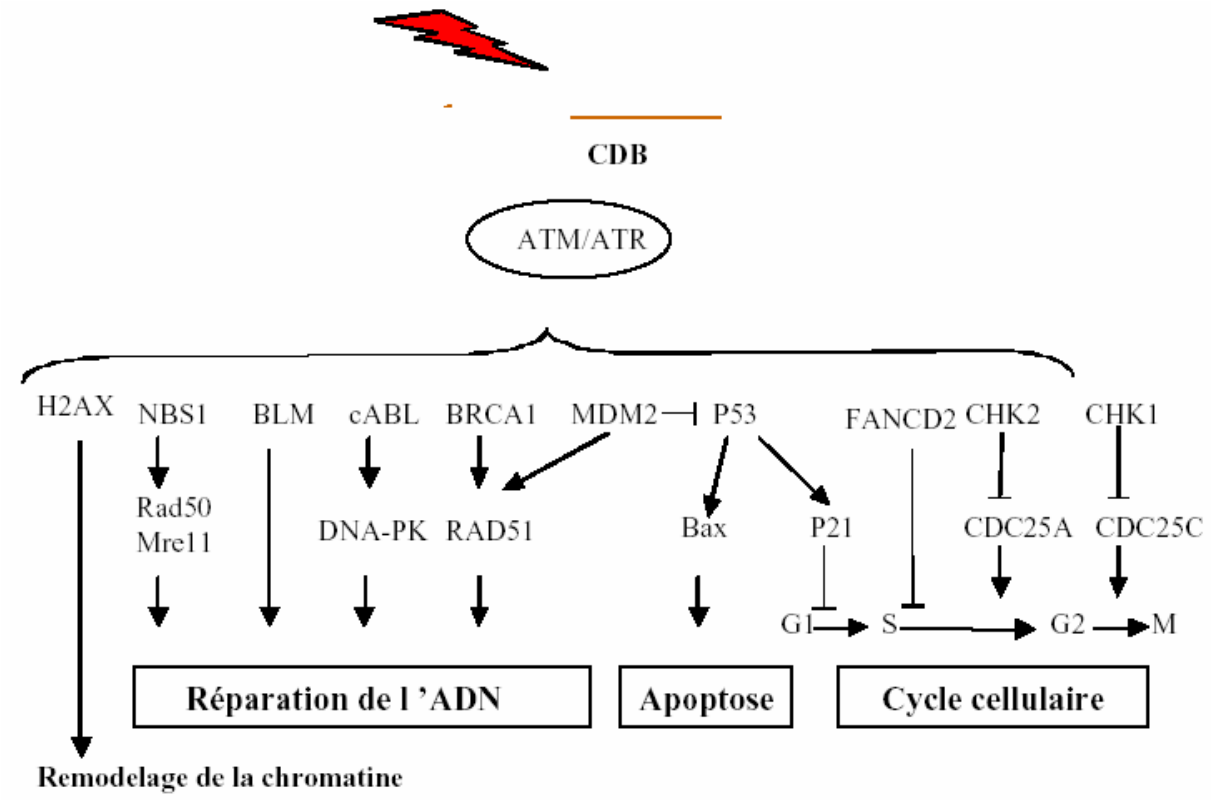

Figure 15. Signalisation des cassures double-brins via les proteines ATM et ATR (tiré de Maurisse, 2003).

La PARP, poly-(ADP ribose) polymérase, se fixe au niveau des cassures de l'ADN pour recruter les protéines de la réparation par excision de base. Pour cela, elle transfère des poly-(ADP riboses) sur différentes protéines telles que les histones, la lamine B, la polymérase α et sur elle-même. Cet ajout de charges négatives diminue l'affinité des protéines pour l'ADN rendant l'accès aux protéines de réparation plus facile (Oliver *et al*., 1999). De plus, ces polymères permettraient d'éviter la recombinaison illégitime en occupant les sites des coupures au cours de l'intervalle de temps nécessaire au recrutement des enzymes de réparation. Par ailleurs, la PARP transmet d'autres signaux que ceux de réparation stricte puisqu'elle pourrait recruter p53, p21, DNA-PKcs, Ku70 etc. (Pleschke *et al*., 2000).

DNA-PKcs, la sous-unité catalytique du complexe DNA-PK de la NHEJ, phosphoryle plusieurs protéines dont P53 comme décrit dans la figure 16. Cependant, le rôle de DNA-PKcs dans la régulation de l'activité P53 n'est pas clairement établi. Elle pourrait agir

indirectement en phosphorylant MDM2 diminuant ainsi l'interaction P53-MDM2 et favorisant la stabilisation de P53 (Mayo *et al*., 1997).

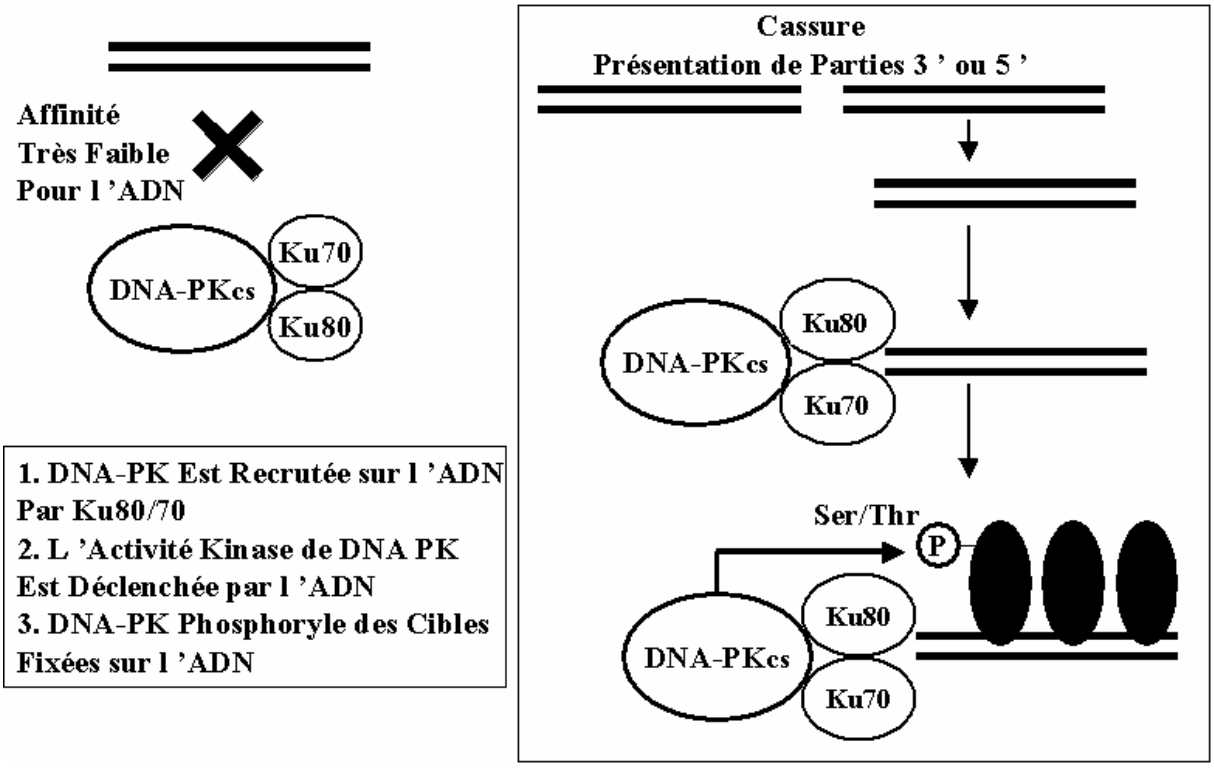

Figure 16. Schéma d'activation de DNA-PK.

ATM (pour revue, Kurz et Lees-Miller, 2004) est une kinase activée après liaison à l'ADN endommagé (Meyn, 1995; Canman et Lim, 1998; Suzuki *et al*., 1999) (Figure 17). Elle est mutée dans les cas d'ataxie télangiectasie, maladie dont les symptômes comprennent une hypersensibilité aux rayonnements ionisants. Les cellules ATM -/- ne s'arrêtent pas en G1 et n'accumulent pas de P53 (Kastan *et al*., 1992). En effet, ATM phosphoryle P53 (Siliciano *et al*., 1997; Banin *et al*., 1998; Canman *et al*., 1998). Les cellules ATM -/- pourraient en fait présenter un retard de phosphorylation et de stabilisation de P53 montrant ainsi la possible implication d'autres kinases telles qu'ATR (ATM and Rad3-related) plus souvent reliée aux irradiations UV (Tibbetts *et al*., 1999). Par ailleurs, ATM pourrait aussi phosphoryler et activer l'ABL kinase qui se complexe avec ATM et phosphoryle P53 et pRB.

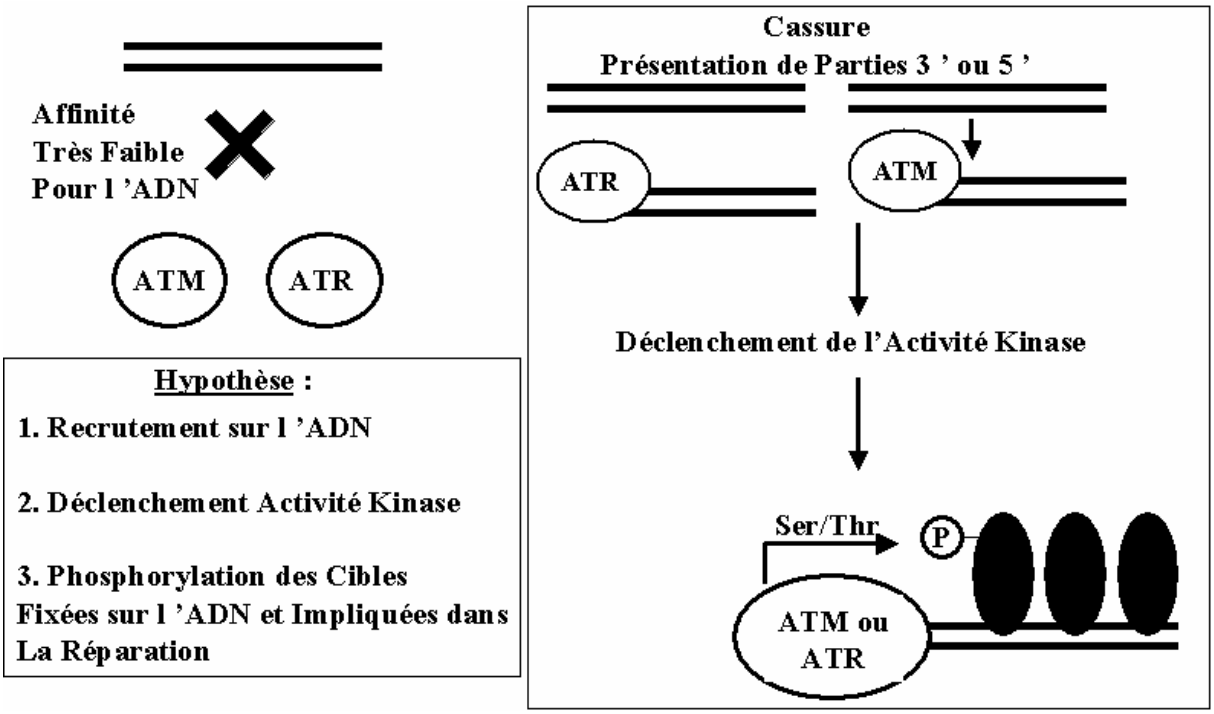

Figure 17. Schéma d'activation d'ATM et ATR.

P53 (pour revue, (Harris et Levine, 2005))

P53, mutée dans plus de 50% des tumeurs humaines, a des réponses variables selon la nature de l'agent génotoxique (Kobayashi *et al*., 1998). Cette protéine agissant comme facteur de transcription joue un rôle central dans la réponse aux rayonnements ionisants (pour revue, Amundson *et al*., 1998). Sa réponse peut également être indépendante de son rôle de facteur de transcription. Après irradiation, son taux augmente (une CDB suffit à l'activer) et celle-ci est transportée dans le noyau où elle se fixe sur des séquences régulatrices provoquant la transcription de protéines impliquées dans le contrôle du cycle cellulaire telles que p21, PCNA, GADD45 et dans l'apoptose. Elle a une demi-vie très courte. Sa phosphorylation sur un résidu sérine (Siliciano *et al*., 1997; Mayo *et al*., 2005;) conduit à l'affaiblissement des interactions avec MDM2, qui participe à sa dégradation, stabilisant P53 (Kubbutat *et al*., 1997). D'autre part, P53 pourrait interagir directement avec l'ADN endommagé (Jayaraman et Prives, 1995).

Arrêts en phase G1 ou G2 du cycle cellulaire

Après irradiation, un blocage peut se produire en fin de phase G1 pour éviter la réplication de l'ADN endommagé ou en fin de phase G2 pour éviter la ségrégation des chromosomes altérés (Figure 18).

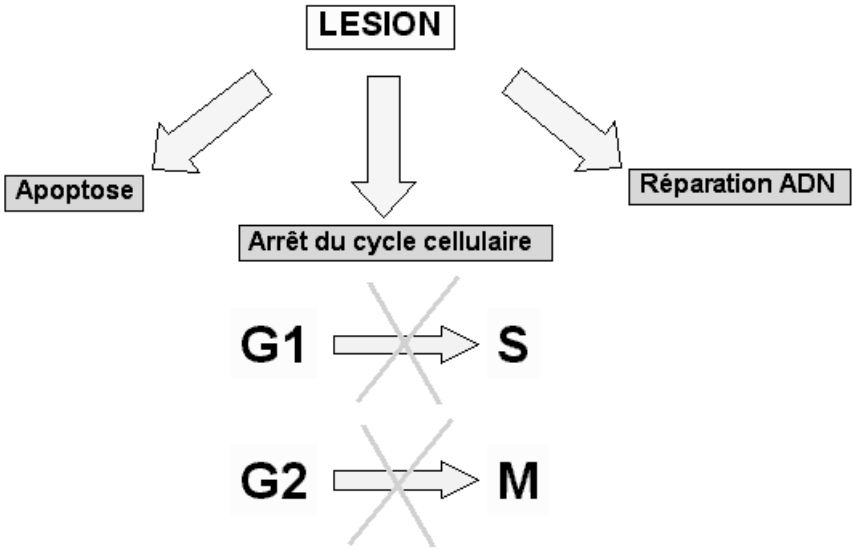

Figure 18. Réponses cellulaires aux lésions de l'ADN.

L'arrêt du cycle cellulaire en phase G1 dépend du statut de P53. En effet, des cellules déficientes en p53 n'ont pas montré de blocage en G1 et la transfection de P53 a restauré l'arrêt (Kastan *et al*., 1991; Kuerbitz *et al*., 1992). Comme décrit précédemment, p53 entraîne la transcription de $p21^{WAF1}$ qui inhibe l'activité des cyclines kinases dépendantes (Xiong *et al*., 1993). Ainsi, par exemple, Rb, protéine cible du complexe cycline D/Cdk 4, n'est pas phosphorylée or sa phosphorylation est nécessaire à l'activation des facteurs de transcription E2F qui régulent l'expression des gènes de la phase S (Black et Azizkhan-Clifford, 1999). Les histones sont également des cibles de phosphorylation pour les complexes cycline/Cdk et l'inhibition par $p21^{WAF1}$ de ces complexes inhibe aussi cette phosphorylation participant probablement au blocage de l'entrée en phase S (el-Deiry *et al*., 1994). D'autre part, $p21^{WAF1}$ se lie à PCNA après irradiation (Savio *et al*., 1996) conduisant à la diminution de son activité or PCNA intervient dans la réplication de l'ADN. En revanche, cette diminution d'activité de PCNA n'inhiberait pas complètement son action dans le système de réparation de l'ADN par excision de base et resynthèse (Li *et al*., 1994).

Les arrêts en phases G1 et G2 ne sont pas complètement indépendants puisqu'il a pu être montré que l'arrêt en phase G2 est prolongé en cas d'absence d'arrêt en G1 (Pellegata *et al*., 1996). P53 jouerait un rôle indirect sur ce blocage. D'autres études ont montré une implication directe de p53 dans le blocage en G2 (Agarwal *et al*., 1995). Ce blocage proviendrait de l'inhibition de l'expression de la cycline B1 (Innocente *et al*., 1999) et de Cdc 2 (Azzam *et al*., 1997) de manière p53-dépendante. Or, le complexe cycline B1/Cdc 2 promoteur de mitose est impliqué dans le blocage en phase G2 après lésion de l'ADN (pour revue Piwnica-Worms, 1999). Une autre étude a montré que ce complexe est séquestré par la protéine 14.3.3 σ, induite par p53, dans des cellules épithéliales irradiées, empêchant sa migration au noyau et donc l'entrée en mitose (Chan *et al*., 1999). Ce complexe est aussi régulée par Chk1, Wee1 et Cdc25C (pour revue, Teyssier *et al*., 1999).

c) les systèmes de réparation

La réparation des lipides s'effectue par les phospholipases A_2 et C et la GPx. Celle des protéines se produit par la dégradation de celles-ci grâce à la MOP (macroxyprotéinase) avant une nouvelle synthèse à partir des acides aminés libérés.

Etant donné l'importance de la réparation des dommages de l'ADN et leur possible implication dans les lésions cutanées radio-induites tardives, nous avons plus particulièrement développé les systèmes de réparation de l'ADN qui peuvent aboutir à de nouvelles cassures.

Réparation par excision de base et resynthèse

Ce système est utilisé pour réparer les bases modifiées, les sites abasiques et les cassures simple-brins. Il est considéré comme un mécanisme de réparation fidèle de l'ADN car il utilise le brin complémentaire comme matrice. Cependant, si deux lésions sont produites en des sites proches sur les deux brins complémentaires, elles peuvent aboutir, par ce système, à

une cassure double-brin (Harrison *et al.*, 1999). La figure 19 présente les différentes étapes de ce mécanisme. Certaines des protéines sont aussi impliquées dans la réplication de l'ADN.

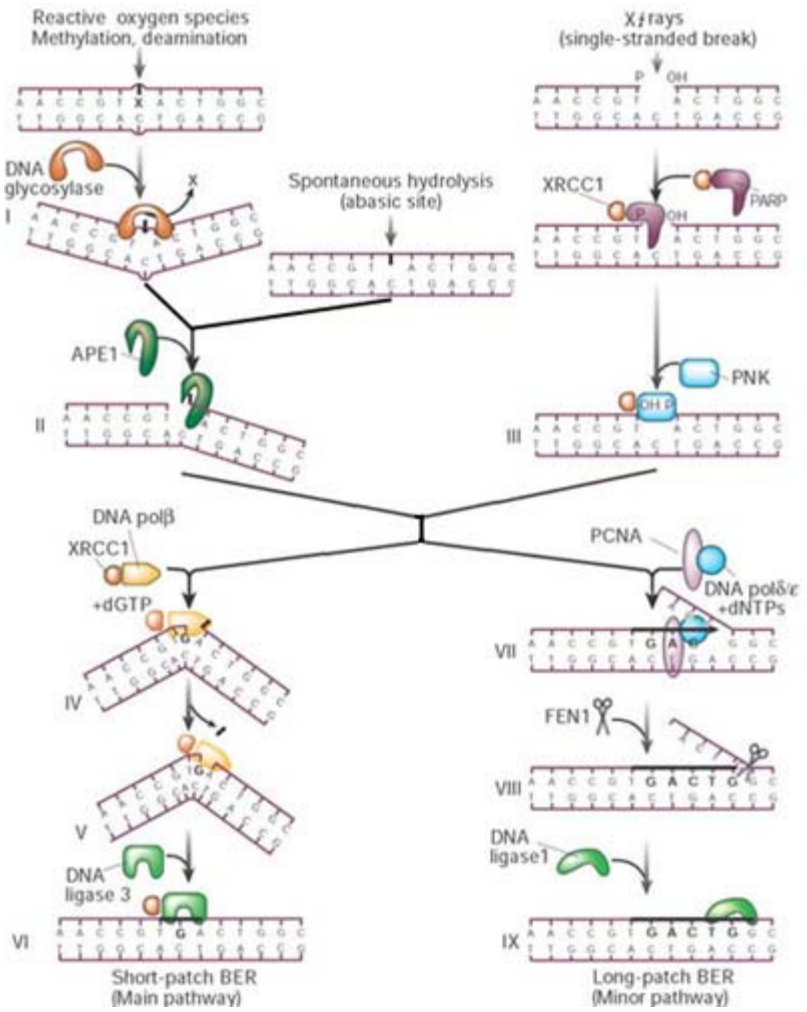

Figure 19. Schéma de la réparation de l'ADN par excision de base et resynthèse.

Réparation par excision de nucléotides et resynthèse

Ce mécanisme est impliqué dans la réparation des lésions de l'ADN produites principalement par les ultraviolets et minoritairement par les rayonnements ionisants que sont les adduits, les pontages intra-chaînes ou protéines-ADN. Plusieurs protéines, telles que PCNA, sont impliquées à la fois dans la réparation par excision de base et par excision de nucléotides, ainsi que dans la réplication de l'ADN.

Jonction des extrémités non-homologues

Les cassures double-brins provoquées par l'irradiation peuvent être de deux natures : à extrémités franches (peu probable) ou à extrémités 3' et 5' cohésives. Elles sont réparées soit par le système NHEJ (Non-Homologous End Joining), c'est-à-dire par la jonction des extrémités non-homologues, soit par le mécanisme de recombinaison homologue (RH). La RH est la voie de réparation des CDB prépondérante chez les levures tandis que la NHEJ est celle qui prédomine chez les eucaryotes supérieurs. La NHEJ conduit à la réparation des CDB franches ou cohésives « appariables » sur la totalité du bout sortant ou sur une seule paire de bases (microhomologie) (Mason *et al*., 1996; Kabotyanski *et al*., 1998). Les mécanismes permettant l'alignement des microhomologies et précédant la ligation ne sont pas encore totalement décrits.

Quatre protéines ont été découvertes par homologie génétique avec celles de sensibilisation aux rayons X chez le hamster : Ku70, Ku86, DNA-PKcs et XRCC4 codées respectivement par xrcc 5, 6, 7 et 4. Les protéines Ku forment un hétérodimère qui se lie avec une très forte affinité aux extrémités libres de l'ADN double-brin (Paillard et Strauss, 1991; Pang *et al*., 1997) permettant de protéger les extrémités de la dégradation (Liang et Jasin, 1996) et facilitant leur ligation (Ramsden et Gellert, 1998). Comme décrit sur la figure 20A, cet hétérodimère recrute la DNA-PKcs formant ainsi le complexe DNA-PK (kinase ADN-dépendante). XRCC4 permet finalement de stabiliser le complexe ADN/DNA-PK et stimule l'activité Ligase IV aboutissant à la ligation (Critchlow *et al*., 1997; Grawunder *et al*., 1998).

La NHEJ n'est pas un mécanisme de réparation des CDB infaillible puisqu'il peut aboutir à des délétions ou insertions. Il interviendrait préférentiellement en phase G1 et en début de phase S du cycle cellulaire (Takata *et al*., 1998).

Par ailleurs, les protéines de la NHEJ sont aussi impliquées dans la recombinaison V(D)J (remaniements des chaînes d'immunoglobulines indispensables à la maturation du système immunitaire).

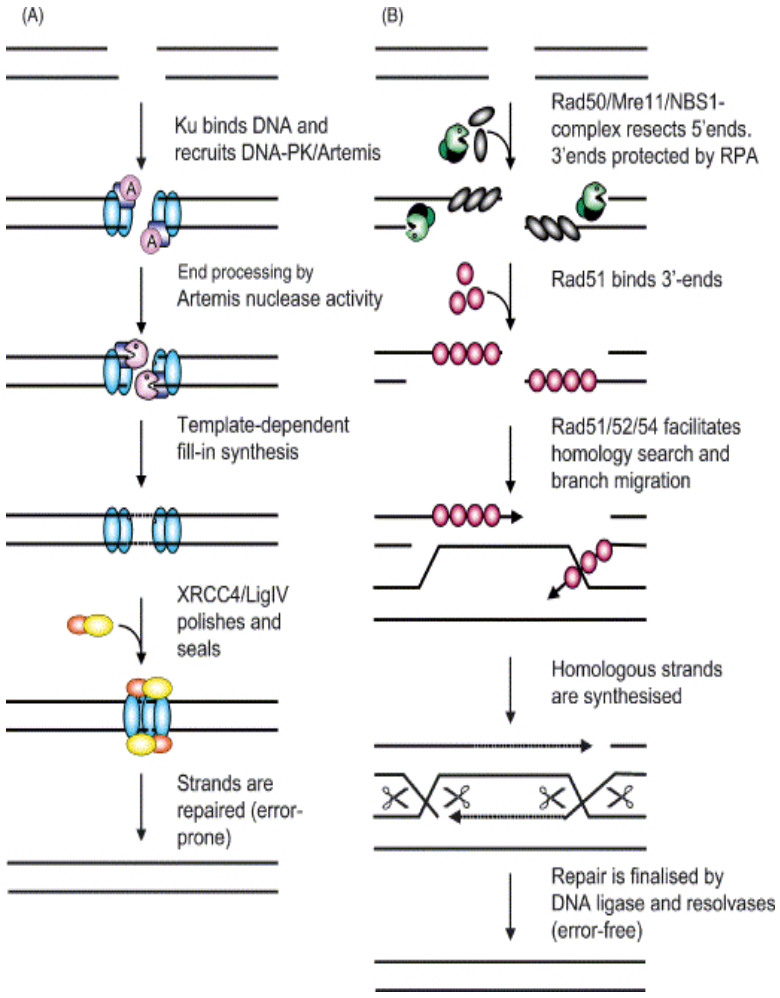

Figure 20. Mécanismes de jonction des extrémités non-homologues (A) et de recombinaison homologue (B) (Slupphaug *et al*., 2003).

Recombinaison homologue

Ce système a été très bien caractérisé chez la levure. Ses mécanismes sont décrits dans la figure 20B. Il serait également utilisé préférentiellement pour réparer les cassures générées lors de la réplication de l'ADN (Haber, 1999) et aboutit à une réparation fidèle car utilisant le brin complémentaire comme matrice.

Contrairement à la NHEJ, la RH agirait plutôt en fin de phase S et en phase G2 du cycle cellulaire (Takata *et al*., 1998).

d) la mort cellulaire radio-induite

Lorsque tous les systèmes de défenses, de réparations et d'arrêts du cycle n'ont pas permis de restaurer le contenu cellulaire, la dernière alternative possible est la mort cellulaire (pour revue, Favaudon, 2000). Celle-ci peut présenter des effets bénéfiques puisqu'elle permettra d'éliminer les cellules endommagées.

La quiescence (ou arrêt en G1) et la sénescence

Dans les fibroblastes humains normaux, l'exposition aux rayonnements conduit à un arrêt complet en G1 évoluant vers l'entrée en quiescence ou sénescence. La sénescence prématurée, ou SIPS (« stress-induced premature senescence »), diffère de la sénescence réplicative. Elle a été observée dans les fibroblastes après des stress prolongés ou répétés (Chainiaux *et al*., 2002; Debacq-Chainiaux *et al*., 2005; Duan *et al*., 2005) et aussi après exposition aux rayonnements ionisants (Gorbunova *et al*., 2002; Naka *et al*., 2004). L'arrêt en G1 est lié à l'augmentation de p53 qui entraîne la transcription de $p21^{WAF1}$ inhibant des complexes cycline/Cdk et PCNA conduisant à l'arrêt de la progression des fourches de réplication comme décrit précédemment. Dans les cellules normales et particulièrement dans les lignées fibroblastiques, cet arrêt devient irréversible contrairement à l'arrêt transitoire en G1 précédant les phénomènes d'apoptose ou permettant la réparation de l'ADN. Naka *et al.* (Naka *et al*., 2004) ont montré, grâce à des fibroblastes mutés pour ATM, que la voie conduisant à la sénescence prématurée des fibroblastes à la suite d'un stress oxydatif ou d'une exposition aux rayonnements ionisants pouvait aussi être ATM-indépendante et pourrait agir via la $p38^{MAPK}$ et $p16^{INK4A}$ (Fig. 21).

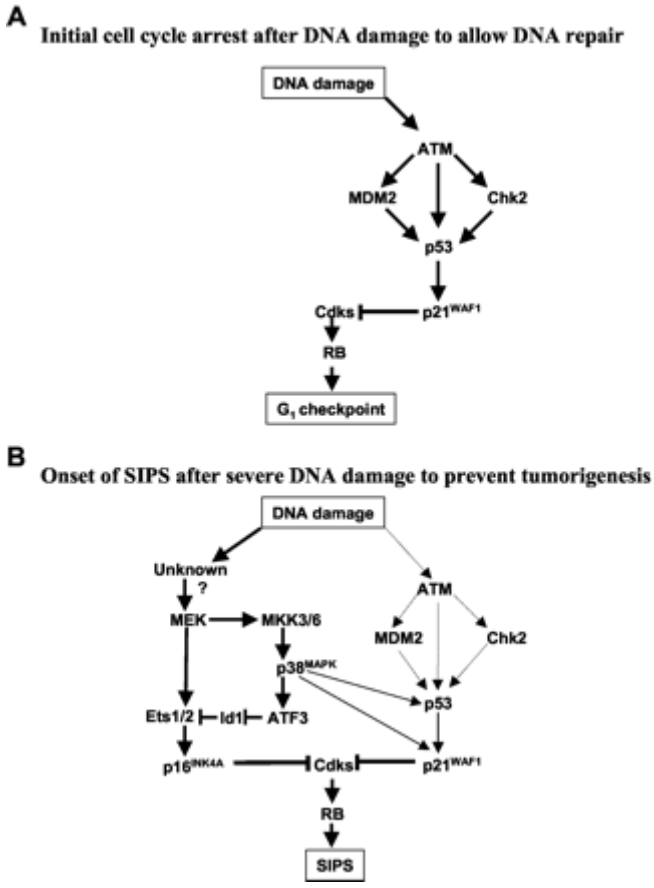

Figure 21. Schéma des voies conduisant des dommages de l'ADN à l'arrêt en G1 (A) ou à la sénescence (B) (Naka *et al*., 2004). SIPS : Stress Induced Premature Senescence.

La mort cellulaire différée et la mort mitotique

Le processus de mort cellulaire différée est dû à la mort d'une partie des cellules ayant subi des remaniements chromosomiques à la suite de l'irradiation. En effet, l'exposition aux rayonnements ionisants conduit à des lésions des chromosomes qui peuvent être transitoires ou stables. La nature de ces aberrations dépend de la phase du cycle cellulaire dans laquelle les cellules ont été irradiées et le temps laissé entre l'irradiation et l'observation.
Certaines de ces aberrations conduiront à une mort cellulaire rapide tandis que d'autres, telles que les translocations, les inversions ou les courtes délétions, survivront en donnant une descendance qui peut évoluer et conduire à la mort d'une partie des cellules.

La mort mitotique, perte de la capacité à achever une mitose, apparaît aussi du fait de l'accumulation d'aberrations chromosomiques mais se caractérise par la formation de cellules géantes, de cellules binucléées indiquant que la cytodiérèse n'a pas eu lieu, et de micronoyaux conduisant à la perte progressive de matériel génétique par exocytose. C'est le mécanisme de mort prépondérant dans les tissus épithéliaux.
Les étapes finales de ces mécanismes de mort passent par la sénescence, l'apoptose ou la nécrose.

La mort cellulaire immédiate

Ce mode de mort cytolytique est peu connu et souvent confondu avec l'apoptose. Elle survient dans les minutes ou heures suivant une exposition à de très fortes doses d'irradiation. Sa rapidité provient de l'activation des lysosomes et de la lyse des membranes et des organites cellulaires.

L'oncose

L'oncose se caractérise par un gonflement du cytoplasme et des organites, une augmentation de la perméabilité membranaire, une caryolyse ou chromatolyse et une cytolyse. Elle a lieu en 24 heures et provient d'une exposition à des inhibiteurs de la phosphorylation oxydative ou d'une ischémie. Elle est souvent confondue avec l'apoptose et certains de ses effecteurs pourraient d'ailleurs être identiques.

L'apoptose (ou mort cellulaire programmée)

C'est un processus transcriptionnellement actif et rapide. Ce processus prend une part importante dans les lignées hématopoïétiques, les cellules acineuses salivaires, les cellules des villosités des cryptes de l'intestin, les cellules endothéliales, les thymocytes et les lymphocytes et une part faible dans les lignées épithéliales avec un taux de 10% seulement après irradiation, et même jusqu'à 2% dans les fibroblastes irradiés.

De nombreux phénomènes peuvent aboutir à ce processus. Les CDB représentent l'un de ces principaux phénomènes avec l'activation de voies de transduction par les céramides produits par la sphyngomyélinase. L'entrée en apoptose peut se produire à partir de toutes les phases du cycle mais a souvent lieu après un arrêt en G1. Elle est sous le contrôle de nombreux gènes promoteurs tels que p53, Bax, Fas et répresseurs tels que MDM2, Bcl-2. Elle conduit à la condensation de la chromatine, à des bourgeonnements de la membrane plasmique puis à la formation de corps apoptotiques phagocytés par les macrophages évitant les réactions inflammatoires. Par ailleurs, l'ADN est digéré en fragments internucléosomaux, des protéines-cibles sont dégradées par les caspases et on observe une disparition de l'asymétrie de la répartition des lipides de la membrane plasmique.

IV- Stress oxydatif et syndrome cutané radio-induit

1. Stress oxydatif et effets tardifs

A de faibles concentrations, les espèces réactives de l'oxygène, ou de l'azote, sont impliquées dans la modulation de la fonction cellulaire (différentiation, prolifération) et jouent un rôle dans les réactions inflammatoires et dans la signalisation en tant que seconds messagers (Murrell *et al*., 1990; Allen, 1991). A des concentrations plus élevées, les radicaux peuvent être néfastes. Afin de s'en protéger, la cellule a mis en place des systèmes de défense. S'ils sont dépassés ou inefficaces, un déséquilibre se produit en faveur des radicaux libres, il y a alors stress oxydatif, pathologique pour les tissus et cellules (Darley-Usmar et Halliwell, 1996; Chaudiere et Ferrari-Iliou, 1999; Evans et Halliwell, 1999).

Les espèces produites peuvent en effet altérer des cibles biologiques telles que l'ADN ou les membranes cellulaires. Le stress oxydatif conduit à l'activation de gènes et protéines

impliqués dans divers processus primordiaux tels que la réparation de l'ADN, les arrêts dans le cycle cellulaire, la sécrétion de facteurs (TNFα, IL-1, PDGF), l'induction de c-fos, la ribosylation des protéines, l'activation de la phosphorylation de PKC et l'induction de la Mn-SOD. Il peut aussi affecter la dégradation de la matrice extracellulaire, la phagocytose et le chimiotactisme pour les leucocytes, la thrombomoduline en surface des cellules endothéliales et l'activation des fibroblastes (Denham et Hauer-Jensen, 2002).

Les ERO sont fortement impliquées dans la réponse à l'irradiation (Riley, 1994; Mikkelsen et Wardman, 2003). Elles sont produites par l'irradiation elle-même et par les phénomènes inflammatoires. En particulier, au cours de l'exsudation, des vagues d'ERO sont générées par les polynucléaires et les macrophages stimulés par les produits de dégradation du collagène, ce processus étant auto-entretenu (Toussaint *et al*., 2000). Enfin, une augmentation du niveau d'ERO se produit à la suite de l'hypoxie du tissu, résultant de l'atteinte de la microvascularisation, perturbant la balance entre espèces réactives de l'oxygène et espèces réactives de l'azote entraînant la déplétion du monoxyde d'azote (NO) tissulaire (Steiner *et al.*, 2002).
Des réactions liées au stress oxydatif ont également été observées dans de nombreux cas de fibrogenèse. L'inflammation chronique qui s'installe à long terme après irradiation résulte en une série de stress qui peuvent conduire à une sénescence prématurée ou à la mort des cellules par apoptose ou nécrose (Toussaint *et al*., 2002).

Même si l'origine des lésions tardives est encore matière à débat, le rôle du stress oxydatif dans l'apparition des effets tardifs de l'irradiation semble être prépondérant (pour revue Robbins et Zhao, 2004). Ceci a été démontré au niveau du rein (Massy et Nguyen-Khoa, 2002; Locatelli *et al*., 2003), au niveau du poumon (Kinnula et Crapo, 2003) et au niveau du système nerveux central (Castagne *et al*., 1999). Cependant, il n'existe pas de preuves directes de l'existence de phénomènes oxydatifs dans le tissu cutané après irradiation à fortes doses. On ne dispose donc que de preuves indirectes :

- la CuZnSOD/MnSOD sous forme liposomale conduit à la réversion de la fibrose et permet la restauration du tissu normal 6 mois après irradiation (Baillet *et al*., 1986; Delanian *et al*., 1994; Lefaix *et al*., 1996),

- l'association pentoxifylline/alpha-tocophérol conduit à la réversion des effets tardifs (Delanian *et al*., 1999; Lefaix *et al*., 1999; Delanian *et al*., 2003; Chiao et Lee, 2005; Delanian *et al*., 2005).

2. La pentoxifylline et l'α-tocophérol

La pentoxifylline

La pentoxifylline (Figure 22) est un inhibiteur de phosphodiesterase non-spécifique qui conduit à l'augmentation du niveau cellulaire d'AMPc impliqué dans la signalisation cellulaire. Elle est également impliquée dans la régulation de l'expression de TNFα et d'autres cytokines pro-inflammatoires (Rube *et al*., 2002). Elle est un anti-oxydant phytochimique qui pourrait agir par piégeage des radicaux libres (Freitas *et al*., 1995; Horvath *et al*., 2002).

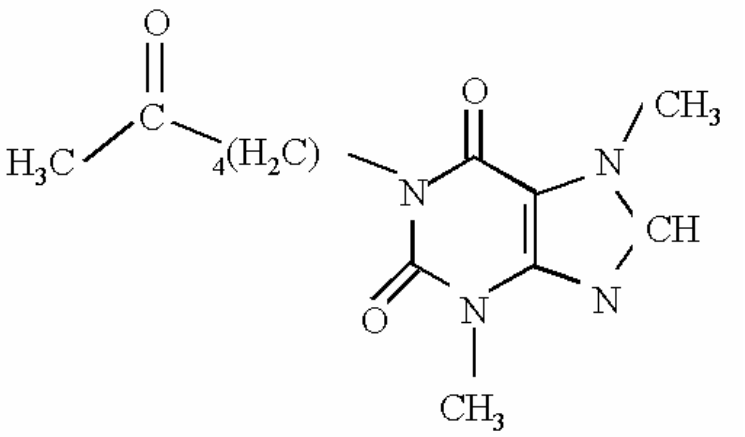

Figure 22. Structure de la pentoxifylline.

La PTX affecte la réponse cellulaire après exposition aux rayonnements ionisants comme montré dans des études effectuées *in vitro*. En effet, elle inhibe l'arrêt radio-induit en phase G2 du cycle cellulaire (Russell *et al*., 1996; Strunz *et al*., 2002; Eley *et al*., 2002) ce qui conduit à la radiosensibilisation des cellules tumorales p53-déficientes (Russell *et al*., 1996; Theron *et al*., 2000; Strunz *et al*., 2002). D'autre part, certaines études ont montré que la PTX inhibait la réparation des CDB de l'ADN (Theron *et al*., 2000; Binder *et al*., 2002), la voie ATM (Sarkaria et Eshleman, 2001) et induisait des aberrations chromosomiques, des échanges de chromatides sœurs ainsi que la formation de micronoyaux (Bozsakyova *et al*., 2001).

L'α-tocophérol

L'α-tocophérol (αT) (Figure 23) est un nutriment anti-oxydant appartenant à la famille des tocophérols ou vitamines E. Cette famille forme le plus important des groupes antioxydants liposolubles. En dehors de ses capacités anti-oxydantes, l'αT a montré *in vitro* des propriétés d'inhibition de l'inflammation, de l'adhésion cellulaire, de l'agrégation plaquettaire et de la prolifération des des cellules musculaires lisses (pour revue, Rimbach *et al*., 2002).

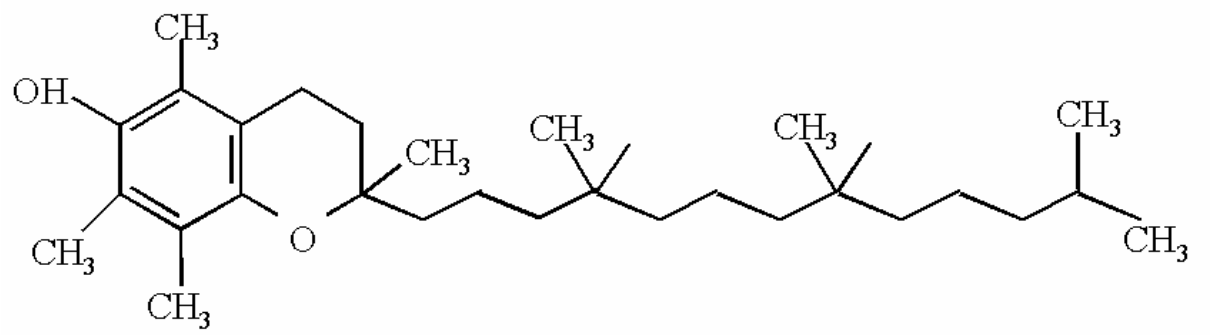

Figure 23. Structure de l'*α*-tocophérol.

Les derivés de l'αT présentent des effets protecteurs contre les dommages de l'ADN dans les cellules lymphoblastoïdes irradiées (Sweetman *et al*., 1997). Le D-alpha-tocopheryl succinate réduit également les dommages chromosomiques radio-induits dans les cellules normales mais pas dans les cellules tumorales (Kumar *et al*., 2002).

In vitro, les mécanismes d'action du traitement associant la pentoxifylline et l'α-tocophérol restes méconnus.

OBJECTIFS

Le rôle du stress oxydatif semble prépondérant dans l'apparition des effets tardifs dans le tissu cutané après irradiation. L'état des connaissances des phénomènes à l'origine des effets cellulaires produits lors du syndrome cutané radio-induit ne permet pas de répondre à plusieurs questions :

- Le stress oxydatif initial radio-induit conduit-il à l'accumulation de lésions de l'ADN radio-induites dans les cellules à renouvellement lent (fibroblastes, cellules endothéliales) ?

- Existe-il des phénomènes oxydatifs tardifs et sont-ils impliqués dans l'apparition d'effets tardifs ?

- Observe-t-on un phénomène de sénescence prématurée qui conduirait à une accumulation des lésions avant la mort cellulaire ?

- Quel est le rôle de l'association pentoxifylline et α-tocophérol ? Quels sont ses mécanismes d'action sur les voies étudiées ?

Nos premiers travaux ont mesuré le taux d'aberrations chromosomiques dans les fibroblastes du derme provenant d'une victime exposée aux rayonnements ionisants. Ils ont mis en évidence une accumulation des lésions de l'ADN pouvant s'expliquer par un phénomène de sénescence prématurée et pouvant servir d'indicateur de dose lors d'une exposition localisée (**article 1**, cas de l'accident en Géorgie). Afin d'élucider le rôle du stress oxydatif dans le développement du syndrome cutané radio-induit, nous avons conduit une étude chez le rat exposé localement aux rayons X visant à corréler les signes cliniques aux variations de plusieurs paramètres du stress oxydatif (**article 2**). Afin de mieux appréhender les mécanismes mettant en jeu le stress oxydatif dans l'apparition des lésions cutanées, nous avons ensuite conduit des études reposant sur l'utilisation de modèles *in vitro*.

Ces travaux ont permis d'étudier une éventuelle modulation de la production d'ERO et de lésions de l'ADN dans des cultures primaires de fibroblastes et de cellules endothéliales du derme en fonction du temps et de la dose d'irradiation et par l'utilisation d'anti-oxydants. L'association pentoxifylline et α-tocophérol, dont on sait l'efficacité *in vivo*, a été administrée à différents temps avant et après l'irradiation afin d'évaluer l'efficacité de ce traitement sur les dommages oxydatifs (**article 3** et **article 4**). La contribution de chacune des drogues dans les effets observés a été déterminée et est présentée dans l'**article 5**. Les résultats obtenus, confortés par les données de la littérature indiquant l'implication des deux drogues dans les mécanismes de réparation de l'ADN, nous ont conduit à mesurer le taux de formation des cassures double-brins et le taux d'expression de protéines impliquées dans les voies de la réparation ou de la sénescence prématurée (**article 6**).

RESULTATS

I- Etudes préliminaires in vivo

Article 1 : Application de la technique PCC-FISH aux fibroblastes de peau pour évaluer la dose reçue localement : cas de l'accident radiologique de Géorgie de 2001

L'objectif de ce travail était d'établir une méthode de dosimétrie biologique applicable au tissu cutané en cas d'irradiation accidentelle localisée.

Pour cela, le taux de formation des aberrations chromosomiques stables a été mesuré par la technique de PCC-FISH dans les fibroblastes cutanés isolés à partir de biopsies de peau. Une courbe de calibration établie à partir de biopsies de peau irradiées *ex vivo* et reliant le nombre d'aberrations chromosomiques à la dose d'irradiation a été établie. Cette courbe a été utilisée dans le cas de l'accident radiologique de Géorgie de 2001, mettant en jeu l'irradiation de plusieurs personnes par une source de ^{90}Sr, pour déterminer la dose reçue par l'une des vitimes au niveau du dos.
La victime a subi une éxérèse du tissu lésé (épithélite exsudative) 12 semaines après irradiation, suivie de greffes de derme et d'épiderme successives. Le tissu excisé a été recueilli, divisé en secteurs et a servi de support à la dosimétrie biologique selon la technique citée ci-dessus. Le taux de formation des aberrations chromosomiques a été mesuré dans chacune des métaphases des fibroblastes isolés et mis en culture à partir des différents secteurs.
A partir de la courbe de calibration établie *ex vivo*, il a été possible de convertir le taux d'aberrations en dose d'irradiation reçue. Une cartographie du territoire irradié a ainsi été établie.

Cette étude a mis en évidence la présence, au sein du tissu irradié, de fibroblastes fortement endommagés qui ne se divisent plus. Ce phénomène pourrait s'expliquer par l'apparition d'un phénotype sénescent. D'autre part, il faudrait prendre en compte les phénomènes infectieux locaux liés à la plaie. Par ailleurs, il s'est avéré que les kératinocytes, compte tenu de leur renouvellement rapide et de leur réponse à l'irradiation, ne constituaient pas un bon modèle de support à la dosimétrie biologique. Toutefois, une meilleure connaissance des phénomènes de

remodelage et de réparation tissulaire mettant en jeu les fibroblastes est nécessaire afin d'évaluer la validité de notre approche quant aux paramètres du temps post-irradiation. En effet, de tels phénomènes pourraient conduire à la perte des fibroblastes les plus endommagés, porteurs de l'information dosimétrique, et à la colonisation du tissu lésé par des cellules périphériques moins fortement irradiées.

Cette étude, outre la mise au point d'une méthode de dosimétrie biologique, ouvre la question de l'implication des phénomènes oxydatifs dans le tissu cutané irradié.

RADIATION RESEARCH 162, 365–376 (2004)
0033-7587/04 $15.00

PCC-FISH in Skin Fibroblasts for Local Dose Assessment: Biodosimetric Analysis of a Victim of the Georgian Radiological Accident

J-P. Pouget,[a,1] C. Laurent,[a] M. Delbos,[a] M. Benderitter,[a] I. Clairand,[a] F. Trompier,[a] J. Stéphanazzi,[b] H. Carsin,[b] F. Lambert,[b] P. Voisin[a] and P. Gourmelon[a]

[a] *Institut de Radioprotection et de Sûreté Nucléaire, Direction de la Radioprotection de l'Homme, 92262 Fontenay-aux-Roses, France; and* [b] *Centre de Traitement des Brûlés, Hôpital Percy, 92140 Clamart, France*

Pouget, J-P., Laurent, C., Delbos, M., Benderitter, M., Clairand, I., Trompier, F., Stéphanazzi, J., Carsin, H., Lambert, F., Voisin, P. and Gourmelon, P. PCC-FISH in Skin Fibroblasts for Local Dose Assessment: Biodosimetric Analysis of a Victim of the Georgian Radiological Accident. *Radiat. Res.* 162, 365–376 (2004).

We propose a new method of biodosimetry that could be applied in cases of localized irradiation. The approach is based on excess chromosome segments determination by the PCC-FISH technique in fibroblasts isolated from skin biopsy. Typically, 0 to 10 Gy *ex vivo* γ-irradiated human skin biopsies were dissociated and fibroblasts were isolated and grown for several days. Cells next underwent PCC-FISH painting of whole chromosome 4, and the number of excess chromosome segments per metaphase was determined. An *ex vivo* reference curve correlating the number of excess chromosome segments per metaphase to the radiation dose was established and used to assess the dose delivered to the skin of one of the victims of the radiological accident that occurred at Lia in Georgia in December 2001. Specifically, the victim suffering from moist desquamation underwent skin excision in Hospital Percy (France). Measurement of excess chromosome segments per metaphase was done in fibroblasts isolated and grown from removed wounded skin and subsequent conversion to radiation doses was performed. The radiation dose map obtained was shown to be in accordance with clinical data and physical dosimetry as well as with conventional biodosimetry. These results demonstrated that PCC-FISH painting applied to skin fibroblasts may be a suitable technique for dose estimation. To assess its worth, this approach needs to be extended to future accidents involving localized radiation exposure.

INTRODUCTION

Over the last 50 years, most accidental overexposure to radiation has occurred in the industrial setting, and 54% of these accidents resulted in localized irradiations of the body (*1*). Dose determination, which is the most important factor in helping medical staff to choose the best therapeutic approach, can be estimated using either biological or physical approaches.

Biological dosimetry is based on changes occurring in biological structures or parameters. In particular, conventional biological dosimetry relies on the determination of the frequency of chromosomal aberrations such as dicentrics in circulating lymphocytes (*2*). This approach is satisfactory and reliable when the dose is distributed uniformly over the whole body, but in the case of localized irradiations, only a small fraction of the circulating lymphocytes are irradiated. Dose assessment is still possible using Dolphin or Qdr methods (*3, 4*). Nevertheless, the calculated dose estimation remains reliable only when at least 20% of the whole body volume is exposed. Other alternative approaches exist and may be based on physical dosimetry (*5*), determination of skin blood flow (*6–8*), infrared thermography (*9*), X-ray tomography (*10*), or nuclear magnetic resonance (*11*). However, the latter methods cannot be considered as biological indicators of dose, and no real biological dosimeter is currently available in the case of acute localized irradiation.

Skin is the first targeted organ in all localized overexposure situations and the injured people suffer from more or less severe burns. In most cases, surgery has to be performed to remove wounded tissue, and a skin sample could thus be available for dose reconstruction. Since determination of chromosome changes in lymphocytes is well established as a biological indicator of dose in the case of whole-body irradiation, we proposed to apply a cytogenetic technique to skin fibroblasts. Specifically, among the available latter techniques, the premature chromosome condensation assay associated with fluorescence *in situ* hybridization (PCC-FISH) (*12–14*) was adapted for use with skin tissue. In contrast to unstimulated blood lymphocytes, which are normally a postmitotic tissue, skin is a renewing tissue, and most of the unstable aberrations would be lost between radiation exposure and dosimetric estimation. Therefore, FISH painting, which allows the measurement

[1] Address for correspondence: Immunociblage des tumeurs et Ingénierie des Anticorps, EMI 0227 INSERM, Centre de Recherche en Cancérologie, CRLC Val d'Aurelle-Paul Lamarque, F-34298 Montpellier Cedex 5, France; e-mail: jppouget@valdorel.fnclcc.fr.

of stable chromosomal aberrations such as translocations, appeared to be the most appropriate technique to detect chromosomal rearrangements in skin fibroblasts. The technique could be combined with the use of calyculin A, a chemical compound that increases the number of analyzable metaphase spreads by prematurely condensing the chromosomes of cells in G_1 and G_2 phases. This is of interest in situations in which few mitotic cells are available for analysis, which is the case for fibroblasts isolated from dermis. One possible approach to assess the radiation dose received by the skin would be to study the correlation between radiation-induced translocations in skin fibroblasts and the delivered dose. However, in practice, this is difficult because doses received in accidental situations are often very high so that chromosomal exchanges are too numerous and their analysis by PCC-FISH is complex and uncertain. The second point is that calyculin A-induced metaphase spreads make the analysis of chromosomal exchanges more tedious because of very marked chromosome condensation. Therefore, we proposed a more rapid and sensitive method based on PCC-FISH painting. The approach consisted of painting a single pair of chromosomes, specifically chromosome 4, and of measuring the number of excess chromosome segments per metaphase. Excess chromosome segments are determined to exist when more than two segments are present within the metaphase spread. The term "metaphase" is used to denote cells in mitosis proper, as well G_1 and G_2 pseudomitoses induced by PCC. They include stable chromosomal aberrations like translocations and insertions but also unstable ones like fragments. Determination of segments makes microscopic analysis easier than studies of chromosomal exchanges. In addition, the formation of excess chromosome segments per metaphase in fibroblasts isolated from *ex vivo* γ-irradiated skin biopsies was shown to increase as a function of dose. Therefore, this parameter could be used as an indicator of radiation exposure. An *ex vivo* standard reference curve was established and available for further dose determination. We next applied this new approach to measure the dose delivered to the skin of one of the victims of the radiological accident that occurred in Georgia in December 2001.[2] Several Georgians were exposed to radiation emitted by a ^{90}Sr source used in radioisotope thermoelectric generators. The activity of the ^{90}Sr in equilibrium with its daughter ^{90}Y was 2.6×10^{15} Bq (70,000 Ci). The electrons emitted by ^{90}Sr and ^{90}Y produce X rays by bremsstrahlung with energies ranging from 0 to 2.28 MeV. The dose rate was estimated by Monte Carlo calculations to be about 230 Gy h^{-1} in contact with the source.[3] The patient involved in the present study suffered from a whole-body irradiation associated with a major cutaneous radiation syndrome with a huge moist epidermitis without necrosis. The observations of a marked initial syndrome on the first day and severe bone marrow failure with spontaneous recovery after 3 weeks were indicative of a mean body dose around 3 Gy with a heterogeneous distribution. The cutaneous radiation syndrome was treated by several wounded skin excisions followed by skin grafts. At the first surgery, removed wounded skin was used for excess chromosome segments per metaphase measurement by applying the PCC-FISH assay to isolated cultured fibroblasts. Subsequent conversion into radiation doses was performed using the *ex vivo* reference curve; this permitted a mapping of the radiation exposure.

[2] P. Gourmelon, IAEA Mission to Tbilissi, Georgia. Final mission report. Institute for Protection and Nuclear Safety, Fontenay aux Roses, France, 2000.

[3] I. Clairand, J. F. Bottollier-Depois, E. Gaillard-Lecanu and P. Gourmelon, Radiological accident at Lia, Georgia, in December 2001; Dose reconstruction by calculation. SDOS/02-009, Institute for Radiological Protection and Nuclear Safety (IRSN), Fontenay-aux Roses, France, 2002.

MATERIALS AND METHODS

Chemicals

Fetal calf serum (FCS), phosphate-buffered saline (PBS), trypsin, penicillin, streptomycin, DMEM and Colcemid were obtained from Life Technologies (Paisley, UK). Collagenase P, calyculin A and RNase A were obtained from Roche Diagnostics (Mannheim, Germany). Collagen Type I culture flasks were obtained from VWR International (Fontenay-sous-Bois, France). The painting probe for chromosome 4, DAPI-antifade solution, and phosphate-buffered detergent (PBD) were from Oncor International. Pepsin and $DiOC_6(3)$ were obtained from Sigma Co (St. Louis, MO). Mouse polyclonal anti-human Ki67 was purchased from Dako (Glostrup, Denmark).

Ex Vivo Skin Biopsies and Irradiation Procedure

Four normal skin biopsies were obtained from abdominal esthetic surgeries performed on four Caucasian women who were 35, 53, 45 and 62 years old. Written consent was obtained from each of the women. Skin explants were chopped into six 2-cm^2 pieces and were immersed in a 5% Betadine bath to avoid contamination before being rinsed twice in PBS. The skin fragments were placed in petri dishes containing 10 ml PBS + 10% penicillin/streptomycin and were γ-irradiated using a ^{137}C source at doses of 1, 3, 5, 8 and 10 Gy at a dose rate of 60 Gy h^{-1}. The ^{137}Cs irradiator produced a continuous Compton diffusion spectrum ranging from 0 to 661 keV due to interaction between emitted photons and irradiator walls. The spectrum mean energy, measured with a NaI spectrometer, was estimated to be 440 keV. Irradiation was performed at room temperature. Skin biopsies were then kept in DMEM for 2 h at 37°C in a 95% air/5% CO_2 atmosphere before they were disaggregated.

Skin Excision from Irradiated Victim

One of the most exposed victims of the accident that occurred at Lia was treated for a moist desquamation. The cutaneous lesion involved the whole posterior side of the thorax from the waist up to the point of the scapulae. The lesion was a wide moist epidermal denudation of about 8% of the body surface without signs of deep necrosis.[2] The lesion was surrounded by a 5-cm pinkish inflammatory halo and by a second desquamation halo of about 10 cm due to peripheral desquamation. On the 88th day postirradiation, wounded skin was excised and disaggregated to isolate fibroblasts that were grown as described below.

Isolation and Culture of Primary Fibroblasts

Primary fibroblast cultures were obtained from *ex vivo* γ-irradiated skin biopsies or from the wounded skin as described as follows. The dermis was dissociated from the epidermis by mincing with sterile scalpel blades

and tweezers. The dermis was then enzymatically dissociated in a 20-ml solution of 0.25% collagenase/0.5% trypsin/EDTA for 30 min at 37°C with stirring. Fresh collagenase-trypsin cocktail was added to the remaining pieces of dermis and the operation was repeated twice. Cells were then counted and plated in DMEM containing 10% FCS at a density of about 20×10^3 cells/cm^2. Culture medium was replaced every 4 days. Cells underwent the PCC-FISH assay when flasks reached 50% confluence (passage P0), corresponding to around $50–100 \times 10^3$ cells/25-cm^2 flask.

Ki67 Immunostaining of Isolated Cells

To determine the proportion of proliferating cells, i.e. of cells moving through G_1, S and G_2/M phase of the cell cycle, the proliferation marker pKi-67 (Ki-67 antigen) was used. The protein pKi-67 is commonly used in clinical and research pathology, since it is expressed only during cell cycle progression. Cell suspensions containing around 30×10^4 fibroblasts were dropped onto polylysine slides and dried at room temperature for 1 h. The cells were fixed for 20 min in acetone at 4°C and permeabilized with 0.1% Triton X-100 for 2 min. Slides were gently rinsed with PBS. Mouse polyclonal anti-Ki67 antibody (100 μl, 1/100 dilution) was added and incubated at 37°C for 1 h before being rinsed with PBS. Secondary rhodamine-labeled goat anti-mouse antibody IgG (100 μl, 1/200 dilution) was then added and incubated at room temperature in the dark for 1 h. Slides were next rinsed with PBS and wash solution (Dako, Denmark). DAPI-antifade solution was added and the slides were placed at 4°C in the dark until microscope analysis. The proliferation index was estimated as the ratio between the number of Ki67-positive cells and the total number of cells counted from observation of at least 500 cells.

For each experiment, positive and negative control experiments for Ki67 staining were performed using either proliferating or feeder cells.

Ki67 Immunohistochemistry on Skin Tissue from Georgian Accident Victim

Skin fragments were dropped into cold isopentane and stored at −80°C. Frozen sections (6 μm) were cut, fixed twice in cold acetone for 10 min, air-dried for 15 min at room temperature, and then permeabilized with 0.1% Triton X-100 for 20 min at room temperature. The following steps were performed on a Ventana automated immunohistochemistry system (Ventana Medical System). Mouse polyclonal anti-human Ki67 antibody was added at concentration of 2.5 μg/100 μl (dilution 1/75) and incubated for 30 min. Slides were next incubated in 0.05% glutaraldehyde for 4 min at 37°C. Slides were then incubated in secondary antimouse antibody coupled to biotin and biotin was detected as described by the manufacturer (Ventana).

Determination of Viability and Apoptosis-Associated Alterations

Cell viability was estimated using trypan blue at a final concentration of 0.2%. The cationic dye $DiOC_6$ (3,3′dihexyloxacarbocyanine iodide) identifies the reduction in mitochondrial transmembrane potential that occurs in the early stages of apoptosis. $DiOC_6(3)$ was stored in DMSO at a concentration of 1 m*M*, further diluted in ethanol, and added (final concentration 80 n*M*) to 1×10^6 cells. Cells were incubated at 37°C in the dark for 15 min and propidium iodide was added at a final concentration of 50 μg/ml. Cells were next analyzed with a FacsSort cytometer (Becton Dickinson, single excitation 488 nm). $DiOC_6(3)$ was monitored in FL1 (emission 530 nm) relative to PI in FL2 (emission 575 nm). Cells with compromised cell membrane permeability allow PI to bind to the cellular DNA and thus discriminate between apoptotic and necrotic cells. Three different cell subpopulations can thus be distinguished: viable cells ($DiOC_6$ high/PI−), necrotic cells ($DiOC_6$ low/PI+), and apoptotic cells ($DiOC_6$low/PI−).

Premature Chromosome Condensation and Fluorescence In Situ Hybridization

Flasks containing fibroblasts that were 50% confluent (passage P0) were incubated in the presence of 0.1 μg/ml Colcemid for 3 h at 37°C in a 95% air/5% CO_2 atmosphere. After 2 h, 80 n*M* calyculin A was added for the remaining hour. Cells were then trypsinized, washed and resuspended in 10 ml of hypotonic KCl solution (0.075 *M*) and maintained at 37°C for 10 min. The cells were centrifuged for 5 min at 240*g* and the pellet was resuspended in a fixative solution of methanol/acetic acid (3:1) with vortexing. Cells were centrifuged again and the fixation was repeated. At this step, cells could be kept at 4°C for several weeks. The cell suspension was dropped onto clean slides and dried overnight at 37°C. Slides were then dried in 100% ethanol, incubated with 250 μl RNase A (100 mg/ml) in 2× SSC (0.3 *M* NaCl, 0.03 *M* Na citrate) for 1 h at 37°C, washed for 5 min in PBS, and incubated with pepsin (0.005%) in 10 m*M* HCl for 10 min at 37°C. After washing in PBS for 5 min, slides were incubated for 10 min at room temperature in a postfixative solution (50 m*M* $MgCl_2$, 0.27% formaldehyde). They were rinsed in PBS for 5 min and dehydrated in successive 3-min 75%, 85% and 100% ethanol solution baths. Slides were dried at room temperature before 10 μl of PBD mixed with 3 μl of whole-chromosome probe for human chromosome 4 was added. Cover slips were added and hybridization was performed using a HYBrite® (Vysis, IL). DNA was denatured at 72°C for 2 min, and hybridizing occurred overnight at 37°C in a dark and humidified atmosphere. Slides were then rinsed in a 0.5× SSC solution at 72°C for 5 min and rinsed in a PBD solution maintained at room temperature for 1.5 min. Counterstaining was performed by overlaying 30 μl of a DAPI-antifade solution. The average number of excess chromosome segments per metaphase, which could be translocations, chromosome fragments or insertions, was determined using a fluorescence microscope (Nikon, Microphot-FXA) equipped with an HBO lamp and filters for observation of DAPI and Texas Red staining. An excess number of segments occurred when more than two segments/metaphase were present. In all experiments, the number of metaphase spreads analyzed corresponded to the maximal number of available metaphase spreads that it was possible to collect by the PCC-FISH assay. Data dispersion was estimated by calculation of *U*-test values.

Mitotic Index

Metaphase spreads were obtained in the presence or absence of calyculin A, according to the procedure used for PCC-FISH experiments, and Giemsa staining was performed. The mitotic index was calculated for 1000 counted fibroblasts, either immediately after skin disaggregating (day 0) or at passage P0.

RESULTS

Culture Growth of Fibroblasts Isolated from Ex Vivo Irradiated Skin Biopsies

The primary cell culture conditions allowed the growth of fibroblasts isolated from nonirradiated skin biopsies and from biopsies exposed to doses up to 10 Gy. For higher radiation doses, cell growth was not observed. When cells were isolated and grown from nonirradiated skin biopsies, $50–100 \times 10^4$ fibroblasts per 25-cm^2 flask (passage P0) were obtained on the 6th day after seeding. The same number of fibroblasts grown from biopsies irradiated with 10 Gy was obtained after 15 days.

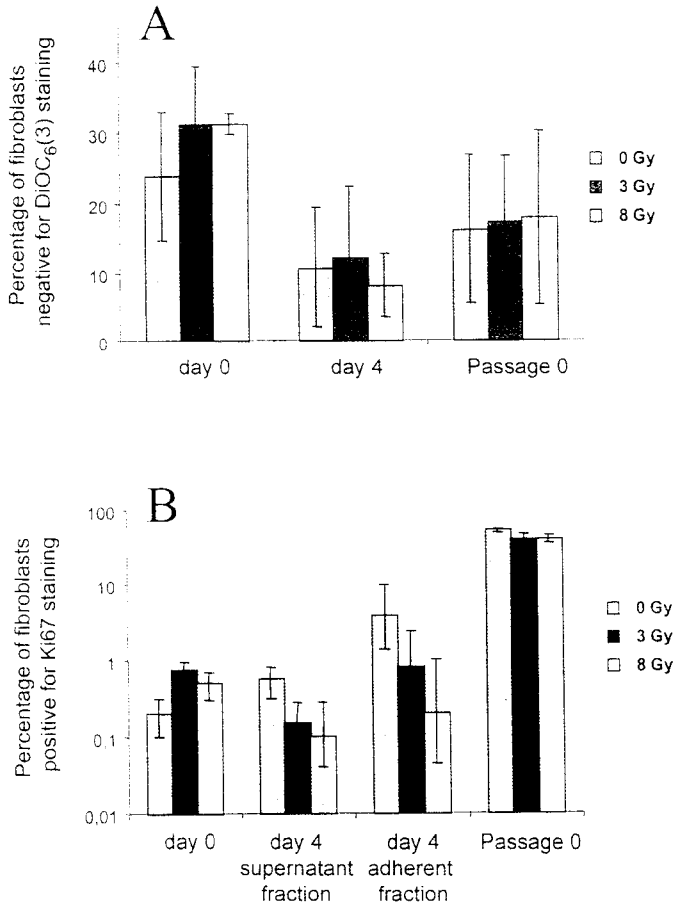

FIG. 1. $DiOC_6(3)$ (panel A) and Ki 67 (panel B) staining of fibroblasts isolated from unirradiated skin biopsies or biopsies irradiated with 3 or 8 Gy. The values represent the means ± SD calculated from 1500 cells isolated from four different donors. Staining was done immediately after skin disaggregation (day 0), at day 4 on both the supernatant and the adherent fraction of culture, and at passage P0.

Cell Viability and Apoptosis of Fibroblasts Isolated from Ex Vivo Irradiated Skin Biopsies

Cell viability and apoptosis were investigated at different times after disaggregation of control and irradiated skin biopsies: immediately after skin disaggregation (day 0), on day 4 (both for the supernatant and for the adherent fraction of the culture) when the cell culture medium was first changed, and when flasks reached 50% confluence (passage P0). Viability assessed by trypan blue dye exclusion was around 80–85% (data not shown). No dose effect and no time-dependent effect were observed over the period studied. Early apoptosis was assessed by $DiOC_6$ staining and subsequent flow cytometry analysis. The cationic dye $DiOC_6(3)$ identifies the reduction in mitochondrial transmembrane potential that occurs in the early stages of apoptosis. Figure 1A indicates that the proportion of cells isolated from either control or irradiated biopsies that were negative for $DioC_6(3)$ staining immediately after skin disaggregation was between 23.9 ± 9.2% and 31.3 ± 1.5%. These percentages decreased slightly on day 4, before increasing to values between 16.2 ± 10.7% and 17.8 ± 12.4% at passage P0. Again, no dose effect and no time-dependent effect were observed over the period studied.

TABLE 1
Mitotic Index (%) Calculated by Giemsa Staining of 1000 Fibroblasts Isolated from Control and Irradiated Skin Biopsies either Immediately after Skin Disaggregation (day 0) or at the First Trypsinization (passage P0) in the Presence or Absence of Calyculin A

	Day 0		passage 0	
Dose (Gy)	Without calyculin A	With calyculin A	Without calyculin A	With calyculin A
0	0.0	0.0	0.7	6.2
3	0.0	0.0	0.7	4.2
8	0.0	0.0	0.0	3.5

Proliferation and Mitotic Indices of Fibroblasts Isolated from Ex Vivo-Irradiated Skin Biopsies

To determine the numbers of cycling and noncycling fibroblasts, antibody against the Ki67 protein was used (Fig. 1B). Ki67 immunostaining was performed at the same time after disaggregation as the assessment cell viability and apoptosis and showed that the proliferation index increased in the early days after cells were seeded. The proportions of fibroblasts isolated from either control or irradiated biopsies, which were positive for Ki67, ranged from 0.20 ± 0.1% to 0.75 ± 0.2% immediately after disaggregation and increased with cell culture time up to values between 39.3 ± 4.8% and 51.7 ± 3.4% at passage P0. Only a small fraction of the cells were mitotic. No metaphase spreads were observed on day 0 among fibroblasts even in the presence of calyculin A (Table 1). It must be noted that under our experimental conditions, the term mitotic index includes mitosis proper, as well as G_1- and G_2-phase pseudomitoses induced by PCC. At the first trypsinization (passage P0) and in the absence of calyculin A, the mitotic index was around 0.7% for cells isolated from skin biopsies irradiated with 3 Gy or from unirradiated biopsies, metaphase was observed among cells isolated from skin biopsies irradiated with 8 Gy. When calyculin A was used, metaphases spreads were observed for all three radiation doses, and the mitotic index increased up to values between 3.5% and 6.2% (Table 1). Analysis of slides stained with Giemsa prior to measurements of the mitotic index confirmed that most of the metaphase spreads possessed a single chromatid. This indicates that the majority of the damage scored is from cells in G_1 at the time of PCC and that the calyculin A is efficient in increasing the mitotic index by recruiting nondividing cells. Figure 2A and B shows the two kinds of FISH images we observed in our experiments, corresponding to mitotic or G_1-phase recruited cells.

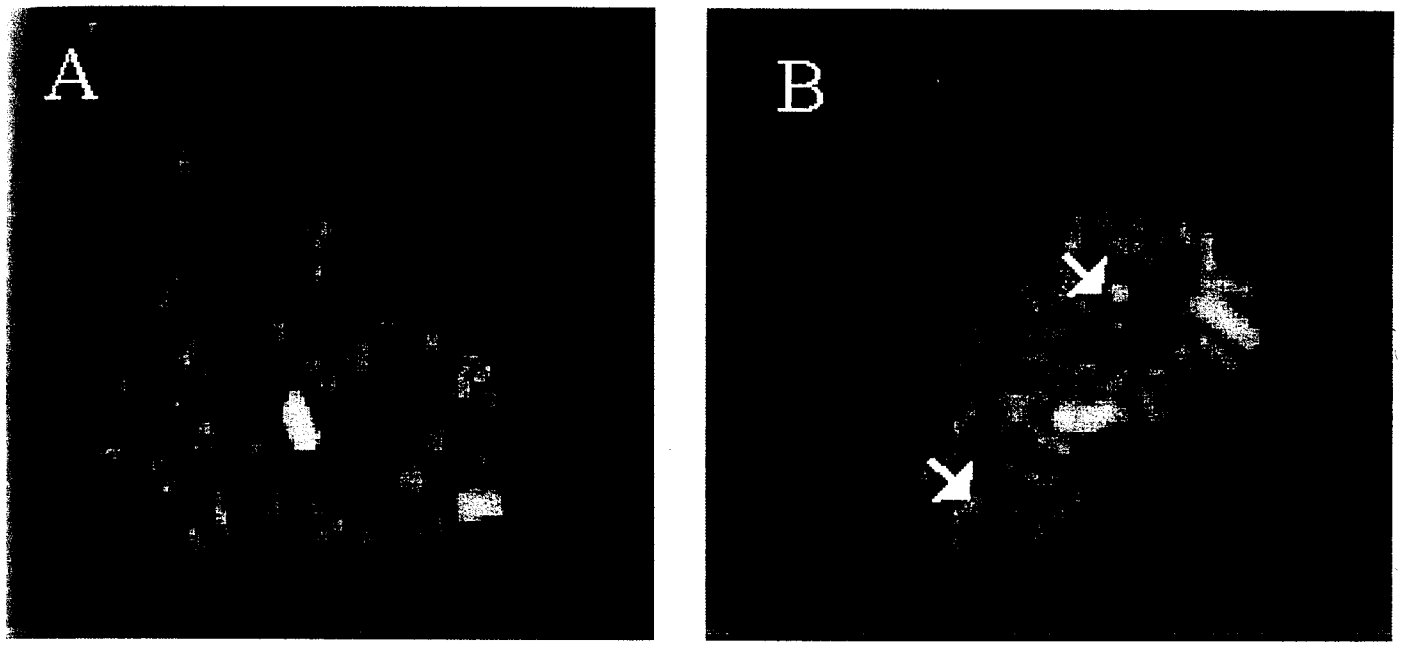

FIG. 2. Panel A: Whole chromosome 4 painting in M-phase fibroblasts. No excess chromosome segments are observed. Panel B: Whole chromosome 4 painting in G_1-phase fibroblasts. Arrows indicate two excess chromosome segments.

Measurement of Excess Chromosome Segments in Fibroblasts Isolated from Skin Biopsies Irradiated Ex Vivo

PCC-FISH was applied to fibroblasts isolated and grown from control and *ex vivo* γ-irradiated skin biopsies obtained from four donors. It allowed measurement of the number of excess chromosome segments per metaphase involving chromosome 4 of fibroblasts at passage P0. For each radiation dose, the interdonor variability was weak, so it was possible to pool the data obtained from the four donors. As shown in Table 2, the ratio between the standard deviation and the mean number of excess chromosome segments per metaphase calculated from the four donors did not exceed 25% except for a dose of 1 Gy (Table 2). The number of metaphase spreads analyzed depended on cell growth rate and was inversely correlated with the radiation dose (Table 3). A total of 794 fibroblast metaphase spreads were analyzed among fibroblasts isolated from nonirradiated skin biopsies, whereas this value decreased to 350 in the case of fibroblasts isolated from skin biopsies irradiated with 10 Gy. The number of excess chromosome segments per metaphase ranged from zero for control to a maximal yield of three for cells isolated from biopsies irradiated with 5, 8 or 10 Gy. As indicated by *U*-test values, for most of the radiation doses, the distribution of excess chromosome segments per metaphase did not differ significantly from a Poisson distribution (Table 3). The formation of additional segments increased as a function of dose, and data analysis by the iteratively reweighed least-squares method (*15*) showed that it could be fitted by a linear-quadratic relationship, $y = 0.0024x^2 + 0.0136x + 0.000119$ (Fig. 3).

TABLE 2
Excess Chromosome Segments per Metaphase Measured in Fibroblasts Isolated and Grown from Unirradiated Skin Biopsies or Biopsies Irradiated with 0–10 Gy γ Rays

Dose (Gy)	Mean	SD	SD/Mean
0	0.000	0.000	
1	0.020	0.013	0.65
3	0.055	0.015	0.27
5	0.145	0.029	0.21
8	0.216	0.029	0.13
10	0.411	0.030	0.07

Notes. Biopsies were obtained from four donors. To assess interdonor variability, for each radiation dose, the mean number of excess chromosome segments per metaphase together with standard deviations and the ratio SD/mean were calculated by pooling the data obtained from the four donors.

Measurement of Excess Chromosome Segments in Fibroblasts Isolated from Excised Skin of the Irradiated Georgian and Subsequent Dose Determination

The removed wounded tissue had a rectangular shape of about 40 × 20 cm and was used for dose assessment (Fig. 4A and B). Three concentric areas could be distinguished. The central part of the biopsy showed moist desquamation characterized by denudation of the epidermis and serum exudation. It was surrounded by an inflammatory area characterized by reddening of the skin and by a third area with no visible clinical signs. The skin sample was divided into 41 pieces of 2- to 4-cm^2 identified squares, and 18 domains (Fig. 5A) were used for PCC-FISH analysis while the oth-

TABLE 3
Fibroblasts Isolated from *Ex Vivo* γ-Irradiated Skin Biopsies Exposed to Doses between 0 and 10 Gy and Grown for PCC-FISH Analysis by Painting Chromosome 4

Number of excess chromosome segments per metaphase	0 Gy	1 Gy	3 Gy	5 Gy	8 Gy	10 Gy
0	794	771	769	273	284	236
1	0	16	41	31	51	88
2	0	0	2	4	12	22
3	0	0	0	2	0	4
Total metaphases	794	787	812	310	347	350
Total aberrations	0	16	45	45	75	144
Mean		0.020	0.055	0.145	0.216	0.411
Var/mean		0.98	1.03	1.30	1.11	1.06
U test		−0.39	0.71	3.81	1.42	0.85

Notes. An excess number of segments occurred when more than two segments/metaphase were present. For each radiation dose, the total number of fibroblasts analyzed as a metaphase spread is reported together with the number of cells possessing zero or more excess chromosome segments. When *U*-test values exceeded ±1.96, the excess chromosome spot distribution was considered as nonuniform with a 95% certainty, and the corresponding distribution was considered non-Poissonian. Except for excess chromosome segments measured in cells isolated from skin biopsies irradiated with 5 Gy, *U*-test values indicate that the distribution of excess chromosome segments per metaphase did not differ significantly from a Poisson distribution.

ers were dropped into isopentane for immunohistochemical experiments.

Two weeks after the neodermis graft, two other 0.2-cm² skin biopsies were excised. The first one was performed at the left inguinal area and the second at the back of the left ear. Finally, fibroblasts were isolated and grown from 20 sectors according to the method described previously (Table 4).

The number of fibroblasts collected in the moist central area of the excised tissue ranged from 0.03×10^6 cells to 0.36×10^6 cells per cm² of skin (Table 4). Values in the inflammatory part were slightly higher and ranged from 0.11×10^6 to 0.52×10^6 fibroblasts per cm² of skin (Table 4). In the peripheral zone, the density ranged from 0.12 to 0.34×10^6 fibroblasts/cm², whereas in the back it increased to 1.2 and 1.5×10^6 fibroblasts/cm² for the left ear and left inguinal area sectors, respectively (Table 4).

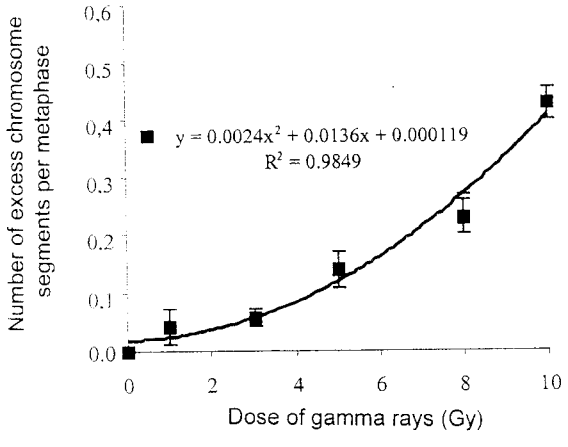

FIG. 3. Formation of excess chromosome segments measured in P0 fibroblasts isolated from four skin biopsies from women exposed to γ-radiation doses of 0 to 10 Gy. The values represent the means ± SD of 310 to 812 metaphases counted among cells isolated from four skin biopsies.

The time to reach 50% confluence in cell culture for applying the PCC-FISH assay was dependent on the area studied (Table 4). Experiments could thus be performed on day 5 or 6 after seeding for fibroblasts isolated from sectors 1, 3, 9, left ear and left inguinal area (Table 4), whereas fibroblasts isolated from domains 27 and 29 were analyzed on day 12. It must be noted that analysis could not be performed for some sectors because cells did not grow. The number of metaphases analyzed ranged from 21 to 209 (Table 4). The number of excess chromosome segments per metaphase ranged from one for cells isolated from sector 1 to a maximum of five for cells isolated from sector 24. As indicated by *U*-test values (Table 4), for most sectors, the distribution of excess chromosome segments per metaphase did not differ significantly from a Poisson distribution.

On the basis of the number of excess chromosome segments per metaphase analyzed, the sectors could be divided into three categories (Table 4). The highest number of excess chromosome segments formatted was determined in metaphase spreads obtained from sectors bordering domain 32, with yields between 0.86 and 1.35 excess chromosome segments per metaphase (Table 4). The yield of excess chromosome segments per metaphase in the peripheral area decreased to values between 0.13 and 1.08 and dropped to 0.04 and 0.0 for the left inguinal site and the back of the left ear, respectively (Table 4).

Conversion of the numbers of excess chromosome segments per metaphase into radiation doses was done using the *ex vivo* calibration curve pre-established in the experiments described above (Fig. 5B). Doses were found to be below or equal to 3.4 Gy for the less exposed zones such as the left inguinal area and the back of the left ear. Doses of about 5 and 6.5 Gy were found on the side of the body

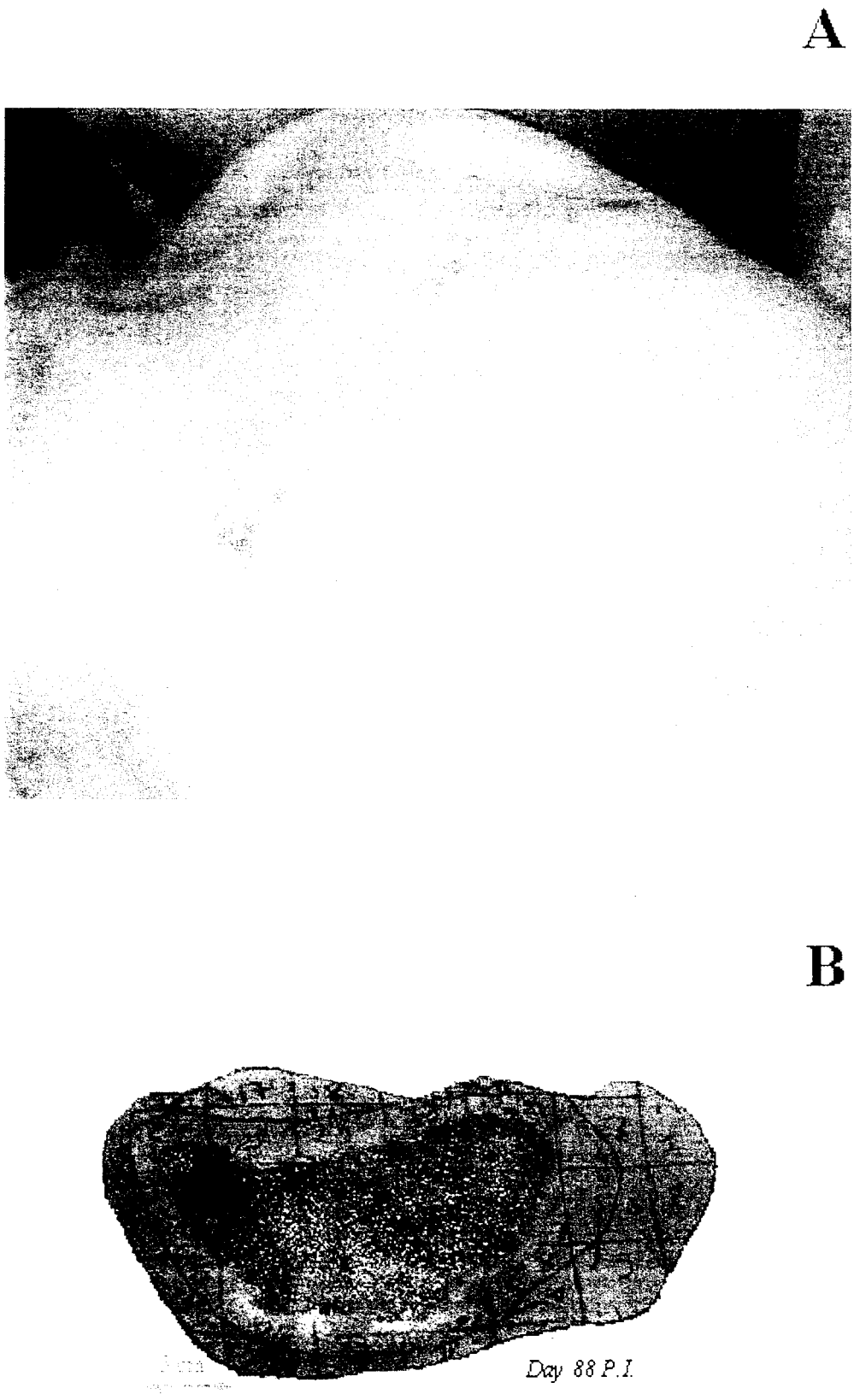

FIG. 4. Panel A: The radiation cutaneous syndrome in the Georgian involved the whole posterior side of the thorax from the waist up to the end point of the scapulae. The lesion was a moist epidermal denudation of about 8% of the body surface without signs of necrosis. On the day 88 postirradiation, wounded skin was excised and a neodermis graft was performed. Panel B: Skin fragment from the back after excision on day 88 postirradiation. Three concentric domains can be distinguished. The inflammatory zone surrounds the moist desquamated zone situated at the center. The third area located at the periphery is characterized by the absence of visible clinical signs.

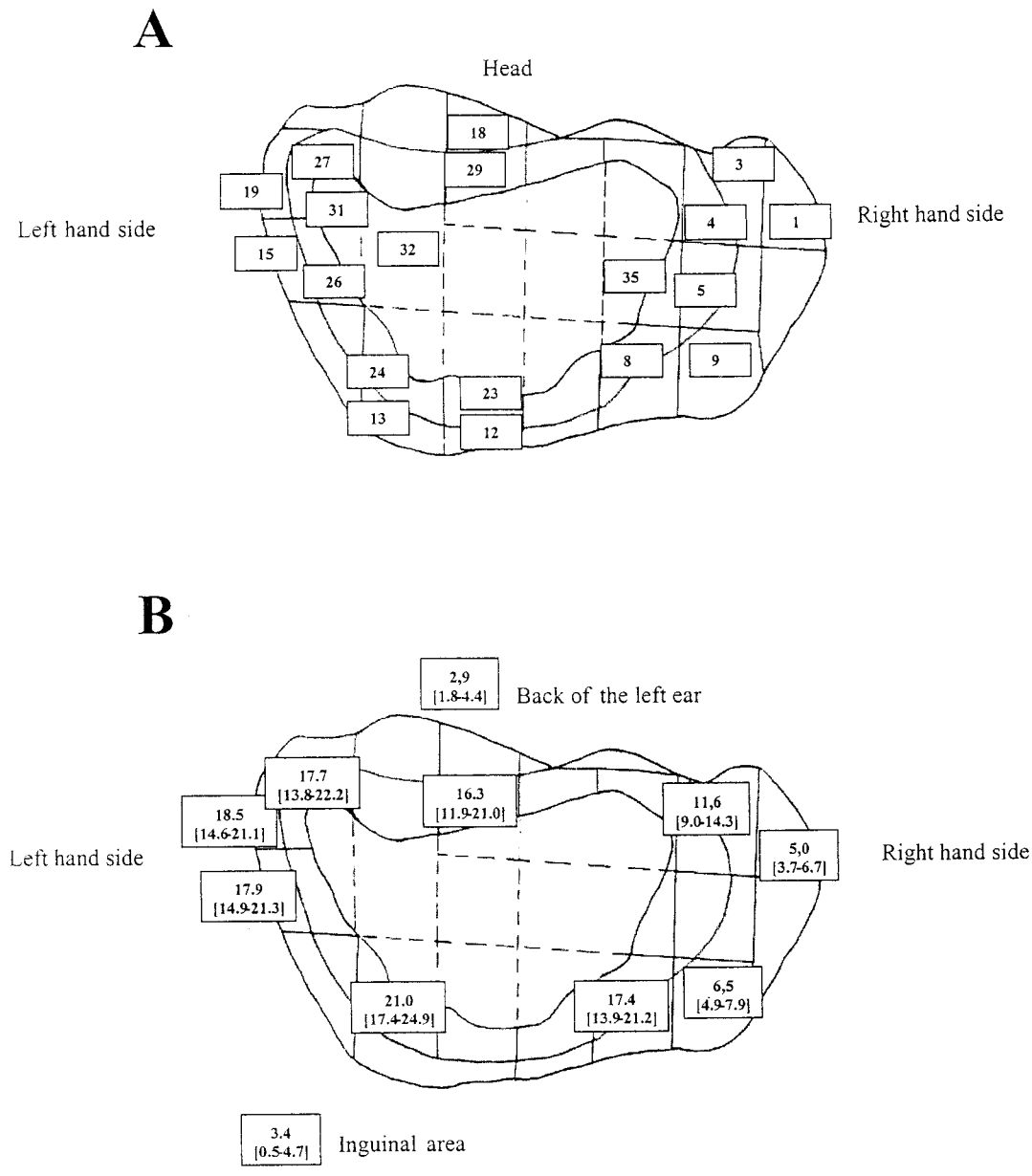

FIG. 5. Panel A: Eighteen identified sectors from the three clinical domains were designed for cytogenetic analysis. Additional sector 5 tissue was used for Ki67 immunostaining. Panel B: Corresponding radiation doses calculated from *ex vivo* calibration curves on the basis of the number of excess chromosome segments per metaphase determined in fibroblasts at passage P0.

(Fig. 5B). A third domain was distinguished by doses higher than 11.6 Gy and up to 21 Gy and corresponded to sectors located in the back of the body. Interestingly, the dose distribution followed an isodose curve bordering sector 32, which appears to be the epicenter of the radiation exposure (Fig. 5B).

DISCUSSION

We propose here a new method for dose estimation in the case of localized radiation overexposure. This approach relies on the measurement by PCC-FISH of excess chromosome segments involving chromosome 4 of fibroblasts isolated from the skin. Excess chromosome segments can be translocations, insertions or chromosome fragments. The background level of excess chromosome segments in cells isolated from nonirradiated skin biopsies was shown to equal zero. This level differs from the one measured in another study which indicates that the background level of complete and incomplete translocations involving chromosomes 2, 4 and 8 is about 13 per 5015 scored lymphocytes sampled from the blood of two women aged 50 to 59 years (*16*). After conversion of metaphase cells to the whole genome equivalent, Ramsey *et al.* estimated that the frequency of stable aberrations in blood lymphocytes of 48-year-old people was about 12 stable aberrations per 1000

TABLE 4
Measurement of Excess Chromosome Segments per Metaphase by PCC-FISH of Whole Chromosome 4 after Seeding in Fibroblasts Isolated and Grown from 11 Sectors

Sector	Number of isolated cells ($\times 10^6$/cm^2)	Day[a]	Number of excess chromosome segments per metaphase						Total			
			0	1	2	3	4	5	Metaphase analyzed	Excess chromosome segments	Excess chromosome segments per metaphase	*U* test
1	0.12	6	148	23	0	0	0	0	171	23	0.13	−1.22
3	0.16	6	37	22	5	0	0	0	64	32	0.50	−1.00
4	0.52	18										
5	0.11	6	14	10	4	3	1	0	32	31	0.97	−1.19
9	0.21	5	137	29	1	0	0	0	167	31	0.19	−1.07
2	0.36	∞										
3	0.34	∞										
5	0.26	6	14	15	11	2	0	0	42	43	1.02	−0.98
8	0.18	∞										
0	0.19	6	11	19	7	2	1	0	40	43	1.08	−0.76
3	0.17	13										
4	0.23	10	6	15	6	2	1	1	31	42	1.35	0.04
6	0.21	6										
7	0.15	12	12	4	8	2	0	0	26	26	1.00	0.43
9	0.23	12	9	7	4	1	0	0	21	18	0.86	−0.11
1	0.36	[b]										
2	0.03	[b]										
5	0.10	[b]										
Left ear	1.20	5	198	9	2	0	0	0	209	13	0.06	2.67
Inguinal area	1.50	5	75	3	0	0	0	0	78	3	0.04	−0.20

Notes. The total number of metaphases analyzed and the number of excess chromosome segments per metaphase are reported. *U*-test values are shown. When *U*-test values exceeded ±1.96, the excess chromosome spot distribution was considered as nonuniform with a 95% certainty, and the matching distribution was considered non-Poissonian. Therefore, *U*-test values indicate that except for the left ear sector, the distribution of excess chromosome segments per metaphase did not differ significantly from a Poisson distribution.

[a] Delay in number of days between seeding stage (day 0) and the day of PCC-FISH experiment.

[b] Total lack of cell culture growth.

cells analyzed (*17*). A possible explanation for the observed lack of excess chromosome segments in skin fibroblasts could be the rather small "target" involved (i.e. chromosome 4 only) or the relatively low number of metaphase spreads that could be analyzed. The mitotic index that was calculated for skin fibroblasts at passage P0 must be compared to that of 5% obtained in conventional cytogenetic analysis. The latter value means that for a total of 1×10^6 blood lymphocytes generally collected, around 1×10^5 cells are available for analysis. In our experiments, for each 25-cm^2 flask, of the 500×10^3 seeded cells, around $50–100 \times 10^3$ cells were collected on the day of the experiment. Considering the mitotic index, this means that fewer than 10×10^3 cells were theoretically and actually available for cytogenetic analysis.

The second possible explanation for the lack of excess chromosome segments in cells isolated from control biopsies is based on fibroblast status. While blood lymphocytes can be considered as quiescent and blocked at first mitosis for cytogenetic analysis, skin fibroblasts can divide during the first days after seeding. Such mitosis would lead to the loss of the most damaged cells, in particular those bearing unstable aberrations such as dicentrics and centric rings. However, such a cell death process would lead to a modification of the linear-quadratic shape of the dose–response curve for formation of aberrations, which is in disagreement with that obtained for production of excess chromosome segments per metaphase in skin fibroblasts analyzed at passage P0. Therefore, it is reasonable to assume that the number of divisions undergone by one fibroblast after isolation from a skin biopsy must be low. This hypothesis was also supported by the lack of a dose–effect relationship observed when trypan blue and $DiOC_6(3)$ staining was performed in the first days after disaggregation. The latter results suggest that the cell death observed during the first days is caused largely by the process of cell isolation and is not radiation-induced mitotic death and consequently is not dependent on dose. From these data, we would expect that the yield of excess chromosome segments per metaphase in skin fibroblasts would be close to that measured in irradiated quiescent cells such as blood lymphocytes. Interestingly, Prasanna *et al.* (*12*) determined a yield of 0.035 and 0.236 excess chromosome segments per metaphase in chromosome 1 of lymphocytes irradiated with 0.5 and 7.5 Gy, respectively. For the same doses, 0.016 and 0.237 excess chromosome segments per metaphase were measured in fibroblasts isolated from skin biopsies exposed to 1 and 7.5 Gy, respectively. If we consider now that divisions can

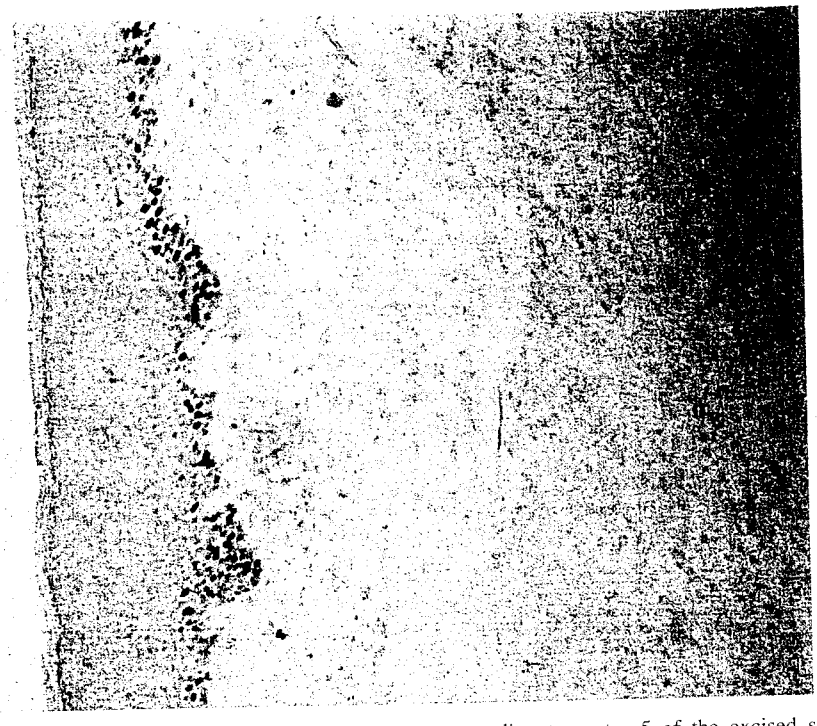

FIG. 6. Immunostaining for Ki67 protein on skin tissue corresponding to sector 5 of the excised skin from Georgian victim on day 88 postirradiation. Arrow indicates proliferating cells at the base of the epidermis.

also occur *in situ*, Ki67 immunostaining performed on sector 5 tissue from the Georgian accident victim or on isolated cells immediately after skin disaggregation provides interesting information. The latter stainings indicated that the Ki67 protein was absent in most of the fibroblasts (Fig. 6). This suggests that skin fibroblasts maintained *in situ* can be considered as quiescent even a few months postirradiation. The lack of divisions occurring *in situ* in irradiated skin fibroblasts is of particular interest in the case of accidental irradiations in which high radiation doses are delivered and in which a long delay can occur between accidental overexposure and dose.

Moreover, considering the highly irradiated domains of the Georgian victim, the analysis by PCC-FISH on days 10–12 after seeding of heavily damaged isolated cells that could not pass more than one division supports the previous hypothesis that few divisions occurred either *in situ* or during the first days after seeding.

Another point that needs to be discussed is how representative of the total irradiated cell population the PCC-FISH analysis performed on cells 5 or 7 days after seeding is and the possible role of clonal expansion in the assessment of the radiation dose. As shown by Ki 67 staining, fibroblasts are quiescent at least until days 3–4 after seeding, and most of the PCC-FISH analyses are performed between 5 and 7 days after seeding. Therefore, the time between adherence and analysis ranges from 2 to 4 days. Bearing in mind that between 0.5×10^5 and 1×10^5 cells are collected on the day of PCC-FISH and that the doubling time is at least 24 h and probably longer, this means that the cells have been derived from at least 3000 to 6000 seeded cells.

Prior to conversion of excess chromosome segments per metaphase into radiation doses, consideration was given to the physical characteristics of the ^{137}Cs irradiator used for calibration and X rays produced by the ^{90}Sr-^{90}Y source. Fortunately, conditions appeared to be quite similar for both irradiations. Monte Carlo calculations showed that the mean energy in term of the fluence of the X-ray spectrum emitted by the ^{90}Sr source was around 350 keV.[3] This is similar to the 440 keV corresponding to the measured mean energy of the Compton diffusion spectrum produced by interaction of ^{137}Cs γ-ray photons with the irradiator wall. It was also estimated by Monte Carlo calculation that the dose rate at the surface of the skin of the victim, considering the source localized in the middle of the back at 5 cm from the skin, was around 72 Gy h^{-1},[3] which is close to the measured dose rate for ^{137}Cs.

The resulting calculated radiation doses from measurement of excess chromosome segments per metaphase in fibroblasts isolated and grown from skin tissue from the Georgian accident victim underlined the suitability of fibroblasts as a support model for dose estimation. Specifically, doses determined on the victim's back matched the observed clinical signs and in particular the moist epidermis area bordering sector 32 (Fig. 5A and B). In addition, the highest calculated dose was lower than 25 Gy and was in agreement with the moist epidermitis without necrosis observed 1.5 months after the onset of clinical signs. Dose mapping indicated that the radiation source might have

moved along the back of the victim because all the doses were quite high and over 10 Gy. On the side of the body, the radiation doses decreased because of tissue attenuation of the photons to lower than 6 Gy. Doses next decreased down to around 3 Gy when distant areas such as the back of the left ear and at the left inguinal field were considered. These results were also in good agreement with data obtained from conventional biological dosimetry based on measurements of dicentrics in blood lymphocytes which indicated a whole-body dose of about 4.4 (3.9–4.8) Gy[4].

Interestingly, an absorbed dose of 13.4 Gy was measured in a piece of vertebra that was removed during the exeresis of unhealthy tissue prior to epidermal autograft on day 130 postirradiation and localized under 2 cm of tissue of sector 32.[5] The method used was based on electron spin resonance (ESR) spectroscopy using the dose addition method (*18*). A corresponding dose of 20 Gy at the surface of the skin was determined by Monte Carlo calculations considering the source localized in the middle of the back at 5 cm from the skin and using the ESR measurement as normalization for the calculated depth-dose profile.[5] This was in good agreement with the doses between 16.3 and 21 Gy we calculated in this area. However, the rather good correlation between doses obtained from physical dosimetry and those obtained from PCC-FISH must not hide the uncertainties associated with our approach, which relies on extrapolation between our two models. Indeed, obvious discrepancies exist between cell behavior in *ex vivo* and *in vivo* irradiated skin, so the extrapolation of results from one model to the other must be discussed. One of the main issues that needs to be highlighted is tissue repair that occurs *in vivo* after irradiation. Though the fibroblasts appeared to be quiescent in the case of the Georgian victim (88 days postirradiation), it is clear that tissue repair will take place *in vivo* and will be associated with remodeling, cell division, cell differentiation, cell death or migration, thus modifying the nature of the cells isolated for FISH analysis. Much more must be known about the kinetics of these phenomena. The second issue is related to chromosomal damage in either *ex vivo* or *in vivo* experiments. We do not know enough about repair of potentially lethal damage in isolated skin cells, and this can be of major relevance to the yield of chromosomal aberrations. One can argue that isolated cells do not divide for several days and that such repair would occur. What we to know is that cells from irradiated victims recover from these lesions. The third point that needs to be mentioned is the uncertainty associated with extrapolating the calibration curve from 0–10 Gy to higher doses.

It must be kept in mind that even conventional biological dosimetry based on lymphocytes also relies on extrapolation between *in vitro* and *in vivo* models. This technique has become routine because its application in thousands of cases of exposure has proven its worth. The purpose of this paper is to underscore the rather good agreement between doses estimated by PCC-FISH on fibroblasts and clinical data together with physical measurements and conventional biological dosimetry. To assess the worth of this approach and whether the correlation is fortuitous, the technique needs to be associated with conventional biological and physical dosimetry in many other radiation accident victims with cutaneous syndrome. We think it could be of major value in the surgical management of radiation accident victims.

SUMMARY

We propose a new method for dose estimation that could be used in the case of localized irradiation. The approach relies on the measurement of excess chromosome segments by PCC-FISH painting of whole chromosome 4 in fibroblasts isolated from skin biopsies. The method was used for dose estimation in the case of a victim of radiation overexposure in Georgia in 2001. The data obtained were in good agreement with those obtained from both physical and conventional biological dosimetry and with clinical data. Further studies based on either other accidental localized overexposures in humans or animal models are needed to assess the validity and reliability of this new methodology as a function of time postirradiation and the wound healing process.

ACKNOWLEDGMENTS

The authors would like to thank Stephen J. Mather (CR, UK) and Marc-André Mouthon (IRSN, France) for helpful discussions and for reading the manuscript.

Received: September 11, 2003; accepted: April 2, 2004

REFERENCES

1. J. L. Lefaix and F. Daburon, Diagnosis of acute localized irradiation lesions: Review of the French experimental experience. *Health Phys.* **75**, 375–384 (1998).
2. M. A. Bender, A. A. Awa, A. L. Brooks, H. J. Evans, P. G. Groer, L. G. Littlefield, C. Pereira, R. J. Preston and B. W. Wachholz, Current status of cytogenetic procedures to detect and quantify previous exposures to radiation. *Mutat. Res.* **196**, 103–159 (1988).
3. G. W. Dolphin, Biological dosimetry with particular reference to chromosome aberration analysis. A review of methods. In *Handling of Radiation Accidents*, pp. 215–224. IAEA, Vienna, 1969.
4. M. S. Sasaki and H. Miyata, Biological dosimetry in atomic bomb survivors. *Nature* **220**, 1189–1193 (1968).
5. J. F. Bottollier-Depois, E. Gaillard-Lecanu, A. Roux, Q. Chau, F. Tompier, P. Voisin and P. Gourmelon, New approach for dose recon-

[4] L. Roy, V. Durand, V. Buard, N. Delbos, N. Paillole, E. Grégoire and P. Voisin, Biological dosimetry report of 3 Georgian people accidentally exposed to ionizing radiation. Paper presented at the International Radiation Protection Association (IRPA) meeting, Florence, Italy, 2002.

[5] I. Clairand, F. Trompier and J. F. Bottollier-Depois, Accident radiologique survenu à Lia, Géorgie, en décembre 2001. Reconstitution dosimétrique physique par simulation numérique et par résonnance paramagnétique électronique (RPE). Paper presented at the Société Française de Radioprotection (SFRP) meeting, Montpellier, France, 2003.

struction: Application to one case of localized irradiation with radiological burns. *Health Phys.* **79**, 251–256 (2000).

6. D. Swain and L. J. Grant, Methods of measuring skin blood flow. *Phys. Med. Biol.* **34**, 151–175 (1989).

7. S. Delanian and J. L. Lefaix, Evaluation of late radiation-induced changes in superficial microcirculation. I. Clinical benefit of the cutaneous Doppler laser. *Cancer Radiother.* **4**, 408–414 (2000).

8. J. L. Lefaix and S. Delanian, Evaluation of late radiation-induced changes in superficial microcirculation after acute beta-irradiation. II. Prognostic importance of cutaneous Doppler laser. *Cancer Radiother.* **4**, 415–420 (2000).

9. R. Gongora, E. Strambi, B. Perdereau, M. Le and S. Tormenta, Thermographie et irradiation partielle aigüe. *Arch. Sci. Lav.* **5**, 41–58 (1989).

10. F. Daburon, Biophysical methods for assessing the radiation dose causing lesions in the skin and subcutaneous tissues. *Br. J. Radiol.* **19** (Suppl.), 75–82 (1986).

11. A. Chalansonnet, J. L. Bonnat, Y. Tricaud, J. L. Lefaix and A. Briguet, Dosimetry of ^{60}Co and ^{192}Ir gamma-irradiated agarose gels by proton relaxation time measurement and NMR imaging, in a 0–100 Gy dose range. *Health Phys.* **72**, 708–712 (1997).

12. P. G. Prasanna, C. J. Hamel, N. D. Escalada, K. L. Duffy and W. F. Blakely, Biological dosimetry using human interphase peripheral blood lymphocytes. *Mil. Med.* **167**, 10–12 (2002).

13. J. M. Coco-Martin and A. C. Begg, Detection of radiation-induced chromosome aberrations using fluorescence *in situ* hybridization in drug-induced premature chromosome condensations of tumour cell lines with different radiosensitivities. *Int. J. Radiat. Biol.* **71**, 265–273 (1997).

14. R. Kanda, K. Eguchi-Kasai and I. Hayata, Phosphatase inhibitors and premature chromosome condensation in human peripheral lymphocytes at different cell-cycle phases. *Somat. Cell. Mol. Genet.* **25**, 1–8 (1999).

15. W. Merkle, Statistical methods in regression and calibration analysis of chromosome aberration data. *Radiat. Environ. Biophys.* **21**, 217–233 (1983).

16. S. Pressl, A. Edwards and G. Stephan, The influence of age, sex and smoking habits on the background level of fish-detected translocations. *Mutat. Res.* **442**, 89–95 (1999).

17. M. J. Ramsey, D. H. Moore, 2nd, J. F. Briner, D. A. Lee, L. Olsen, J. R. Senfit and J. D. Tucker, The effects of age and lifestyle factors on the accumulation of cytogenetic damage as measured by chromosome painting. *Mutat. Res.* **338**, 95–106 (1195).

18. J. M. Brady, N. O. Aarestad and H. M. Swartz, *In vivo* dosimetry by electron spin resonance spectroscopy. *Health Phys.* **15**, 43–47 (1968).

Article 2 : Stress oxydatif associé aux symptomes cliniques dans la peau de rats hairless exposés localement aux rayons X : rôle de la Superoxyde Dismutase ?

L'objectif de cette étude est de caractériser les phénomènes oxydatifs au niveau de l'épiderme et du derme de la peau de rats hairless exposés localement au rayonnement X de sorte d'obtenir la dose maximale d'irradiation au niveau de la peau (voir photographie du dispositif ci-dessous). Si ces processus sont de mieux en mieux connus dans le cas d'exposition aux rayonnements ultraviolets, peu d'études traitent de l'exposition de la peau aux rayonnements ionisants. Des travaux militaires ont toutefois été menés sur ce sujet. L'atteinte du tissu cutané constitue un problème fondamental dans le cas du traitement des personnes irradiées accidentellement.

Photographie du dispositif d'anesthésie et d'irradiation (générateur de rayons X, Institut Gustave Roussy, Villejuif). Les rats anesthésiés sont placés sous la tête du générateur. Une protection de plomb limite l'exposition aux pattes postérieures.

Afin de caractériser le stress oxydatif radio-induit, la première approche consiste à évaluer l'efficacité des systèmes de défense du tissu face à la production de radicaux par la mesure de l'activité des enzymes anti-oxydantes (catalase, superoxyde dismutase, glutathion peroxydase) et du niveau de glutathion total et oxydé. Comme nous l'avons dit précédemment, si ces systèmes sont dépassés, il y a atteinte des macromolécules biologiques. Nous avons donc ensuite mesuré le niveau cutané d'un des produits des péroxydations lipidiques, le malonedialdéhyde, et celui de la 8-oxodGuo dans les lymphocytes circulants. Un suivi de l'état général des rats (poids, suivi clinique, numération des cellules sanguines) et de leur alimentation a été effectué. Parmi les signes cliniques majeurs, il a été mis en évidence la présence d'un érythème chez les rats irradiés à 30 Gy 7 jours après l'irradiation. Cet érythème évolue en desquamation sèche puis humide la semaine suivante. On observe toutefois un phénomène de réparation partielle un mois après irradiation qui coïncide avec une amélioration de l'état général des rats. Les modifications les plus significatives des paramètres biochimiques mesurés ont porté sur l'activité de la SOD dans le derme. Une forte diminution de l'activité de cette enzyme a en effet été observée alors que des variations plus modestes ont concerné les deux autres enzymes anti-oxydantes. Par ailleurs, nous avons mis en évidence une expression forte de marqueurs de l'inflammation. Une forte augmentation d'expression de la MPO (myéloperoxydase), du niveau de 8-oxodGuo et de MDA a été mesurée 2 jours après irradiation et du niveau de TNFα 12 j après irradiation.

Les données obtenues ont fourni la preuve directe de l'existence de phénomènes oxydatifs dans la peau irradiée par les rayonnements ionisants. Il apparaît que les phenomènes oxydatifs suivent une cinétique dont l'ampleur est directement reliée à la dose d'irradiation délivrée. Il sera intéressant dans de futurs travaux d'étudier les phénomènes oxydatifs à des temps plus tardifs. Néanmoins, cette étude a également souligné la complexité du modèle *in vivo* dans lequel de nombreux paramètres (nombreux types cellulaires, échanges intercellulaires, phénomènes inflammatoires) sont mis en jeu et peuvent influer directement sur la production de stress oxydatif. Nous avons pour cela, dans la suite du projet, utilisé des modèles *in vitro* plus simples afin de comprendre les mécanismes fondamentaux mis en jeu dans l'action des rayonnements ionisants au niveau des cellules cutanées. Par ailleurs, cette étude a ainsi mis en évidence l'intérêt des traitements anti-oxydants. En particulier, les modèles cellulaires se sont avérés plus adaptés pour comprendre les mécanismes de l'association.

Oxidative stress-associated clinical symptoms in skin of locally X-irradiated hairless rats: role of Superoxide Dismutase ?

J-P Pouget[1,2], J-L Ravanat[3], and C Laurent[1]

[1] Service de Radiobiologie et d'Epidémiologie, DRPH, Institut de Radioprotection et de Sûreté Nucléaire, Fontenay-aux-Roses, France

[2] INSERM EMI 0227, Immunociblage des tumeurs et Ingénierie des Anticorps, Centre de Recherche en Cancérologie, CRLC Val d'Aurelle, Institut Paul Lamarque, Montpellier, France

[3] Laboratoire des lésions des acides nucléiques,DRFMC/SCIB, CEA Grenoble, France

Running title: Oxidative modification of irradiated skin

Keywords: Skin, accidental overexposure, oxidative stress

‡ To whom correspondence should be addressed:

e-mail: jppouget@valdorel.fnclcc.fr

INSERM EMI 0227, Immunociblage des tumeurs et Ingénierie des Anticorps,

Centre de Recherche en Cancérologie,

CRLC Val d'Aurelle, Institut Paul Lamarque,

F-34298 Montpellier, France CEDEX

Abstract

The aim of the present study was to assess the role of oxidative stress parameters in view of clinical signs in skin of locally X-irradiated rats. Typically, hairless rats were exposed to radiation, at posterior legs level, at doses ranging from 0 to 30 Gy. Skin excision was done and the level of the main antioxidant defences systems (SOD, Cat, GPx, glutathione) together with markers of inflammation (Myeloperoxydase and TNF-alpha) were measured in both dermis and epidermis over one month after irradiation. The level of 8-oxodGuo level was measured in DNA of blood lymphocytes and MDA yield was determined in both skin compartments. It was observed that the main modifications in enzyme activity concerned

dermal SOD that might be correlated to dry and moist desquamation in 20 and 30 Gy-irradiated rats. Return of dermal SOD to control level was shown to correspond to onset of healing of tissue lesion. It was also shown a first boost of inflammatory process as demonstrated by MPO immunostaining, 8-oxodGuo and MDA measurement. This was followed from day 12 after irradiation by an increase in TNF-α level which persisted until day 30. Further studies are necessary for precising the role of SOD drop as initiating skin damage.

Introduction

Skin, by its anatomical situation and function is the first organ exposed to external radiation. Skin tolerance may affect therapeutic schedules by limiting dose delivery in treatment of skin, or breast cancer, but it is also of major relevance in preventing delayed injury that may appear from months to years after radiotherapy and may affect vital diagnosis of patient (Delanian and Lefaix, 2004; Dubray *et al*., 1997).

Predicting skin response to irradiation is also essential in the treatment of victims of accidental overexposure. Indeed, most of the radiological accidents are localised irradiation, and high irradiation doses are delivered to a reduced area of the body. Then victims suffer most of the time from more or less severe burns which can evolve from blister to tissue necrosis. Then, the major problem encountered by the medical staff for taking in charge such victims is that time course and magnitude of clinical symptoms gathered under the radiological cutaneous syndrome depend on the irradiation dose and on irradiation quality. In this respect, we proposed in a previous work (Pouget *et al*., 2004), methodology for assessing irradiation dose delivered to the skin fibroblasts. Radiological cutaneous syndrome includes a plethora of lesions that can be divided in early and delayed effects (Archambeau *et al*., 1995). Early effects include erythema, pigmentation and depilation, dry and wet epidermitis, and appear from days to weeks after irradiation. Delayed effects appear from months to years after irradiation and may include clinical signs like telangiectasia, fibrosis or necrosis.

Magnitude and time course of clinical symptoms is highly dependent on the radiobiology associated to skin constituents.

It is generally considered that early effects are a consequence of irradiation of germinatum stratum of epidermis. By contrast, late effects would be associated to dermis alteration (Peters and Withers, 1982; Rudolph *et al*., 1988). They would be caused by change in architecture and number of functional units *i.e.* by lost of endothelial cells and subsequent alteration of

microvessels organisation, and by activation of secreting cells such as fibroblasts. A common feature to these phenomenons might be oxidative stress. Oxidative stress occurs when an imbalance between reactive oxygen and defence systems exists. In this respect the role of oxidative stress in the becoming of irradiated tissue was demonstrated in brain, lung but not in the case of irradiated skin (Robbins and Zhao, 2004).

Interestingly, since the eighties, therapies based onto antioxidants substances showed they could be a useful and beneficial strategy in protecting victims against the development of fibrosis but also in some particular circumstances, in reversing radionecrosis (Baillet *et al*., 1986; Lefaix *et al*., 1999; Delanian *et al*., 2001; Delanian and Lefaix, 2002; Delanian and Lefaix, 2004; Delanian *et al*., 2005). In addition, the presence three months after exposure to irradiation of heavily damaged fibroblasts in the exposed area (Pouget *et al*., 2004) might be explained by stress induced prematurely senescence phenomenon (SIPS) (Remacle *et al*.., 1995). The origin of oxidative stress in irradiated skin can be multiple (Robbins and Zhao, 2004). Indeed, many reactive oxygen species can be produced in skin, either by irradiation itself or later, during tissue response including remodelling and inflammatory processes. It is known for long that cells developed defence systems against reactive oxygen species like (ROS) like superoxide radicals, hydrogen peroxide and hydroxyl radicals but also nitric oxide radicals or hypochlorous acid. Defence systems are made of non enzymatic system (vitamin C, vitamin E, gluthatione, thioredoxine, ubiquinone etc.) and of enzymatic ones constituted by superoxide dismutase, catalase and glutathione peroxidase. When defence systems are exceeded, oxidative damage occurred. DNA, lipids and proteins constituting cells or participating to tissue ultrastructure are potential targets for oxidative stress.

Most of the studies dealing with oxidative stress induced in skin were based on UV or visible radiation, but to our knowledge, no studies dealt with modifications in oxidative parameters induced in skin in case of localised exposure to ionising radiation. Therefore, the aim of the present study is to assess the level of the main antioxidant enzymes and of oxidative parameters in view of clinical signs that developed among locally irradiated hairless rats. Typically, rats were exposed at posterior legs level to X-irradiation for doses ranging from 0 to 30 Gy and study was followed up over one month after exposure. It was thus observed that in response to irradiation, the main changes in antioxidants defences, concerned dermis and particularly dermal SOD activity which was strongly decreased. A strong implication of inflammatory process was also underlined. Our results demonstrated that oxidative stress occur in irradiated skin and might be connected to clinical symptoms.

Materials and methods

Animals

A total of 96 hairless rats was obtained from Charles River (Lyon, France). Rats were 5 weeks old on arrival and were acclimated for three weeks before the beginning of the experiments. They were housed individually in polycarbonate cages under standard conditions of temperature, humidity and light/darkness (12/12 hours). Food and water were available ad libitum. Rats were weighed twice a week until their euthanasia. The work was approved by the Animal Ethics Committee.

Irradiation

Irradiation was performed using X-ray 125 keV generator. Irradiation was localised to the posterior legs using lead shield and dosimetry was done using Fli thermoluminescent dosimeter. Dose rate was 0.73 $Gy.min^{-1}$. Rats were maintained anesthetised using isoflurane gas during irradiation and were maintained at 37°C. Doses of 10, 20 and 30 Gy were delivered to respective groups of rats.

Sample preparation

Skin biopsies and blood sampling were performed under anesthesia either at 6, 24, 48 hours and 7, 12 or 30 days post-irradiation. After skin excision, epidermis was then separated from dermis using sterile scalpel. Skin samples were then immediately dropped into liquid nitrogen for biochemical analysis or into cold isopentane before being frozen at -80°C for immunohistochemistry experiments. Blood samples were used for cells counting and for DNA base damage measurement. Three rats were used for each irradiation dose, at each time of analysis.

Skin disaggregating

Prior to biochemical analysis, epidermis and dermis were thawed and immediately immersed in cold phosphate buffer (10mM KH_2PO_4, 40mM Na_2HPO_4, 0.01 mM EDTA, pH 7.5). Samples were then disaggregated using ultraturrax T-25 homogenizer for 20 min. Homogenate was then centrifuged at 15,000×g for 5 min. Supernatant was collected and stored at -80°C prior biochemical analysis or protein concentration determination.

Protein concentration

Concentration of proteins was determined on an aliquot fraction of homogenates using Bradford method. Typically 10 µL samples homogenates were mixed with 300 µL Coomassie® (Interchim, France) and absorbance was measured at 570 nm using microplate spectrophotometer.

Blood sampling

Blood cells counting was performed using MS9 automat (France). For DNA base damage measurement, lymphocytes were isolated from blood using red blood cells lysis buffer. Typically, lysis buffer (NH_4Cl 156 mM, $NaHCO_3$ 11.9 mM, Na_2EDTA 0.11 mM) was added to blood sample in a ratio 10:1 (v/v). Mixture was incubated at 37°C for 7 min and centrifuged for 10 min at 5,000×g. Supernatant was discarded and the pellet containing lymphocytes rinsed twice with PBS.

Superoxide dismutase

The superoxide dismutase activity was measured according to the method described in (Flohe and Otting, 1984) by assessing increase in absorbance of reduced NBT. Typically, x µL of samples homogenate were mixed with 15 µL NBT and incubated for 10 min at 30°C. Then 100µL xanthine oxydase prepared in bicarbonate buffer (50 mM $NaHCO_3$, 50 mM Na_2CO_3, 0.5 mM DTPA. Absorbance was then measured at 560 nm for 1.5 min. Slope was measured and compared to the one obtained with xanthine (8.7 mg/ml). Results were expressed in inhibitory units. One unit was defined as the amount leading to 50% inhibitory effects. Results were then normalised to value measured in control at each considered time.

Catalase

Catalase activity was assayed spectrophometriccaly on a Beckman DU650 spectrophotometer according to the method of Clairbone and Aebi (Aebi, 1984). Typically, 900 µL H_2O_2 were mixed with 100 µL sample homogenate and the decrease in absorbance of H_2O_2 at 240 nm was followed for 1 min. One enzyme unit is defined as equivalent to 1 µmole of substrate disappearance per min under the defined conditions. Results were then normalised to value measured in control at each considered time.

Glutathione peroxidase

Glutathione peroxidase activity was assessed spectrophotometricaly on a Beckman DU650 apparatus by following the decrease in absorbance of NADPH. Typically volume x of sample homogenate was mixed with 125 µL buffer (0.5 M Na_2HPO_4, 0.5 M NaH_2PO_4, 0.1 M EDTA, 0.4 M KCN, pH 7), 50 µL 0.1 mM GSH, 10 µL NADPH diluted in 0.1 % $NaHCO_3$, 25 µL Glutathione reductase (10 IU/mL buffer) and 690-x µL of H_2O. Mixture was incubated for 15 min at 30°C before addition of 100µL TerButylHydroperoxide. Absorbance was then measured at 340 nm at 30°C for 10 min. Results were normalised to value measured in control at each considered time.

Dosage of glutathione

Total Glutathione and oxidised glutathione were determined according to the method described by Lord-Fontaine and Averill-Bates (Lord-Fontaine and Averill-Bates, 2002) and slightly modified as follows. Sample homogenate were deproteinized by using 5-sulfosalicylic acid (4% w/v), incubated for 15 min at room temperature and then centrifuged (15000×g, 15 min). Supernatant was collected and 100 µL were mixed with 680 µL of a solution of 0,143 M sodium phosphate containing 6.3 mM EDTA (pH7.5), 70 µL NADPH (0.248 mg/mL) and 0.1 mL of 6 mM 5,5'-dithiobis(2-nitrobenzoic acid) and 50 µL TEAM. After 10 min at 30°C, 10 µL Glutathion reducatse (100 U/mL) were then added and the rate of formation of 5-thio-2-nitrobenzoic acid was followed at 412 nm during 3 min at 30°C. Oxidised glutathione was measured by using the same method after preincubation for 60 min of sample with 2 µL of 1 M 2-vinylpyridine. Ratio between oxidised and total glutathione was then calculated and resulting data were normalised to value measured in control at each considered time of analysis.

DNA base damage measurement

Lymphocytes pellets of about 15.10^6 cells/sample were used for DNA base damage measurement. The chaotropic method was used for DNA extraction and analysis by HPLC-MS/MS was described by Pouget *et al*. (Pouget *et al*., 2002).

Malonedialdehyde

Lipid peroxidation was assessed by the formation of malonedialdehyde which was separated from others thiobarbituric acid-reactive substances by HPLC. Typically, around 500 mg epidermis and dermis were cryomilled before being mixed with 800 µL 0.44 M phosphoric acid. Then, 250 µL thiobarbituric acid 42 mM and 450 µL H_2O were added and the mixture

was heated at 70°C for 1 h. Samples were kept on ice prior to HPLC-Spectrofluorimetry analysis. Before analysis, proteins were precipitated. For this purpose, 500 µL samples were mixed with 500 µL NaOH 90 mM (in methanol 90%). Samples were then centrifuged at 9,500×g for 5 min. HPLC column was rinsed with a methanol/H_2O solution 1:1 (v/v), equilibrated with mobile phase (4.17 g KH_2PO_4 dissolved into 0.6 L H_2O, pH 6.8 and complete with methanol to 1L). Flow rate was 0.75 mL/min. TBARS were detected by spectrofluorimeter ($\lambda_{excitation}$ = 515 nm and $\lambda_{emission}$ = 553 nm). Malonedialdehyde retention time was around 8.6 min.

TNFα

Tumor necrosis factor alpha (TNF-α) is produced by activated macrophages and other cell types including T and B cells, endothelial and smooth muscle cells. It is a mediator of inflammatory process. It was quantified by ELISA using Human TNF alpha ELISA Kits (R&D systems, France). For this purpose, one hundred µL of sample homogenates were used for each analysis and the procedure was as recommended by the manufacturer. Results in pg/mg proteins were normalised to value measured in control at each considered time.

MPO immunohistochemistry

MPO is a protein found in granules of neutrophilic polymorphonuclear leukocytes and may be used as a marker of inflammation. MPO was measured on skin tissue by immunhistochemistry. Typically, skin fragments were dropped into cold isopentane and stored at –80°C. Frozen sections (6 µm) were cut, fixed twice in cold acetone for 10 min, air-dried for 15 min at room temperature and then permeabilized with Triton X100 for 10 min at room temperature. The following steps were performed on a Ventana automated immunohistochemistry system (Ventana Medical system, Ar, USA) with primary rabbit polyclonal (1/200) antibody and secondary goat anti-rabbit antibody coupled to biotin. Biotin was detected as described by the manufacturer (Ventana, medical system Inc., Ar, USA). Qualitative assessment of MPO immunostaining was done by scoring the number of fluorescent spots/ slide.

Results

CLINICAL SYMPTOMS

Clinical symptoms including, skin manifestation, blood cells counting and rat's weight were followed in hairless rats locally exposed to doses of X-ray ranging from 0 to 30 Gy.

Tissue reaction after localized irradiation

Tissue reaction was time and dose dependent. None skin modification was observed in controls and only slight changes in pigmentation was observed in 10 Gy-irradiated rats (Figure 1). Erythema was observed for rats exposed to 20 Gy and 30 Gy on days 7 and 15, respectively after irradiation. Erythema evolved into dry and next moist desquamation only for 30 Gy-exposed rats between days 12 and 15. Erythema attenuated and disappeared from skin of rats exposed to 20 Gy around day 20. Onset of moist desquamation healing was observed for 30 Gy-irradiated rats from day 20 and was still progressing until day 30 without being totally achieved.

Rats' weight and food intake

Food intake was assessed daily all over the considered period (data not shown). Initial decrease was observed for the four groups of rats (0, 10, 20 and 30 Gy). Subsequent rat's weight was shown to decrease in irradiated groups until day 12 but raise was then observed for all of them, more markedly for 20 and 30 Gy irradiated rats.

Blood cells count

In order to assess changes in haematopoietic tissue in bone marrow, blood cells counting was done. Radiation-induced cell lost is generally replaced by newly formed cells from the bone marrow according to their blood transit. Changes in granulocytes, thrombocytes and lymphocytes concentration is a major phenomenon which occur during the first hours following irradiation and participate to the haematological syndrome. If granulocytes loss is involved in inflammatory process and thrombocytes in bleeding, lymphocytes is generally considered as a good and reliable marker of irradiation.

Blood cells counting indicated that granulocytes concentration diminished for the three irradiation dose groups (0.7 10^9/L, 0.3 10^9/L, 0.4 10^9/L, respectively) as soon as 6 hours after irradiation and remained at this level around until day 12. At that time, an increase in concentration was observed and progressed until day 30 with a slightly greater level than the one measured in control group (data not shown). Thrombocytes concentration was shown to

decrease from day 7 in all irradiated groups (332 10^9/L, 452 10^9/L, 353 10^9/L, respectively) and then returned to control group level on day 30.

Concerning blood lymphocytes strong decrease was also observed from 6 hours after irradiation in all the irradiated groups (Figure 2). This decrease was emphasized and reached the nadir on day 1 post-irradiation in a dose-dependant manner (2.8 10^9/L, 2.5 10^9/L, 2.0 10^9/L, respectively). It then persisted until day 12 and return to control values was observed on day 30. Decrease was statistically significant for 10 Gy- and 20 Gy-irradiated groups from day 2 to day 12.

BIOCHEMICAL ANALYSIS

Antioxidant enzymes activities and markers of oxidative stress were also measured in both epidermis and dermis of rats locally exposed to irradiation as described previously. Typically, Superoxide dismutase (SOD) which converts superoxide anion into H_2O_2, glutathione peroxidase (GPx) and catalase (Cat) activities which reduce H_2O_2 into H_2O and 0_2 were measured. Skin biopsies were performed at different time post irradiation and then disaggregated before being homogenized into an appropriate enzymatic buffer. Enzymatic activities were then assayed as described above. Results are normalised to value measured in control at each considered time.

SOD activity

In control rats, SOD activity was found to be 43% lower in dermis than in epidermis (130 IU/mg of proteins). In response to irradiation, SOD activity measured in both epidermis (Fig. 3A) and dermis (Fig. 3B) was found to vary according to successive rises and decreases as a function of time and of the irradiation dose.

In epidermis of 10 Gy- and 20 Gy-irradiated groups, as compared to control, SOD activity was shown to increase in and to reach a peak on day 2 (×1.42 and ×2.32, respectively). Increase was statistically significant for 20 Gy-irradiated rats. Then a decrease was observed, before a second raise was measured on day 30 (×2.73 and ×1.96, respectively). By contrast, for 30 Gy-exposed rats, a decrease was measured on day 2 (×0.45) followed by a return to control values on day 7 and by a strong increase in activity on day 30 (×1.86).

In dermis, modifications in SOD activities were more pronounced. A strong decrease was observed on day 1 for the three irradiations doses groups (×0.08, ×0.22 and ×0.16, respectively). Return to control group values was observed on day 2 for 10 Gy-irradiated rats

but was followed by a second temporary decrease on day 12 (×0.20). By contrast, the level measured in the two other irradiated groups was maintained until day 30 with values lower by a factor (×0.50). Decrease was statistically significant on day 7, 12. On day 30 a strong increase was observed in all the irradiated groups of rats with levels about 2.37, 1.8 and 1.09 fold greater in 10 Gy, 20 Gy and 30 Gy respectively, compared to controls.

Catalase activity

Catalase activity measured in control rats was shown to be lower in dermis (40 IU/mg of proteins) than in epidermis (50 IU/mg of proteins).

As compared to control values, modifications in catalase activities were measured both in epidermis (Fig. 4A) and dermis (Fig. 4B), as a function of time and of the irradiation dose.

In epidermis of 10 Gy-irradiated rats two similar falls were observed 6 hours after irradiation and on day 2 (×0.7). Then values returned to control level. By contrast, although never statistically significant, decrease was observed as soon as 6 hours after irradiation for the 30 Gy irradiated rats (×0.6) and from day 2 for 20 Gy-irradiated group (×0.49). Catalase activity measured in 20 Gy-irradiated rats returned to control values on day 30 but remained lower for 30 Gy irradiated rats (×0.7).

In dermis of rats exposed to irradiation doses of 10 and 20 Gy, decrease in catalase activity was observed as soon as 6 hours post-irradiation (×0.8 and ×0.6, respectively). A Significant decrease was also observed in 30 Gy-irradiated rats from day 1 (×0.6). Values measured in 10 Gy-irradiated rats returned to control values on day 2, whereas climb and return to control level was progressive until day 30 in dermis of 20 Gy-irradiated rats. By contrast, level in catalase activity measured in 30Gy-irradiated rats was shown to be subject to more pronounced variations. Indeed, from day 2 (×0.9) to day 7 (×1.3) a strong increase in Catalase activity was followed by strong decrease until day 30 with a level 0.6 fold lower than in controls.

GPx activity

Basal level in GPx activity measured in control rats was shown to be 27% lower in dermis than in epidermis. Response to irradiation of GPx activity was measured both in epidermis (Fig. 5A) and in dermis (Fig. 5B). In the latter compartment, main changes in GPx activity, although non significant, concerned 30 Gy-irradiated rats group. In this respect, successive rises, on day 1 (×1.7) and on day 12 (×1.6) were measured. The only marked decrease was observed on day 30 (×0.6). No changes in activities measured in 10- and 20 Gy-irradiated rats

was observed until day 30, time at which a significant decrease was measured for 20 Gy dose (×0.6).

In dermis, no major modifications in GPx activity measured in 10 Gy exposed rats was noticed all over the considered period. By contrast, although non significant, slight increases in GPx activity were measured in 20 Gy- and 30 Gy-irradiated rats with on days 1, 2 and 12. In addition, small decrease was measured in all irradiated groups on day 30.

Oxidized and reduced glutathione

Glutathione system is a major antioxidant system. GSH is a three amino acids that can give an electron or hydrogen atom to a peroxide in an oxidation reaction catabolized by GPx. Glutathione is then under its reduced (GSH) or under its oxidised form (GSSG). GSSG must be reduced again into GSH by the action of glutathione reductase. The ratio GSSG/GSH is usually used as an indicator of redox potential of the cells as an high ratio can be responsible for the accumulation of hydrogen peroxide and create sever oxidative stress. This ratio was determined in both epidermis (Table 1) and dermis (Table 2) of control and irradiated rats as described previously. Values were normalised to 100% in control group at each time of analysis.

In epidermis, Table 1 shows that ratio is generally greater than 1, for all considered times, suggesting formation of GSSG. A statistically significant increase in GSSG level compared to control was observed in 20 and 30 Gy-irradiated groups on day 7 and on day 30 in all irradiated ones (data not shown). Similar trends were observed in dermis. Increase in ratio was thus observed at any considered time, excepted on day 12 with values about ratio measured in controls. A statistically significant increase in GSSG level compared to control was observed in 20 and 30 Gy-irradiated groups on day 7 (data not shown).

DNA base damage level

The measurement of DNA base damage induced in DNA of blood lymphocytes of rats exposed to doses ranging from 0 to 30 Gy was done using LC-MS/MS method after DNA extraction followed by enzymatic DNA hydrolysis. Initial DNA base damage measurement concerned several purines and pyrimidines modifications. However, no significant modification in the level of Thymidine glycols, 5 HmdUrd, 5-FordUrd, 8-oxodAdo compared to controls were observed. By contrast, significant modifications according to time and

irradiation dose concerned the level of the major marker of oxidative stress which is 8-oxodGuo (Figure 6).

In this respect, it was observed that 8-oxodGuo slightly increased in irradiated rats as soon as 6 hours after irradiation and reached a maximal value on day 2 about 2.2 8oxodGuo/10^5 dGuo for rats exposed to 20 and 30 Gy compared to a mean value of about $1/10^5$ dGuo all over the considered period in controls. Then a decrease and a return to value slightly higher than in control rats was observed and return to control values was effective on day 30.

Malonedialdehyde

ROS lead to polyunsaturated fat acids peroxidation. Lipidic hydroperoxides are degradated mainly in malonedialhedyde and 4-hydroxynonenal which react in a covalent manner with proteins and inactivate them. MDA level was measured in both epidermis and dermis of irradiated rats as described above. Increase in MDA level, although non significant, was measured in all irradiated samples either on day 1 for epidermis or day 2 for dermis (data not shown). Increase was then about 100% in epidermis and about 50% in dermis. Then, surprisingly, values decreased from day 7 to day 12, in all irradiated samples and were shown to rise again on day 30. In this respect, MDA level was about 50 % greater than in controls in both compartments of 10 and 20 Gy-irradiated rats. Values in 30 Gy-irradiated rats were similar to level measured in control.

TNFα

Tumor necrosis factor alpha is a mediator of inflammatory response and is secreted by stimulated macrophages and T cells, smooth muscle cells and fibroblasts. TNFα was measured both in epidermis (Figure 7A) and dermis (Figure 7B) of irradiated hairless rats.

In epidermis TNFα level remained unchanged for all irradiation doses until day 7 when a slight increase was observed. This increase was confirmed on day 12, with a drastic raise in 30 Gy-irradiated group (×9) and less pronounced rise in 20 Gy-exposed group (×1.7). Interestingly, on day 30, values measured in 10 Gy- and 20 Gy-irradiated sample showed a strong rise with values 2, 2.1 times higher than in controls, respectively. Level measured in 30 Gy-irradiated rats was still high with a statistical difference (×3).

Changes in TNFα level as a function of time and of irradiation doses were also observed in irradiated dermis. As early as 6 hours post irradiation, a slight increase was measured in all

the irradiated samples. Next, values remained slightly higher or around those measured in controls until day 7. On day 12, whereas values were similar to controls in both 10 and 20 Gy, value quantified in 30 Gy–irradiated rats drastic raised (× 4.5). Then, as observed in epidermis, this value was shown to decrease but remained about 2.5 fold higher than controls on day 30. Increase, although no statistically significant, was also observed in 10 and 20 Gy samples.

Myeloperoxidase activity

MPO is an iron-containing protein found in granules of neutrophilic polymorphonuclear leukocytes and, in less extent, in the lysosomes of monocytes. When neutrophils become activated, like during phagocytosis, they undergo a process which causes production of superoxide, hydrogen peroxide, and other reactive oxygen derivatives, which are all toxic to microbes. Therefore, MPO staining is a marker of inflammatory process and subsequent release of reactive oxygen species. In addition presence of MPO hydrogen peroxide and chloride ions (Cl) are converted into the highly toxic into hypochlorous acid.

MPO was strongly expressed in the first 48 hours after irradiation; the most being in 30 Gy exposed rat skin at day 2 (Figure 8). In addition, MPO was also detected at day 12 in 20 Gy irradiated rat skin.

Discussion

Predicting skin response to radiation is of major importance in the care or overexposure casualties or in preventing delayed effects consecutive to radiotherapy that may appear in any patients from months to years after radiotherapy. It has been for long considered that mitotic death of keratinocytes, fibroblasts and endothelial cells was the main process involved in radiological cutaneous syndrome. However, the success of antioxidant therapies in restoring integrity of damaged skin indicated that oxidative stress would play a significant role in skin becoming.

To our knowledge, this is the first study dealing with the measure of several markers of oxidative stress and of inflammation in skin of rats locally exposed to ionizing radiation. Typically, hairless rats were exposed at posterior legs level, to X-ray doses ranging from 0 to

30 Gy. The level of antioxidant enzymes SOD, Cat, Gpx and the level of oxidized and total glutathione level together with MDA were measured in both epidermis and dermis. The presence of Myeloperoxidase, a marker of inflammation, was investigated by immunostaining and TNF-alpha, a pro-inflammatory cytokine, was also quantified. At last, 8-OxodGuo level, a marker of oxidative stress, was determined in DNA of blood lymphocytes. All these parameters were studied in regards of clinical signs.

In this respect, changes in blood cells concentration consisted of a decrease in blood lymphocytes and granulocytes concentration and few days later in thrombocytes concentration. These changes participated to the haematological syndrome. We may consider, under our experimental conditions, that all blood cells have been irradiated during their passage in the irradiation field, and that the quarter or the third of bone marrow was irradiated since femurs were exposed. However, considering life span of blood cells and considered time course, decrease was due to death of circulating cells or sequestering by tissue, more than to death of genitor cells.

Visible clinical symptoms consisting of erythematic reaction were visible as soon as day 7 and day 12 post-irradiation in 30 Gy- and 20 Gy-irradiated rats. Erythema evolved into moist desquamation only in the most irradiated group two weeks after irradiation, whereas a slight dry desquamation was observed in 20 Gy. Interestingly, as soon as day 15, onset of healing was observed and almost achieved on day 30. These modifications in skin lesions may be correlated to inflammatory process together with modification of enzymatic activities or non enzymatic level.

Indeed, MPO immunostaining was shown to be present in irradiated tissue with a maximal level two days after irradiation suggesting presence of neutrophilic polymorphonuclear leukocytes participating to inflammation. Concomitant oxidative damage to DNA of circulating lymphocytes, and peroxidation of lipids constituting exposed skin was also observed. The origin of such lesions might not be due to irradiation itself because such damage are repaired in the hours following irradiation. Then, one possible origin might be oxidative stress associated to inflammatory process. Another marker of inflammation, namely TNF-α level was also shown to strongly increase in both epidermis and dermis, but only from day 12 (in 30 Gy-irradiated rats) to day 30 for the three irradiation doses. Such development of inflammatory process might also be correlated to oxidation of reduced glutathione into its oxidized form and to modulation of enzymatic response.

Measurement of antioxidant enzymes activities in both epidermis and dermis homogenates showed modifications according to time after irradiation and to irradiation dose.

Unexpectedly, epidermis and dermis responses to irradiation were shown to be associated to a decrease in catalase and to a small raise (although non significant) in GPx activities. The origin of the modifications in antioxidant enzyme activities remains unclear. One would expect an increase in antioxidant enzyme activity to counteract formation of reactive oxygen species. However, previous studies dealing for most of them with superoxide dismutase, indicated a contradictory effects of ionizing radiation on antioxidant enzymes depending on cell types used and on doses applied (Akashi *et al*., 1995; Joksic *et al*., 2000; Pajovic et al., 2000). In addition, studies based on UVA and UVB radiation which are not ionizing radiation but nevertheless at the origin of reactive oxygen species, also indicated modifications in catalase, SOD which were shown to depend on nature of irradiation (chronic or acute) and on nature of irradiation (UVA or UVB). However, no changes in GPx activities were determined (Pence and Naylor, 1990; Okada *et al*., 1994; Shindo and Hashimoto, 1997). In the present study, the main significant modifications in antioxidant enzymatic concerned SOD activity. A strong decrease was thus observed in dermis during the first two weeks with the lowest values measured on days 1 and 12. For 20 Gy and 30 Gy-irradiated groups this level was maintained until day 30 before a strong increase was observed. This depletion in dermal SOD might be connected to development of dry and moist desquamation, apparent on day 12 in the most irradiated groups, and return of SOD to normal values is concomitant with ongoing healing on day 30. In the same way, lack of visible clinical signs at skin level of 10 Gy-irradiated rats group could be correlated to much less severe decrease in SOD activity. By contrast in epidermis, changes are less radical and even appear to be contrary with a strong increase in SOD activity on days 2 and 30. In such a case, correlation with clinical signs is not obvious. It was also shown that TNF-alpha and other cytokines induce increase in MnSOD *in vitro* and *in vivo* (Golstein *et al*., 1991) so that return to control values on day 30 might be due to strong increase in TNF-α observed on day 12.

In addition, time course of events must be taken into account and connected to the period of observation. In this respect, a second decrease in SOD activity was for example observed in 10 Gy-irradiated rats, and subsequent clinical consequences might only be expressed more than one month after irradiation. Therefore, they would be out of the frame of the present study and would require investigation of oxidative stress parameters in view of clinical signs several weeks to months after irradiation. Nevertheless, our results clearly indicate that oxidative stress in involved in onset of skin radiation injury. To precise role of SOD, it would be interesting in further work to assess the effect of SOD administration on such a decrease and on radiological cutaneous syndrome development. It was demonstrated in *in vitro* study

that administration of liposomal bovine SOD was accompanied with a phenotypic reversion of fibroblasts implicated in fibrosis and subsequent proliferation arrest and onset of differentiation (Delanian *et al*., 2001). In addition, antioxidant therapies based on bovine or liposomal SOD showed in vivo their effectiveness in reducing radiation-induced fibrosis (Baillet *et al*., 1986; Perdereau *et al*., 1994; Lefaix *et al*., 1999).

Another alternative to SOD might rely on the use of PTX. Indeed, PTX which is an antioxidant methylxanthine and a non-specific phosphodiesterase inhibitor, was shown to act as a radical scavenger (Freitas *et al*., 1995; Horvath *et al*., 2002) and to down-regulate the expression of TNFα and other inflammatory cytokines (Rube *et al*., 2002). PTX could therefore be also an interesting candidate for counteracting the strong increase in TNF-alpha measured between days 12 and 30. PTX was shown to reduce late radiation-induced skin injury in mice (Dion *et al*., 1989) and delayed toxicity in lung of rats (Koh *et al*., 1995). This compound was also shown to induce healing of soft tissue in patients suffering from late radiation necrosis (Dion *et al*., 1990) and to have a significant protective effect against early and late lung radiotoxicity in patients undergoing radiotherapy (Ozturk *et al*., 2004). However, by contrast, no beneficial effects on acute (Dion *et al*., 1989; Ward *et al*., 1992) and late radiation-induced skin injury were observed in other studies (Koh *et al*., 1995; Lefaix *et al*., 1999; Delanian *et al*., 2003).

In conclusion, this study dealt with the effects of X-irradiation delivered to posterior legs of hairless rats in range of dose between 0 and 30 Gy. Antioxidant enzymatic and non enzymatic defence levels together with several markers of inflammation were measured over one month after irradiation. If inflammatory process were shown to take place all over the considered period, main modifications in enzyme activity concerned dermal SOD which was shown to drastically decrease and was connected to alteration of clinical signs. However, the time course of the present study needs to be extended from one to several months, and the precise role of depletion in SOD as an initiating event in radiation skin injury needs to be clarified. In this respect, therapeutic approach based onto SOD administration could be of major interest.

Acknowledgements

This work was supported by EDF-Service de Radioprotection and Région Ile-de-France.

References

Aebi, H. (1984). "Catalase in vitro." Methods Enzymol **105**: 121-6.

Akashi, M., M. Hachiya, et al. (1995). "Irradiation increases manganese superoxide dismutase mRNA levels in human fibroblasts. Possible mechanisms for its accumulation." J Biol Chem **270**(26): 15864-9.

Archambeau, J. O., R. Pezner, et al. (1995). "Pathophysiology of irradiated skin and breast." Int J Radiat Oncol Biol Phys **31**(5): 1171-85.

Baillet, F., M. Housset, et al. (1986). "Treatment of radiofibrosis with liposomal superoxide dismutase. Preliminary results of 50 cases." Free Radic Res Commun **1**(6): 387-94.

Delanian, S., A. Bravard, et al. (2001). "In vitro modulation by liposomal superoxide dismutase of the fibroblast phenotype in human skin with chronic radiotherapy damage." Radiother Oncol **58**: 325-31.

Delanian, S., J. Depondt, et al. (2005). "Major healing of refractory mandible osteoradionecrosis after treatment combining pentoxifylline and tocopherol: a phase II trial." Head Neck **27**(2): 114-23.

Delanian, S. and J.-L. Lefaix (2004). "The radiation-induced fibroatrophic process: therapeutic perspective via the antioxidant pathway." Radiother Oncol **73**: 119-131.

Delanian, S. and J. L. Lefaix (2002). "Complete healing of severe osteoradionecrosis with treatment combining pentoxifylline, tocopherol and clodronate." Br J Radiol **75**(893): 467-9.

Delanian, S., R. Porcher, et al. (2003). "Randomized, placebo-controlled trial of combined pentoxifylline and tocopherol for regression of superficial radiation-induced fibrosis." J Clin Oncol **21**(13): 2545-50.

Dion, M. W., D. H. Hussey, et al. (1990). "Preliminary results of a pilot study of pentoxifylline in the treatment of late radiation soft tissue necrosis." Int J Radiat Oncol Biol Phys **19**(2): 401-7.

Dion, M. W., D. H. Hussey, et al. (1989). "The effect of pentoxifylline on early and late radiation injury following fractionated irradiation in C3H mice." Int J Radiat Oncol Biol Phys **17**(1): 101-7.

Dubray, B., S. Delanian, et al. (1997). "[Late effects of mammary radiotherapy on skin and subcutaneous tissues]." Cancer Radiother **1**(6): 744-52.

Flohe, L. and F. Otting (1984). "Superoxide dismutase assays." Methods Enzymol **105**: 93-104.

Freitas, J. P., P. Filipe, et al. (1995). "[Potential antioxidative effects of pentoxifylline]." C R Seances Soc Biol Fil **189**(3): 401-5.

Golstein, P., D. M. Ojcius, et al. (1991). "Cell death mechanisms and the immune system." Immunol Rev **121**: 29-65.

Horvath, B., Z. Marton, et al. (2002). "In vitro antioxidant properties of pentoxifylline, piracetam, and vinpocetine." Clin Neuropharmacol **25**(1): 37-42.

Joksic, G., S. B. Pajovic, et al. (2000). "Chromosome aberrations, micronuclei, and activity of superoxide dismutases in human lymphocytes after irradiation in vitro." Cell Mol Life Sci **57**(5): 842-50.

Koh, W. J., K. J. Stelzer, et al. (1995). "Effect of pentoxifylline on radiation-induced lung and skin toxicity in rats." Int J Radiat Oncol Biol Phys **31**(1): 71-7.

Lefaix, J. L., S. Delanian, et al. (1999). "Striking regression of subcutaneous fibrosis induced by high doses of gamma rays using a combination of pentoxifylline and alpha-tocopherol: an experimental study." Int J Radiat Oncol Biol Phys **43**(4): 839-47.

Lord-Fontaine, S. and D. A. Averill-Bates (2002). "Heat shock inactivates cellular antioxidant defenses against hydrogen peroxide: protection by glucose." Free Radic Biol Med **32**(8): 752-65.

Okada, K., Y. Takahashi, et al. (1994). "Time-dependent effect of chronic UV irradiation on superoxide dismutase and catalase activity in hairless mice skin." J Dermatol Sci **8**(3): 183-6.

Ozturk, B., I. Egehan, et al. (2004). "Pentoxifylline in prevention of radiation-induced lung toxicity in patients with breast and lung cancer: a double-blind randomized trial." Int J Radiat Oncol Biol Phys **58**(1): 213-9.

Pajovic, S. B., G. Joksic, et al. (2000). "Role of antioxidant enzymes in radiosensitivity of human blood cells." J Environ Pathol Toxicol Oncol **19**(4): 325-31.

Pence, B. C. and M. F. Naylor (1990). "Effects of single-dose ultraviolet radiation on skin superoxide dismutase, catalase, and xanthine oxidase in hairless mice." J Invest Dermatol **95**(2): 213-6.

Perdereau, B., F. Campana, et al. (1994). "[Superoxide dismutase (Cu/Zn) in cutaneous application in the treatment of radiation-induced fibrosis]." Bull Cancer **81**(8): 659-69.

Peters, L. J. and H. R. Withers (1982). "Critique of "Radiobiological basis of total body irradiation with different dose rate and fractionation: repair capacity of hemopoietic cells"." Int J Radiat Oncol Biol Phys **8**(10): 1819-20.

Pouget, J. P., S. Frelon, et al. (2002). "Formation of modified DNA bases in cells exposed either to gamma radiation or to high-LET particles." Radiat Res **157**(5): 589-95.

Pouget, J. P., C. Laurent, et al. (2004). "PCC-FISH in skin fibroblasts for local dose assessment: biodosimetric analysis of a victim of the Georgian radiological accident." Radiat Res **162**(4): 365-76.

Robbins, M. E. and W. Zhao (2004). "Chronic oxidative stress and radiation-induced late normal tissue injury: a review." Int J Radiat Biol **80**(4): 251-9.

Rube, C. E., F. Wilfert, et al. (2002). "Modulation of radiation-induced tumour necrosis factor alpha (TNF-alpha) expression in the lung tissue by pentoxifylline." Radiother Oncol **64**(2): 177-87.

Rudolph, R., J. Vande Berg, et al. (1988). "Slowed growth of cultured fibroblasts from human radiation wounds." Plast Reconstr Surg **82**(4): 669-77.

Shindo, Y. and T. Hashimoto (1997). "Time course of changes in antioxidant enzymes in human skin fibroblasts after UVA irradiation." J Dermatol Sci **14**(3): 225-32.

Ward, W. F., Y. T. Kim, et al. (1992). "Pentoxifylline does not spare acute radiation reactions in rat lung and skin." Radiat Res **129**(1): 107-11.

Legends

Figures legends

Figure 1. Picture of posterior legs of rats exposed to X-irradiation. Pictures were taken 7 days after irradiation at 10 Gy (A), 20 Gy (B), 30 Gy (C), 12 days after irradiation at 10 Gy (D), 20 Gy (E), 30 Gy (F) or 30 days after irradiation at 10 Gy (G), 20Gy (H), 30 Gy (I). No clinical signs are visible in 10 and 20 Gy irradiation groups 7 days after irradiation whereas erythema appears in rats exposed to 30 Gy. Erythema in rats exposed to 20 Gy, and moist desquamation in rats exposed to 30 Gy are visible on day 12. No clinical signs are visible on day 30 in 10 Gy and 20 Gy groups and healing is observed in 30 Gy-irradiated rats.

Figure 2. Blood lymphocytes concentration in rats locally irradiated at 0, 10, 20 and 30 Gy. Concentration in lymphocytes is normalised to 1 10^9 cells/L for controls. Values are means ± SEM (three experiments). *$p < .05$ vs. control (t-test).

Figure 3. SOD activity in epidermis (A) and dermis (B) of rats exposed locally to irradiation dose of 0, 10, 20 or 30 Gy. SOD activity was measured as previously described in epidermis and dermis homogenates. Values are compared with control values. Values are means ± SEM (three experiments). *$p < .05$ vs. control (t-test).

Figure 4. Catalase activity in epidermis (A) and dermis (B) of rats exposed locally to irradiation dose of 0, 10, 20 or 30 Gy. Catalase activity was measured as previously described in epidermis and dermis homogenates. Values are compared with control values. Values are means ± SEM (three experiments). *$p < .05$ vs. control (t-test).

Figure 5. GPx activity in epidermis (A) and dermis (B) of rats exposed locally to irradiation dose of 0, 10, 20 or 30 Gy. GPx activity was measured in epidermis and dermis homogenates as described in Materials and Methods section. Values are compared with control values. Values are means ± SEM (three experiments). *$p < .05$ vs. control (t-test).

Figure 6. Formation of 8-oxodGuo in DNA of blood lymphocytes of rats locally exposed to irradiation doses of 0, 10, 20 or 30 Gy. 8-oxodGuo level was quantified by HPLC-

MS/MS after DNA extraction(Helbock et al., 1998). Values are compared with control values. Values are means ± SEM (three experiments). *p < .05 vs. control (t-test).

Figure 7. TNFα measurement in epidermis (A) and dermis (B) of rats exposed locally to irradiation dose of 0, 10, 20 or 30 Gy. TNFα was assayed by ELISA. Values are compared with control values. Values are means ± SEM (three experiments). *p < .05 vs. control (t-test).

Figure 8. MPO immunostaining performed two days after irradiation on skin exposed to irradiation dose of 30 Gy.

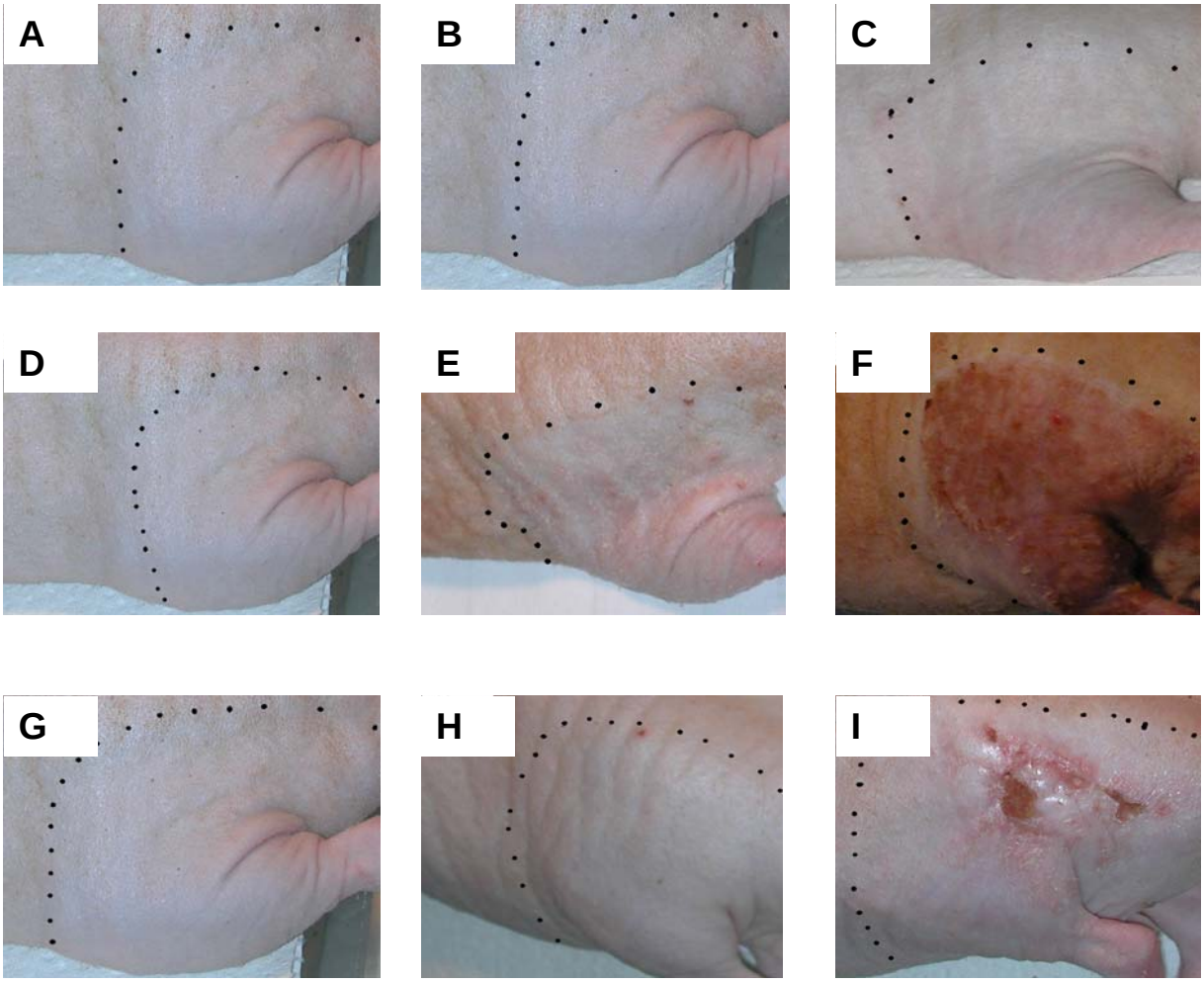

Figure 1

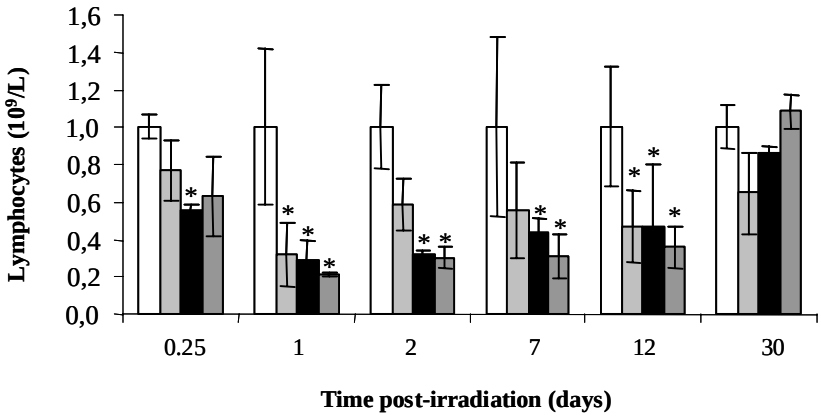
1,6
1,4
1,2
1,0
0,8
0,6
0,4
0,2
0,0
Lymphocytes (10^9/L)
0.25
1
2
7
12
30
Time post-irradiation (days)

Figure 2

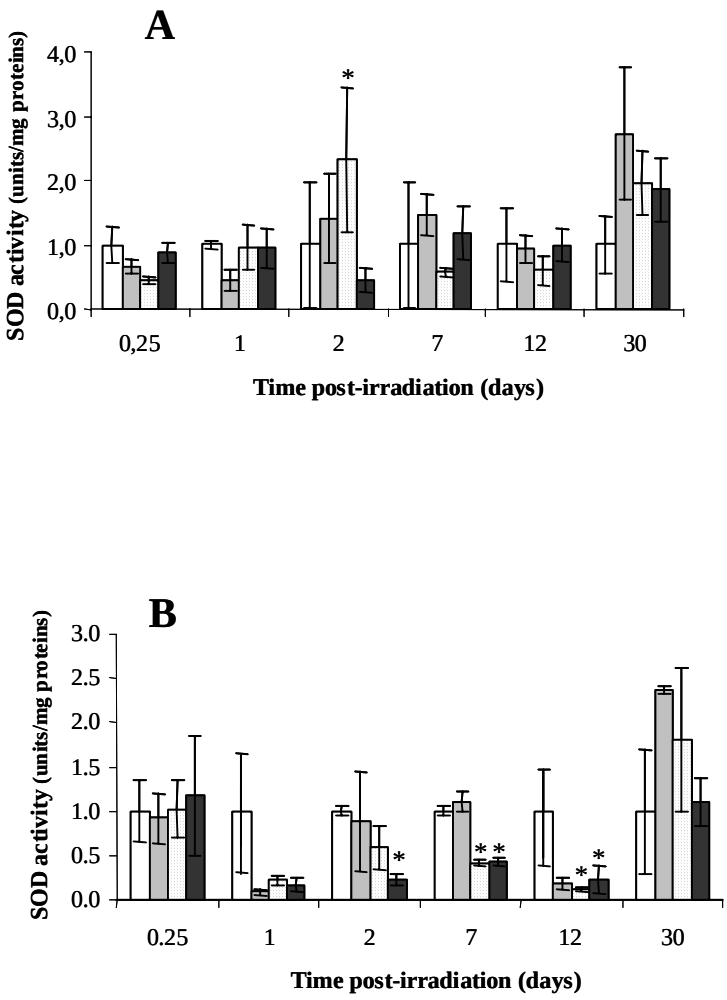
A
SOD activity (units/mg proteins)
4,0
3,0
2,0
1,0
0,0
*
0,25
1
2
7
12
30
Time post-irradiation (days)
B
SOD activity (units/mg proteins)
3.0
2.5
2.0
1.5
1.0
0.5
0.0
* * *
0.25
1
2
7
12
30
Time post-irradiation (days)

Figure 3

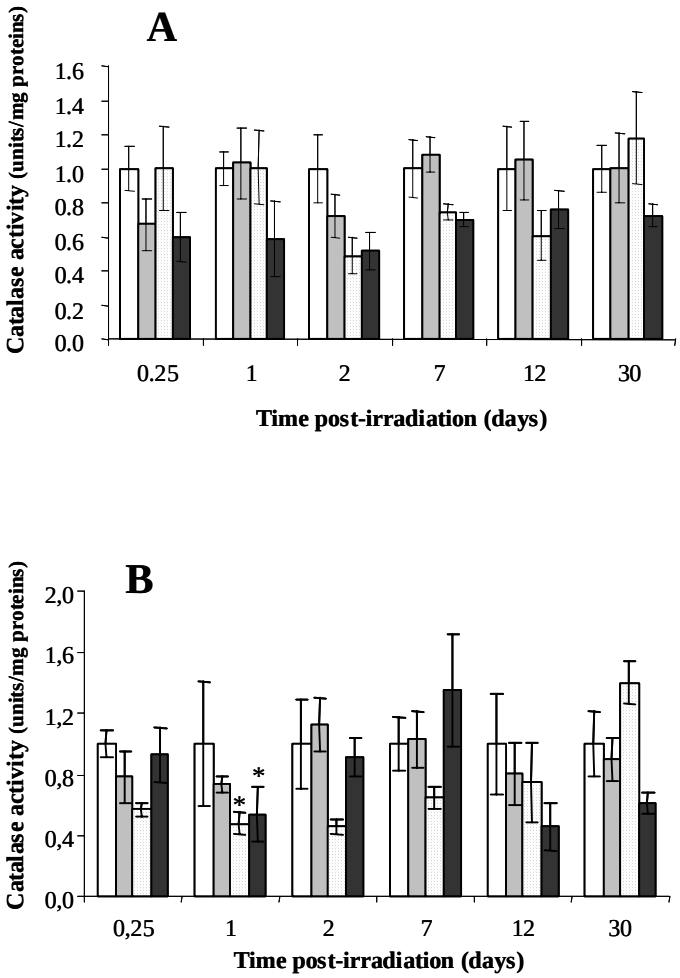
A
Catalase activity (units/mg proteins)
1.6
1.4
1.2
1.0
0.8
0.6
0.4
0.2
0.0
0.25
1
2
7
12
30
Time post-irradiation (days)
B
Catalase activity (units/mg proteins)
2,0
1,6
1,2
0,8
0,4
0,0
0,25
1
2
7
12
30
Time post-irradiation (days)

Figure 4

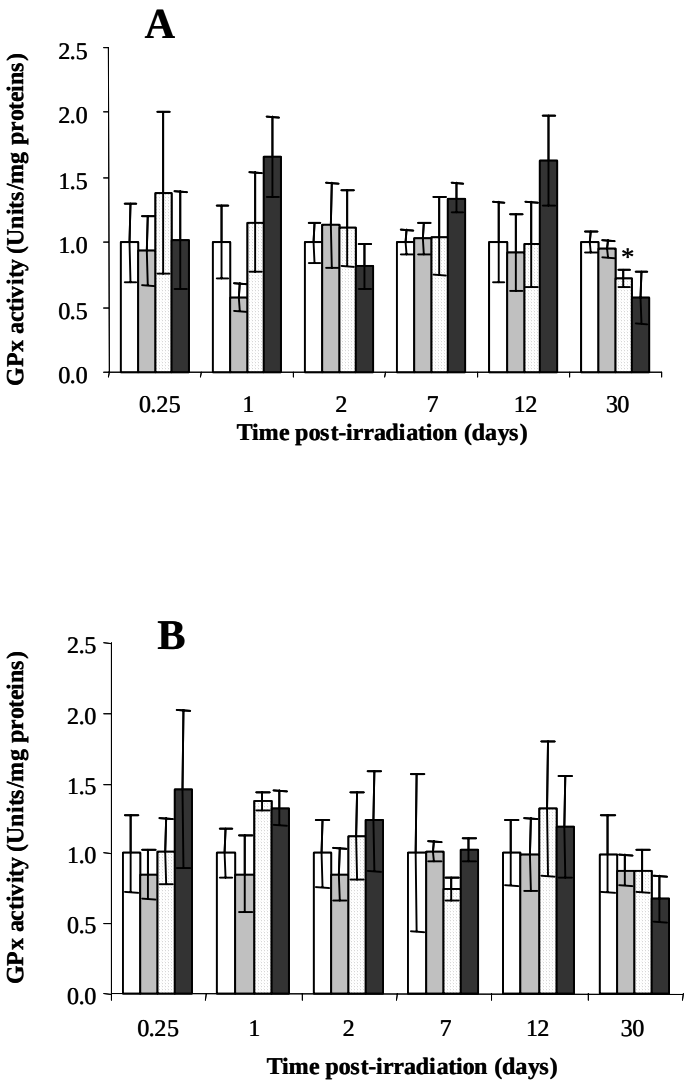
A
GPx activity (Units/mg proteins)
2.5
2.0
1.5
1.0
0.5
0.0
*
0.25
1
2
7
12
30
Time post-irradiation (days)
B
GPx activity (Units/mg proteins)
2.5
2.0
1.5
1.0
0.5
0.0
0.25
1
2
7
12
30
Time post-irradiation (days)

Figure 5

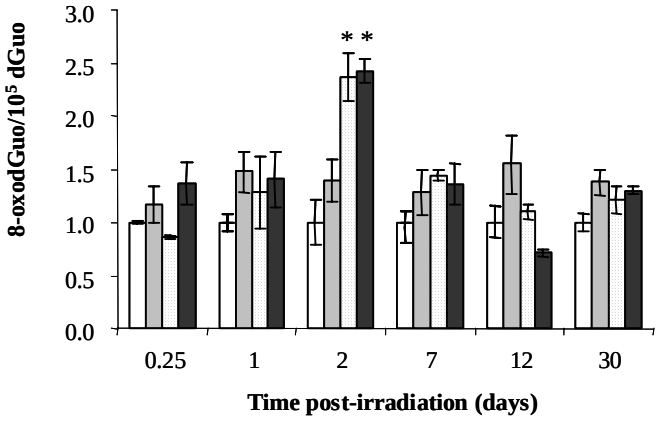
8-oxodGuo/10^5 dGuo
3.0
2.5
2.0
1.5
1.0
0.5
0.0
* *
0.25
1
2
7
12
30
Time post-irradiation (days)

Figure 6

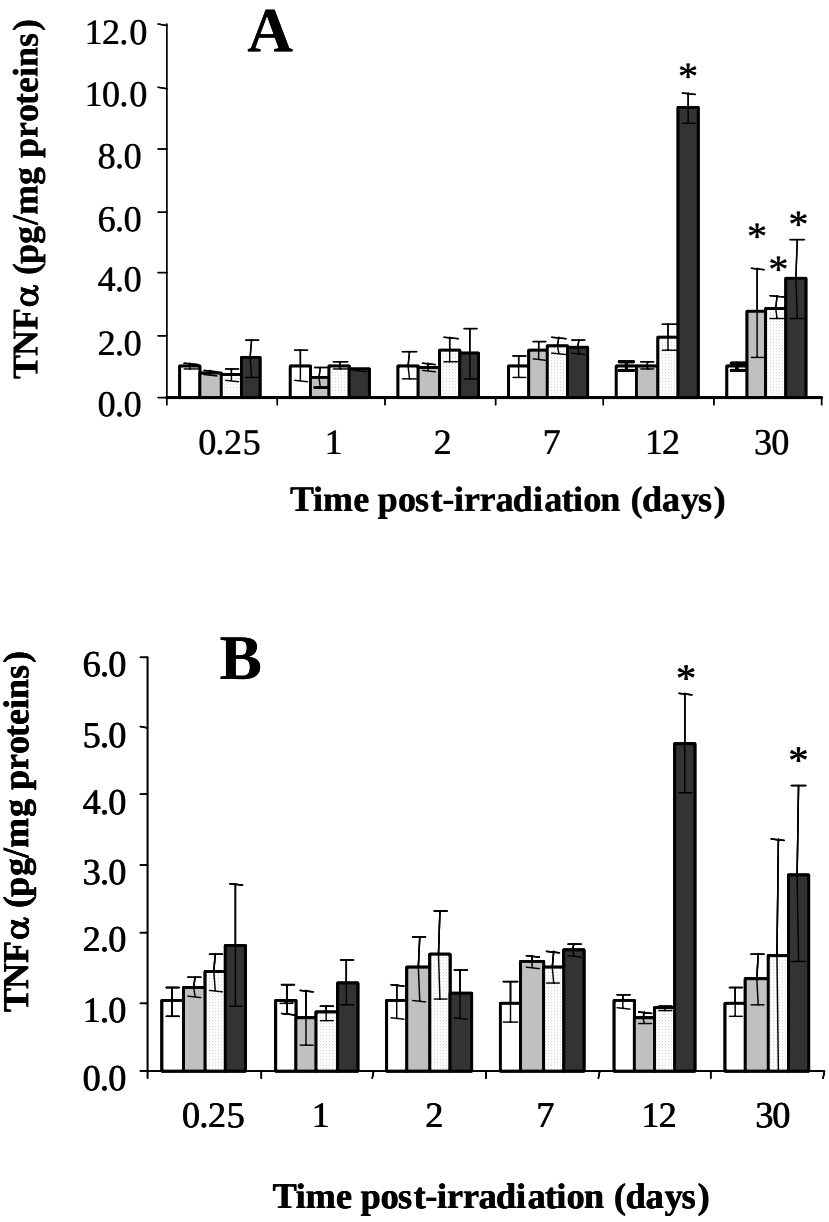
A
TNFα (pg/mg proteins)
12.0
10.0
8.0
6.0
4.0
2.0
0.0
0.25
1
2
7
12
30
Time post-irradiation (days)
B
TNFα (pg/mg proteins)
6.0
5.0
4.0
3.0
2.0
1.0
0.0
0.25
1
2
7
12
30
Time post-irradiation (days)

Figure 7

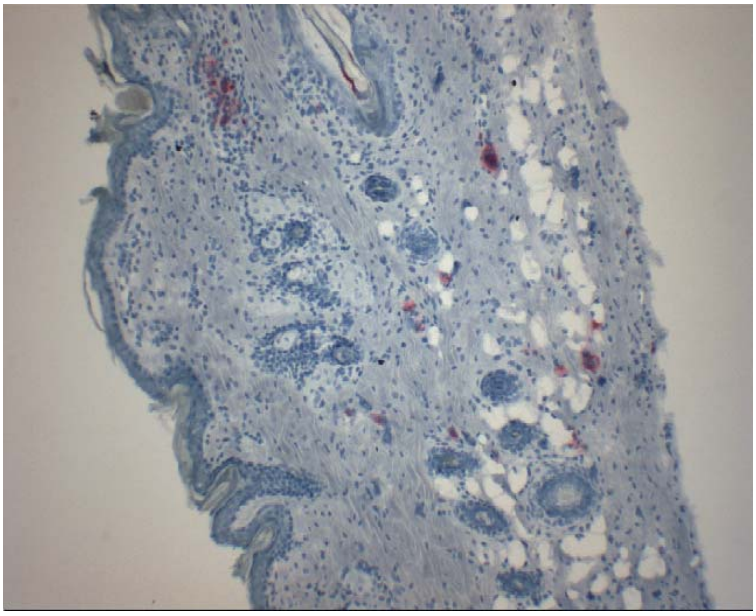

Figure 8

Table 1: Time course of ratio GSSG/Total glutathione in epidermis of locally X-irradiated rats. GGSG and total GSH were measured as described in Materials and Methods and ratio was then calculated.

	Time post-irradiation (days)					
Dose (Gy)	**0.25**	**1**	**2**	**7**	**12**	**30**
0 Gy	1.00±0.1	1.00±0.16	1.00±0.10	1.00±0.04	1.00±0.10	1.00±0.20
10 Gy	1.08±0.04	1.51±0.23	1.25±0.15	1.70±0.35	1.04±0.15	1.81±0.15
20 Gy	0.61±0.09	1.16±0.10	1.44±0.10	2.52±0.20	0.82±0.12	1.76±0.10
30 Gy	1.16±0.07	1.67±0.26	1.18±0.07	2.08±0.39	1.20±0.13	1.53±0.12

Table 2: Time course of ratio GSSG/Total glutathione in dermis of locally X-irradiated rats. GGSG and total GSH were measured as described in Materials and Methods and ratio was then calculated.

	Time post-irradiation (days)					
Dose (Gy)	**0.25**	**1**	**2**	**7**	**12**	**30**
0 Gy	1.00±0.12	1.00±0.17	1.00±0.14	1.00±0.13	1.00±0.20	1.00±0.09
10 Gy	1.43±0.08	1.80±0.29	1.28±0.27	1.90±0.28	0.73±0.11	1.26±0.12
20 Gy	1.20±0.04	1.19±0.17	1.34±0.38	2.31±0.09	0.94±0.15	1.20±0.13
30 Gy	1.37±0.18	4.29±0.04	0.93±0.26	2.03±0.06	0.77±0.20	1.03±0.17

Table 3: Qualitative assessment of MPO staining. Number medium of spots was calculated/analysed slide and the mean number was calculated from three different slides. Immunostaining magnitude varied from absence of signal (-) in control group to strong signal (+++++++) in 30Gy-irradiated group.

	Time post-irradiation (days)				
dose (Gy)	**0,25**	**2**	**7**	**12**	**30**
0	**-**	**-**	**-**	**-**	**-**
10	**+++**	**+++**	**++**	**-**	**-**
20	**+**	**+++**	**-**	**+++**	**+**
30	**++++**	**+++++++**	**-**	**-**	**-**

II- Mise en place des modèles cellulaires, choix des doses d'irradiation et de la concentration en traitement

1. Caractérisation et mise en place des modèles cellulaires

Cultures primaires de fibroblastes de derme

Les cultures primaires de fibroblastes de derme (NHF-d, normal human fibroblasts from dermis) à partir d'explants de peau humaine ont été mises en place dans le cadre de la dosimétrie biologique appliquée aux fibroblastes isolés à partir de biopsies de peau (article 1). Ces dernières proviennent d'adultes sains (BIO-EC, Clamart) consentants de type caucasien ayant subi une chirurgie plastique (réduction mammaire ou abdominale). Brièvement, le derme est séparé de l'épiderme à l'aide d'un scalpel et digéré dans trois bains successifs de trypsine/collagénase P (0,5%/0,25%). La suspension cellulaire est collectée et resuspendue dans du DMEM supplémenté (20% SVF, 100 µg/ml L-glutamine, 10 mM HEPES, 100 unités/ml pénicilline, 100 µg/ml streptomycine). Les cellules sont ensuite ensemencées dans des flacons de cultures recouverts de collagène I et cultivées à 37°C dans une atmosphère humidifiée avec 5% de CO_2 jusqu'au premier passage.

Cultures primaires de cellules endothéliales de microvascularisation de derme

Différents essais de cultures primaires de cellules endothéliales de microvascularisation du derme (HMVEC-d, human microvascular endothelial cells from dermis) ont été effectués.
Plusieurs méthodes de dissociation de la peau ont ainsi été testées : trypsine, trypsine/collagénase, pendant différents temps et à différentes températures.
Après obtention de l'homogénat de derme, différentes méthodes ont été utilisées pour sélectionner les cellules endothéliales :

- sélection positive par le système MACS (Miltenyi Biotec, Paris) grâce aux anticorps CD105 : la sélection est effectuée après dissociation ou après différents temps de culture ou après plusieurs passages,
- adhésion différentielle, etc.

Les résultats les plus intéressants sont présentés sur la Figure 1 :

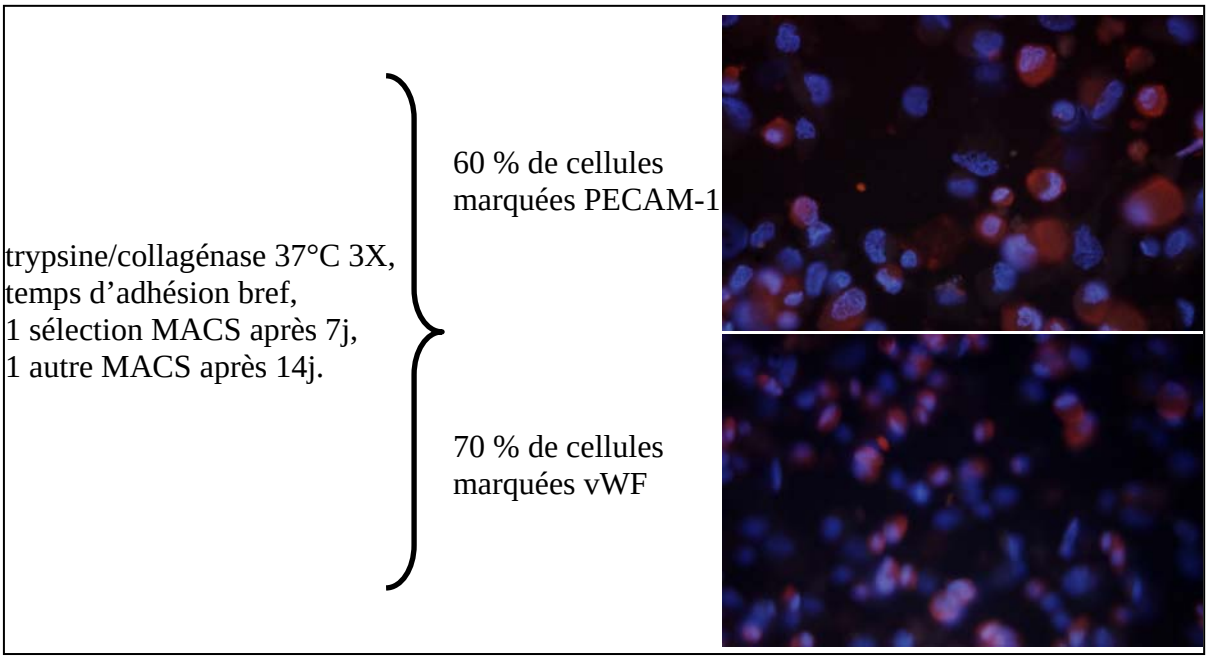

Figure 1. Marquage par PECAM et vWF des cellules endothéliales de microvascularisation de derme obtenues après isolement et sélection (MACS, Miltenyi Biotec).

Le pourcentage de cellules endothéliales obtenu montre que cette méthode ne permet pas de disposer de cultures primaires de cellules endothéliales à partir d'explants de peau. En effet, le pourcentage de cellules endothéliales ne dépasse pas 70% 14 jours après sélection. Le reste de la population étant majoritairement constitué de fibroblastes, ceux-ci vont rapidement envahir la culture.

Nous avons testé un second modèle de cellules endothéliales : des cellules humaines provenant de la microvascularisation (HMEC) et transformées par l'antigène T de SV40.
Cependant, ce modèle s'est révélé inadéquat pour les raisons suivantes :

- la morphologie des HMEC transformées est plus proche de celle des fibroblastes que des cellules endothéliales primaires,

- les HMEC ne présentent ni de marquage vWF, ni de marquage PECAM-1 comme présenté Figure 2.

Nous avons donc choisi d'utiliser des cellules endothéliales primaires d'origine commerciale : les cellules endothéliales de la microvascularisation du derme provenant d'adultes sains de type caucasien (Cambrex, Verviers, Belgique).

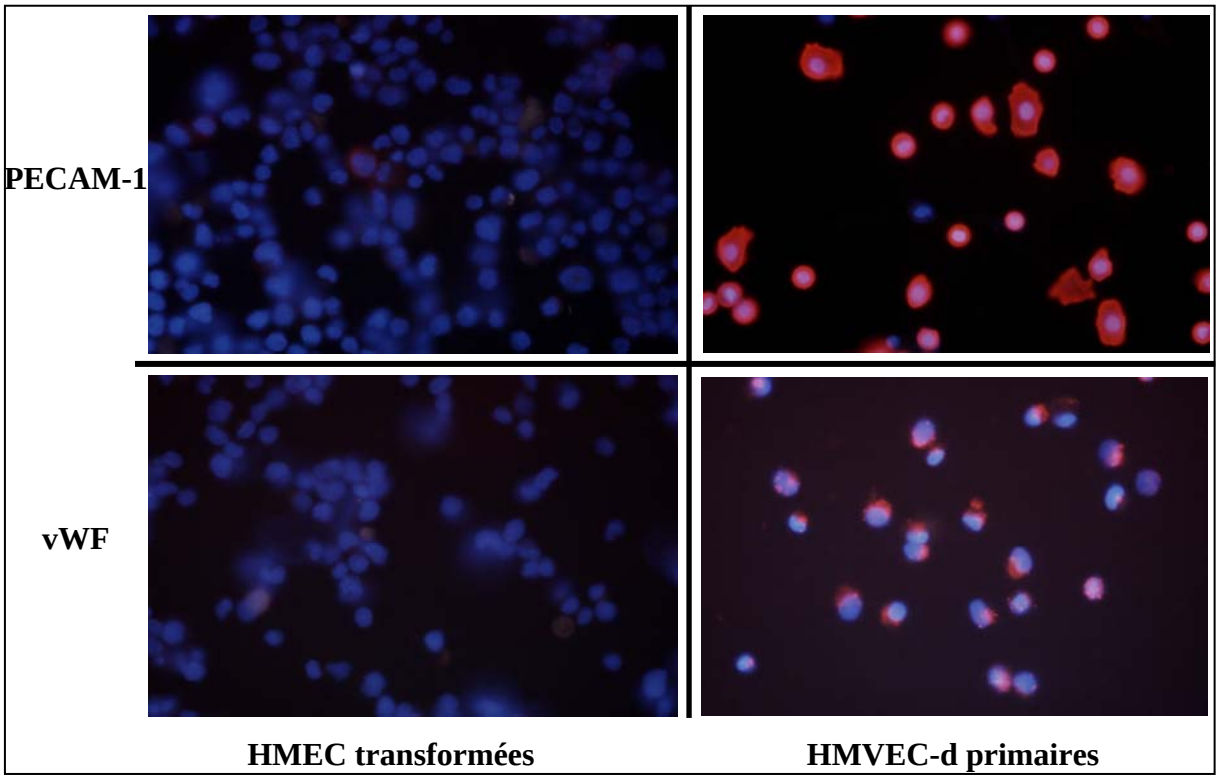

Figure 2. Marquages vWF et PECAM-1 dans les cellules endothéliales primaires et transformées.

2. Choix des doses d'irradiation

Les doses d'irradiation sont : 0 Gy, 3 Gy et 10 Gy. Celles-ci ont été choisies sur la base des données de la littérature et de nos résultats de survie clonogénique (Figure 3).

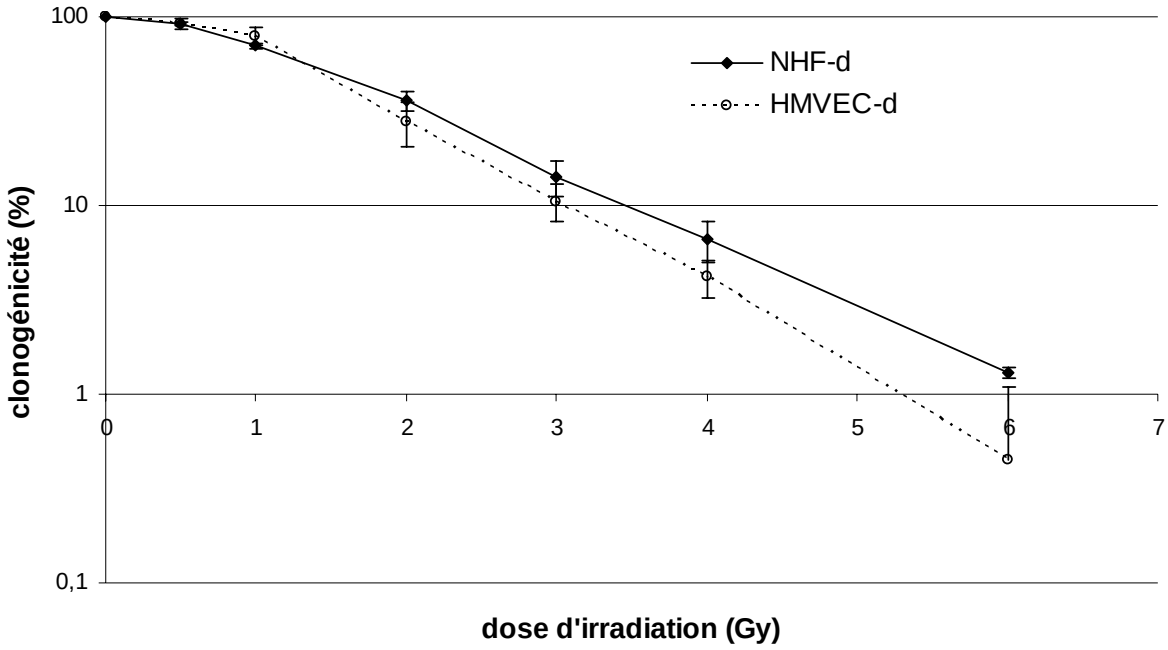

Figure 3. Courbes de survie clonogénique des cultures primaires de fibroblastes (NHF-d) et de cellules endothéliales de la microvascularisation (HMVEC-d) de derme.

Les D_0 obtenues sont en accord avec celles données dans la littérature : D_0 HMVEC-d = 1,5 Gy et D_0 NHF-d = 1,7 Gy.

Ces courbes de clonogénicité ont mis en évidence que la dose pour laquelle 10% des cellules sont encore capables de proliférer est de 3 Gy.

La dose d'irradiation de 10 Gy a été choisie pour se placer dans le domaine de doses des surexpositions accidentelles. A 10 Gy, les fibroblastes et les cellules endothéliales ne sont plus capables de proliférer.

3. Choix de la concentration en traitement

Les concentrations en pentoxifylline et en α-tocophérol ont été choisies d'après les données de la littérature et de façon à être non cytotoxique, non génotoxique et anti-oxydant.

Les courbes de cytotoxicité ont montré une DL_{50} de 6,7 mM pour la pentoxifylline (PTX) et de 7,2 mM pour le trolox (Tx) (Figure 4), l'analogue hydrosoluble de l'α-tocophérol, dans les fibroblastes. Concernant les cellules endothéliales, les DL_{50} sont beaucoup plus basses avec 1,2 mM pour PTX et 1,7 mM pour Tx.

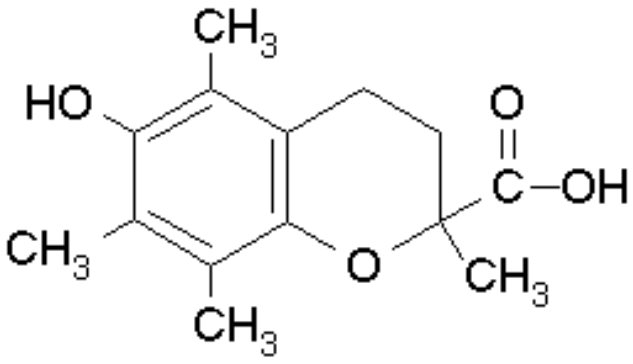

Figure 4. Structure du Trolox.

Le test ORAC, qui mesure la capacité anti-oxydante des drogues en absence du contexte cellulaire, a montré que le pouvoir anti-oxydant maximal était obtenu pour la concentration de 0,5 mM pour les deux drogues utilisées séparément ou ensemble (cf article 3 et article 5).

La concentration en PTX et Tx retenue est donc 0,5 mM pour les deux drogues qu'elles soient utilisées seules ou en association.

III- Phénomènes oxydatifs radio-induits et leur modulation par l'association PTX/Tx dans les fibroblastes et les cellules endothéliales cutanés

Article 3 : Modulation des lésions de l'ADN par la pentoxifylline et l'alpha-tocophérol dans les fibroblastes de peau exposés au rayonnement gamma

Cet article a pour objectif d'évaluer les phénomènes oxydatifs dans les cultures primaires de fibroblastes de derme conduisant à la production d'ERO (Espèces Réactives de l'Oxygène) et à la formation de lésions de l'ADN. L'accumulation de lésions de l'ADN peut être responsable d'une mort mitotique décalée dans le temps. En parallèle, nous avons évalué l'effet du traitement pentoxifylline et α-tocophérol, très efficace *in vivo*, sur la production de ces phénomènes oxydatifs.

Les fibroblastes confluents ont été irradiés au ^{137}Cs et le traitement pentoxifylline et trolox, l'analogue hydrosoluble de l'α-tocophérol, a été administré 15 minutes avant, 30 minutes après ou 24 heures après irradiation.
Le niveau d'ERO, mesuré grâce au test du DCFH-DA, évolue par phases après l'irradiation. Le taux de formation des micronoyaux, lésions considérées comme résultant d'une mauvaise réparation des CDB (Cassures Double-Brins), augmente aux temps tardifs (14 et 21 jours) après irradiation à 10 Gy alors qu'aucune formation de dommages de l'ADN n'a été mise en évidence par la technique des comètes en milieu alcalin. Ces résultats suggèrent une mauvaise réparation des CDB à 10 Gy.
Le traitement PTX/Tx a conduit à la diminution de la production d'ERO immédiatement et tardivement après irradiation. Par ailleurs, il conduit à une diminution du niveau basal mesuré dans les cellules contrôles. Le même effet a été observé même lorsque le traitement a été administré après l'irradiation. Une diminution du niveau des lésions de l'ADN a été mesurée que le traitement soit administré avant ou après irradiation. Toutefois, elle s'accompagne d'une augmentation tardive du taux de micronoyaux dans les cellules irradiées à 10 Gy. Le traitement pourrait donc interférer avec les mécanismes de réparation des lésions de l'ADN. De plus, ces phénomènes seraient assez tardifs puisque le traitement administré 24 heures après irradiation conduit à la même augmentation du taux des micronoyaux.

Cet article met en évidence la présence de phénomènes oxydatifs par phases successives dans les cultures primaires confluentes de fibroblastes de derme exposées au rayonnement gamma. Ces phénomènes oxydatifs peuvent être partiellement inhibés par le traitement PTX/Tx. Un niveau élevé de formation de micronoyaux persiste plusieurs semaines après exposition à de fortes doses d'irradiation et le traitement en augmente l'ampleur. Une étude plus précise du taux de formation des CDB est nécessaire.

RADIATION RESEARCH 164, 63–72 (2005)
0033-7587/05 $15.00

Modulation of DNA Damage by Pentoxifylline and α-Tocopherol in Skin Fibroblasts Exposed to Gamma Rays

Carine Laurent,[a] Jean-Pierre Pouget[b,c,1] and Philippe Voisin[c]

[a] *Laboratoire de Dosimétrie Biologique, DRPH/SRBE, Institut de Radioprotection et de Sûreté Nucléaire, F-92262 Fontenay-aux-Roses, France;* [b] *Immunociblage des tumeurs et Ingénierie des Anticorps, EMI 0227, INSERM, Centre de Recherche en Cancérologie, CRLC Val d'Aurelle, Institut Paul Lamarque, F-34298 Montpellier, France; and* [c] *Service de Radiobiologie et d'Epidémiologie, DRPH, Institut de Radioprotection et de Sûreté Nucléaire, F-92262 Fontenay-aux-Roses, France*

Laurent, C., Pouget, J-P. and Voisin, P. Modulation of DNA Damage by Pentoxifylline and α-Tocopherol in Skin Fibroblasts Exposed to Gamma Rays. *Radiat. Res.* 164, 63–72 (2005).

Previous *in vivo* studies showed the combination pentoxifylline (PTX) and α-tocopherol was highly efficient in reducing late radiation-induced skin damage. The present work aimed at investigating the molecular and cellular mechanisms involved in the effects of this combination. Primary cultures of confluent dermal fibroblasts were γ-irradiated in the presence of PTX and trolox (Tx), the water-soluble analogue of α-tocopherol. Drugs were added either before or after radiation exposure and were maintained over time. Their antioxidant capacity and their effect on radiation-induced ROS production was assessed together with cell viability and clonogenicity. DNA damage formation was assessed by the alkaline comet assay and by the micronucleus (MN) test. Cell cycle distribution was also determined. The combination of PTX/Tx was shown to reduce both immediate and late ROS formation observed in cells after irradiation. Surprisingly, decrease in DNA strand breaks measured by the comet assay was observed any time drugs were added. In addition, the micronucleus test revealed that for cells irradiated with 10 Gy, a late significant increase in MN formation occurred. The combination of PTX/Tx was shown to be antioxidant and to decrease radiation-induced ROS production. The observed effects on DNA damage at any time the drugs were added suggest that PTX/Tx could interfere with the DNA repair process. © 2005 by Radiation Research Society

INTRODUCTION

High doses of radiation used for cancer therapy or encountered in accidental radiological overexposure may lead to the appearance of the cutaneous radiological syndrome. Such syndrome is characterized by early (rash, desquamation) and delayed cutaneous effects (telangiectasia, fibrosis and necrosis). Their appearance and severity are dependent on time and radiation dose. Although clinical symptoms associated with cutaneous radiological syndrome have been described in detail (*1–3*), the cellular and molecular mechanisms at their origin together with the parameters influencing their appearance have not been clarified. It has long been assumed that radiation-induced late cutaneous injury was due only to the delayed mitotic death of dermal parenchymal (*4*) or vascular cells (*5, 6*), indicating that the lesions were progressive and inevitable. Moreover, recent studies have demonstrated an active role for these cells in the cutaneous response to ionizing radiation exposure (*7–9*). Therefore, dermal cells appeared to be interesting candidates for pharmacological treatments aimed at preventing late radiation injury by modulating events that lead to this injury, such as production of ROS (*2*). Many studies have used antioxidant therapy, and bovine superoxide dismutase (SOD) was shown to induce a fast regression of radiation-induced fibrosis. This was observed in a three-dimensional co-culture model of skin (*10*) in pigs (*11*) and in patients (*12*). However, since bovine SOD could not be used safely in the clinic, research focused on an alternative approach based on the combination of pentoxifylline (PTX) and α-tocopherol, which demonstrated a similar effectiveness but required a longer treatment period.

PTX was first delivered to patients who suffered from vascular disease because of its capacity to improve tissue oxygenation. The molecule is a methylxanthine with a plethora of *in vitro* activities. PTX is a non-specific phosphodiesterase inhibitor that leads to an increased level of cellular cAMP, which is involved in cell signaling. It is a phytochemical antioxidant that acts as a radical scavenger (*13, 14*), and it may regulate the expression of TNFA and other inflammatory cytokines (*15*). In addition, PTX was also shown to affect cellular response to ionizing radiation. It is an inhibitor of radiation-induced G_2 arrest (*16–18*), which may result in radiation sensitization of TP53-deficient tumor cells (*16, 17, 19*). PTX was also shown to inhibit DNA double-strand break (DSB) repair (*19, 20*) and

[1] Address for correspondence: Immunociblage des tumeurs et Ingénierie des Anticorps, EMI 0227, INSERM, Centre de Recherche en Cancérologie, CRLC Val d'Aurelle, Institut Paul Lamarque, F-34298 Montpellier, France; e-mail: jppouget@valdorel.fnclcc.fr.

the *ATM* gene (*21*) and to induce chromosomal aberrations, sister chromatid exchanges, and micronuclei (*22*). *In vivo*, the administration of PTX alone was found to reduce late radiation-induced skin injury in mice (*23*) and late lung toxicity in rats (*24*). Clinical studies showed that it led to the healing of soft tissue in patients suffering from late radiation necrosis (*25*) and has a significant protective effect against early and late lung radiotoxicity in patients undergoing radiotherapy (*26*). However, other studies indicated that PTX had no beneficial effects on acute (*23, 27*) and late radiation-induced skin injury in both rats (*24*) and pigs (*28*) and that radiation-induced fibrosis was not reduced by PTX alone in patients treated by radiotherapy (*29*).

The other compound of interest is α-tocopherol. It is an antioxidant nutrient and a constituent of the vitamin E family, which forms the most important lipid-soluble antioxidant group. Besides its known antioxidant properties, α-tocopherol was shown to inhibit *in vitro* inflammation, cell adhesion, platelet aggregation and smooth muscle cell proliferation; for a review, see ref. (*30*). Its derivatives also exhibited protective effects against DNA damage in irradiated lymphoblastoid cells (*31*). D-Alpha-tocopheryl succinate (αTS) reduced radiation-induced chromosomal damage in normal cells but not in tumor cells (*32*). Few *in vivo* studies have reported the effects of α-tocopherol on radiation-induced injury. However, a water-soluble vitamin E was shown to reduce the number of aberrant metaphases and to decrease micronucleus yield in the bone marrow of mice exposed to radiation (*33, 34*). Clinical trials associated with radiotherapy have shown an improvement in oral mucositis (*35*), but no modification was observed in radiation-induced skin fibrosis (*29*).

When used in combination, PTX and α-tocopherol appeared to be very effective in reducing late radiation-induced skin injuries. This combination was very valuable in provoking the regression of radiation-induced skin fibrosis in irradiated pigs (*28*). Clinical trials on patients undergoing radiotherapy showed that the combination was responsible for a continuous regression of chronic damage (*29, 36*) and for a reduction of radiation-induced fibroatrophic uterine lesions (*37*). When administered with clodronate, the complete reversion of osteoradionecrosis and radiation-induced fibrosis was observed (*38*).

Up to now, the mechanisms underlying the success of the combination of PTX/α-tocopherol have not been elucidated. Our work aimed at investigating the antioxidant properties of the combination of PTX and trolox (Tx), a water-soluble analogue of α-tocopherol, and at assessing its effects on DNA damage in normal human dermal fibroblasts exposed to γ rays. We assessed the effectiveness of the treatment when drugs were administered either before or at different times after radiation exposure. Our results suggest that the combination was an antioxidant and consequently reduced both radiation-induced ROS production and subsequent DNA strand breaks. However, it was also shown to be accompanied by an increase in micronucleus yield and in radiation sensitivity, suggesting that the DNA repair process could be affected by the combination of drugs.

MATERIALS AND METHODS

Reagents

Dulbecco's modified Eagle medium (DMEM), fetal bovine serum (FBS), *N*-(2-hydroxyethyl)piperazine-*N'*-(2-ethanesulfonic acid) (Hepes) buffer, Dulbecco's phosphate-buffered saline (PBS), trypsin/EDTA, L-glutamine, penicillin and streptomycin were purchased from Gibco BRL Life Technologies (Gaithersburg, MD). Collagenase P and alkaline phosphatase were obtained from Roche (Indianapolis, IN). Dichlorodihydrofluorescein diacetate (H_2DCFDA) was purchased from Molecular Probes (Eugene, OR). 2,2′-Azo-bis(2-amidinopropane) dihydrochloride (AAPH) was obtained from Interchim (Montluçon, France). Protease was provided by Qiagen (Hilden, Germany). All others chemicals were purchased from Sigma (St. Louis, MO).

Cell Cultures

Primary cultures of NHF-d dermal fibroblasts (normal human fibroblasts from dermis) were established from skin of two healthy Caucasian women 22 and 40 years old who were undergoing elective surgery (mammary reduction and abdominoplasty, respectively). No significant individual variability in response to treatment and to radiation was observed among isolated fibroblasts. Written consent was obtained from both subjects. Immediately after surgery, collected skin was first dropped into a 5% betadine bath for 15 min and rinsed with PBS. Then epidermis was separated from dermis with a scalpel blade, and the resulting dermal tissue was incubated in three successive baths of trypsin/collagenase P (0.5%/0.25%) at 37°C for 30 min under stirring to isolate cells. Cell suspensions were collected, centrifuged and resuspended in DMEM supplemented with 20% FBS, 100 μg/ml L-glutamine, 10 m*M* Hepes and antibiotics (100 U/ml penicillin and 100 μg/ml streptomycin). Cells were next plated into flasks coated with collagen I and grown at 37°C in a humidified atmosphere of 95% air/5% CO_2 up to the first passage and were then grown in uncoated flasks for the following passages. Experiments were performed when cells reached passage 4–7.

Assay of Oxygen Radical Absorbing Capacity

Antioxidant status was assessed by the oxygen radical absorbing capacity (ORAC) assay as described by Cao *et al.* (*39*) using a spectrofluorimeter (Kontron Instruments, model SFM 25, Germany) with excitation wavelength of 540 nm and emission wavelength of 565 nm. ORAC values were obtained from the area under the quenching curve of β-phycoerythrin in the presence of both the peroxyl radical generator, 2,2′-azobis(2-amidinopropane) dihydrochloride (AAPH), and the molecules studied, PTX and Tx. PTX and Tx were used either separately or together at concentrations ranging from 0.5 to 4 m*M*. One ORAC unit was equal to the antioxidant status of 1 μ*M* trolox as presented by Cao *et al.* (*39*).

Cell Treatment and Gamma Irradiation

Confluent cells were irradiated at room temperature at doses of 0, 3 and 10 Gy using a ^{137}Cs source (IBL 637, Cis bio International) at a dose rate of 1 Gy/min. Pentoxifylline (PTX) and trolox (Tx) were added either before (15 min before) or after (30 min or 24 h) radiation exposure and maintained during the entire period considered (21 days). PTX was first dissolved in water at a concentration of 100 m*M*, and Tx was dissolved in methanol at a concentration of 100 m*M* before dilution in culture medium.

Cell Viability Assay

Cell viability was assessed by the trypan blue exclusion assay on confluent fibroblasts plated in 96-well microplates and exposed to γ rays at doses of 0, 3 or 10 Gy in the presence or absence of PTX/Tx. PTX/Tx was added either 15 min before or 30 min or 24 h after irradiation. Cells were incubated with Trypan blue (0.4%) and scored in a hemocytometer. The percentage of viable cells was expressed as the ratio between cell numbers in irradiated samples and in controls. For each experimental condition, experiments were done in triplicate and repeated three times.

Determination of ROS

Cytoplasmic ROS generation was determined in control fibroblasts and fibroblasts irradiated with 3 and 10 Gy treated or not treated with the combination of PTX/Tx. Drugs were either added 15 min before or 30 min or 24 h after irradiation. Typically, 2′,7′-dichlorofluorescein diacetate (DCFH-DA) was used. DCFH-DA is a permeable compound that penetrates into both the cytoplasm and the nucleus but that can be hydrolyzed only by a cytoplasmic esterase. The hydrolyzed form, DCFH, is nonpermeable and reacts with intracellular ROS to form a fluorescent compound, 2′,7′-dichlorofluorescein (DCF), analyzed by flow cytometry. Fibroblasts were incubated in the presence of 1 μ*M* DCFH-DA for 15 min. They were then trypsinized, washed with PBS and fixed in 1% paraformaldehyde. For measurement of immediate ROS generation, cells were treated with DCFH-DA just before radiation exposure. For each sample, the fluorescence intensity of 10,000 cells was analyzed by flow cytometry using a FACSort (Becton Dickinson). For each experimental condition, the experiments were repeated three times in triplicate.

Clonogenicity

The clonogenicity of the cells was assessed according to the method of Puck and Marcus (*40*). Briefly, a defined number of cells, ranging from 400 to 5000 fibroblasts for radiation doses between 0 and 6 Gy, were plated in 25-cm² tissue culture flasks. Four hours after seeding, cells were irradiated. Drugs were added 15 min before or 30 min or 24 h after irradiation. Cells were then grown for 10 days. Colonies were stained with crystal violet (2.5 g/liter in 45:5 methanol/paraformaldehyde 30%). Those containing 50 or more cells were scored and the surviving fraction was calculated. Experiments were repeated three times in triplicate.

Cell Cycle

The effect of PTX/Tx, which was added 15 min before irradiation, on the movement of control and 10-Gy-irradiated cells through the cell cycle was measured. Typically, since the cells were in plateau phase (93% in G_0/G_1 phase), they were first trypsinized at given times postirradiation, reseeded and grown for 24 h more, corresponding to one population doubling time. They were next trypsinized again, fixed and permeabilized with 70% ice-cold ethanol, and kept overnight at 4°C. Prior to analysis, cells were incubated 30 min at 37°C with RNase A (final concentration 10 μg/ml) and stained with propidium iodide (final concentration 50 μg/ml). For each sample, 10,000 cells were analyzed by flow cytometry (FACSort, Becton Dickinson) with the software CELLQuest (Becton Dickinson). The percentages of cells in the G_1/G_0, S and G_2/M phases were then calculated (mean of three experiments in triplicate).

Alkaline Single-Cell Gel Electrophoresis

The alkaline single-cell gel electrophoresis assay (comet assay) was used to measure single- and double-strand breaks together with alkali-labile sites in the DNA of confluent fibroblasts irradiated with 0, 3 or 10 Gy and treated either 15 min before or 30 min after irradiation. The method of Pouget *et al.* (*41*) was used with slight modifications. Briefly, 20,000 cells were suspended in 1.2% low-melting-point agarose and laid onto frosted glass microscope slides precoated with a 1% normal-melting-point agarose layer. Slides were kept for 10 min at 4°C to allow the agarose to solidify. Slides were then immersed in a lysis buffer (2.5 *M* NaCl, 100 m*M* Na_2EDTA, 10 m*M* Tris at pH 10, 1% sodium sarcosinate v/v, 1% Triton X-100 v/v, and 10% DMSO v/v) and maintained at 4°C overnight to lyse cell membranes. Slides were then placed in an electrophoresis tank containing 300 m*M* NaOH and 1 m*M* Na_2EDTA. Electrophoresis was performed at 25 V (corresponding to 1.15 V/cm), 300 mA, for 45 min before nuclei were stained with propidium iodide (500 μg/ml). Analysis was performed using a fluorescence microscope (Olympus, AX-70). The Olive tail moment, defined as the product of the distance between the head and center of gravity of DNA in the tail by the ratio of the intensity between the head and the tail (corresponding to DNA migrated), was the parameter retained for analysis. The mean tail moment was calculated by the computer image analysis software from IMSTAR (Paris, France) immediately after irradiation and 1, 3 and 24 h postirradiation. For each experimental condition, the mean tail moment of 50 cells per slide was determined and three slides obtained from three different wells were analyzed. In addition, experiments were repeated three times.

TABLE 1
Oxygen Radical Antioxidant Capacity (ORAC) of the Combination PTX and Tx

	ORAC value
0.5 m*M* PTX/Tx	4.02
1.5 m*M* PTX/Tx	2.83
4 m*M* PTX/Tx	2.08

Notes. Antioxidant capacity of PTX/Tx was assayed and ORAC values were calculated as described by Cao *et al.* (*39*). One ORAC unit is equal to the antioxidant status of 1 μ*M* trolox.

Micronucleus Assay

The micronucleus assay was used to measure chromosomal loss in confluent fibroblasts exposed to doses of 0, 3 or 10 Gy and incubated in the presence of PTX/Tx added either 15 min before or 30 min or 24 h after radiation exposure. Fibroblasts were then trypsinized at different times postirradiation and plated in 12-well plates. Twenty-four hours after, cytochalasin B was added to the culture medium at a final concentration of 5 μg/ml to block cytokinesis, and the culture was maintained for 24 h. Cells were then harvested and centrifuged. The supernatant was carefully discarded, and the pellet was treated with 125 m*M* KCl under constant shaking to induce hypotonic chock. Cells were then fixed three times in acetic acid:ethanol (1:6), dropped onto slides under a humidified atmosphere, and air-dried. Before analysis, slides were stained with propidium iodide (500 μg/ml). The number of micronuclei and binucleated cells was determined among 500 cells using a fluorescence microscope (Nikon, Microphot-FXA). Three slides obtained from three different wells were counted per experimental condition, and the experiments were repeated three times.

Statistical Analysis

Data are depicted as means ± SEM; $P < 0.05$ was considered statistically significant (one-way ANOVA with Tukey test). Each experiment was repeated three times in triplicate.

RESULTS

Antioxidant Capacity of Pentoxifylline and Trolox

The antioxidant capacity of PTX and Tx used at concentrations ranging from 0.5 to 4 m*M* was assessed by the oxygen radical absorbing capacity (ORAC) test (Table 1). ORAC values were calculated as described in the Materials

and Methods section. The highest ORAC value, corresponding to the highest antioxidant capacity of the drugs was obtained for the concentration of 0.5 m*M*. Interestingly, trolox had a higher ORAC value than PTX (ORAC values of 3.70 and 2.96, respectively). When drugs were used together at 0.5 m*M*, a stronger antioxidant power was observed, with an ORAC value of 4.02. The concentration of 0.5 m*M* of the combination was thus chosen for all subsequent experiments since no toxic effects were observed on viability or DNA damage.

Modulation of Fibroblast Viability Induced by PTX/Tx after Radiation Exposure

Confluent fibroblasts were γ-irradiated with doses of 0, 3 and 10 Gy. Cell viability was assessed by trypan blue exclusion from the first day to day 21 after irradiation (Fig. 1). Cell viability was shown to decrease after irradiation and dropped to about 67% for cells irradiated with 3 Gy and 53% for cells irradiated with 10 Gy on day 3. This number remained around 50% over the observation period.

No significant modifications in fibroblasts numbers were observed when PTX/Tx was used. It must be emphasized that higher concentrations of drugs were shown to be nontoxic (data not shown).

Modulation of ROS Production by the Combination of PTX/Tx after Irradiation

The effect of the combination of PTX/Tx on ROS production was measured by the DCFH-DA method in fibroblasts immediately and up to 21 days after radiation exposure at doses of 0, 3 and 10 Gy (Fig. 2). The DCFH-DA assay allows detection of reactive intermediates like hydrogen peroxide and oxidants produced during the reduction of hydrogen peroxide by peroxidase. The highest level of reactive intermediates was produced immediately after exposure, with values of about 263% or 309% for cells irradiated with 3 or 10 Gy, respectively. All values were compared to the value for nonirradiated cells normalized at 100%. Reactive intermediate formation decreased rapidly and reached 48% and 60% of the control value 1 and 3 h after exposure, respectively. Reactive intermediate production was similar to that measured in controls and fluctuated between 100% and 130% of control level over the last 20 days of the observation period.

When PTX/Tx was added 15 min before irradiation, an immediate 1.4- (nonsignificant) and 1.8-fold (significant) decrease was observed in the production of reactive intermediates in cells irradiated with 3 and 10 Gy, respectively. For the next 3 h, the level of reactive intermediates was not diminished by the treatment at any time drugs were added. However, from day 1 to day 21, this level was significantly lower in treated cells, and this trend was observed for the three radiation doses.

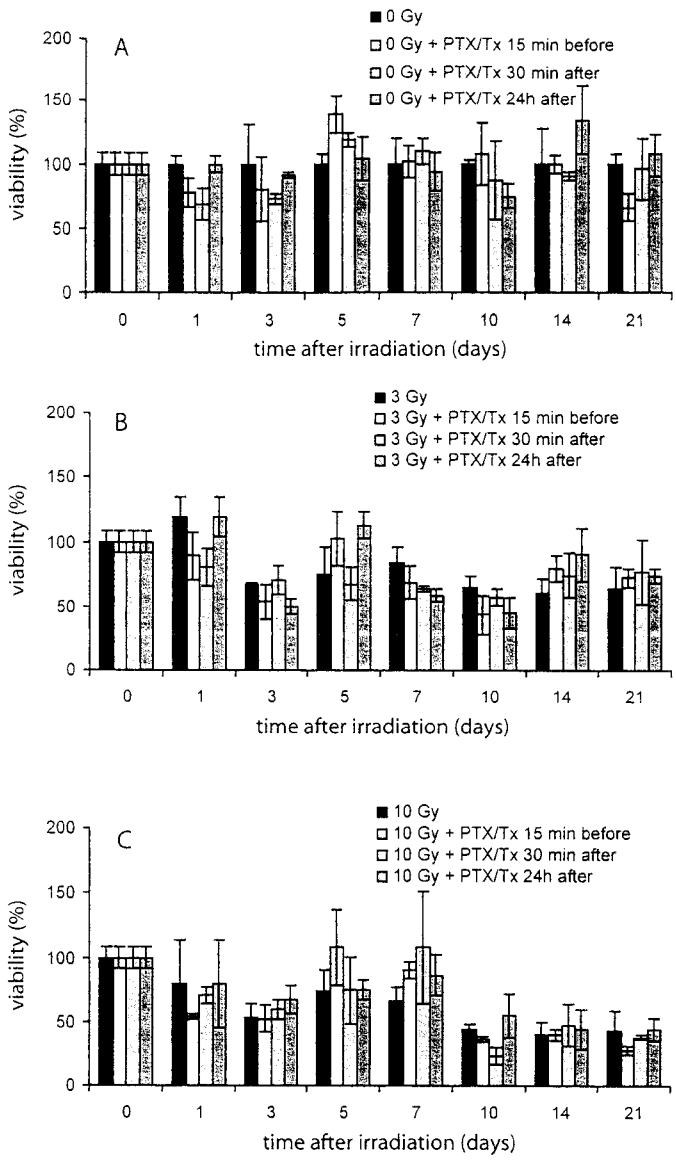

FIG. 1. Death of fibroblasts after radiation exposure. Cell viability was determined by the trypan blue exclusion assay. NHF-d cells were irradiated at confluence in the presence or absence of PTX/Tx at doses of 0 (panel A), 3 (panel B) or 10 Gy (panel C). Values are means ± SEM (three experiments). $*P < 0.05$ or $**P < 0.005$ compared to control (one-way ANOVA with Tukey test).

Modulation of Clonogenicity by the Combination of PTX/Tx

Figure 3 shows the survival curves obtained for treated (15 min before and 30 min and 24 h after irradiation) and untreated normal human fibroblasts exposed to doses ranging from 0 to 6 Gy. A clonogenic index of 10% was obtained for untreated cells exposed to a dose of 3 Gy, and no colony formation was observed for doses greater than 6 Gy.

In the presence of 0.5 m*M* of PTX/Tx, no significant modification in clonogenicity was observed for doses below 3 Gy, and the time at which the drugs were added did not affect these results. However, for cells exposed to doses of

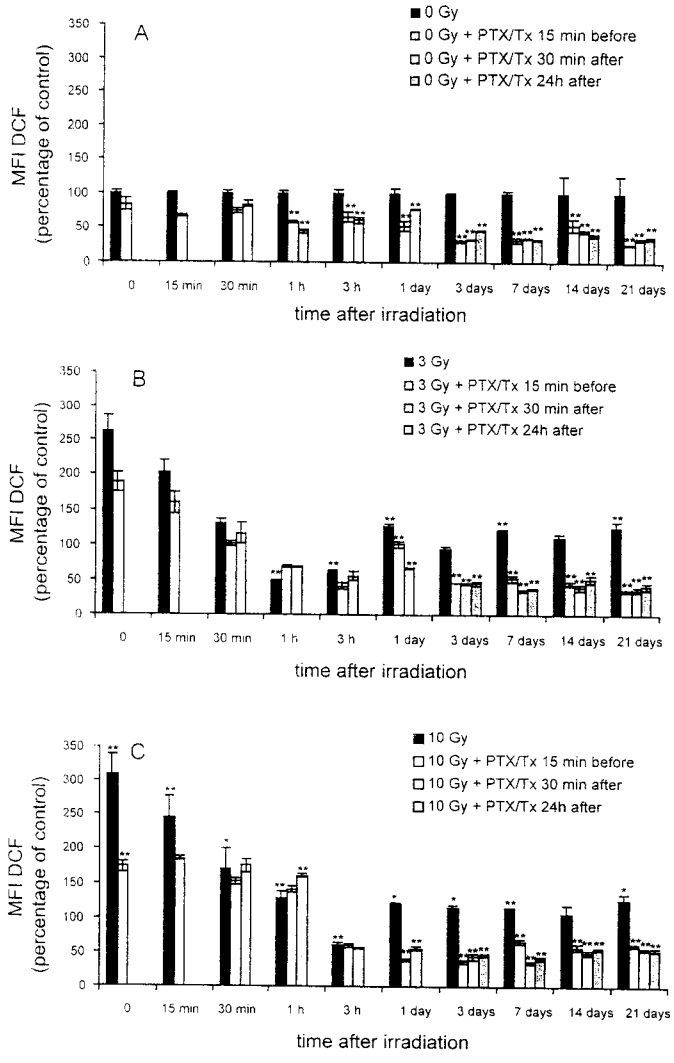

FIG. 2. Production of peroxide in fibroblasts after radiation exposure. Peroxide production was assayed by DCFH oxidation measured by flow cytometry (MFI = mean fluorescence intensity) after radiation exposure at doses of 0 (panel A), 3 (panel B) or 10 Gy (panel C). The combination of PTX/Tx was administered before or after irradiation. Values are means ± SEM (three experiments). $^*P < 0.05$ or $^{**}P < 0.005$ compared to control for untreated cells and compared to untreated cells for the treated cells (one-way ANOVA with Tukey test).

4 and 6 Gy, radiation sensitization was observed whenever the drugs were added.

Modulation of DNA Damage by PTX/Tx

The alkaline comet assay was used to measure DNA strand breaks together with alkali-labile sites after irradiation with 0, 3 and 10 Gy of γ rays (Fig. 4). An increase in the Olive tail moment was observed immediately after irradiation and reached around 35 arbitrary units and about 100 arbitrary units in cells irradiated with 3 and 10 Gy, respectively. Then a decrease in the tail moment was observed, and values returned to the background level of 2 arbitrary units measured in control cells. The background

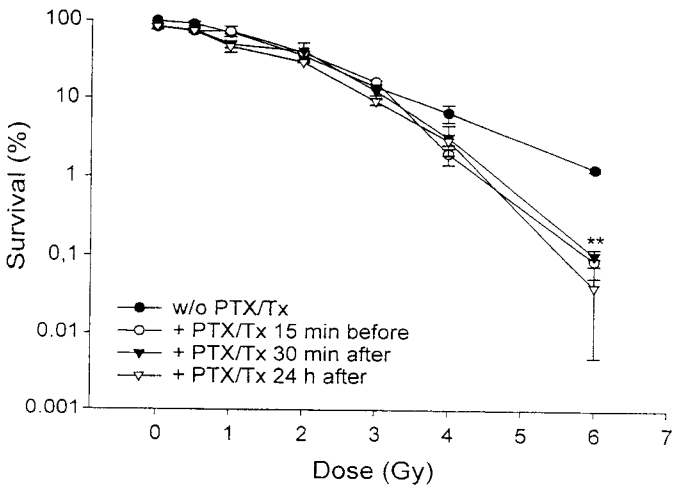

FIG. 3. Clonogenic survival of fibroblasts after radiation exposure. Clonogenic survival was assayed by colony formation (*40*). The combination of PTX/Tx was administered before or after irradiation. Values are means ± SEM (three experiments). $^*P < 0.05$ or $^{**}P < 0.005$ compared to untreated cells (one-way ANOVA with Tukey test).

level was thus reached in 1 or 3 h after irradiation for cells irradiated with 3 and 10 Gy, respectively.

When the combination of PTX/Tx was administered before irradiation, an initial 1.6- or 1.4-fold decrease in the tail moment was observed for cells irradiated with 3 or 10 Gy, respectively. One hour after irradiation, the tail moment measured in cells irradiated with 3 Gy was similar to that measured in nontreated cells and was about 2 arbitrary units. Interestingly, for cells irradiated with 10 Gy, the level of DNA strand breaks was shown to be 2.2-fold lower than in the absence of treatment.

More surprisingly, when PTX/Tx was added 30 min after irradiation, a similar decrease in the tail moment (1.6-fold decrease) was observed. This would suggest that drugs do not simply act as radical scavengers that interfere with initial events but could act in a significant manner with secondary events that occur during the first hours after irradiation.

Modulation of Micronucleus Formation by the Combination of PTX/Tx

The micronucleus (MN) assay was used to assess chromosomal loss. The percentage of binucleated cells in control cells was around 45% with the incubation times used in the studies (data not shown). This percentage dropped to 18% and 20% on day 3 in fibroblasts irradiated with 3 and 10 Gy, respectively (data not shown). Then, from day 3 to day 21, the percentage of binucleated cells increased in fibroblasts irradiated with 3 Gy and reached about 37% on day 21 postirradiation, whereas it remained around 16% in cells irradiated with 10 Gy (data not shown). After the administration of PTX/Tx, both the percentage of binucleated cells and the MN frequency remained unchanged during the first week postirradiation (data not shown). MN formation measured 24 h postirradiation in fibroblasts irradi-

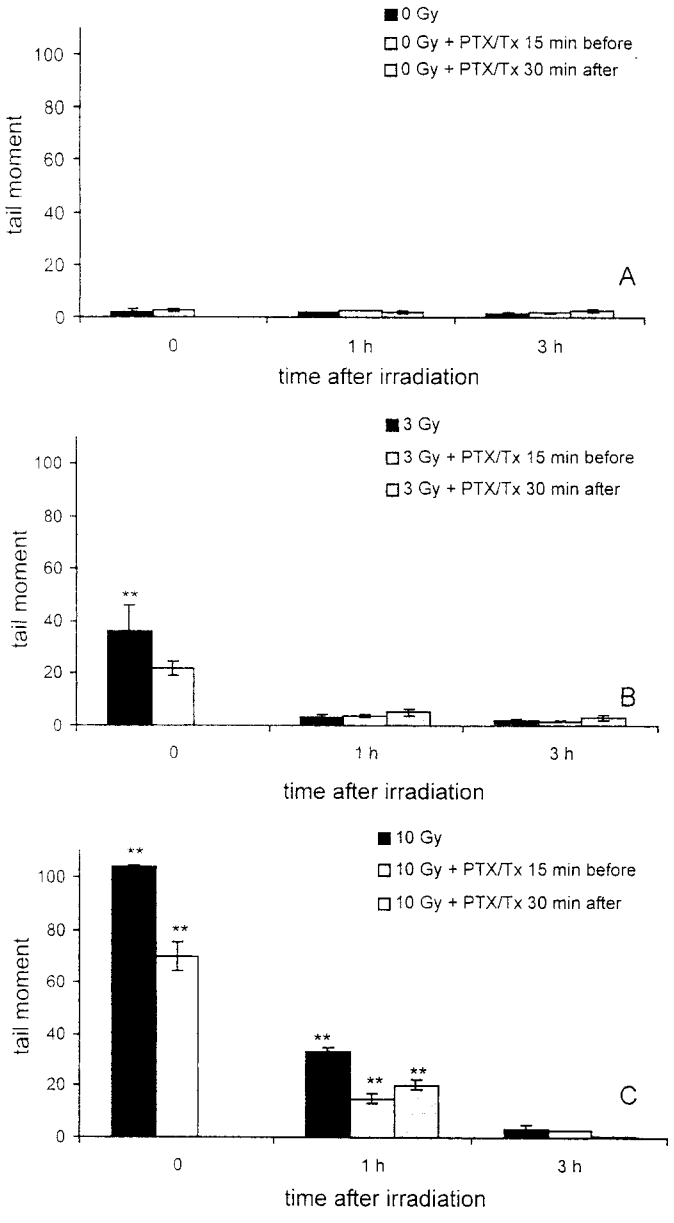

FIG. 4. DNA damage in fibroblasts after radiation exposure. Single- and double-strand breaks together with alkali-labile sites were measured by the alkaline single-cell gel electrophoresis assay in fibroblasts exposed to radiation doses of 0 (panel A), 3 (panel B) or 10 Gy (panel C) and treated with the combination of PTX/Tx either 15 min before or 30 min after radiation exposure. Values are means ± SEM (three experiments). $^{*}P < 0.05$ or $^{**}P < 0.005$ compared to control for untreated cells and compared to untreated cells for treated cells (one-way ANOVA with Tukey test).

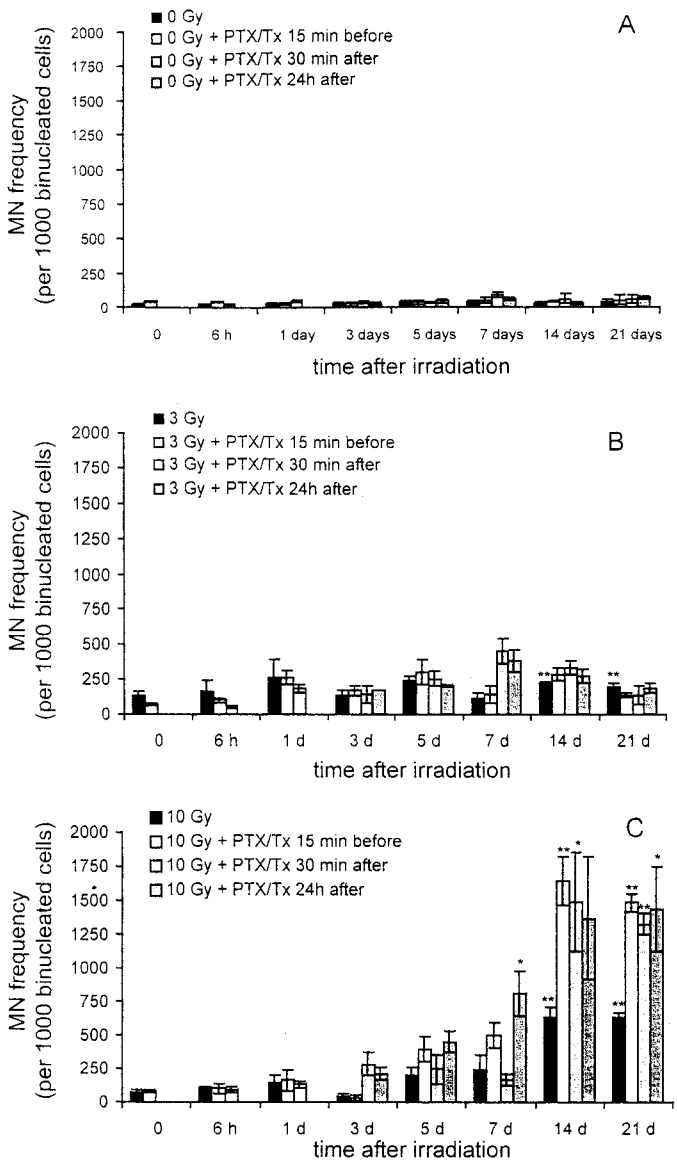

FIG. 5. Micronucleus frequency in fibroblasts after radiation exposure. NHF-d cells irradiated with 0 (panel A), 3 (panel B) or 10 Gy (panel C) were reseeded and grown for different times after irradiation. They were incubated with cytochalasin B for 24 h before hypotonic shock and fixation. Then they were stained with propidium iodide before analysis of 500 cells using a fluorescence microscope. Values are means ± SEM (three experiments). $^{*}P < 0.05$ or $^{**}P < 0.005$ compared to control for untreated cells and compared to untreated cells for treated cells (one-way ANOVA with Tukey test).

ated with 3 and 10 Gy was 7.4 and 4.2 times higher than in controls, respectively (Fig. 5). The MN yields were similar until day 21 in cells irradiated with 3 Gy. In cells irradiated with 10 Gy, a strong increase was observed on day 7, and the number of micronuclei per binucleated cell reached a plateau, around 635 micronuclei per 1000 binucleated cells, that was maintained between days 14 and 21 and corresponded to a level about 18.7-fold higher than in control cells.

When PTX/Tx was administered, a 1.8-fold increase in MN yield measured in fibroblasts irradiated with 10 Gy was observed on day 7. This phenomenon occurred any time the drugs were added.

Modulation of Cell Cycle Distribution of Fibroblasts Exposed to Radiation by PTX/Tx

The ability of cells to progress through the cell cycle was assessed. Typically, the distribution of fibroblasts in cell cycle phases (Fig. 6) was measured after exposure to doses

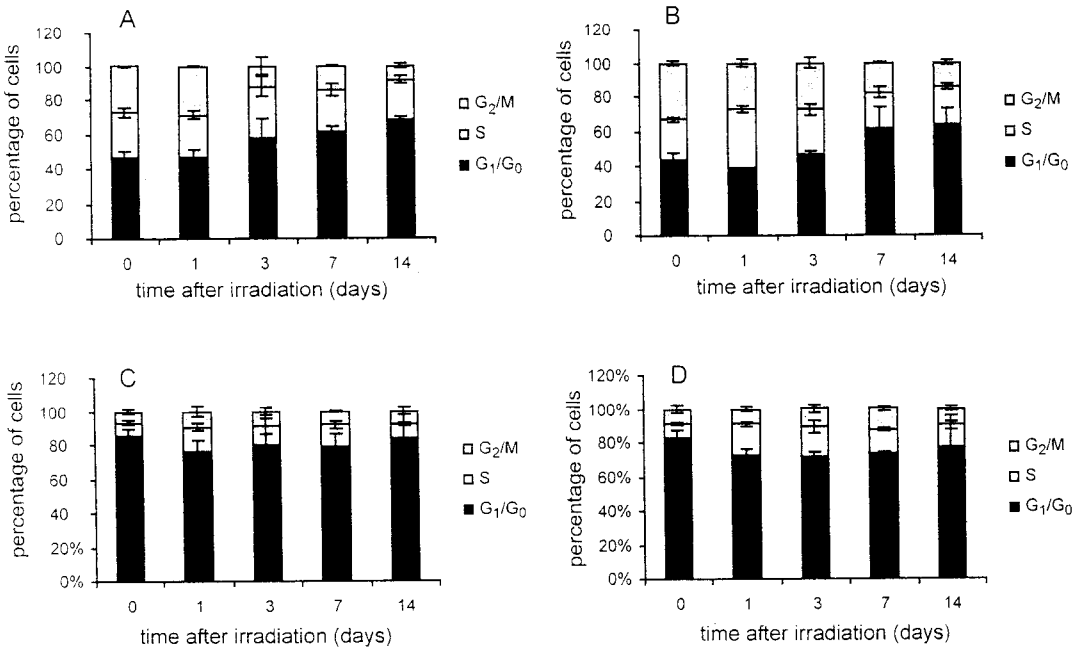

FIG. 6. Distribution of fibroblasts in cell cycle phases after radiation exposure. NHF-d cells were irradiated with 0 Gy in the absence (panel A) or presence of PTX/Tx added 15 min before irradiation (panel B) or with 10 Gy in the absence (panel C) or presence of PTX/Tx added 15 min before irradiation (panel D) and were reseeded to allow them to grow. Fibroblasts were fixed and nuclei were stained with propidium iodide before analysis by flow cytometry. Values are means ± SEM (three experiments). $^*P < 0.05$ or $^{**}P < 0.005$ compared to control for untreated cells and compared to untreated cells for the treated cells (one-way ANOVA with Tukey test).

of 0 or 10 Gy. For this purpose, confluent cells were irradiated and treated with PTX/Tx 15 min before irradiation. Since the cells were confluent, primary cell cycle analysis by flow cytometry indicated that about 93% of the cells were in G_1/G_0 phase. Therefore, at different times postirradiation, they were first trypsinized and replated for 24 h corresponding to one doubling time before being trypsinized again and fixed in ethanol. Figure 6C shows that 86% of fibroblasts irradiated with 10 Gy were in G_1/G_0 phase from the first day, whereas the corresponding value was only about 46% in control cells (Fig. 6A). This arrest was shown to persist for 14 days in irradiated cells, but the proportion of control cells in G_0/G_1 phase increased up to 68% over this period. The percentages of fibroblasts irradiated with 10 Gy in S and G_2/M phase were markedly lower than in control cells (by 3.5 and 4.2, respectively), and this percentage did not change over 2 weeks. In contrast, a decrease by a factor of 3 in the proportion of cells in G_2/M phase was observed for controls over this period.

The distribution of unirradiated fibroblasts (Fig. 6B) and fibroblasts irradiated with 10 Gy (Fig. 6D) in the cell cycle phases was not significantly changed by the administration of PTX and trolox 15 min before irradiation.

DISCUSSION

Radiation-induced DNA damage and its subsequent error-free or error-prone repair are considered as critical factors for cell survival and are controlled by cell cycle checkpoints. Radiation sensitivity is closely linked to cell cycle position and to progression through the cell cycle. Typically, the low mitotic index of dermal skin cells would explain the time between radiation exposure and the occurrence of the clinical symptoms of the cutaneous radiological syndrome observed after exposure to high radiation doses (*4–6*). Cells bearing unstable chromosomal aberrations would die during the first or second mitosis postirradiation and thus would be responsible for the delayed skin injuries involved in the cutaneous radiological syndrome. Most low-LET radiation-induced DNA damage is produced by ROS originating from water radiolysis. Therefore, one could expect that antioxidant treatment might counteract these effects. This work aimed at understanding the molecular mechanisms involved in the effects of treatment with the combination of pentoxifylline and α-tocopherol, which was shown to reduce late radiation-induced skin injury (*28, 29, 36, 37*). The focus was on oxidative DNA damage.

The combination PTX/Tx was added to the culture medium of confluent dermal fibroblasts either before or after exposure to γ rays. The fibroblasts had been isolated from skin biopsies obtained from two patients. No difference was observed in the results for cells from these two patients. No effect of passage number (passage 4–7 and 2–4), which might reflect clonal expansion and selection, was observed.

The concentrations of PTX and Tx were chosen based on previously published values and on ORAC test results (Table 1). Published *in vitro* studies generally used concentrations of PTX or Tx ranging from 0 to 2 m*M*. A concen-

tration of 0.5 m*M* for both PTX and Tx was shown to exhibit the highest antioxidant capacity. We determined by trypan blue exclusion and by comet assays that such concentrations were not cytotoxic or genotoxic in control cells.

The antioxidant properties of the drug combination were confirmed by the DCFH assay (Fig. 2). This assay allows detection of several reactive intermediates like hydrogen peroxide and oxidants produced during the reduction of hydrogen peroxide by peroxidase (reactive intermediates) and gives an overall view of cytoplasmic oxidative stress. However, ROS like superoxide anion and hydroxyl radical were excluded from this analysis (*42*). The DCFH assay indicated that the treatment produced a decrease both in early reactive intermediate production and also in the subsequent production of ROS that occurred during 3 weeks postirradiation. In addition, treatment was shown to be efficient at any time it was administered. Interestingly, from 3 h postirradiation, PTX/Tx was shown to reduce the background level of reactive intermediates in nonirradiated cells. We also observed that the production of reactive intermediates in irradiated cells was abrogated at any time the drugs were added. Therefore, these results highlight the great efficiency of the combination in reducing both endogenous and radiation-induced reactive intermediates, not only during the irradiation but also during the minutes, hours and days postirradiation.

When the drugs were present at the time of irradiation, a decrease in initial oxidative DNA damage, such as strand breaks and alkali-labile sites measured by the alkaline comet assay (Fig. 4), was observed. It must be emphasized that this correlation was not obvious because most of DNA damage was induced by ROS, such as hydroxyl radical or superoxide anion, two species that are not detected by ORAC and DCFH oxidation assays. One hour after irradiation, the numbers of strand breaks and alkali-labile sites measured in cells irradiated with 3 Gy returned to control levels in both treated and nontreated cells. However, for cells irradiated with 3 Gy, DNA repair did not occur, so the effect of the treatment on DNA repair can be partly appreciated (Fig. 4). Interestingly, the level of DNA strand breaks and alkali-labile sites measured in cells irradiated with 10 Gy that were treated with drugs was shown to be significantly lower than in the absence of the drugs. One could expect that the level of DNA strand breaks was lower when the drugs were added 15 min before irradiation because, as mentioned above, the initial level of DNA strand breaks, probably due to reactive species quenching, was lower. However, even when the drugs were added 30 min after irradiation, they reduced the level of strand breaks to the same degree as when they were added before radiation exposure. The reasons for this are not clear, but we propose the following three hypotheses: (1) Strand breaks are produced by initial radiation-induced reactive species and also by secondary reactive species Therefore, the progressive decrease in strand breaks that is usually observed after radiation exposure (half-time of single-strand break repair is about 30 min) would be the result of both DNA repair and secondary DNA breaks, and PTX/Tx treatment would interfere with their development. (2) Secondary strand breaks are produced during DNA repair as intermediate breaks before DNA ligation. This suggests that around 30% (15 arbitrary units) of the breaks observed 1 h postirradiation are DNA repair-induced secondary strand breaks. Treatment with PTX/Tx would prevent the formation of such secondary strand breaks. (3) The third hypothesis, which may be not so different from the previous one, is that PTX/Tx treatment would interfere with DNA repair processes. This would result in an apparent reduction of DNA strand breaks. At this step, more must be known about the possible interference with the DNA repair process or enzymes. However, in our opinion, this is the most likely hypothesis, because several earlier studies emphasized the role of PTX and α tocopherol on cell cycle arrest, DNA repair and subsequent chromosomal damage like micronuclei (*16–21, 42, 43*).

Our results clearly showed that micronuclei, which are a result of impaired repair of DNA double-strand breaks, increased at week 2 postirradiation in 10-Gy-irradiated cells treated by drugs regardless of when the drugs were added.

We can exclude any toxic effect of the drugs PTX/Tx, because at this concentration, neither increased DNA break formation nor a decrease in cell viability was measured in control fibroblasts. The apparent opposing effects of a reduction in tail moment and an increase in MN formation can be explained by the nature of the lesions that are measured by the two genotoxic assays. The comet assay measures radiation-induced DNA strand breaks (single- and double-strand breaks together with alkali-labile sites), whereas micronucleus formation reflects impaired DNA repair, mainly of double-stand breaks. In addition, in the case of γ irradiation, most of the strand breaks measured by the alkaline comet assay are single-strand breaks. Considering that around 1000 single-strand breaks (SSBs) are produced per 40 double-strand breaks (DSBs) per cell per gray, the alkaline comet assay is not sensitive enough to measure variations in DSB levels or possible misrepair of these lesions. Therefore, one cannot assume that a decrease in tail moment will be accompanied by an increase or decrease in DSBs. What is likely is that most of the decrease in tail moment is due to a reduction of DNA SSBs. As mentioned previously, this phenomenon remains unexplained. One indication about formation and possible residual level of DSBs could be provided by cell cycle analysis. DSBs represent one of the major lesions involved in radiation-induced cell cycle arrest. In addition, PTX was known to affect G_2 arrest, probably by interfering with the activities of the DNA sensor system like ATM (*43*), which participates in DSB detection. Therefore, the effect of the treatment on cell cycle progression and possible impaired checkpoint that could explain increase in MN frequency was investigated. It was observed that treatment had very little effect on cell cycle redistribution. For that reason, it

appears unlikely that cell cycle dysfunction could explain impaired DNA damage repair. Moreover, we confirmed that the radiation sensitization that was observed was due to PTX (data not shown). In this respect, it must be kept in mind that many studies underlined the role of PTX in sensitizing TP53-deficient cells to radiation (*43*) by abrogating cell cycle arrest in G_2. However, NHF-d cells were TP53 proficient, which is supported by the observation of G_1 arrest in irradiated cells, and it was shown that TP53 mutations are a general requirement for radiation sensitization by pentoxifylline and that the level of radiation sensitization was dependent on the location of the TP53 mutation (*20*). Therefore, other mechanisms might be involved in the action of PTX. Therefore, the observed in increase in MN frequency and decrease in OTM when drugs were added 30 min after irradiation is still not understood. Further investigations dealing with the effect of this treatment on the two main DNA repair systems, namely the non-homologous end joining (NHEJ) and the homologous recombination (HR) repair systems, would be valuable in understanding these phenomena. More specifically, the main system involved in restoring the integrity of DNA in G_0/G_1 cells is described as being the NHEJ pathway, which is an error-prone system responsible for misrejoined DSBs (*44*).

In conclusion, this work investigated the effects of pentoxifylline and a watery soluble α-tocopherol analog on DNA damage formation in fibroblasts exposed to γ rays. Our results showed that for fibroblasts irradiated with 10 Gy, treatment with PTX/Tx at any time was accompanied by a significant decrease in DNA strand breaks observed during the first 3 h postirradiation. However, it was accompanied by a significant increase in micronucleus yield during the following weeks. These results suggest that PTX/Tx could interfere with the DNA repair process in a way that needs to be elucidated in further work. In addition, it would be of major interest to study the effects of the individual drugs on these systems.

From a clinical point of view, the effects of the combination of drugs in DNA repair would be of major interest because it would suggest that in the case of high production of reactive intermediates, an apparent initial decrease in reactive species and subsequent DNA damage could be accompanied by a delayed toxicity.

ACKNOWLEDGMENTS

We are very grateful to Dr. J-L. Lefaix and Dr. S. Delanian for helpful discussions. We also thank Dr. J. Lallemand and Dr. P-Y. Hémidy. This work was supported by Electricité de France-Service de Radioprotection and Région Ile-de-France.

Received: August 30, 2004; accepted: February 9, 2005

REFERENCES

1. J. O. Archambeau, R. Pezner and T. Wasserman, Pathophysiology of irradiated skin and breast. *Int. J. Radiat. Oncol. Biol. Phys.* **31**, 1171–1185 (1995).
2. B. Dubray, S. Delanian and J. L. Lefaix, Late effects of mammary radiotherapy on skin and subcutaneous tissues. *Cancer Radiother.* **1**, 744–752 (1997).
3. R. U. Peter and P. Gottlober, Management of cutaneous radiation injuries: Diagnostic and therapeutic principles of the cutaneous radiation syndrome. *Mil. Med.* **167**, 110–112 (2002).
4. K. Masuda, N. Hunter and H. R. Withers, Late effect in mouse skin following single and multifractionated irradiation. *Int. J. Radiat. Oncol. Biol. Phys.* **6**, 1539–1544 (1980).
5. P. Rubin and G. W. Casarett, Clinical radiation pathology as applied to curative radiotherapy. *Cancer* **22**, 767–778 (1968).
6. P. Rubin, The Franz Buschke lecture: Late effects of chemotherapy and radiation therapy: A new hypothesis. *Int. J. Radiat. Oncol. Biol. Phys.* **10**, 5–34 (1984).
7. J. E. Moulder, M. E. Robbins, E. P. Cohen, J. W. Hopewell and W. F. Ward, Pharmacologic modification of radiation-induced late normal tissue injury. *Cancer Treat. Res.* **93**, 129–151 (1998).
8. K. R. Trott, Experimental radiotherapy of late-responding tissues—recent advances and future development. *Front. Radiat. Ther. Oncol.* **37**, 9–16 (2002).
9. H. B. Stone, W. H. McBride and C. N. Coleman, Modifying normal tissue damage postirradiation. Report of a workshop sponsored by the Radiation Research Program, National Cancer Institute, Bethesda, Maryland, September 6–8, 2000. *Radiat. Res.* **157**, 204–223 (2002).
10. M. C. Vozenin-Brotons, V. Sivan, N. Gault, C. Renard, C. Geffrotin, S. Delanian, J. L. Lefaix and M. Martin, Antifibrotic action of Cu/Zn SOD is mediated by TGF-β1 repression and phenotypic reversion of myofibroblasts. *Free Radic. Biol. Med.* **30**, 30–42 (2001).
11. J. L. Lefaix, S. Delanian, J. J. Leplat, Y. Tricaud, M. Martin, A. Nimrod, F. Baillet and F. Daburon, Successful treatment of radiation-induced fibrosis using Cu/Zn-SOD and Mn-SOD: An experimental study. *Int. J. Radiat. Oncol. Biol. Phys.* **35**, 305–312 (1996).
12. S. Delanian, F. Baillet, J. Huart, J. L. Lefaix, C. Maulard and M. Housset, Successful treatment of radiation-induced fibrosis using liposomal Cu/Zn superoxide dismutase: Clinical trial. *Radiother. Oncol.* **32**, 12–20 (1994).
13. J. P. Freitas, P. Filipe and F. Guerra Rodrigo, Potential antioxidative effects of pentoxifylline. *C. R. Seances Soc. Biol. Fil.* **189**, 401–405 (1995).
14. B. Horvath, Z. Marton, R. Halmosi, T. Alexy, L. Szapary, J. Vekasi, Z. Biro, T. Habon, G. Kesmarky and K. Toth, *In vitro* antioxidant properties of pentoxifylline, piracetam, and vinpocetine. *Clin. Neuropharmacol.* **25**, 37–42 (2002).
15. C. E. Rube, F. Wilfert, D. Uthe, K. W. Schmid, R. Knoop, N. Willich, A. Schuck and C. Rube, Modulation of radiation-induced tumour necrosis factor alpha (TNF-α) expression in the lung tissue by pentoxifylline. *Radiother. Oncol.* **64**, 177–187 (2002).
16. K. J. Russell, L. W. Wiens, G. W. Demers, D. A. Galloway, T. Le, G. C. Rice, J. A. Bianco, J. W. Singer and M. Groudine, Preferential radiosensitization of G_1 checkpoint-deficient cells by methylxanthines. *Int. J. Radiat. Oncol. Biol. Phys.* **36**, 1099–1106 (1996).
17. A. M. Strunz, P. Peschke, W. Waldeck, V. Ehemann, M. Kissel and J. Debus, Preferential radiosensitization in p53-mutated human tumour cell lines by pentoxifylline-mediated disruption of the G_2/M checkpoint control. *Int. J. Radiat. Biol.* **78**, 721–732 (2002).
18. K. W. Eley, S. H. Benedict, T. D. Chung, B. D. Kavanagh, W. C. Broaddus, R. K. Schmidt-Ullrich and P. S. Lin, The effects of pentoxifylline on the survival of human glioma cells with continuous and intermittent stereotactic radiosurgery irradiation. *Int. J. Radiat. Oncol. Biol. Phys.* **54**, 542–550 (2002).
19. T. Theron, A. Binder, F. Verheye-Dua and L. Bohm, The role of G_2-block abrogation, DNA double-strand break repair and apoptosis in the radiosensitization of melanoma and squamous cell carcinoma cell lines by pentoxifylline. *Int. J. Radiat. Biol.* **76**, 1197–1208 (2000).
20. A. Binder, T. Theron, H. Donninger, M. Parker and L. Bohm, Radiosensitization and DNA repair inhibition by pentoxifylline in NIH3T3 p53 transfectants. *Int. J. Radiat. Biol.* **78**, 991–1000 (2002).

21. J. N. Sarkaria and J. S. Eshleman, ATM as a target for novel radiosensitizers *Semin. Radiat. Oncol.* **11**, 316–327 (2001).

22. E. Bozsakyova, I. Chalupa, L. Sebova and D. Slamenova, Chromosomal aberrations, sister chromatid exchanges and micronuclei induced by pentoxifylline in *in vitro* cultivated Chinese hamster cells (V79) and human blood lymphocytes. *Mutat. Res.* **497**, 63–70 (2001).

23. M. W. Dion, D. H. Hussey and J. W. Osborne, The effect of pentoxifylline on early and late radiation injury following fractionated irradiation in C3H mice. *Int. J. Radiat. Oncol. Biol. Phys.* **17**, 101–107 (1989).

24. W. J. Koh, K. J. Stelzer, L. M. Peterson, B. L. Staker, W. F. Ward, K. J. Russell and T. W. Griffin, Effect of pentoxifylline on radiation-induced lung and skin toxicity in rats. *Int. J. Radiat. Oncol. Biol. Phys.* **31**, 71–77 (1995).

25. M. W. Dion, D. H. Hussey, J. F. Doornbos, A. P. Vigliotti, B. C. Wen and B. Anderson, Preliminary results of a pilot study of pentoxifylline in the treatment of late radiation soft tissue necrosis. *Int. J. Radiat. Oncol. Biol. Phys.* **19**, 401–407 (1990).

26. B. Ozturk, I. Egehan, S. Atavci and M. Kitapci, Pentoxifylline in prevention of radiation-induced lung toxicity in patients with breast and lung cancer: A double-blind randomized trial. *Int. J. Radiat. Oncol. Biol. Phys.* **58**, 213–219 (2004).

27. W. F. Ward, Y. T. Kim, A. Molteni, C. Ts'ao and J. M. Hinz, Pentoxifylline does not spare acute radiation reactions in rat lung and skin. *Radiat. Res.* **129**, 107–111 (1992).

28. J. L. Lefaix, S. Delanian, M. C. Vozenin, J. J. Leplat, Y. Tricaud and M. Martin, Striking regression of subcutaneous fibrosis induced by high doses of gamma rays using a combination of pentoxifylline and alpha-tocopherol: An experimental study. *Int. J. Radiat. Oncol. Biol. Phys.* **43**, 839–847 (1999).

29. S. Delanian, R. Porcher, S. Balla-Mekias and J. L. Lefaix, Randomized, placebo-controlled trial of combined pentoxifylline and tocopherol for regression of superficial radiation-induced fibrosis. *J. Clin. Oncol.* **21**, 2545–2550 (2003).

30. G. Rimbach, A. M. Minihane, J. Majewicz, A. Fischer, J. Pallauf, F. Virgli and P. D. Weinberg, Regulation of cell signalling by vitamin E. *Proc. Nutr. Soc.* **61**, 415–425 (2002).

31. S. F. Sweetman, J. J. Strain and V. J. McKelvey-Martin, Effect of antioxidant vitamin supplementation on DNA damage and repair in human lymphoblastoid cells. *Nutr. Cancer* **27**, 122–130 (1997).

32. B. Kumar, M. N. Jha, W. C. Cole, J. S. Bedford and K. N. Prasad, D-Alpha-tocopheryl succinate (vitamin E) enhances radiation-induced chromosomal damage levels in human cancer cells, but reduces it in normal cells. *J. Am. Coll. Nutr.* **21**, 339–343 (2002).

33. L. Sarma and P. C. Kesavan, Protective effects of vitamins C and E against gamma-ray-induced chromosomal damage in mouse. *Int. J. Radiat. Biol.* **63**, 759–764 (1993).

34. M. Satyamitra, P. Uma Devi, H. Murase and V. T. Kagiya, *In vivo* postirradiation protection by a vitamin E analog, α-TMG. *Radiat. Res.* **160**, 655–661 (2003).

35. H. V. Worthington, J. E. Clarkson and O. B. Eden, Interventions for treating oral mucositis for patients with cancer receiving treatment. *Cochrane Database Syst. Rev.* CD001973 (2002).

36. S. Delanian, S. Balla-Mekias and J. L. Lefaix, Striking regression of chronic radiotherapy damage in a clinical trial of combined pentoxifylline and tocopherol. *J. Clin. Oncol.* **17**, 3283–3290 (1999).

37. H. Letur-Konirsch, F. Guis and S. Delanian, Uterine restoration by radiation sequelae regression with combined pentoxifylline-tocopherol: A phase II study. *Fertil. Steril.* **77**, 1219–1226 (2002).

38. S. Delanian and J. L. Lefaix, Complete healing of severe osteoradionecrosis with treatment combining pentoxifylline, tocopherol and clodronate. *Br. J. Radiol.* **75**, 467–469 (2002).

39. G. Cao, H. M. Alessio and R. G. Cutler, Oxygen-radical absorbance capacity assay for antioxidants. *Free Radic. Biol. Med.* **14**, 303–311 (1993).

40. T. T. Puck, P. I. Marcus and S. J. Cieciura, Clonal growth of mammalian cells *in vitro*; Growth characteristics of colonies from single HeLa cells with and without a feeder layer. *J. Exp. Med.* **103**, 273–283 (1956).

41. J. P. Pouget, T. Douki, M. J. Richard and J. Cadet, DNA damage induced in cells by gamma and UVA radiation as measured by HPLC/GC-MS and HPLC-EC and Comet assay. *Chem. Res. Toxicol.* **13**, 541–549 (2000).

42. C. P. LeBel, H. Ischiropoulos and S. C. Bondy, Evaluation of the probe 2′,7′-dichlorofluorescin as an indicator of reactive oxygen species formation and oxidative stress. *Chem. Res. Toxicol.* **5**, 227–231 (1992).

43. J. N. Sarkaria, E. C. Busby, R. S. Tibbetts, P. Roos, Y. Taya, L. M. Karnitz and R. T. Abraham, Inhibition of ATM and ATR kinase activities by the radiosensitizing agent, caffeine. *Cancer Res.* **59**, 4375–4382 (1999).

44. M. R. Lieber, Y. Ma, U. Pannicke and K. Schwarz, Mechanism and regulation of human non-homologous DNA end-joining. *Nat. Rev. Mol. Cell. Biol.* **4**, 712–720 (2003).

Article 4 : Lésions de l'ADN dans les cellules endothéliales de la microvascularisation de la peau exposées au rayonnement gamma et traitées par l'association pentoxifylline / alpha-tocophérol

L'article 4 traite des effets des rayonnements ionisants sur les cellules endothéliales du derme. Ces dernières constituent en effet le deuxième type cellulaire majeur impliqué dans l'apparition des effets cutanés tardifs radio-induits. Les cellules endothéliales sont décrites comme pouvant être à l'origine d'une mort décalée dans le temps du fait de leur faible index mitotique (inférieur à 0,5%).

L'approche méthodologique utilisée dans cette étude est identique à celle décrite dans l'article 3. Les cellules ont été irradiées à confluence et le traitement PTX/Tx a été administré avant ou après irradiation.
Cette étude a montré une production d'ERO (Espèces Réactives de l'Oxygène) maximale immédiatement après l'irradiation et variant ensuite en fonction du temps et de la dose d'irradiation. Le niveau des lésions de l'ADN mesuré par la méthode des comètes en milieu alcalin atteint également un niveau maximal immédiatement après irradiation. Il revient au niveau basal dans les 3 heures qui suivent du fait de la réparation cellulaire. Ce niveau reste inchangé jusqu'à des temps plus tardifs (14 jours). En revanche, une augmentation de la fréquence des micronoyaux a lieu immédiatement après irradiation et persiste dans les deux semaines qui suivent l'irradiation. Elle augmente même à 21 jours dans les cellules irradiées à 10 Gy.
D'autre part, nous avons observé que le traitement diminuait la production d'ERO, de dommages de l'ADN mais augmentait la fréquence de micronoyaux dans les cellules irradiées à 10 Gy même lorsqu'il est administré 24 heures après l'irradiation.

Comme dans le cas des fibroblastes, on observe la présence de phénomènes oxydatifs et de lésions de l'ADN plusieurs semaines après l'irradiation dans les cellules endothéliales du derme. L'association PTX/Tx permet de moduler les phénomènes oxydatifs radio-induits. Elle ne semble pas agir uniquement par piégeage des radicaux mais pourrait interférer avec les voies de réparation des lésions de l'ADN et, plus particulièrement, des CDB (Cassures Double-Brins).

DNA damage in cultured skin microvascular endothelial cells exposed to gamma-rays treated by the combination of pentoxifylline and α-tocopherol

Carine Laurent[1], Philippe Voisin[2], Ph.D, and Jean-Pierre Pouget[2, 3†], Ph.D.

[1] Laboratoire de Dosimétrie Biologique, DRPH/SRBE, Institut de Radioprotection et de Sûreté Nucléaire, Fontenay-aux-Roses, France

[2] Service de Radiobiologie et d'Epidémiologie, DRPH, Institut de Radioprotection et de Sûreté Nucléaire, Fontenay-aux-Roses, France

[3] INSERM EMI 0227, Immunociblage des tumeurs et Ingénierie des Anticorps, Centre de Recherche en Cancérologie, CRLC Val d'Aurelle, Institut Paul Lamarque, Montpellier, France

Running title: Modulation of DNA damage in skin endothelial cells by PTX/Tx

[†] Address correspondance to: Jean-Pierre Pouget, Immunociblage des tumeurs et Ingénierie des Anticorps, EMI 0227, INSERM, Centre de Recherche en Cancérologie, CRLC Val d'Aurelle, Institut Paul Lamarque, 34298 Montpellier Cedex, France ; Tel: +33 4 67 61 37 08; E-mail: jppouget@valdorel.fnclcc.fr.

Abstract

This *in vitro* study aims at evaluating the effect of the combination of pentoxifylline (PTX) and Trolox (Tx), the water-soluble analogue of αT, on oxidative state and DNA damage in dermal microvascular endothelial cells exposed to a high dose of ionizing radiation. Confluent primary cultures of dermal endothelial cells were gamma-irradiated at 3 and 10 Gy and 0.5 mM of PTX and Tx were added either before or after irradiation. Both, Reactive Oxygen Species (ROS) yield, measured by DCFH-DA assay, and DNA damage assessed by the comet and micronuclei (MN) assays, were measured at different times after exposure. We observed that treatment was counteracting early and delayed ROS yield. Moreover, strand breaks level as measured by the comet assay, was shown to be reduced, even when drugs were added after exposure. However, more unexpected was the raise in MN frequency observed on day 7 post-irradiation. This increase in chromosomal damage was not correlated to extend of radiation sensitivity in the considered range of doses. These results suggest that oxidative stress and DNA damage induced in dermal microvascular endothelial cells by radiation, can be modulated by PTX/Tx, and that drugs do not simply act as radical scavenger but might interfere with DNA repair process in a way that needs to be further explored.

Author Keywords

Ionizing radiation; Reactive Oxygen Species; Microvascular endothelial cells; DNA damage; Pentoxifylline; α-tocopherol

1. INTRODUCTION

The origin of delayed radiation skin injury, including telangiectasia, fibrosis and necrosis, that may occur from several months to several years after exposure (Archambeau *et al*., 1995; Dubray *et al*., 1997; Peter and Gottlober, 2002) is still a matter of debate. It may occasionally occur after radiotherapy treatment or subsequently to accidental overexposure. It depends tightly of the irradiation dose delivered to the skin tissue and we proposed in a previous work a method for assessing dose delivered to the skin (Pouget *et al*., 2004) in situation where skin exeresis has to be done. The present study aims at understanding the mechanisms involved in the activity of the combination pentoxifylline/alpha-tocopherol. The latter combination demonstrated its efficiency in restoring skin integrity after fibrosis or necrosis took place in the exposed tissue long time after irradiation.

Development of radiation-induced fibrosis or necrosis, which are the two most important delayed symptoms that may affect vital prognosis of irradiated people, is thought to be the result of multicellular process of interacting cell types, such as endothelial cells, epithelial cells, fibroblasts, macrophages and leukocytes (Hill *et al*., 2001). Fibrosis can be divided into initial pre-fibrotic and constitutive fibrotic phases (Dubray *et al*., 1997; Delanian and Lefaix, 2004). In the initial pre-fibrotic phase, endothelial cells play a very important role by releasing cytokines that would attract leukocytes which are next involved in inflammatory processes. Subsequent inflammation is accompanied by destruction of endothelial cells and vascular thrombosis that may lead to necrosis of micro-vessels and local ischemia. Loss of endothelial barrier leads to direct exposure of conjonctive cells to stimuli that are normally foreign to them (Dubray *et al*., 1997; Delanian and Lefaix, 2004). Activated and senescent fibroblasts (myofibroblasts and fibrocytes, respectively) and extracellular matrix are next the major actors of the following phase, namely the constitutive phase, made of densely synthesis of extracellular matrix under cytokine controls. It precedes late fibroatrophic phase characterized by densified and poorly vascularised and cellularised tissue. Therefore dermis and especially vascular system alteration might play a major role as an initiating event in radiation injury development (Phillips, 1966; Rubin and Casarett, 1968; Law, 1981; Adamson and Bowden, 1983; Ts'ao *et al*., 1983). In this respect, it was shown that modification of microvascularisation was effectively responsible for loss of gastrointestinal tract integrity (Paris *et al*., 2001). More specifically, it was demonstrated that death of endothelial cells was due to ceramide-mediated apoptosis which is triggered within the first five minutes following irradiation. However, the mechanisms involved in cutaneous radiological syndrome (CRS) might be different because symptoms appear long time after irradiation whereas described

loss of endothelial cells in intestine is fast. It has been for long considered that radiation-induced mitotic death was the main process involved (Phillips, 1966; Rubin and Casarett, 1968; Law, 1981; Adamson and Bowden, 1983; Ts'ao *et al*., 1983). Such mechanism of death relies on the statement that irradiation produces unstable chromosomal aberrations such as dicentrics. Cells bearing such type of DNA damage could not pass division and would then die. Consequently, the long time observed between irradiation and apparition of clinical signs would be due to the low mitotic index of endothelial cells. In addition, this would explain why lesions were assumed to be progressive and inevitable because of their early origin.

Another hypothesis dealing with delayed apparition of radiation skin injury was based on chronic inflammation that takes place in the exposed tissue. These phenomenon would produce reactive species causing damage within the cell and their subsequent death mediated by an apoptotic, a necrotic or a mitotic process (for review, Robbins and Zhao, 2004). Interestingly, in several published works, regression of radiation-induced skin lesions was observed (Delanian *et al*., 1994; Lefaix *et al*., 1996) when pharmacological treatments based on antioxidant therapy were used. Studies thus showed a regression of fibrosis with the administration of superoxide dismutase (SOD) both in animal and in patients (Delanian *et al*., 1994; Lefaix *et al*., 1996). However, as SOD could not be produced for a safe clinical treatment, clinical research focused on another antioxidant therapy based on the combination of pentoxifylline (PTX) and α-tocopherol (αT) for the reasons exposed below. Fortunately, a similar efficiency in healing than with SOD was observed but just required a longer period of treatment.

PTX was first delivered to patients that had vascular disease because of its properties to improve tissue oxygen (Ehrly and Schroeder, 1977; Ehrly, 1979). Recent studies showed that PTX could act as a radical scavenger (Freitas *et al*., 1995; Horvath *et al*., 2002) and could regulate the production of TNFα and of other inflammatory cytokines (Rube *et al*., 2002). PTX was also shown to inhibit G2 arrest induced by radiation exposure (Russell *et al*., 1996; Eley *et al*., 2002; Strunz *et al*., 2002), resulting in the radiosensitization of p53-deficient tumour cells (Theron *et al*., 2000), and was shown to be responsible for clastogenic effects such as chromosomal aberrations, sister chromatide exchanges and micronuclei (Bozsakyova et al., 2001). In addition, it was shown to inhibit DNA double-strand breaks (DSB) repair (Theron *et al*., 2000; Binder *et al*., 2002) and ATM gene expression (Sarkaria and Eshleman, 2001).

The second compound is alpha-tocopherol which is a major lipid-soluble antioxidant. More specifically, it was shown to inhibit *in vitro* inflammation, cell adhesion, platelet aggregation

and smooth muscle cell proliferation (for review: Rimbach *et al*., 2002; Weiss and Landauer, 2003). Its derivatives exhibited protective effects against DNA damage (Sweetman *et al*., 1997; Kumar *et al*., 2002). The combination of these two molecules, PTX and αT, was shown to reduce late chronic damage, fibrosis and necrosis *in vivo* (Delanian *et al*., 1999; Lefaix *et al.*, 1999; Delanian and Lefaix, 2002; Letur-Konirsch *et al*., 2002; Delanian *et al*., 2003; Chiao and Lee, 2005) whereas single compound had no beneficial or toxic effects (Delanian et al., 2003; Chiao and Lee, 2005).

The mechanisms involved in the efficient action of the combination of PTX/αT in restoring skin integrity are still unexplained. In a previous study, we investigated the role of this combination on dermal fibroblast exposed to gamma-rays (Laurent *et al*., 2005). We propose now to study its effects on microvascular endothelial cells.

Typically, endothelial cells from skin microvascularisation were gamma-irradiated at confluence stage in presence or not of the treatment. Oxidative stress and DNA damage formation was next assessed. It was thus observed that oxidative phenomenon occurred at early and late times after radiation exposure. Treatment was shown to reduce ROS production and early DNA damage. Nevertheless, a delayed increase in micronuclei frequency was observed several weeks after irradiation at irradiation dose of 10 Gy. This enhancement of DNA damage in presence of the drugs would suggest that the combination does not simply act as a radical scavenger but could be involved in several mechanisms of cell response to radiation and would participate to acute toxicity at the highest irradiation doses.

2. MATERIALS AND METHODS

2.1. Materials

Dulbecco's phosphate-buffered saline (PBS) and trypsin/EDTA were purchased from Gibco BRL Life Technologies (Gaithersburg, MD, USA). Dichlorodihydrofluorescein diacetate (H_2DCFDA) was purchased from Molecular Probes (Eugene, OR, USA). All others chemicals were purchased from Sigma (St. Louis, MO, USA).

2.2. Cell cultures

Primary cultures of endothelial cells were established from commercial human dermal microvascular endothelial cells (HMVEC-d). HMVEC-d cells were derived from an healthy caucasian 45-years old woman undergoing elective surgery and were obtained from Cambrex

(Verviers, Belgium). Cells were cultured in EGM-2 MV provided by the supplier, at 37°C in a humidified atmosphere of 5% CO_2 and 95% air and were used at passages 5-7.

2.3. Cell treatment and gamma-radiation

Confluent HMEC-d cells were exposed to gamma-irradiation at doses of 3 and 10 Gy using a ^{137}Cs source (IBL 637, Cis bio International). Irradiation was performed at room temperature at a dose rate of 1 Gy/min. Pentoxifylline (PTX) and Trolox (Tx) were added either 15 min before irradiation, 30 min or 24 h after radiation exposure at final concentration of 0.5 mM. Concentration of 0.5 mM was determined in a previous work on fibroblasts [35]. However, it was checked that such a concentration was appropriate for conducting the present study in regards of the balance toxicity/efficiency on endothelial cells.

PTX (100 mM) was dissolved in water and Tx (100 mM), the water-soluble analogue of αT, in methanol. The treatment was maintained during the whole considered period.

2.4. Determination of ROS

2',7'-dichlorofluorescein diacetate (DCFH-DA) was used to determine cytoplasmic ROS generation in 0 Gy-, 3 Gy- and 10 Gy-irradiated confluent endothelial cells treated with the combination PTX/Tx 15 min before, 30 min or 24 h after IR exposure. Cells were incubated in presence of 1 µM DCFH-DA for 15 min at 37°C, trypsinized, washed with PBS and fixed in 1% paraformaldehyde. For measurement of immediate ROS generation, incubation with DCFH-DA was done at the time of radiation exposure. Formation of 2', 7'-dichlorofluorescein (DCF), a fluorescent compound, was analysed by flow cytometry using a FACSort (Becton Dickinson) with the software CELLQuest (Becton Dickinson).

2.5. Alkaline single-cell gel electrophoresis (comet assay)

The alkaline single-cell gel electrophoresis assay was used to measure DNA damage (single- and double-strand breaks together with alkali-labile sites) in 0 Gy-, 3 Gy- and 10 Gy-irradiated confluent endothelial cells treated either 15 min before or 30 min after irradiation. The method described by Pouget et al. (Pouget et al., 2000) was slightly modified. Twenty thousands cells were embedded in 1.2% low melting point agarose and laid onto frosted glass microscope slides precoated with 1% normal melting point agarose. Lysis was performed overnight at 4°C (2.5 M NaCl, 100 mM Na_2EDTA, 10 mM Tris at pH 10, 1% sodium sarcosinate v/v, 1% Triton X-100 v/v, and 10% DMSO v/v) before electrophoresis (25 V, 1.15 V/cm, 300 mA) for 45 min at 4°C in 300 mM NaOH and 1 mM Na_2EDTA. DNA was

stained with propidium iodide (500 µg/ml). Analysis was performed using a fluorescence microscope (Olympus, AX-70). Olive Tail Moment of 50 cells per slide was obtained by the computer image analysis software from IMSTAR (Paris, France).

2.6. Micronuclei assay

Micronuclei assay was used to measure chromosomic loss in reseeded gamma-irradiated confluent endothelial cells. For this purpose, cells were exposed to irradiation doses of 0 Gy, 3 Gy or 10 Gy at the plateau phase and treated by PTX/Tx either 15 min before IR exposure or 30 min or 24 h after irradiation. At different times post-irradiation, they were reseeded and incubated in presence of cytochalasin B (final concentration = 5 µg/mL) for 24 h to block cytokinesis. Cells were then harvested and centrifuged before hypotonic chock consisting of KCl 125 mM under constant shaking. They were then fixed in acetic/acid:ethanol (1:6), dropped onto slides under humidified atmosphere and air dried. Slides were stained with propidium iodide. Micronuclei frequency was determined among 200 cells using a fluorescence microscope (Nikon, Microphot-FXA).

2.7. Cell Cycle

Proportion of cells in the different cell cycle phases was measured in control- and 10 Gy-irradiated cells according PTX/Tx was added or not 15 min before irradiation. Typically, cells were first re-seeded at given times post-irradiation and grown for 24 h to perform one population doubling. They were next trypsinized, fixed and permeabilized with 70% ice-cold ethanol, and kept overnight at 4°C. Cells were incubated 30 minutes at 37°C with RNAse A (final concentration 10 µg/mL) and stained with propidium iodide (final concentration 50 µg/mL). For each sample, 10 000 cells were analyzed by flow cytometry (FACSort, Becton Dickinson) with the software CELLQuest (Becton Dickinson). The percentage of cells in the G1/G0, S and G2/M phases was then calculated (mean of three experiments in triplicate).

2.8. Clonogenic assay

For clonogenicity assay, endothelial cells were plated in 25 cm² tissue culture flasks. Cloning efficiency was about 40%. Six hours after seeding, they were irradiated at doses ranging from 0 to 6 Gy. Drugs were either added 15 min before, 30 min or 24 h after irradiation. Cells were then grown for 14 days and colonies were stained with Crystal violet (2.5 g/L of 45:5 methanol/paraformaldehyde 30%). Colonies containing 50 or more cells were scored and the surviving fraction was calculated.

2.9. Statistical analysis

Data are depicted as mean ± SEM; *p < .05 and ** p < .005 were considered statistically significant (one-way ANOVA with Tukey test). Each experiment was repeated three times in triplicate.

3. RESULTS

3.1. Radiation-induced ROS production in HMVEC-d treated by PTX/Tx

ROS production was assessed by DCF measurement in gamma-irradiated confluent cells at early and late times after radiation exposure (Fig. 1). The highest levels of peroxides were measured immediately after irradiation according to a dose effect relationship. Typically boosts of about 224% and 448%, compared to controls, were observed in 3 Gy and 10 Gy-irradiated cells, respectively. Next, during the 3 hours following irradiation, yield decreased down to the basal level, defined as the level measured in non-irradiated cells. This decrease was pursued during the 14 following days by successive rises and declines but levels never reached initial values observed immediately after irradiation.

Addition of the treatment, consisting of 0.5 mM of PTX and Tx, 15 min before irradiation resulted in the inhibition of early ROS production in HMVEC-d cells. The combination was very efficient so that yield of ROS was divided by a factor 2.8 (from 448% to 162% for 10 Gy-irradiated cells). Administration of PTX/Tx 30 min or 24 h after irradiation led to similar effects. In addition, it must be underlined that treatment was able to reduce the level of ROS in control cells (background level), at any time it was added.

3.2. DNA damage in irradiated HMVEC-d treated by PTX/Tx

The alkaline comet assay was used to measure DNA single and double strand breaks together with alkali-labile sites formation in cells exposed to irradiation, according treatment was present or not at the time of exposure. An increase in DNA damage was thus observed immediately after radiation exposure (Fig. 2). This increase was dose-dependent and OTM values of 32 and 76 units were measured in 3 Gy- and 10 Gy-irradiated cells, respectively. Corresponding values of 2 units were in contrast determined in unirradiated cells. One hour after irradiation, DNA damage level was reduced down to 21 units and to 58 units at 3 Gy and at 10 Gy, respectively. OTM values continued decreasing and returned to basal level 3 hours

after radiation exposure. Then, this level kept unchanged even several days after irradiation (data not shown).

When the combination of PTX/Tx was administered before irradiation, a decrease in the level of initial DNA damage was observed. DNA damage yield was thus reduced to 56% and to 41% of values measured in 3 Gy (OTM value of 14 units) and in 10 Gy-irradiated cells (OTM value of 45 units), in absence of treatment. Surprisingly, addition of PTX/Tx 30 min after irradiation provoked the same reduction in DNA damage measured one hour post-irradiation. Therefore, treatment was shown to reduce strand breaks level as measured by the comet assay and this at any time it was added. In this respect, no statistically significant differences were observed between OTM values according treatment was added before or after irradiation.

3.3. Radiation-induced micronuclei formation in HMVEC-d treated by PTX/Tx

Chromosomal damage was assessed by the micronuclei (MN) assay (Fig. 3). Typically, at different time after exposure, gamma-irradiated HMVEC-d cells maintained at confluence stage were trypsinised and reseeded for 24hours to re-enter cell cycle. The number of MN per binucleated cells was then determined. Figure 3 thus showed a strong increase in MN frequency immediately after radiation exposure representing a rise of about 825% compared to the incidence measured in unirradiated cells. This boost was maintained until day 5 in a dose-dependent manner. Then, MN frequency decreased down to a level similar to the one measured in controls. Surprisingly, a second augment was observed from day 10. Whereas MN frequency determined in 3 Gy-irradiated cells then returned to control frequency at day 21, the increase was emphasized in 10 Gy-irradiated cells reaching a level of around 678% of control level.

Administration of PTX/Tx had no effect on MN formation in 0 Gy- and 3 Gy-irradiated cells, and this at any time treatment was added. In contrast, the delayed MN formation in 10 Gy-irradiated cells, which was described above, was enhanced so that MN yield was multiplied by a factor 2.2 to 3.6 at day 10 and 14. Then decrease was observed on day 21.

3.4. Cell cycle modulation in irradiated HMVEC-d treated by PTX/Tx

Proportion of HMVEC-d in each cell cycle phase was measured by flow cytometry after DNA staining (Fig. 4). As cells were irradiated at confluence and were for most of them in G0/G1 stage (data not shown), they were first trypsinised and reseeded at each analysis time to re enter cell cycle. Therefore, it is their ability to re-enter cell cycle and to move through cell cycle that was assessed. It was thus observed that in non-irradiated cells, proportion of

HMVEC-d cells in G1/G0 phase was strongly increased from the first day post-irradiation. Cells exposed to 10 Gy exhibited an immediate enhancement of the G1/G0 phase by a factor 1.6. In contrast, proportion of cells in S and G2/M phases were decreased by a factor 0.8 and 0.7, respectively. For following considered analysed times, the proportion of cells in G1/G0 phase was increased as for unirradiated cells.

Administration of PTX/Tx 15 min before irradiation enhanced proportion of cells in G1/G0 phase immediately after irradiation in 0 Gy- and 10 Gy-irradiated cells whereas it decreased proportion of cells in S and G2/M phases. Then, no significant differences could be detected according treatment was added or not.

3.5. HMVEC-d survival and modulation by PTX/Tx

Endothelial cells survival (Fig. 5) was shown to decline with increasing irradiation doses. At the dose of 3 Gy, only 10% of cells could form colonies, and no colonies were observed at irradiation dose of 6 Gy.

Clonogenicity was unchanged by the addition of PTX/Tx whatever the time of administration of the combination.

4. DISCUSSION

Dermis constituent and more specifically microvascular endothelial cells were described as being sensitive targets to radiation and probably one of the major actor involved in the occurrence of delayed skin alteration. Delayed skin alteration includes telangiectasia, fibrosis and /or necrosis. They may appear from several months to years after irradiation in the exposed area and may affect the vital diagnosis of patients.

Interestingly, the combination PTX/Tx demonstrated, *in vivo,* its ability in reducing delayed radiation-induced skin injuries (Delanian *et al*., 1999; Lefaix *et al*., 1999; Delanian and Lefaix, 2002; Letur-Konirsch *et al*., 2002; Delanian *et al*., 2003), but the mechanisms involved in these process are still misunderstood. In a previous work, we investigated the effect of these drugs on irradiated dermal fibroblasts (Laurent *et al*., 2005) which constitutes the other major cell type of dermis. The present study focus on the effect of gamma-irradiation on confluent skin endothelial cells in presence of the combination of pentoxifylline/trolox (PTX/Tx). Typically, ROS formation together with DNA damage and subsequent consequences on cell viability and cell cycle were investigated. For this purpose,

human microvascular endothelial cells from adult dermis were irradiated at confluence stage in presence or not of the two drugs. Confluent stage was chosen in order to mimic quiescent cellular status in cutaneous tissue. For treated cells, 0.5 mM of PTX/Tx was added 15 min before, 30 min after or 24 h after irradiation. Irradiation doses of 3 and 10 Gy were chosen in regards of clonogenic values which indicated that 10% of irradiated cells were able to produce a colony at a dose of 3 Gy and no growth was observed at 10 Gy. It must also be added that PTX and Tx concentrations were chosen on the basis of previous published works and both on cytotoxicity assessment together with antioxidant capacity measured in preliminary works.

Antioxidant capacity of the combination of drugs on fibroblasts exposed to gamma rays was shown in a previous work (Laurent *et al*., 2005) and was corroborated in the present study in regards of its effect on ROS production measured by the DCFH-DA assay (Fig. 1). Early and delayed formations of reactive species that were observed after radiation exposure were thus shown to be counteracted when drugs were added. This effect was observed at any time drugs were added. It must be kept in mind that DCFH-DA assay gives an overall view of cytoplasmic oxidative stress as it detects several reactive intermediates like hydrogen peroxide and oxidants produced during the reduction of hydrogen peroxide by peroxidase but not superoxide anion and free hydroxyl radical (LeBel *et al*., 1992).

The decrease in ROS formation observed in presence of treatment was accompanied by a decrease in DNA strand breaks yield as revealed by the comet assay. Indeed, a greater kinetic of DNA repair was observed in presence of treatment so that OTM values (Fig. 2) returned to control values one hour post-irradiation, whereas three hours were necessary in absence of drugs. Unexpectedly, the administration of PTX/Tx 30 min after irradiation was also accompanied by a similar decrease in DNA damage level and subsequent OTM value reached control levels. These results would indicate that time of administration (15 min before or 30 min after irradiation) had no influence, and that in both conditions, DNA damage level is strongly decreased. Moreover, this would indicate that drugs do not simply act as radical scavenger preventing formation of initial damage but could possibly interfere with the mechanisms involved in cellular response to ionizing radiation during the first hours after exposure.

In addition, it was observed that, in absence of treatment, DNA strand breaks measured by the comet assay were decreasing during the first hours post irradiation and then remained at the basal level long term after exposure (data not shown). However, this decrease was also accompanied by a strong and delayed augment in micronuclei frequency (Fig. 3) in 10 Gy-irradiated cells. This raise remained high until three weeks post-irradiation. More surprisingly,

when the combination PTX/Tx was used, a very marked increase in MN frequency at day 10 and 14 followed by a decrease at day 21 was observed. This was previously demonstrated for PTX alone (Bozsakyova *et al*., 2001) or for the combination of drugs used in gamma-irradiated skin fibroblasts (Laurent *et al*., 2005). The first hypothesis which needs to be addressed and that could explain the delayed increase in micronuclei frequency could be prooxidant properties that are sometimes associated to antioxidants such as alpha-tocopherol or pentoxifylline. Indeed, it was shown that under certain circumstances, antioxidant compounds may exhibit unexpected oxidants-associated toxic effects (for review (Burkitt, 2001; Yoshida *et al*., 2003)). However, such phenomenon seems, under our experimental conditions, at least partly excluded because no increase in initial DNA damage as measured by the comet assay or alteration in cell viability parameters are observed in non-irradiated cells. Its involvement, if it exists, would be associated to irradiation.

The second hypothesis that might explain such raise in MN frequency associated to the decrease in early DNA strand breaks could be the interference of PTX/Tx with DNA repair pathways. Indeed, similar decrease in OTM was observed at any time treatment was added *i.e.* either before or after irradiation, suggesting that drugs-associated radical scavenging properties are not required. In this respect, previous published works underlined the interference of PTX and alpha-tocopherol with DNA repair and subsequent chromosomal damage like micronuclei (MN) (Theron *et al*., 2000; Bozsakyova *et al*., 2001; Binder *et al*., 2002) and ATM gene (Sarkaria and Eshleman, 2001). Considering that most of the cells in the present study are in G0/G1 phase, one possible DNA repair involved could be the error prone DNA double-strand breaks (DSB) repair process pathway, namely NHEJ (Non-Homologous End Joining). However, as alkaline comet assay allows to detect both single and double-strand breaks (SSB) together with alkali-labile sites, and considering that most of low-LET radiation-induced strand breaks are single strand breaks, it is not possible at this stage, to determine if decrease in DNA strand breaks measured by the comet assay concerns single or double lesions or both of them. Moreover, increase in MN frequency would suggest that it is DNA double strand breaks repair that would be implicated in the striking observed effects. However, at this stage further investigations are necessary to determine effects of drugs on both kinds of lesions and their involvement in DNA repair.

As mentioned, another effect of drugs described in literature is their role on cell cycle arrest. In particular, PTX was shown to inhibit G2 block induced by radiation exposure (Russell *et al.*, 1996; Eley *et al*., 2002; Strunz *et al*., 2002) and could subsequently sensitize cells to radiation. However, cell cycle analysis (Fig. 4) did not highlight any inhibition of cell cycle

arrest in presence of PTX/Tx after irradiation (Strunz *et al*., 2002) and clonogenic assay did not show any sensitization to radiation (Fig. 5). The latter results appear to be opposite to what was observed in fibroblast (Laurent *et al*., 2005) and the exact reason for such discrepancy remains unexplained.

In conclusion, this work showed the effectiveness of the combination PTX/Tx in reducing early and late ROS productions and in reducing DNA damage, as measured by the comet assay. However, PTX/Tx was shown not to simply act as radical scavenger because effects on DNA damage were observed even when drugs were added after irradiation. In addition, for the irradiation dose of 10 Gy, PTX/Tx was shown to strongly increase late micronuclei frequency but no sensitization to radiation was shown as measured by clonogenic assay between 0 and 6 Gy. Further works are now necessary to investigate the role of both drugs on DNA repair systems. Possible effects on the quality of DNA repair would be of major interest for clinical use of the combination.

Acknowledgements

The authors are thankful to Dr. J.-L. Lefaix and Dr S. Delanian for helpful discussions. This work was supported by Electricité de France-Service de Radioprotection and Région Ile-de-France.

References

Adamson, I. Y. and D. H. Bowden (1983). "Endothelial injury and repair in radiation-induced pulmonary fibrosis." Am J Pathol **112**(2): 224-30.

Archambeau, J. O., R. Pezner, et al. (1995). "Pathophysiology of irradiated skin and breast." Int J Radiat Oncol Biol Phys **31**(5): 1171-85.

Binder, A., T. Theron, et al. (2002). "Radiosensitization and DNA repair inhibition by pentoxifylline in NIH3T3 p53 transfectants." Int J Radiat Biol **78**(11): 991-1000.

Bozsakyova, E., I. Chalupa, et al. (2001). "Chromosomal aberrations, sister chromatid exchanges and micronuclei induced by pentoxifylline in in vitro cultivated Chinese hamster cells (V79) and human blood lymphocytes." Mutat Res **497**(1-2): 63-70.

Burkitt, M. J. (2001). "A critical overview of the chemistry of copper-dependent low density lipoprotein oxidation: roles of lipid hydroperoxides, alpha-tocopherol, thiols, and ceruloplasmin." Arch Biochem Biophys **394**(1): 117-35.

Chiao, T. B. and A. J. Lee (2005). "Role of pentoxifylline and vitamin E in attenuation of radiation-induced fibrosis." Ann Pharmacother **39**(3): 516-22.

Delanian, S., F. Baillet, et al. (1994). "Successful treatment of radiation-induced fibrosis using liposomal Cu/Zn superoxide dismutase: clinical trial." Radiother Oncol **32**(1): 12-20.

Delanian, S., S. Balla-Mekias, et al. (1999). "Striking regression of chronic radiotherapy damage in a clinical trial of combined pentoxifylline and tocopherol." J Clin Oncol **17**(10): 3283-90.

Delanian, S. and J.-L. Lefaix (2004). "The radiation-induced fibroatrophic process: therapeutic perspective via the antioxidant pathway." Radiother Oncol **73**: 119-131.

Delanian, S. and J. L. Lefaix (2002). "Complete healing of severe osteoradionecrosis with treatment combining pentoxifylline, tocopherol and clodronate." Br J Radiol **75**(893): 467-9.

Delanian, S., R. Porcher, et al. (2003). "Randomized, placebo-controlled trial of combined pentoxifylline and tocopherol for regression of superficial radiation-induced fibrosis." J Clin Oncol **21**(13): 2545-50.

Dubray, B., S. Delanian, et al. (1997). "[Late effects of mammary radiotherapy on skin and subcutaneous tissues]." Cancer Radiother **1**(6): 744-52.

Ehrly, A. M. (1979). "The effect of pentoxifylline on the deformability of erythrocytes and on the muscular oxygen pressure in patients with chronic arterial disease." J Med **10**(5): 331-8.

Ehrly, A. M. and W. Schroeder (1977). "Oxygen pressure values in the ischemic muscle tissue of patients with chronic occlusive arterial disease." Adv Exp Med Biol **94**: 401-5.

Eley, K. W., S. H. Benedict, et al. (2002). "The effects of pentoxifylline on the survival of human glioma cells with continuous and intermittent stereotactic radiosurgery irradiation." Int J Radiat Oncol Biol Phys **54**(2): 542-50.

Freitas, J. P., P. Filipe, et al. (1995). "[Potential antioxidative effects of pentoxifylline]." C R Seances Soc Biol Fil **189**(3): 401-5.

Hill, R. P., H. P. Rodemann, et al. (2001). "Normal tissue radiobiology: from the laboratory to the clinic." Int J Radiat Oncol Biol Phys **49**(2): 353-65.

Horvath, B., Z. Marton, et al. (2002). "In vitro antioxidant properties of pentoxifylline, piracetam, and vinpocetine." Clin Neuropharmacol **25**(1): 37-42.

Kumar, B., M. N. Jha, et al. (2002). "D-alpha-tocopheryl succinate (vitamin E) enhances radiation-induced chromosomal damage levels in human cancer cells, but reduces it in normal cells." J Am Coll Nutr **21**(4): 339-43.

Laurent, C., J. P. Pouget, et al. (2005). "Modulation of DNA damage by pentoxifylline and a-tocopherol in skin fibroblasts exposed to gamma-rays." Radiat Res **Under Press**.

Law, M. P. (1981). "Radiation-induced vascular injury and its relation to late effects in normal tissue." Adv Radiat Biol **9**: 37.

LeBel, C. P., H. Ischiropoulos, et al. (1992). "Evaluation of the probe 2',7'-dichlorofluorescin as an indicator of reactive oxygen species formation and oxidative stress." Chem Res Toxicol **5**(2): 227-31.

Lefaix, J. L., S. Delanian, et al. (1996). "Successful treatment of radiation-induced fibrosis using Cu/Zn-SOD and Mn-SOD: an experimental study." Int J Radiat Oncol Biol Phys **35**(2): 305-12.

Lefaix, J. L., S. Delanian, et al. (1999). "Striking regression of subcutaneous fibrosis induced by high doses of gamma rays using a combination of pentoxifylline and alpha-tocopherol: an experimental study." Int J Radiat Oncol Biol Phys **43**(4): 839-47.

Letur-Konirsch, H., F. Guis, et al. (2002). "Uterine restoration by radiation sequelae regression with combined pentoxifylline-tocopherol: a phase II study." Fertil Steril **77**(6): 1219-26.

Paris, F., Z. Fuks, et al. (2001). "Endothelial apoptosis as the primary lesion initiating intestinal radiation damage in mice." Science **293**(5528): 293-7.

Peter, R. U. and P. Gottlober (2002). "Management of cutaneous radiation injuries: diagnostic and therapeutic principles of the cutaneous radiation syndrome." Mil Med **167**(2 Suppl): 110-2.

Phillips, T. L. (1966). "An ultrastructural study of the development of radiation injury in the lung." Radiology **87**(1): 49-54.

Pouget, J. P., T. Douki, et al. (2000). "DNA damage induced in cells by gamma and UVA radiation as measured by HPLC/GC-MS and HPLC-EC and Comet assay." Chem Res Toxicol **13**(7): 541-9.

Pouget, J. P., C. Laurent, et al. (2004). "PCC-FISH in skin fibroblasts for local dose assessment: biodosimetric analysis of a victim of the Georgian radiological accident." Radiat Res **162**(4): 365-76.

Rimbach, G., A. M. Minihane, et al. (2002). "Regulation of cell signalling by vitamin E." Proc Nutr Soc **61**(4): 415-25.

Robbins, M. E. and W. Zhao (2004). "Chronic oxidative stress and radiation-induced late normal tissue injury: a review." Int J Radiat Biol **80**(4): 251-9.

Rube, C. E., F. Wilfert, et al. (2002). "Modulation of radiation-induced tumour necrosis factor alpha (TNF-alpha) expression in the lung tissue by pentoxifylline." Radiother Oncol **64**(2): 177-87.

Rubin, P. and G. W. Casarett (1968). "Clinical radiation pathology as applied to curative radiotherapy." Cancer **22**(4): 767-78.

Russell, K. J., L. W. Wiens, et al. (1996). "Preferential radiosensitization of G1 checkpoint-deficient cells by methylxanthines." Int J Radiat Oncol Biol Phys **36**(5): 1099-106.

Sarkaria, J. N. and J. S. Eshleman (2001). "ATM as a target for novel radiosensitizers." Semin Radiat Oncol **11**(4): 316-27.

Strunz, A. M., P. Peschke, et al. (2002). "Preferential radiosensitization in p53-mutated human tumour cell lines by pentoxifylline-mediated disruption of the G2/M checkpoint control." Int J Radiat Biol **78**(8): 721-32.

Sweetman, S. F., J. J. Strain, et al. (1997). "Effect of antioxidant vitamin supplementation on DNA damage and repair in human lymphoblastoid cells." Nutr Cancer **27**(2): 122-30.

Theron, T., A. Binder, et al. (2000). "The role of G2-block abrogation, DNA double-strand break repair and apoptosis in the radiosensitization of melanoma and squamous cell carcinoma cell lines by pentoxifylline." Int J Radiat Biol **76**(9): 1197-208.

Ts'ao, C. H., W. F. Ward, et al. (1983). "Radiation injury in rat lung. III. Plasminogen activator and fibrinolytic inhibitor activities." Radiat Res **96**(2): 301-8.

Weiss, J. F. and M. R. Landauer (2003). "Protection against ionizing radiation by antioxidant nutrients and phytochemicals." Toxicology **189**(1-2): 1-20.

Yoshida, Y., E. Niki, et al. (2003). "Comparative study on the action of tocopherols and tocotrienols as antioxidant: chemical and physical effects." Chem Phys Lipids **123**(1): 63-75.

Figures legends

Figure 1. Modulation of peroxide production in endothelial cells exposed to radiation by PTX/Tx. Peroxide production was assayed in HMVEC-d cells exposed to 0 Gy (A), 3 Gy (B) or 10 Gy (C) according PTX/Tx were added either before or after irradiation. DCFH oxidation was measured by flow cytometry (MFI = mean fluorescence intensity). Data are depicted as mean ± SEM of three experiments. *p < .05 or **p < .005 vs. control.

Figure 2. DNA damage in endothelial cells after radiation exposure and modulation by PTX/Tx. HMVEC-d cells were gamma-irradiated at confluent stage at doses of 0 Gy (A), 3 Gy (B) or 10 Gy (C) and PTX/Tx was added either before or after irradiation. Alkaline comet assay was performed and Olive Tail Moment (OTM) was calculated by analysis software. Data are depicted as mean ± SEM of three experiments.

Figure 3. Micronuclei frequency in endothelial cells after radiation exposure and modulation by PTX/Tx. HMVEC-d were irradiated at 0 Gy (A), 3 Gy (B) or 10 Gy (C) and PTX/Tx was added either before or after irradiation. Cells were reseeded at different times post-irradiation and grown for 24 h. They were next incubated with cytochalasin B for 24 h before hypotonic shock and fixation were done. Then, staining was done using propidium iodide and determination of micronuclei was done among 200 cells using a fluorescence microscope. Data are depicted as mean ± SEM (three experiments). *p < .05 or **p < .005 vs. control for untreated cells and vs. untreated cells for the treated one.

Figure 4. Cell cycle after irradiation in endothelial cells and modulation by PTX/Tx. HMVEC-d were irradiated at confluent stage at dose of 0 Gy in absence (A) or in presence (B) of PTX/Tx added 15 min before irradiation and at doses of 10 Gy in absence (C) or in presence (D) of PTX/Tx added 15 min before irradiation. Cells were reseeded at different times post-irradiation and grown for 24 h before fixation and staining with propidium iodide. Analysis was performed by flow cytometry. Data are depicted as mean ± SEM.

Figure 5. Endothelial cells survival and modulation by PTX/Tx. Clonogenic survival of HMVEC-d cells was assayed as described by Puck and Marcus. The combination PTX/Tx was administered either before or after irradiation. Data are depicted as mean ± SEM of three

experiments. *p < .05 or **p < .005 vs. control for untreated cells and vs. untreated cells for the treated one.

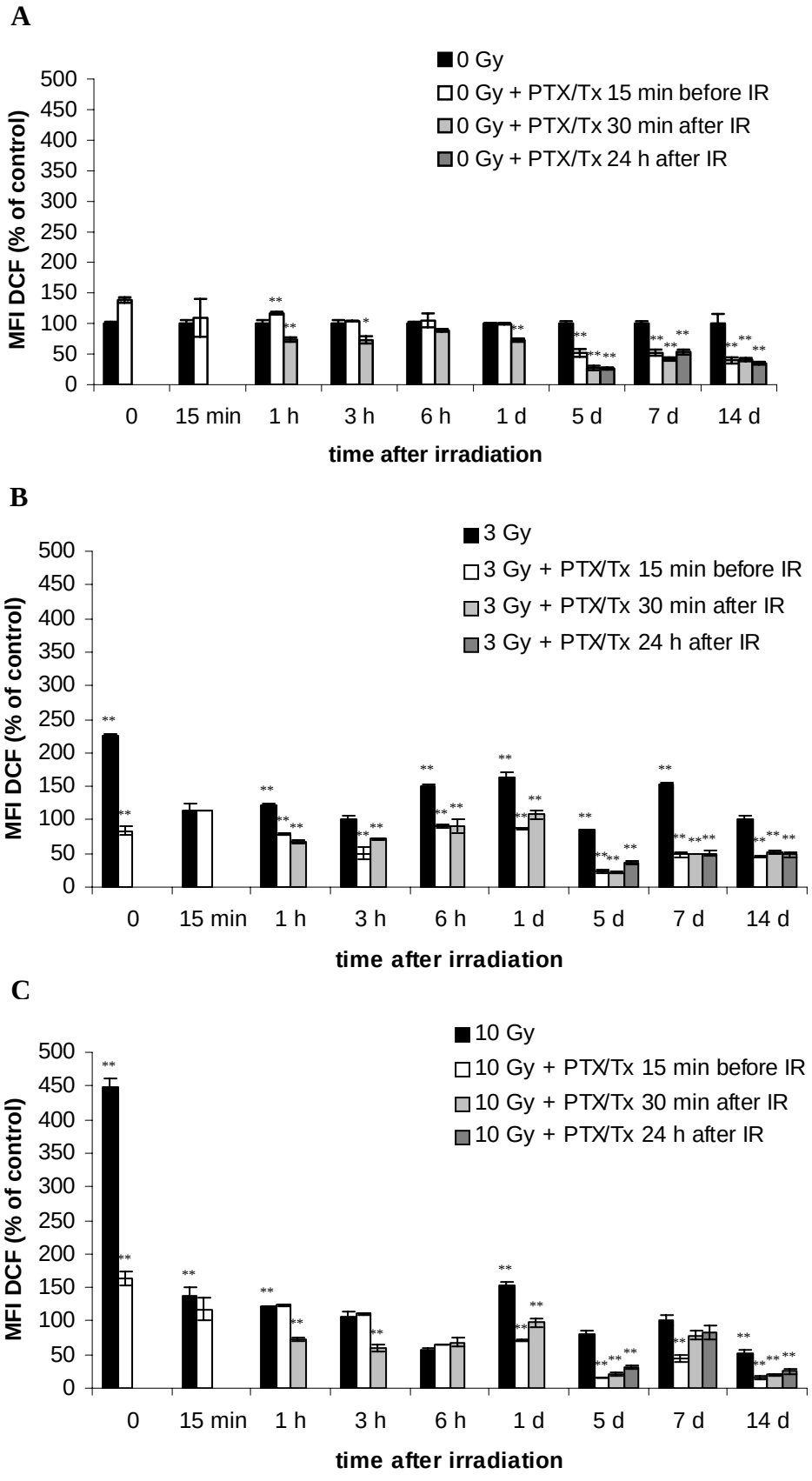
A
0 Gy
0 Gy + PTX/Tx 15 min before IR
0 Gy + PTX/Tx 30 min after IR
0 Gy + PTX/Tx 24 h after IR
MFI DCF (% of control)
time after irradiation
0
15 min
1 h
3 h
6 h
1 d
5 d
7 d
14 d
B
3 Gy
3 Gy + PTX/Tx 15 min before IR
3 Gy + PTX/Tx 30 min after IR
3 Gy + PTX/Tx 24 h after IR
MFI DCF (% of control)
time after irradiation
C
10 Gy
10 Gy + PTX/Tx 15 min before IR
10 Gy + PTX/Tx 30 min after IR
10 Gy + PTX/Tx 24 h after IR
MFI DCF (% of control)
time after irradiation

Figure 1

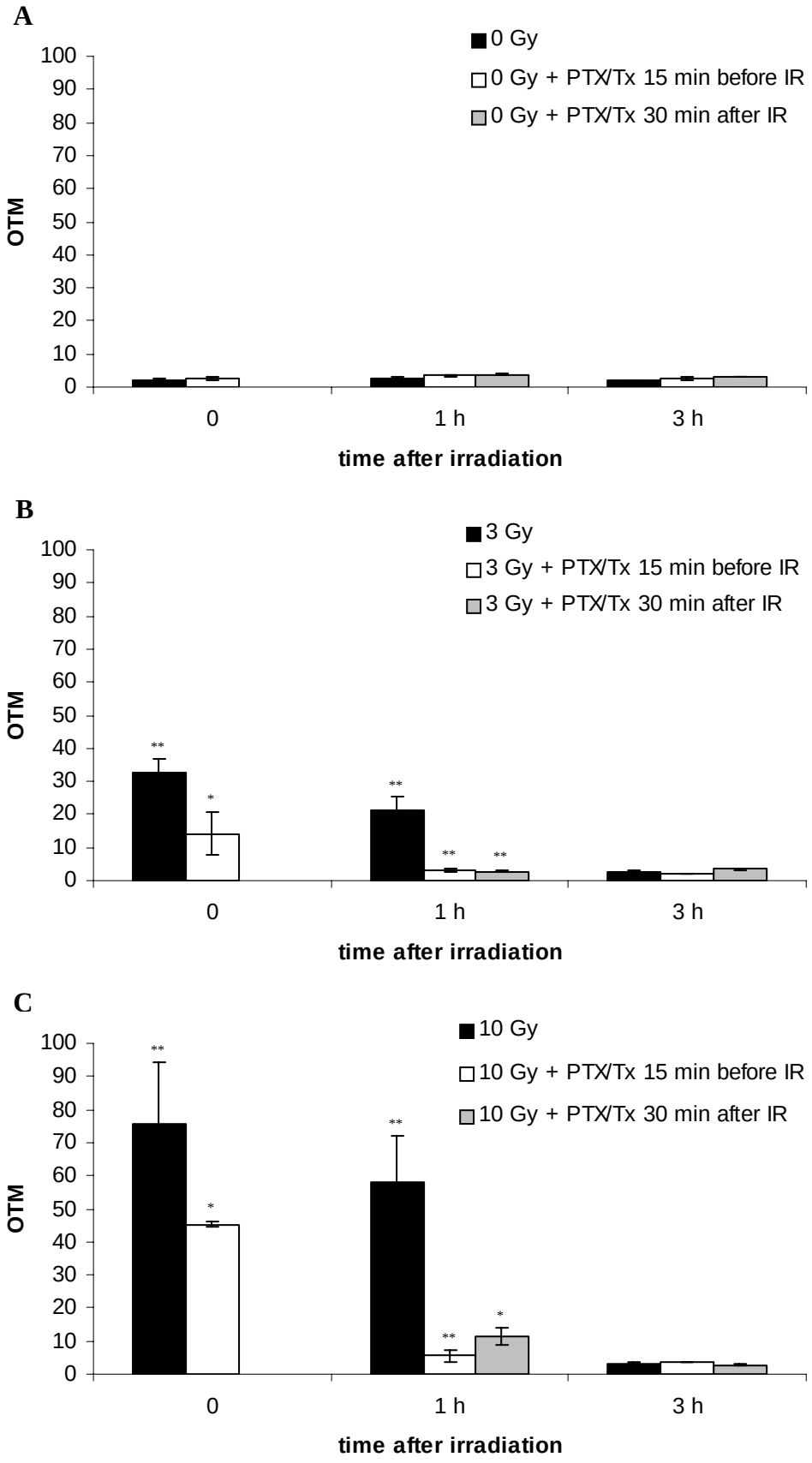
A
0 Gy
0 Gy + PTX/Tx 15 min before IR
0 Gy + PTX/Tx 30 min after IR
OTM
time after irradiation
B
3 Gy
3 Gy + PTX/Tx 15 min before IR
3 Gy + PTX/Tx 30 min after IR
OTM
time after irradiation
C
10 Gy
10 Gy + PTX/Tx 15 min before IR
10 Gy + PTX/Tx 30 min after IR
OTM
time after irradiation
0
1 h
3 h

Figure 2

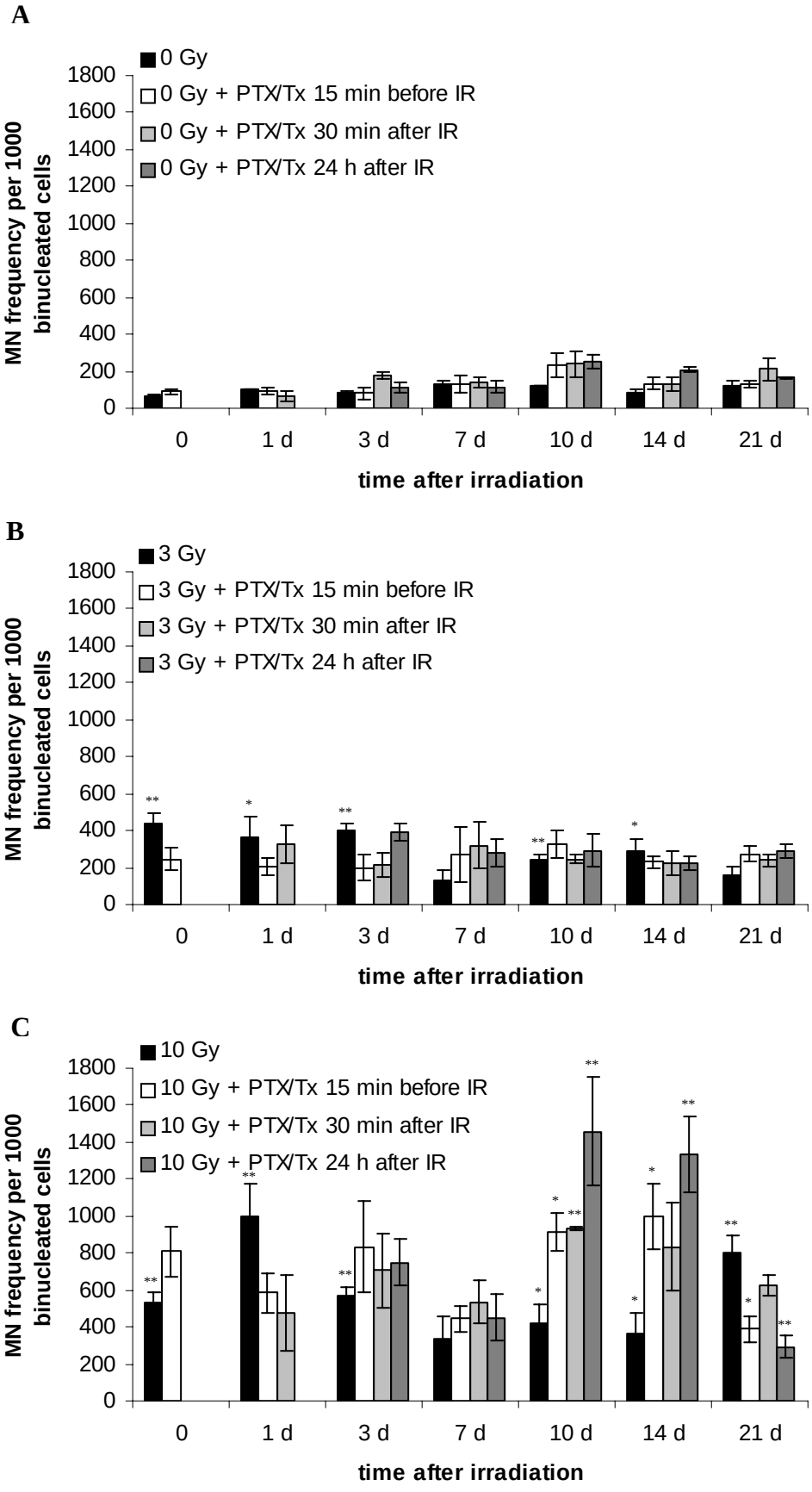
A
0 Gy
0 Gy + PTX/Tx 15 min before IR
0 Gy + PTX/Tx 30 min after IR
0 Gy + PTX/Tx 24 h after IR
MN frequency per 1000 binucleated cells
time after irradiation
B
3 Gy
3 Gy + PTX/Tx 15 min before IR
3 Gy + PTX/Tx 30 min after IR
3 Gy + PTX/Tx 24 h after IR
MN frequency per 1000 binucleated cells
time after irradiation
C
10 Gy
10 Gy + PTX/Tx 15 min before IR
10 Gy + PTX/Tx 30 min after IR
10 Gy + PTX/Tx 24 h after IR
MN frequency per 1000 binucleated cells
time after irradiation
0
1 d
3 d
7 d
10 d
14 d
21 d

Figure 3

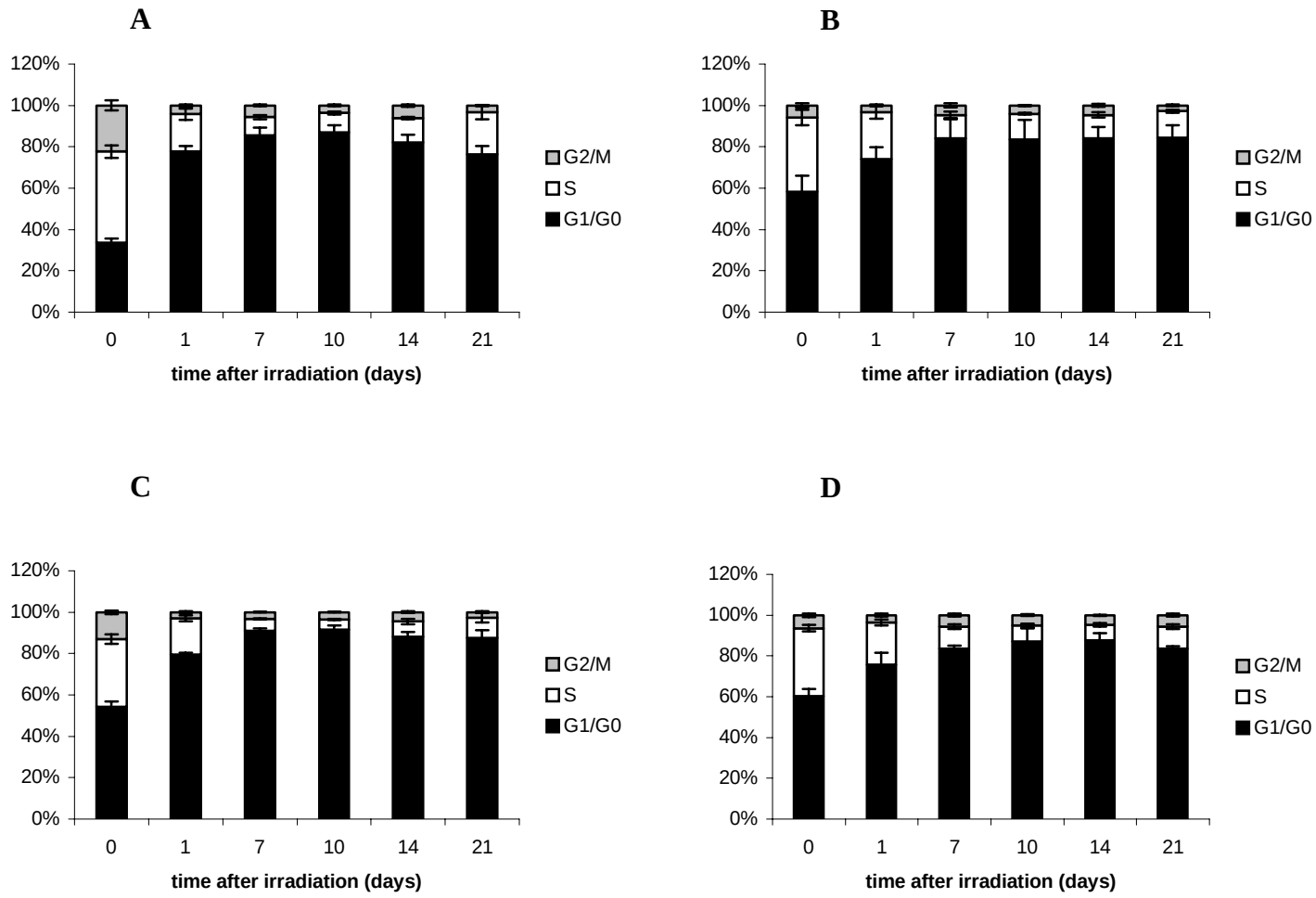
A
B
C
D
120%
100%
80%
60%
40%
20%
0%
0
1
7
10
14
21
time after irradiation (days)
G2/M
S
G1/G0

Figure 4

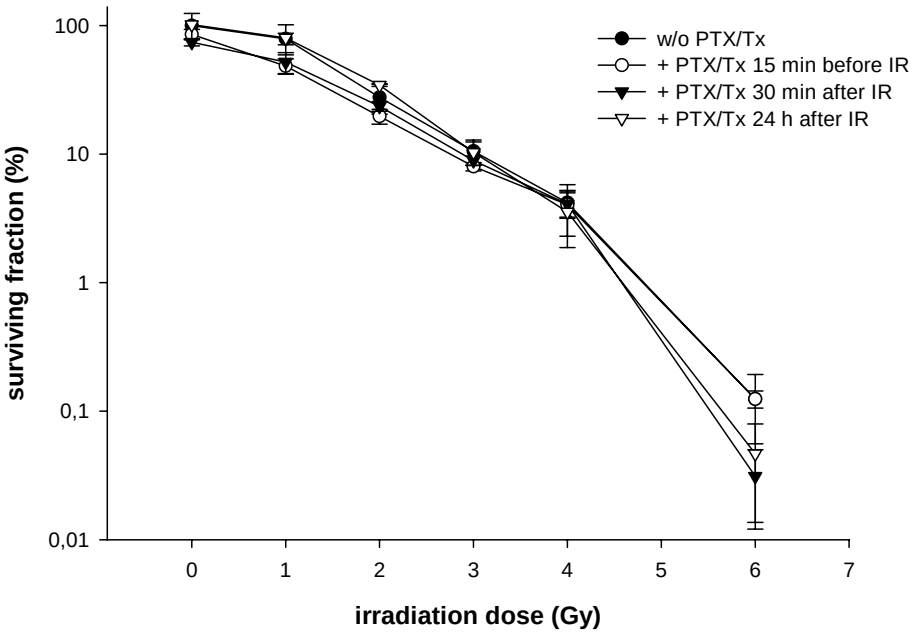
w/o PTX/Tx
+ PTX/Tx 15 min before IR
+ PTX/Tx 30 min after IR
+ PTX/Tx 24 h after IR
surviving fraction (%)
100
10
1
0,1
0,01
0
1
2
3
4
5
6
7
irradiation dose (Gy)

Figure 5

IV- Effets différentiels de PTX et Tx sur l'association

Article 5 : Effets différentiels de la pentoxifylline et de l'α-tocophérol sur les lésions de l'ADN radio-induites dans les fibroblastes de peau

Afin d'étudier les mécanismes d'action de l'association PTX et Tx, il est apparu essentiel de mesurer l'effet de chacune des deux drogues utilisées séparément.

Pour cela, les propriétés anti-oxydantes des drogues, leurs effets sur les lésions de l'ADN et sur la survie cellulaire ont été mesurés dans les fibroblastes de derme.
Nous avons ainsi pu montrer que PTX et Tx agissaient différemment. PTX a un pouvoir anti-oxydant plus faible que celui de Tx et est aussi moins efficace à réduire les lésions de l'ADN mesurées par la méthode des comètes. Par ailleurs, il faut noter que ces mêmes lésions sont plus vite réparées lorsque l'association des deux drogues est utilisée que lorsque celles-ci sont utilisées de façon séparée ce qui suggère un effet coopératif entre les deux substances. En revanche, PTX diminue la fréquence des micronoyaux contrairement à Tx qui l'augmente. On peut émettre l'hypothèse que PTX et Tx agissent par des voies différentes sur la réparation de l'ADN. Ainsi, PTX pourrait être impliquée dans l'activation d'un système de réparation fidèle des CDB alors que Tx, comme l'association PTX/Tx, pourrait lui conduire à une réparation infidèle. Les résultats de survie clonogénique que nous avons obtenus sont cependant opposés à cette hypothèse puisque PTX s'est avérée être un composé radiosensibilisateur et Tx radioprotecteur. Une telle contradiction apparente pourrait s'expliquer par l'action de PTX sur la progression des cellules dans le cycle cellulaire. Le nombre de cellules binuclées en présence de PTX est largement inférieur à celui obtenu avec Tx ou avec l'association des deux drogues, jusqu'au 21ème jour. Par conséquent, le taux de formation des micronoyaux/cellule binucléée l'est aussi et comme peu de cellules s'engagent dans le cycle, il en résulte que peu de colonies se forment et sont mesurées par le test de survie clonogénique analysé 12 jours après irradiation.

Si nous avons confirmé le caractère antioxydant des deux substances, nous avons aussi mis en évidence l'interférence de Tx et PTX avec les voies de réparation de l'ADN.

Differential effects of pentoxifylline, α-tocopherol and the combination on radiation-induced DNA damage in skin fibroblasts

Carine Laurent[1], Philippe Voisin[2], Ph.D., and Jean-Pierre Pouget[2,3†], Ph.D.

[1] Laboratoire de Dosimétrie Biologique, DRPH/SRBE, Institut de Radioprotection et de Sûreté Nucléaire, Fontenay-aux-Roses, France

[2] Service de Radiobiologie et d'Epidémiologie, DRPH, Institut de Radioprotection et de Sûreté Nucléaire, Fontenay-aux-Roses, France

[3] INSERM, EMI 0227, Immunociblage des tumeurs et Ingénierie des Anticorps, Centre de Recherche en Cancérologie, CRLC Val d'Aurelle, Institut Paul Lamarque, Montpellier, France

Running title: DNA damage modulation by pentoxifylline and α-tocopherol

† Address correspondance to : Jean-Pierre Pouget, Immunociblage des tumeurs et Ingénierie des Anticorps, EMI 0227, INSERM, Centre de Recherche en Cancérologie, CRLC Val d'Aurelle, Institut Paul Lamarque, 34298 Montpellier Cedex, France ; Tel: +33 4 67 61 37 08; E-mail: jppouget@valdorel.fnclcc.fr.

Abstract

Pentoxifylline (PTX) and α-tocopherol (αT) were shown to reduce the late radiation-induced skin damage only when administered in combination. The effects of the two separate compounds remain to be elucidated. Antioxidant capacity of separate drugs or of the combination was first assessed. Trolox (Tx), the water-soluble analogue of αT, was shown to be a stronger antioxidant than PTX and the combination was slightly more antioxidant than Tx used alone. Confluent primary cultures of dermal fibroblasts were gamma-irradiated and incubated in presence of PTX and/or Tx. Marked decrease in DNA strand-breaks level, as measured by the comet assay, was measured when combination was used. It was shown that Tx was statistically even more efficient than combination (or PTX) in reducing strand breaks either immediately or 1 hour after irradiation. However, the lack of additive effect between the two drugs in their ability in reducing strand breaks immediately after irradiation, would suggest they might act in different and partially opposite ways. By contrast one hour after irradiation, additive effect was observed so that strand breaks level was lower when the combination was used. Considering delayed production of micronuclei (MN), an increase was observed when PTX+Tx or Tx alone were used whereas PTX was shown to decrease MN frequency. Surprisingly, clonogenic values highlighted a radioprotective effect of Tx, whereas PTX was shown to be a radiosensitizing. Such apparent discrepancy between clonogenic survey and MN yield could be due to the effect of PTX on cell cycle progression. Indeed the number of binucleated cells was much lower in presence of PTX until two weeks after irradiation, *i.e.* after clonogenic survey was analysed. Therefore, the number of cells entering mitosis at the origin of a colony would be lower when PTX was used alone. Opposite effect was observed with Tx, which therefore was shown to be radioprotective. Therefore, this study would indicate that if Tx and PTX are antioxidants and decrease initial level of DNA strand breaks, they would interfere with DNA repair processes leading to modulation of MN yield. However, radiosensitizing effect was only observed with PTX.

Author Keywords

Ionizing radiation; DNA damage; pentoxifylline; α-tocopherol; skin fibroblasts; trolox

1. INTRODUCTION

Oxidative phenomenon that occur after ionizing radiation exposure, are often considered as the initiators of injury (Dubray *et al*., 1997) as directly produced by irradiation itself or by tissue response including inflammatory mechanisms. Pharmacological treatments which aimed at reducing radiation effect have thus focused on antioxidants such as the detoxification enzyme, superoxide dismutase (SOD), which was shown to allow a fast regression of radiation-induced fibrosis either in patients (Delanian *et al*., 1994), in pigs (Lefaix *et al*., 1996) or in a three-dimensional co-culture model of skin (Vozenin-Brotons *et al*., 2001). However, as it could not be produced for a safe clinical treatment, the combination of pentoxifylline (PTX), an antioxidant phytochemical, and of α-tocopherol (αT), an antioxidant nutrient, was preferred and showed a similar effectiveness.

PTX, a synthetic antioxidant methylxanthine, was first delivered to patients that had vascular disease because of its properties to improve tissue oxygenation. PTX is a non-specific phosphodiesterase inhibitor which leads to an increased cellular level of cAMP. Recent studies have shown that PTX could act as a radical scavenger (Freitas *et al*., 1995; Horvath *et al*., 2002) and could regulate the expression of TNFα and other inflammatory cytokines (Rube *et al*., 2002). By contrast to p53-mutated or -disrupted cells, p53-wild type tumour cells were not radiosensitized by PTX (Russell *et al*., 1996; Strunz *et al*., 2002; Theron *et al*., 2000) but an inhibition of DNA double-strand breaks (DSB) repair (Binder *et al*., 2002; Theron *et al*., 2000) and an increase in chromosomal aberrations, sister chromatid exchange and micronuclei (Bozsakyova *et al*., 2001) was observed. *In vivo* studies reported opposite effects of the administration of PTX used alone. PTX was found to reduce late radiation-induced skin injury in mice (Dion *et al*., 1989) and delayed toxicity in lung of rats (Koh *et al*., 1995). This compound was also shown to induce healing of soft tissue in patients suffering from late radiation necrosis (Dion *et al*., 1990) and to have a significant protective effect against early and late lung radiotoxicity in patients undergoing radiotherapy (Ozturk *et al*., 2004). However, no beneficial effects on acute (Dion *et al*., 1989; Ward *et al*., 1992) and late radiation-induced skin injury were observed in other studies (Koh *et al*., 1995; Lefaix *et al*., 1999; Delanian *et al*., 2003).

The second compound of interest is αT. αT is a constituent of the Vitamin E family which forms the most important lipid-soluble antioxidant group. Besides of its known antioxidant properties, αT was shown to inhibit *in vitro* inflammation, cell adhesion, platelet aggregation and smooth muscle cell proliferation (for review: Rimbach *et al*., 2002; Weiss and Landauer,

2003). αT and any of its derivatives had protective effects against DNA damage in irradiated lymphoblastoid cells (Sweetman *et al*., 1997), in bone marrow from irradiated mouse (Sarma and Kesavan, 1993) and in normal cells whereas the level of these damage was enhanced in tumour cells (Kumar *et al*., 1999). As for PTX, these results suggest an interesting use of αT to reduced drawbacks associated to radiation therapy. *In vivo*, few studies have reported the effects of αT on radiation-induced injury. In mice, erythrocytes exposed to irradiation were shown to have a reduced percentage of aberrant metaphases, and a decreased number of micronuclei when a water-soluble vitamin E derivative was used (Satyamitra *et al*., 2003). Clinical trials associated to radiotherapy have shown an improvement of oral mucositis (Worthington *et al*., 2002) but no modifications were observed on radiation-induced skin fibrosis (Delanian *et al*., 2003).

When used in combination, PTX and αT appeared to be very effective in reducing the late radiation-induced skin injuries. Lefaix *et al.* used this combination in the treatment of irradiated pigs and showed regression of radiation-induced skin fibrosis (Lefaix *et al*., 1999). Clinical trials based on patients undergoing radiotherapy have also indicated a continuous regression of the chronic damage (Delanian *et al*., 1999; Delanian *et al*., 2003), a reduction of radiation-induced fibroatrophic uterine lesions (Letur-Konirsch *et al*., 2002) and, when the combination was administered with clodronate, a complete reversion of osteoradionecrosis and radiation-induced fibrosis (Delanian and Lefaix, 2002). The role of both drugs in these effects remains to be elucidated.

We showed in previous works (Laurent *et al*., 2005; Laurent *et al*., 2005) that the combination of PTX and Tx, the water-soluble analogue of αT, was accompanied by a decrease in DNA damage as measured by the comet assay in both fibroblasts and endothelial cells exposed to gamma-irradiation. This decrease was observed even when drugs were added after irradiation, suggesting they did not simply act as antioxidants. In addition, it was shown a delayed increased micronuclei formation which occurred on day 7 and lasted until the end of considered period which was about 21 days. Moreover, a radiosensitizing effect was observed in fibroblasts. The present *in vitro* study deals with the effect of either PTX or Tx, on radiation-induced DNA damage in 10 Gy-gamma-irradiated fibroblasts. A comparison with the effects of the combination of drugs was also done. Drugs were added 15 min before irradiation. Clonogenic survey together with antioxidant capacities were also measured.

Our results indicated that if both drugs are antioxidants, a more pronounced reduction in initial DNA strand breaks measured by the comet assay is caused by Tx. In addition, PTX was shown to be radiosensitizing whereas Tx was radioprotective. Considering micronuclei (MN)

formation, opposite effects were observed. Indeed, use of PTX was associated to a decrease in MN yield while a raise was observed in presence of Tx. However such discrepancy between both assays might be due to differential effects of drugs on cell cycle progression. Therefore, these results would indicate that both PTX and Tx would interfere with DNA repair pathways in different ways but only use of PTX is accompanied by a radiosensitizing effect.

2. MATERIALS AND METHODS

2.1. Reagents

Dulbecco's modified Eagle medium (DMEM), fetal bovine serum, N-(2-hydroxyethyl)piperazine-N'-(2-ethanesulfonic acid) (HEPES) buffer, Dulbecco's phosphate-buffered saline (PBS), trypsin/EDTA, L-glutamine, penicillin and streptomycin were purchased from Gibco BRL Life Technologies (Gaithersburg, MD, USA). Collagenase P was obtained from Roche (Indianapolis, IN, USA). All others chemicals were provided by Sigma (St. Louis, MO, USA).

2.2. ORAC assay

Antioxidant status was assessed by the Oxygen Radical Absorbing Capacity (ORAC) assay as described by Cao et al. (Cao et al., 1993) using a spectrofluorimeter (Kontron Instruments, model SFM 25, Germany) with excitation wavelength of 540 nm and emission wavelength of 565 nm. ORAC values were obtained from the area under the quenching curve of β-phycoerythrin in the presence of the peroxyl radical generator, 2,2'-azo-bis(2-amidinopropane) dihydrochloride (AAPH), and of the studied molecules, PTX and Tx. PTX and Tx were used either separately or together at concentrations ranging from 0.5 mM to 4 mM. One ORAC unit was equal to the antioxidant status of 1 µM Trolox as presented by Cao et al. (Cao et al., 1993).

2.3. Cell cultures

NHF-d (normal human fibroblasts from dermis) were obtained from adult healthy individuals undergoing elective surgery. Briefly, after removal of the epidermis with a scalpel blade, dermal tissue was digested in three successive baths of trypsin/collagenase P (0.5%/0.25%) at 37°C for 30 min under stirring. Cell suspension was collected, centrifuged and resuspended in DMEM supplemented with 20% fetal bovine serum, 100 µg/ml L-glutamine, 10 mM HEPES

and antibiotics (100 units/ml penicillin and 100 µg/ml streptomycin). Cells were next plated onto flasks coated with collagen I and grown at 37°C in a humidified atmosphere of 5% CO2 up to the first passage. Then, fibroblasts were plated in uncoated flasks for the following passages. Experiments were performed at passages 4-7.

2.4. Cell treatment and γ-radiation

Two days after reaching confluence, cells were irradiated using a 137Cs source (IBL 637, Cis bio International) at room temperature, at a dose rate of 1 Gy/min. PTX and/or Tx, diluted in medium (final concentration of 0.5 mM), were added 15 min before radiation exposure. PTX was first dissolved in water at a concentration of 100 mM and Tx, the water-soluble analogue of α-T, in methanol at a concentration of 100 mM. The treatment was maintained during the whole considered period of 21 days.

2.5. Clonogenic assay

Clonogenicity was assayed according to the method described by Puck and Marcus (Puck et al., 1956). Briefly, a precise number of cells, depending on irradiation doses ranging from 0 to 6 Gy, was plated. After 4 hours, plated cells were treated 15 min before irradiation as described above. Cells were allowed to grow for 10 days. Colonies were then stained with Crystal violet (2.5 g/L of 45:5 methanol/paraformaldehyde 30%). Colonies containing 50 or more cells were scored and the surviving fraction was calculated. The experiment was repeated three times in triplicate.

2.6. Alkaline single-cell gel electrophoresis (comet assay)

The alkaline single-cell gel electrophoresis assay was used to measure DNA single and double strand breaks together with alkali-labile sites in 10 Gy-irradiated confluent fibroblasts treated 15 min before irradiation. The method described by Pouget et al (Pouget et al., 2000) was slightly modified. Briefly, 20,000 cells were suspended in 1.2% low melting point agarose and laid onto frosted glass microscope slides precoated with a 1% normal melting point agarose layer. Slides were immersed in a lysis buffer (2.5 M NaCl, 100 mM Na2EDTA, 10 mM Tris at pH 10, 1% sodium sarcosinate v/v, 1% Triton X-100 v/v, and 10% DMSO v/v) at 4°C overnight. Electrophoresis was performed at 25 V (corresponding to 1.15 V/cm), 300 mA for 45 min in 300 mM NaOH and 1 mM Na_2EDTA before nuclei were stained with propidium iodide (500 µg/ml). The Olive Tail Moment of 50 cells per slide was calculated by the computer image analysis software from IMSTAR (Paris, France) using a fluorescence

microscope (Olympus). The average Olive Tail Moment was determined using three slides from three different wells and the experiment was repeated three times.

2.7. Micronuclei assay

Micronuclei assay was used in confluent fibroblasts exposed to the irradiation dose of 10 Gy and treated 15 min before irradiation. Fibroblasts were reseeded at different times post-irradiation to perform one cell cycle. Cytochalasin B was added to the medium (final concentration of 5 µg/mL) to block cytokinesis. Twenty four hours later, cells were harvested and treated with KCl 125 mM under constant shaking for hypotonic chock. Then, cells were fixed three times in acetic acid:ethanol 1:6 (v/v) and dropped on slides under humidified atmosphere. Before analyzing, slides were stained with propidium iodide (500 µg/mL). Micronuclei and binucleated cells frequencies were determined for 500 cells using a fluorescence microscope (Nikon, Microphot-FXA). Three slides from three different wells were counted and the experiment was repeated three times. Micronuclei (MN) yield was analysed 7, 14 and 21 days after irradiation, corresponding to time at which increase in MN was measured in previous studies dealing with effect of the combination PTX/Tx (Laurent et al., 2005; Laurent et al., 2005).

2.8. Statistical analysis

Data are depicted as mean ± SEM; *p < .05 and **p < .001 were considered statistically significant (one-way ANOVA with Tukey test). Each experiment comprised three points and was repeated three times.

3. RESULTS

3.1. Antioxidant capacity of PTX, Tx and the combination

Figure 1 shows the Oxygen Radical Absorbing Capacity values obtained for Tx and PTX or for the combination when used in range of concentration between 0 and 4 mM. Such range was chosen in according to values described in the literature. For Tx, PTX and the combination, 0.5 mM was shown to be the concentration most efficient in scavenging ROS, or more specially peroxyl radicals, with values of 3.8, 2.9 and 4.0, respectively. Moreover, Tx was more antioxidant than PTX at 0.5 mM (+ 31%) and at 1.5 mM (+ 20%). At these concentrations, the antioxidant capacity of the combination was shown to be slightly higher

than for Tx (+ 5% at 0.5 mM and + 32% at 1.5 mM). At 4 mM, Tx antioxidant capacity was strongly decreased to 0.7 whereas PTX ORAC value rose to 2.1 without reaching ORAC value obtained at 0.5 mM. At this concentration, the ORAC value of the combination was similar to the one of PTX.

3.2. Modulation of radiation-induced DNA damage by PTX, Tx and the combination

The alkaline comet assay was used to measure single- and double-strand breaks together with alkali-labile sites formation after radiation exposure of NHF-d (Fig. 2). An initial increase in DNA damage was observed immediately after 10 Gy radiation exposure (Fig. 2A) with an OTM around 100 AU (Arbitrary Units). Such DNA damage production was lower in presence of Tx (-42%), PTX (-26%) and of the combination (-33%). Tx was shown to be more efficient than PTX and also than the combination in reducing DNA damage. Then, a rapid decrease in OTM values was observed so that they reached, 3 hours after irradiation, OTM value of 2 AU measured in control cells (data not shown). One hour after irradiation, around 33% of initial DNA damage were not repaired and this proportion of remaining strand breaks was about 21% for Tx, 26% for PTX and 14% for the combination. From these results, it appears that Tx was, as immediately after irradiation, more efficient than PTX in reducing strand breaks level. However, by contrast to what was observed immediately after irradiation, combination of drugs was accompanied by a statistically stronger decrease, suggesting additive effect between Tx and PTX.

If one considers DNA repair kinetic (Fig. 2B), half time of DNA repair in presence of Tx and PTX was shown to be similar to value obtained in absence of treatment whereas combination was accompanied by slight higher DNA repair rate. Consequently, half time of DNA repair values decreased from about 44 min to 38 min.

3.3. Modulation of micronuclei radiation-induced formation by PTX, Tx and the combination

Micronuclei (MN) assay (Fig. 3) was used to assess chromosomic loss and dividing capacity. MN frequency (Fig. 3A) was very strongly increased only for late times (from 7th day to 21th day) after 10 Gy radiation exposure reaching 1008 MN per 1000 binucleated cells versus 43 MN per 1000 binucleated cells in unirradiated fibroblasts at day 21. Moreover, this increase was emphasized in presence of Tx (+ 58% at day 14) whereas it was decreased by PTX (-71% at day 14). The combination of both compounds followed the Tx variations (no significant difference between Tx and PTX+Tx treatments at days 14 and 21).

Concerning dividing capacity as measured by percentage of binucleated (BN) cells (Fig. 3B), it was shown to decrease after 10 Gy radiation exposure with 15% of BN cells versus around 30% in unirradiated fibroblasts. In presence of Tx or PTX/Tx, the decrease of BN cells percentage after 10 Gy radiation exposure was not observed, it remained around 30% as for unirradiated cells. In contrast, PTX did not have this effect on BN cells frequency, except at day 21, since it did not change the value obtained at day 7 for 10 Gy-irradiated cells and even decreased it at day 14.

3.4. Modulation of clonogenic survival by PTX, Tx and the combination

Clonogenicity assay allowed to determine surviving fraction after irradiation doses ranging from 0 to 6 Gy (Fig. 4). Surviving fraction was shown to decrease after radiation exposure reaching 10% at 3 Gy. For irradiation doses greater than 1 Gy and up to 6 Gy, administration of Tx in the culture medium was associated to an increase (average about +90%) in cell survival. By contrast, PTX was shown to be responsible for a statistically significant drop (average about -45.6%) in cell survival for doses greater than 1 Gy. When combination was used a decrease in clonogenic values was also observed but decrease was less pronounced than for PTX (average about -41%).

4. DISCUSSION

The efficiency of the combination of pentoxifylline (PTX) and α-tocopherol (αT) in restoring radiation-induced skin damage injury was underlined in several studies whereas no or less drastic effects were observed when drugs were used separately (Koh *et al*., 1995; Lefaix *et al*., 1999; Delanian *et al*., 2003). In this respect, we showed in previous works (Laurent *et al*., 2005; Laurent *et al*., 2005) that the combination was antioxidant and was able to reduce initial DNA damage produced in dermal fibroblasts and endothelial cell by gamma-irradiation. We also demonstrated that combination was also able to reduce damage measured one hour after irradiation, even when drugs were added 30 min after irradiation. These data suggested that drugs combination would track initial reactive oxygen species but also would interfere with DNA repair. This was supported by micronuclei measurements which indicated that PTX/Tx use was accompanied by a strong increase in MN from 7 days after irradiation. Moreover, combination was shown to be radiosensitizing in fibroblasts. Previous works relying on different models underlined the effects of either PTX or Tx or its analogues on DNA damage

and on DNA repair (Sarma and Kesavan, 1993; Sweetman *et al*., 1997; Kumar *et al*., 1999; Theron *et al*., 2000; Bozsakyova *et al*., 2001; Binder *et al*., 2002). However, no studies compared the effect of drugs used in combination or separately. In the present study, we proposed to study radiation-induced damage effects in fibroblasts after cells were incubated in presence of single or of the association of drugs. For this purpose, cells at confluent stage were exposed to the irradiation dose of 10 Gy since the main striking effects observed in our previous works were at this dose. Moreover, this irradiation dose is more appropriate to mimic radiotherapy schedules where global irradiation doses delivered to patients and subsequent tissue damage may be important.

First, antioxidant capacity of drugs was assayed (Fig. 1) and showed Tx was a strong antioxidant properties PTX for concentrations lower than 4 mM where methanol could have a pro-oxidant effect (Paula *et al*., 2003). The antioxidant capacity of the combination was slightly higher than the one of Tx but no additive effects were observed. This ability of the two drugs in tracking radicals might be responsible for decrease in DNA damage as observed by the alkaline comet assay (Fig. 2). As one could expect, Tx, which is more antioxidant than PTX (+31%), was shown to reduce DNA damage level more markedly than PTX (+28%) immediately but also one hour after radiation exposure.

Although combination was more antioxidant, it was shown to be less efficient than Tx itself in reducing DNA damage immediately after irradiation. This is surprising because it would suggest that drugs are not passive and do not simply act as radical scavengers. Nevertheless, mixture was statistically more proficient one hour after so that the strongest decrease was obtained, at this time, when the combination was used, and suggests an additive effect. Such differential effect of drugs in regards to the considered time of analysis would suggest they do not act in the same way on initial DNA damage and on DNA damage resulting from both initial damage and DNA repair. In addition, half time of DNA repair was shown to be slightly diminished when both drugs were used whereas no changes were observed when drugs were used separately. The reason for such cooperative effect is still unexplained but could be involved into the synergistic effects observed *in vivo* when combination is used while isolated drugs are inefficient.

We showed in previous works that micronuclei (MN) frequency was increased in both 10 Gy-irradiated fibroblasts and endothelial cells when drugs were used either before or after irradiation. Such raise started on day 7 and lasted until day 21 (end of the considered period of observation) after exposure. No increase was observed in non-irradiated cells.

In the present study, compared to non treated cells, a strong increase in 10 Gy-irradiated fibroblasts was observed in presence of Tx on day 14 after irradiation and was enhanced on day 21 (Fig. 3A). By contrast, use of PTX was accompanied by a reduced level of MN. MN frequency measured when both drugs were used indicated a similar level than the one measured in presence of Tx alone. These results would suggest that TX is the drug involved in genotoxic effect of the mixture at high irradiation doses. However considering survival curves, it appears that PTX was radiosensitive while Tx was highly radioprotective. Such discrepancy might be explained in regards to the time at which analysis is done and to the percentage of binucleated cells (Fig. 3B). Indeed, the proportion of cells entering mitosis is much higher in presence of Tx, and this amount is not statistically different when combination is used. Moreover, survival clonogenic curves are established during the first two weeks following irradiation, then at a time when, ratio of cells entering mitosis in presence of PTX is low (Fig. 3B). Therefore, PTX which leads to a lower level of MN in cells appears surprisingly to be more radiosensitive. On day 21, percentage of binucleated cells in presence of PTX increases and subsequent MN is also augmented. Therefore, it is not possible at this stage to exclude PTX might be involved in MN frequency raise but this involvement would be delayed. In addition radioprotective effect of Tx, demonstrated by clonogenic results performed during the two first weeks after irradiation, could be overcome if one considers later times.

Is the origin of raise in MN frequency associated to a stimulation of treated cells a going through cell cycle? PTX was described in literature as being responsible for abrogating G2 cell cycle arrest (Russell *et al*., 1996; Li *et al*., 1998; Eley *et al*., 2002; Strunz *et al*., 2002). However, we did not observe in previous works (Laurent *et al*., 2005; Laurent *et al*., 2005) statistically significant effects of the combination on proportion of cells evolving through the different phases until day 14 after irradiation. Therefore, augment in binucleated cells ratio might be due to noticeable increase in DNA repair and subsequent reduction in OTM. Such DNA repair would permit fibroblasts to go through cell cycle but, faulty DNA repair would be expressed later and would be at the origin of delayed increase in MN frequency.

Considering these data, it would be interesting in a further work to deal with the effects of drugs on DNA repair pathways. In particular, the effect of drugs on systems involved in DNA DSB repair would be of major relevance for investigating micronuclei origin. In this respect, PTX was shown to affect ATM pathway (Sarkaria *et al*., 1999) and to inhibit DSB formation (Theron *et al*., 2000; Binder *et al*., 2002). Effect of Tx against on DNA damage yield in p53-wild type and deficient cells was underlined in previous studies (Sarma and Kesavan, 1993;

Sweetman *et al*., 1997; Kumar *et al*., 1999). However our comet assay results suggest that single-strand breaks or alkali-labile sites might also be involved in combination effects.

In conclusion, this work aimed at investigating contribution of PTX and Tx in observed effects of the combination PTX/Tx on DNA damage and subsequent cell survival induced in cells by gamma irradiation. Both drugs were shown to reduce DNA damage level but additive effect was observed one hour after irradiation. In addition, Tx was shown to be responsible for increase, two weeks after irradiation, in micronuclei frequency that might be correlated to the percentage of cells entering mitosis. PTX was shown to also affect micronuclei yield, but this effect was delayed mainly due to its inhibiting effect on progression of cells through cell cycle. This study suggests that drugs might interfere with DNA repair pathways.

At the clinical level, these compounds act synergistically reducing skin late radiation-induced injury whereas drugs administered separately did not (Koh *et al*., 1995; Lefaix *et al*., 1999; Delanian *et al*., 2003). At the cellular level, additive effect in reducing DNA damage one hour after irradiation, was also accompanied by increase in MN.

Acknowledgements

The authors are very grateful to Dr M Souidi and Dr Y. Gueguen for their readings of the manuscript. We also thank Dr J.-L. Lefaix and Dr S. Delanian for helpful discussions. This work was supported by Electricité de France-Service de Radioprotection and Région Ile-de-France.

References

Binder, A., T. Theron, et al. (2002). "Radiosensitization and DNA repair inhibition by pentoxifylline in NIH3T3 p53 transfectants." Int J Radiat Biol **78**(11): 991-1000.

Bozsakyova, E., I. Chalupa, et al. (2001). "Chromosomal aberrations, sister chromatid exchanges and micronuclei induced by pentoxifylline in in vitro cultivated Chinese hamster cells (V79) and human blood lymphocytes." Mutat Res **497**(1-2): 63-70.

Cao, G., H. M. Alessio, et al. (1993). "Oxygen-radical absorbance capacity assay for antioxidants." Free Radic Biol Med **14**(3): 303-11.

Delanian, S., F. Baillet, et al. (1994). "Successful treatment of radiation-induced fibrosis using liposomal Cu/Zn superoxide dismutase: clinical trial." Radiother Oncol **32**(1): 12-20.

Delanian, S., S. Balla-Mekias, et al. (1999). "Striking regression of chronic radiotherapy damage in a clinical trial of combined pentoxifylline and tocopherol." J Clin Oncol **17**(10): 3283-90.

Delanian, S. and J. L. Lefaix (2002). "Complete healing of severe osteoradionecrosis with treatment combining pentoxifylline, tocopherol and clodronate." Br J Radiol **75**(893): 467-9.

Delanian, S., R. Porcher, et al. (2003). "Randomized, placebo-controlled trial of combined pentoxifylline and tocopherol for regression of superficial radiation-induced fibrosis." J Clin Oncol **21**(13): 2545-50.

Dion, M. W., D. H. Hussey, et al. (1990). "Preliminary results of a pilot study of pentoxifylline in the treatment of late radiation soft tissue necrosis." Int J Radiat Oncol Biol Phys **19**(2): 401-7.

Dion, M. W., D. H. Hussey, et al. (1989). "The effect of pentoxifylline on early and late radiation injury following fractionated irradiation in C3H mice." Int J Radiat Oncol Biol Phys **17**(1): 101-7.

Dubray, B., S. Delanian, et al. (1997). "[Late effects of mammary radiotherapy on skin and subcutaneous tissues]." Cancer Radiother **1**(6): 744-52.

Eley, K. W., S. H. Benedict, et al. (2002). "The effects of pentoxifylline on the survival of human glioma cells with continuous and intermittent stereotactic radiosurgery irradiation." Int J Radiat Oncol Biol Phys **54**(2): 542-50.

Freitas, J. P., P. Filipe, et al. (1995). "[Potential antioxidative effects of pentoxifylline]." C R Seances Soc Biol Fil **189**(3): 401-5.

Horvath, B., Z. Marton, et al. (2002). "In vitro antioxidant properties of pentoxifylline, piracetam, and vinpocetine." Clin Neuropharmacol **25**(1): 37-42.

Koh, W. J., K. J. Stelzer, et al. (1995). "Effect of pentoxifylline on radiation-induced lung and skin toxicity in rats." Int J Radiat Oncol Biol Phys **31**(1): 71-7.

Kumar, S. S., R. C. Chaubey, et al. (1999). "Inhibition of radiation-induced DNA damage in plasmid pBR322 by chlorophyllin and possible mechanism(s) of action." Mutat Res **425**(1): 71-9.

Laurent, C., J. P. Pouget, et al. (2005). "Modulation of DNA damage by pentoxifylline and a-tocopherol in skin fibroblasts exposed to gamma-rays." Radiat Res **Under Press**.

Laurent, C., P. Voisin, et al. (2005). "DNA damage in cultured skin microvascular endothelial cells exposed to gamma-rays treated by the combination of pentoxifylline and alpha-tocopherol." **Submitted**.

Lefaix, J. L., S. Delanian, et al. (1996). "Successful treatment of radiation-induced fibrosis using Cu/Zn-SOD and Mn-SOD: an experimental study." Int J Radiat Oncol Biol Phys **35**(2): 305-12.

Lefaix, J. L., S. Delanian, et al. (1999). "Striking regression of subcutaneous fibrosis induced by high doses of gamma rays using a combination of pentoxifylline and alpha-tocopherol: an experimental study." Int J Radiat Oncol Biol Phys **43**(4): 839-47.

Letur-Konirsch, H., F. Guis, et al. (2002). "Uterine restoration by radiation sequelae regression with combined pentoxifylline-tocopherol: a phase II study." Fertil Steril **77**(6): 1219-26.

Li, Y. X., K. Weber-Johnson, et al. (1998). "Effect of pentoxifylline on radiation-induced G2-phase delay and radiosensitivity of human colon and cervical cancer cells." Radiat Res **149**(4): 338-42.

Ozturk, B., I. Egehan, et al. (2004). "Pentoxifylline in prevention of radiation-induced lung toxicity in patients with breast and lung cancer: a double-blind randomized trial." Int J Radiat Oncol Biol Phys **58**(1): 213-9.

Paula, E. M., D. C. Mathangi, et al. (2003). "Free radical changes in methanol toxicity." Indian J Physiol Pharmacol **47**(2): 207-11.

Pouget, J. P., T. Douki, et al. (2000). "DNA damage induced in cells by gamma and UVA radiation as measured by HPLC/GC-MS and HPLC-EC and Comet assay." Chem Res Toxicol **13**(7): 541-9.

Puck, T. T., P. I. Marcus, et al. (1956). "Clonal growth of mammalian cells in vitro; growth characteristics of colonies from single HeLa cells with and without a feeder layer." J Exp Med **103**(2): 273-83.

Rimbach, G., A. M. Minihane, et al. (2002). "Regulation of cell signalling by vitamin E." Proc Nutr Soc **61**(4): 415-25.

Rube, C. E., F. Wilfert, et al. (2002). "Modulation of radiation-induced tumour necrosis factor alpha (TNF-alpha) expression in the lung tissue by pentoxifylline." Radiother Oncol **64**(2): 177-87.

Russell, K. J., L. W. Wiens, et al. (1996). "Preferential radiosensitization of G1 checkpoint-deficient cells by methylxanthines." Int J Radiat Oncol Biol Phys **36**(5): 1099-106.

Sarkaria, J. N., E. C. Busby, et al. (1999). "Inhibition of ATM and ATR kinase activities by the radiosensitizing agent, caffeine." Cancer Res **59**(17): 4375-82.

Sarma, L. and P. C. Kesavan (1993). "Protective effects of vitamins C and E against gamma-ray-induced chromosomal damage in mouse." Int J Radiat Biol **63**(6): 759-64.

Satyamitra, M., P. Uma Devi, et al. (2003). "In vivo postirradiation protection by a vitamin E analog, alpha-TMG." Radiat Res **160**(6): 655-61.

Strunz, A. M., P. Peschke, et al. (2002). "Preferential radiosensitization in p53-mutated human tumour cell lines by pentoxifylline-mediated disruption of the G2/M checkpoint control." Int J Radiat Biol **78**(8): 721-32.

Sweetman, S. F., J. J. Strain, et al. (1997). "Effect of antioxidant vitamin supplementation on DNA damage and repair in human lymphoblastoid cells." Nutr Cancer **27**(2): 122-30.

Theron, T., A. Binder, et al. (2000). "The role of G2-block abrogation, DNA double-strand break repair and apoptosis in the radiosensitization of melanoma and squamous cell carcinoma cell lines by pentoxifylline." Int J Radiat Biol **76**(9): 1197-208.

Vozenin-Brotons, M. C., V. Sivan, et al. (2001). "Antifibrotic action of Cu/Zn SOD is mediated by TGF-beta1 repression and phenotypic reversion of myofibroblasts." Free Radic Biol Med **30**(1): 30-42.

Ward, W. F., Y. T. Kim, et al. (1992). "Pentoxifylline does not spare acute radiation reactions in rat lung and skin." Radiat Res **129**(1): 107-11.

Weiss, J. F. and M. R. Landauer (2003). "Protection against ionizing radiation by antioxidant nutrients and phytochemicals." Toxicology **189**(1-2): 1-20.

Worthington, H. V., J. E. Clarkson, et al. (2002). "Interventions for treating oral mucositis for patients with cancer receiving treatment." Cochrane Database Syst Rev(1): CD001973.

Figure Legends

Figure 1. Oxygen Radical Absorbing Capacity of Tx, PTX and the combination. ORAC was assayed as described in Materials and Methods. Antioxidant capacity of PTX, Tx and the combination of the both was assessed. One ORAC unit is equal to the antioxidant status of 1 µM Tx.

Figure 2. Modulation of DNA damage (A) and repair kinetic (B) by Tx, PTX and the combination in gamma-irradiated fibroblasts. NHF-d were treated by Tx, PTX or the combination, gamma-irradiated at 10 Gy at confluent stage and alkaline comet assay was performed immediately and one after irradiation. Olive Tail Moment (OTM) was calculated (A) and repair kinetic were measured (B). Data are depicted as mean ± SEM; *p < .05 and **p < .001 was considered statistically significant compared to irradiated untreated cells (one-way ANOVA with Tukey test).

Figure 3. Modulation of micronuclei (A) and binucleated cells (B) frequencies by Tx, PTX and the combination in gamma-irradiated fibroblasts. NHF-d were treated and gamma-irradiated at 10 Gy at confluent stage. They were reseeded at 7, 14 and 21 days after irradiation and grown. Fibroblasts were then incubated with cytochalasin B for 24 h before hypotonic shock and fixation. Then, they were stained with propidium iodide before analysis of 500 cells using a fluorescence microscope. Data are depicted as mean ± SEM; *p < .05 and **p < .001 was considered statistically significant (one-way ANOVA with Tukey test).

Figure 4. Modulation of clonogenic survival by Tx, PTX and the combination in gamma-irradiated fibroblasts. Clonogenic survival was assayed from 0 to 6 Gy. Tx, PTX or the combination was administered before irradiation. Data are depicted as mean ± SEM; *p < .05 and **p < .001 was considered statistically significant (one-way ANOVA with Tukey test).

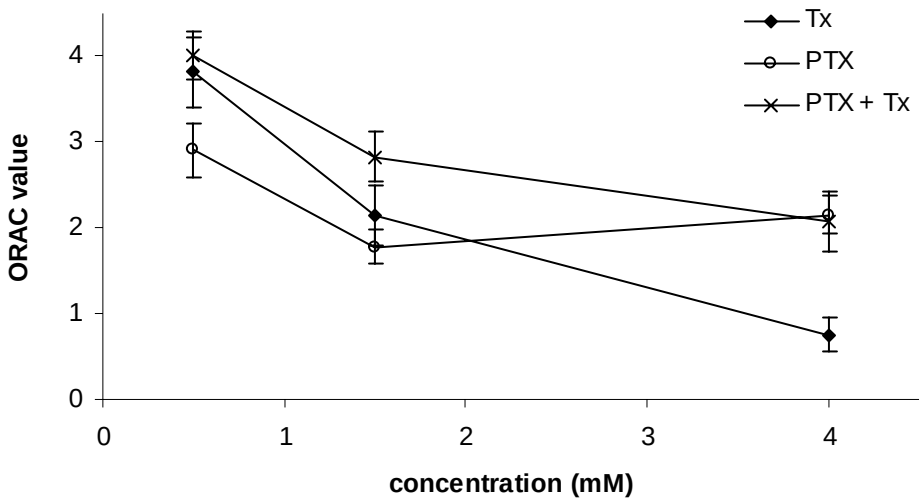

Figure 1

A

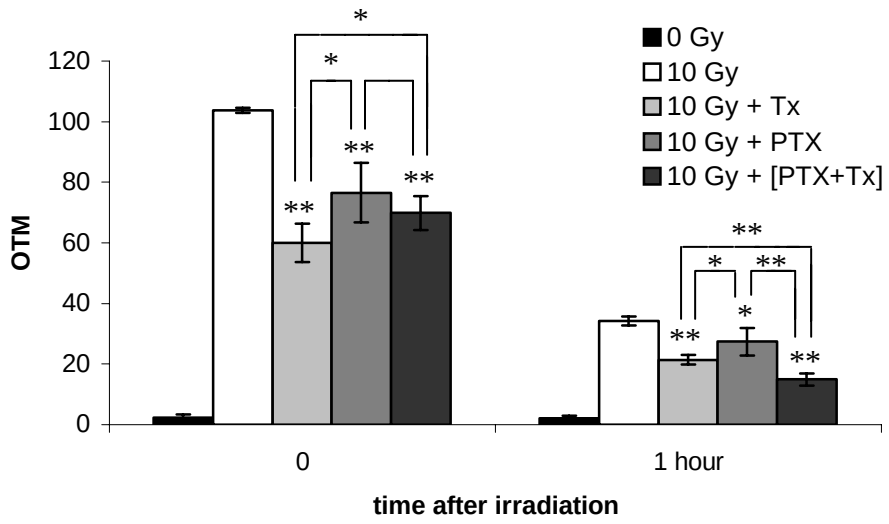

B

	Half time of DNA repair
10 Gy w/o treatment	44 min
10 Gy + Tx	46 min
10 Gy + PTX	46 min
10 Gy + [PTX+Tx]	38 min

Figure 2

A

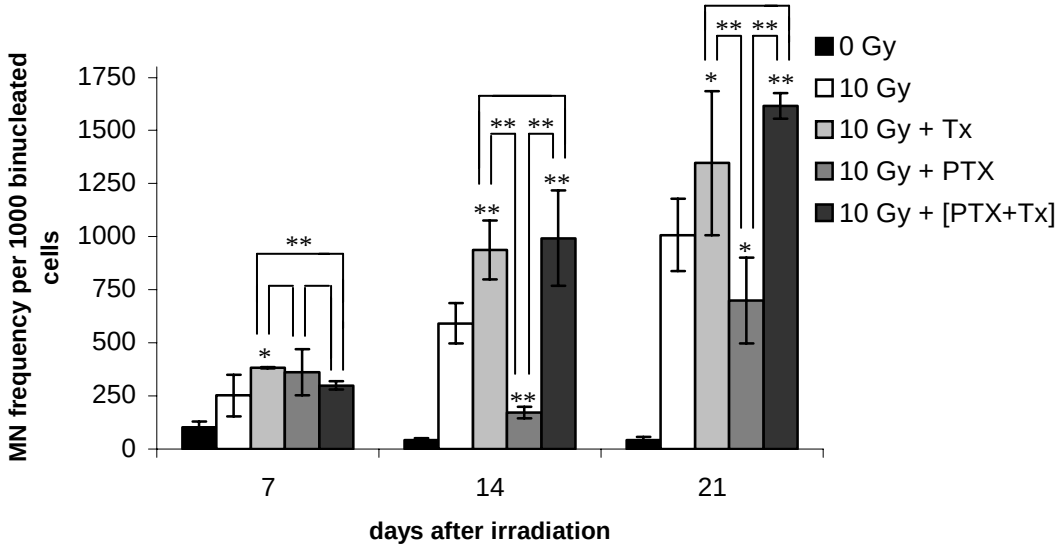
MN frequency per 1000 binucleated cells
1750
1500
1250
1000
750
500
250
0
7
14
21
days after irradiation
0 Gy
10 Gy
10 Gy + Tx
10 Gy + PTX
10 Gy + [PTX+Tx]

B

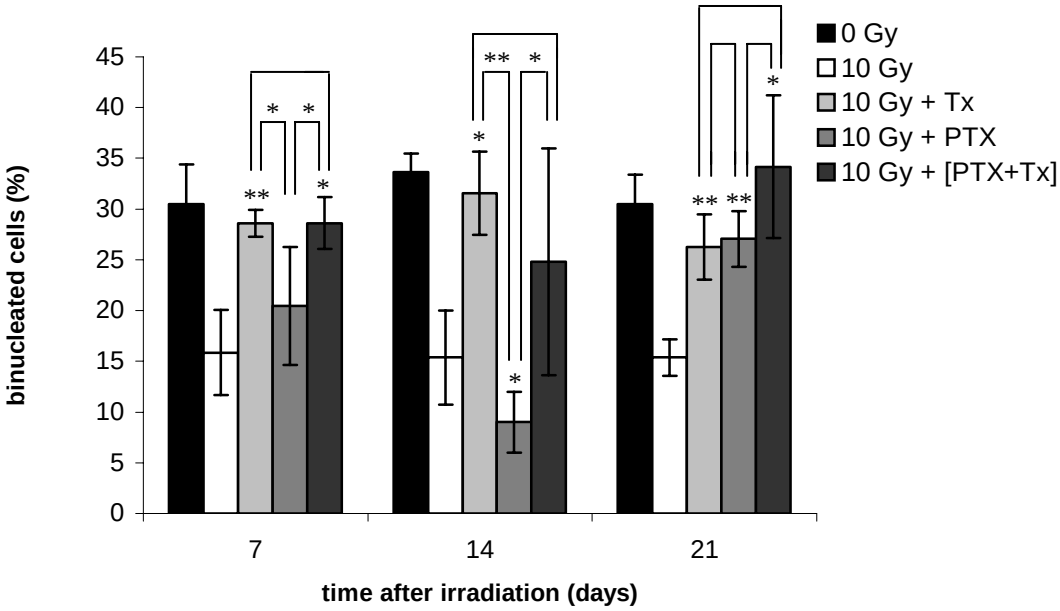
binucleated cells (%)
45
40
35
30
25
20
15
10
5
0
7
14
21
time after irradiation (days)
0 Gy
10 Gy
10 Gy + Tx
10 Gy + PTX
10 Gy + [PTX+Tx]

Figure 3

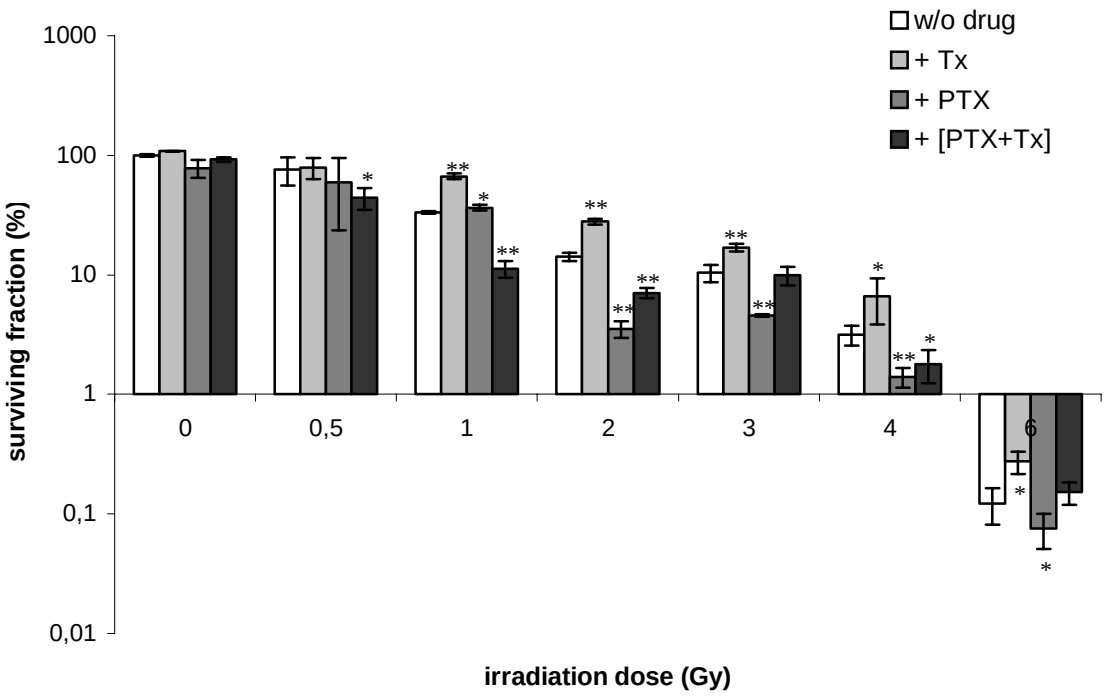
w/o drug
+ Tx
+ PTX
+ [PTX+Tx]
surviving fraction (%)
1000
100
10
1
0,1
0,01
0
0,5
1
2
3
4
6
irradiation dose (Gy)

Figure 4

V- Cassures double-brins, sénescence prématurée et voies de signalisation

Article 6 : Hyperphosphorylation tardive de H2AX associée à une baisse de l'expression de DNA-PKcs et à une sénescence prématurée dans les fibroblastes et les cellules endothéliales de peau irradiés et leur modulation par la pentoxifylline et le trolox

Les résultats obtenus précédemment ont montré l'importance de l'étude de la formation des cassures double-brins (CDB) dans la compréhension des effets de l'association pentoxifylline/trolox sur les dommages de l'ADN dans les cellules exposées à de fortes doses d'irradiation. Nous avons en effet montré que l'administration de l'association même après irradiation s'accompagnait d'une diminution du nombre de cassures mesurées par la méthode des comètes en milieu alcalin, à un niveau équivalent à celui que l'on peut obtenir lorsque les composés sont ajoutés avant l'irradiation. L'hypothèse la plus probable semble être l'interférence des deux composés avec les mécanismes de réparation cellulaire. Par ailleurs, nous avons observé une augmentation tardive de la fréquence des micronoyaux dans les fibroblastes et les cellules endothéliales irradiés à une dose de 10 Gy en présence du traitement. Cette augmentation pourrait être due à une formation accrue de CDB ou à une baisse de leur réparation. Cette augmentation du niveau de micronoyaux n'explique pas à elle seule l'effet radiosensiblisateur du traitement. Nous avons choisi comme mesure des CDB d'utiliser la méthode de détection de l'histone H2AX phosphorylé (γ-H2AX). Cette méthode nécessite d'être spécifique, validée et calibrée. Il faut noter que la méthode des comètes en milieu alcalin permet la détection simultanée des cassures simple- et double-brins de l'ADN ainsi que celle des sites alkali-labiles. Elle ne constitue un outil adapté et sensible à la détection des CDB seules.

Par ailleurs, le système de réparation de l'ADN principalement impliqué dans la réparation des CDB chez les eucaryotes supérieurs en phase G1 du cycle cellulaire, qui correspond à la phase du cycle dans laquelle se trouvent la plupart des cellules dans nos expérimentations, est le système de recombinaison non homologue (NHEJ pour « Non Homologous End Joining). Cette voie implique le complexe DNA-PK et XRCC4 conduisant à la ligation de l'ADN. La mesure de l'activité du complexe DNA-PK nécessitant une mise au point méthodologique très importante et, surtout, une grande quantité de matériel biologique (20 millions de cellules par

analyse), nous nous sommes intéressés à l'expression des trois protéines formant ce complexe : DNA-PKcs, la sous-unité catalytique, et les deux protéines Ku. Il a été montré que le niveau d'expression de DNA-PKcs était lié à l'activité DNA-PK sans qu'un changement de l'expression des proteins Ku (Ader *et al*., 2002) ou du niveau de réparation des CDB (Ortiz *et al*., 2004) ne soit observé. Nous avons mesuré le niveau d'expresion de DNA-PKcs dans les cellules par la technique de « Western Blot ». Dans une deuxième partie nous nous sommes intéressés au phénomène de sénescence prématurée induite par un stress chronique (SIPS pour « stress-induced premature senescence »). Un tel phénomène pourrait expliquer la présence d'un stress chronique au niveau cellulaire qui pourrait expliquer la présence de dommages de l'ADN longtemps après exposition. Il a été montré que la SIPS pouvait se produire après des stress répétés (Duan *et al*., 2005) et aussi après exposition aux rayonnements ionisants (Naka *et al*., 2004). La SIPS présente des caractéristiques morpholigique bien définies, ainsi qu'une apparition de l'activité β-galactosidase (SA-β-gal) et l'augmentation d'expression de la protéine $p21^{WAF1}$.

Nous avons dans le cadre de notre étude montré la présence d'une hyperphosphorylation tardive de l'histone H2AX, i.e. bien au delà de celle induite par l'irradiation elle-même. Nous avons également observé que les variations de niveau de γ-H2AX étaient associées à des changements d'expression de DNA-PKcs. En effet, une diminution de l'expression de DNA-PKcs était accompagnée d'une augmentation de γ-H2AX correspondant à la présence de CDB. L'association PTX/Tx a diminué le niveau de DNA-PKcs à différents temps selon le type cellulaire après irradiation. Cette diminution était associée à une plus forte phosphorylation de H2AX. La SIPS a été observée dans les fibroblastes et les cellules endothéliales irradiés d'une manière temps- et dose-dépendante. Par ailleurs nous avons montré que PTX/Tx conduisait à une baisse de la SIPS. Diminution de la réparation des CDB et sortie des cellules du phénomène de sénescence pourraient participer à l'effet radiosensibilisateur du traitement.

Cette étude a permis de mettre en évidence l'apparition d'une hyperphosphorylation tardive de l'histone H2AX dans les cultures primaires de fibroblastes et de cellules endothéliales de derme exposées, à confluence, a une forte dose de rayonnements ionisants. Cette phosphorylation était associée à une diminution de l'expression de DNA-PKcs et à l'apparition d'un phénotype de sénescence prématurée. Le traitement PTX/Tx a pu conduire à une augmentation de la phosphorylation de H2AX lié à une baisse du niveau de DNA-PKcs.

Nous avons poursuivi ces travaux par des mesures préliminaires, par la technique de « Western Blot », d'expresion d'ATM et de $p16^{INK4A}$, impliquées respectivement dans les voies de signalisation de la réparation des CDB de l'ADN et de sénescence prématurée. Ces premiers résultats ont mis en évidence une augmentation d'expression d'ATM, surtout à 14 jours dans les cellules endothéliales, et de $p16^{INK4A}$ à tous les temps dans les deux types cellulaires après irradiation. Ces résultats mettent en évidence une possible activation des voies conduisant à la sénescence ou à l'arrêt en phase G1 pour la réparation de l'ADN. Le traitement PTX/Tx a conduit à une diminution du niveau de ces deux protéines montrant une éventuelle inhibition de ces voies de signalisation.
De plus, nous avons également montré que l'expression de la Poly-(ADP Ribose)-Polymérase (PARP), qui est une protéine impliquée dans la signalisation des cassures de brins de l'ADN en liaison avec DNA-PKcs et d'autres protéines, augmentait dans les temps précoces après irradiation. En revanche, le traitement PTX/Tx s'est traduit par une diminution, dans les deux types cellulaires, de son niveau à 7 et 14 jours mais par une augmentation à 21 jours dans les cellules endothéliales irradiées alors qu'une diminution est observée dans le fibroblastes. Ces résultats peuvent être associés aux variations de fréquences des micronoyaux qui augmentent fortement dans les fibroblastes irradiés en présence du traitement à 14 jours et encore à 21 jours post-irradiation tandis que cette fréquence diminue dans les cellules endothéliales après traitement à 21 jours. La PARP pourrait donc également jouer un rôle dans l'effet du traitement sur les lésions tardives observées.

Toutes ces données montrent la mise en place d'évènements à des temps tardifs après irradiation dans les fibroblastes et les cellules endothéliales du derme. En effet, une augmentation des CDB est observée à 7 jours après irradiation associée à une diminution d'expression de DNA-PKcs dans les fibroblastes. Dans les cellules endothéliales, l'augmentation à 7 jours des CDB est moins importante et est associée à une augmentation de DNA-PKcs. Le traitement PTX/Tx, à une forte dose d'irradiation, pourrait agir sur les dommages de l'ADN, les voies de signalisation, les systèmes de réparation et la sénescence prématurée pouvant conduire à sa toxicité à long terme par l'augmentation des lésions de l'ADN résultantes.

Late H2AX hyperphosphorylation associated to decreased DNA-PKcs expression and SIPS in irradiated skin fibroblasts and endothelial cells and modulation by pentoxifylline and trolox

Carine Laurent[1], Martine Delbos[1], Pascale Voisin[1], Philippe Voisin[2], Ph.D, and Jean-Pierre Pouget[2, 3†], Ph.D.

[1] Laboratoire de Dosimétrie Biologique, DRPH/SRBE, Institut de Radioprotection et de Sûreté Nucléaire, Fontenay-aux-Roses, France

[2] Service de Radiobiologie et d'Epidémiologie, DRPH, Institut de Radioprotection et de Sûreté Nucléaire, Fontenay-aux-Roses, France

[3] INSERM EMI 0227, Immunociblage des tumeurs et Ingénierie des Anticorps, Centre de Recherche en Cancérologie, CRLC Val d'Aurelle, Institut Paul Lamarque, Montpellier, France

Running title: Radiation-induced formation of DNA double-strand breaks in dermal cells

[†] Address correspondance to: Jean-Pierre Pouget, Immunociblage des tumeurs et Ingénierie des Anticorps, EMI 0227, INSERM, Centre de Recherche en Cancérologie, CRLC Val d'Aurelle, Institut Paul Lamarque, 34298 Montpellier Cedex, France ; Tel: +33 4 67 61 37 08; E-mail: jppouget@valdorel.fnclcc.fr.

Abstract

We observed in previous studies, that the combination of pentoxifylline and trolox (PTX/Tx) was associated to reduction in early DNA damage as measured by the alkaline comet assay but increase in delayed micronuclei frequency in fibroblasts and endothelial cells exposed to high dose of gamma-rays. We then proposed drugs combination might interfere with DNA repair process or with stress-induce premature senescence. Therefore, to investigate the effect of drugs on both phenomena, we measured in irradiated confluent skin fibroblasts and endothelial cells treated or not by PTX/Tx, γ-H2AX expression, as a reflect of double-strand breaks (DSB) yield, DNA-PKcs expression, a protein involved in DSB repair as the level of two proteins involved in SIPS, namely $p21^{WAF1}$ and SA-β-gal. Results showed an immediate phosphorylation of H2AX but also delayed production at day 7 in both irradiated cell types. This was associated to the changes observed in DNA-PKcs expression so that decrease in DNA-PKcs level was linked to an increase in DSB level. Surprisingly, no reduction in phosphorylation of H2AX was observed 10 min after irradiation when the combination PTX/Tx was used. By contrast decreases in DNA-PKcs level were measured at day 7 in irradiated endothelial cells and at day 21 in irradiated fibroblasts and were associated to a stronger phosphorylation of H2AX. SIPS was observed in both cell types long term after irradiation and its level was reduced in presence of PTX/Tx in endothelial cells from day 5 after irradiation. To conclude, a late hyperphosphorylation of H2AX and senescent phenotype was observed in 10 Gy-gamma-irradiated skin fibroblasts and endothelial cells. The effect of PTX/Tx on DSB indicates drugs do not simply act as antioxidant because they were shown to increase DSB level at different time after irradiation. Moreover, treatment was shown to interfere with signaling pathways involved in SIPS.

Author Keywords

Ionizing radiation; DNA double-strand breaks; endothelial cells; fibroblasts; repair; pentoxifylline; α-tocopherol

1. INTRODUCTION

High doses of ionizing radiation may lead to cutaneous radiological syndrome. Early symptoms including rash and desquamation, are considered as caused by epidermis injury since this tissue presents a fast renewal (Devik, 1955; Epstein and Maibach, 1965; Withers, 1967). By contrast, late effects (telangiectasia, fibrosis, and necrosis) appear from months to years after radiation exposure. Several theories could explain such a delay between irradiation and clinical symptoms occurrence. We focused on those relying on mitotic death in cells constituting skin stroma, namely fibroblasts and microvascular endothelial cells (Rudolph *et al*., 1988; Withers *et al*., 1980). According to this theory, accumulation of DNA damage in dermal cells would be expressed only at the first mitosis which may happen a long time after irradiation because of low renewal of these cells.

Many kinds of radiation-induced DNA damage have been identified. They include DNA single- and double-strand breaks, abasic sites, modified bases and DNA-protein adducts (Cadet *et al*., 1997) which are, in case of low-LET radiation, mainly caused by reactive oxygen intermediates produced by water radiolysis. Among these categories of lesions, double-strand breaks (DSB) appeared as being the most lethal damage since cells defaulting in DNA DSB repair were particularly sensitive to ionizing radiation.

We measured in previous works the rate of formation of DNA strand-breaks using the alkaline comet assay in gamma-irradiated fibroblasts or endothelial cells (Laurent *et al*., 2005). Results indicated an immediate increase in DNA damage in primary cultures of skin fibroblasts (Fig.1A) and endothelial cells (Fig.1B) followed by a return to control values during the three hours consecutive to exposure (Laurent *et al*., 2005). No damage were observed at later times. However, a strong delayed increase in micronuclei frequency was measured 14 days after irradiation (Fig. 2) (Laurent *et al*., 2005). This increase could be due to a newly formed DSB since yield of reactive oxygen species (ROS) were measured even several weeks after radiation exposure (Laurent *et al*., 2005). The production of such chronic stress would be at the origin of SIPS (stress-induced premature senescence). SIPS was shown to be produced in fibroblasts after repeated or prolonged stresses (Chainiaux *et al*., 2002; Debacq-Chainiaux *et al*., 2005; Duan *et al*., 2005) and also after ionizing radiation exposure (Gorbunova *et al*., 2002; Naka *et al*., 2004). It would be associated to $p21^{WAF1}$ expression and to oxidative DNA damage and repair (Duan *et al*., 2005).

Another hypothesis that may explain such increase in MN frequency is the presence within dermal cells of unrepaired DSB that would only be expressed at first mitosis.

This theory was supported by striking results obtained when the combination of pentoxifylline (PTX) and trolox (Tx) was administered to cell culture before of after irradiation. PTX and Tx were shown to be very efficient in *vivo* in reducing late injuries observed during cutaneous radiological syndrome (Delanian *et al*., 2003; Chiao and Lee, 2005). Indeed, if these drugs were described as being antioxidant, it was shown that their administration before but also after irradiation was accompanied by a decrease in DNA strand breaks, as measured by the alkaline comet assay, one hour after irradiation. Moreover, delayed micronuclei yield was emphasized. As drugs association was not accompanied by increase in DNA damage in controls, it was then proposed that they might interfere with DNA repair pathways (Laurent *et al*., 2005). However since the alkaline comet assay is dedicated to simultaneous measure of three categories of lesions as mentioned above, the method is not appropriate for highlighting presence of unrepaired DSB which are produced by gamma rays in much lower frequency that single-strand breaks and alkali-labile sites. Therefore, a method exclusively dedicated to the measure of DSB was required.

The origin of unrepaired DSB might be due to a default in the Non-Homologous End Joining (NHEJ) repair system which is the main pathway involved in DSB repair in fibroblasts and endothelial cells blocked in G1 phase of cell cycle (Laurent *et al*., 2005). This system includes DNA-PKcs subunit together with Ku70 and Ku80 which binds DNA ends. The level of DNA-PK activity was shown to be associated to an increased DNA-PKcs overexpression without any change in Ku proteins expression (Ader *et al*., 2002). Conversely, low level of DNA-PKcs was associated to defective DSB repair whereas high level was correlate to a high rate of DSB repair (Ortiz *et al*., 2004).

We propose in the present work to measure DSB formation and DNA-PKcs expression in dermal fibroblasts and endothelial cells exposed to gamma-rays at times ranging from min to weeks after irradiation. To investigate the mechanisms involved in the combination PTX/Tx, both drugs were added to cell culture medium 15 min before exposure. In order to assess involvement of chronic stress, level of SIPS markers was also determined.

Our results indicated a late hyperphosphorylation of H2AX associated to a decrease in DNA-PKcs expression after irradiation and to the appearance of SIPS. Surprisingly, the combination was not shown to decrease initial DSB yield and was even shown to increase H2AX phosphorylation at late times, in irradiated cells, in spite of its antioxidant properties. Increase in DNA-PKcs expression was correlated to raise in H2AX phosphorylation. At last, an increase in SIPS was observed in irradiated cells, but was shown to be reduced when the combination of drugs was used.

2. MATERIALS AND METHODS

2.1. Reagents

Dulbecco's modified Eagle medium (DMEM), fetal bovine serum (FBS), N-(2-hydroxyethyl)piperazine-N'-(2-ethanesulfonic acid) (HEPES) buffer, Dulbecco's phosphate-buffered saline (PBS), trypsin/EDTA, L-glutamine, penicillin and streptomycin were purchased from Gibco BRL Life Technologies (Gaithersburg, MD, USA). Collagenase P was obtained from Roche (Indianapolis, IN, USA). γ-H2AX, DNA-PKcs and $p21^{WAF1}$ antibodies were obtained from Trevigen (Gaithersburg, MD, USA), NeoMarkers (Fremont, CA, USA) and DakoCytomation (Glostrup, Denmark), respectively. All others chemicals were purchased from Sigma (St. Louis, MO, USA).

2.2. Cell cultures

Primary cultures of dermal fibroblasts, NHF-d (normal human fibroblasts from dermis), were obtained from skin of two healthy white Caucasian women of 22 and 40 years of age undergoing elective surgery (mammary reduction and abdominoplasty, respectively). No significant individual variability in response to treatment and to irradiation was observed among isolated fibroblasts. Written consents were obtained from both subjects. Skin was first dropped into 5% betadine bath for 15 min and rinsed with PBS. Then, epidermis was separated from dermis with scalpel blade, and resulting dermal tissue was incubated in three successive baths of trypsin/collagenase P (0.5%/0.25%) at 37°C for 30 min under stirring in order to isolate cells. Cell suspension was collected, centrifuged and resuspended in DMEM supplemented with 20% FBS, 100 µg/mL L-glutamine, 10 mM HEPES and antibiotics (100 units/mL penicillin and 100 µg/mL streptomycin). Cells were next plated onto flasks coated with collagen I and grown at 37°C in a humidified atmosphere of 5% CO_2 up to the first passage and were then grown in uncoated flasks for the following passages. Experiments were performed when cells reached passages 4-7.

Primary cultures of endothelial cells were commercially obtained. Human dermal microvascular endothelial cells (HMVEC-d) were derived from an healthy caucasian 45-years old woman undergoing elective surgery and were obtained from Cambrex (Verviers,

Belgium). Cells were cultured in EGM-2 MV provided by the supplier, at 37°C in a humidified atmosphere of 5% CO_2 and 95% air and were used at passages 5-7.

2.3 Cell treatment and gamma-irradiation

Confluent cells were irradiated at room temperature at doses of 0 and 10 Gy using a ^{137}Cs source (IBL 637, Cis bio International), at a dose rate of 1 Gy/min. Pentoxifylline (PTX) and Trolox (Tx) were added 15 min before radiation exposure and maintained during the whole of the considered period (21 days). PTX was first dissolved in water at a concentration of 100 mM and the water-soluble analogue of αT, Tx, was dissolved in methanol at a concentration of 100 mM before dilution in culture medium.

2.3. γ-H2AX immunocytochemistry

Fibroblasts and endothelial cells, treated or not by PTX/Tx, were fixed in methanol/acetone 1/1 (v/v) at different times postirradiation (10 minutes, 1 hour, 3 hours, 7 days, 14 days, 21 days) in labteks. Cells were then rehydrated with PBS and BSA 1% was added for 10 minutes at room temperature. Slides were incubated for 1 hour at 37°C in presence of primary antibody against phosphorylated H2AX, named γ-H2AX. Then slides were rinsed and secondary antibody was added. Analysis of γ-H2AX was performed using a fluorescence microscope. The MFI (mean fluorescence intensity) was measured by the computer image analysis software (IMSTAR, France).

2.4. Western blot analyses

Total lysates were prepared from fibroblasts and endothelial cells irradiated or not and treated or not by PTX/Tx. Cells were trypsinized at different times post-irradiation and lysed in buffer (Tris/HCl 10 mM, Triton 0.1%, sucrose 200 mM) by three successive incubations in liquid azote and at 37°C. Lysates were centrifuged at 20,000 g for 30 minutes at 4°C and supernatants were aliquoted and conserved at –80°C. Protein concentration was determined (BioRad). For gel electrophoresis, 50 µg of proteins per lane were loaded on 6% sodium dodecyl sulfate polyacrylamide gel electrophoresis (SDS-PAGE) gels following the method of Laemmli (Laemmli, 1970). Protein samples were prepared by addition of loading buffer and were denaturated by incubation 5 min at 95°C. Western blotting was conducted following the procedure of Towbin et al. (Towbin et al., 1979). Proteins separated by SDS-PAGE were transferred to nitrocellulose membranes (Amersham Biosciences) in 48 mM Tris, 39 mM glycine, 1.3 mM SDS, pH 9.2 and 20% methanol. Immunoblots were blocked in 8% non-fat

dry milk and primary antibodies were diluted in 3% non-fat dry milk. The membranes were rinsed three times in TBS containing 0.1% Tween 20 (v / v), and incubated at 4 °C overnight with the antibody. After another wash, the membranes were incubated with a secondary antibody anti-IgG conjugated to HRP (1 : 1000 dilution) at room temperature for 1 h. Detection was performed with the ECL method. Membranes were washed and developed with chemiluminescence substrate and exposed to Hyperfilm (Amersham Biosciences).

2.5. Senescence assay

Senescence was measured via SA-β-galactosidase (SA-β-gal) activity. Indeed, senescent cells present an activity SA-β-gal. In this way, confluent fibroblasts and endothelial cells were reseeded at different times post-irradiation to perform one cycle. They were then washed twice before fixation (formaldehyde 3%) for 5 minutes at room temperature. Cells were rinsed and incubated overnight at 37°C without CO_2 in X-gal solution (citric acid/sodium phosphate 40 mM, NaCl 150 mM, $MgCl_2$ 2 mM, potassium ferrocyanide 5 mM, potassium ferricyanide 5 mM and X-gal 1mg/mL) mixed extemporally. SA-β-gal activity was determined by counting blue cells, expressing SA-β-gal, using microscope.

2.6. Statistical analysis

Data are depicted as mean ± SEM; *p < .05 was considered statistically significant (one-way ANOVA with Tukey test). Each experiment was repeated three times in triplicate.

3. RESULTS

3.1. γ-H2AX formation

H2AX histone is phosphorylated at double-strand breaks site. Phosphorylated H2AX, namely γ-H2AX, was stained by immunocytochemistry and quantified by mean fluorescence intensity in irradiated and unirradiated fibroblasts and endothelial cells treated or not by PTX/Tx.

At the irradiation dose of 3 Gy, γ-H2AX level was returned to control level 1 hour after irradiation (data not shown). After irradiation, phosphorylation of H2AX occurs in 10 minutes and fluorescence intensity was related to the irradiation dose (Fig. 3 I). At the irradiation dose of 10 Gy, foci of γ-H2AX could not be counted and fluorescence intensity gave not

significative results since number of cells on slide was changing with time. In this way, results were presented according to the staining intensity observed.

An immediate phosphorylation was observed in fibroblasts (Fig. 3 II A) and endothelial cells (Fig. 3 II B) exposed to 10 Gy-radiation. Then, repair occurred. In fibroblasts, a strong staining was observed 3 hours after exposure. At day 7 post-irradiation, a new phosphorylation of H2AX happened and was stronger in fibroblasts than in endothelial cells. Finally, fibroblasts presented a low γ-H2AX level increase at day 21 post exposure.

The PTX/Tx combination led to the decrease in γ-H2AX level in irradiated fibroblasts immediately and 3 hours after irradiation but increased this level at 1 hour. Moreover, unirradiated fibroblasts treated by PTX/Tx presented an increased H2AX phosphorylation at 10 minutes and 21 days post-irradiation. In contrast, PTX/Tx treatment induced an increase in H2AX phosphorylation at days 7 and 21 in irradiated endothelial cells.

3.2. DNA-PKcs expression

DNA-PKcs forms, with Ku proteins, an heterotrimer, DNA-PK, involved in NHEJ process, the main DSB repair pathway. DNA-PKcs level was measured by Western blotting in irradiated and unirradiated fibroblasts and endothelial cells treated or not by PTX/Tx. Blots were analysed by image analysis software.

DNA-PKcs expression was shown to increase at day 1 after irradiation: a 1.94-fold increase in fibroblasts (Fig. 4A) against a 1.24-fold increase in endothelial cells (Fig. 4B) compared to unirradiated cells. Then, DNA-PKcs expression dropped in fibroblasts with a 1.69-fold decrease compared to control and remained under control level at day 14 before returning to normal value at day 21 post-irradiation. In endothelial cells, DNA-PKcs expression was still increased at day 7 by a factor 1.55 before decreasing by a factor 1.22 at day 14 and reaching basal level at day 21. However, DNA-PKcs expression was very low at day 21 after irradiation in endothelial cells.

PTX/Tx treatment allowed the decrease in DNA-PKcs level at day 21 after irradiation in fibroblasts by a factor 1.54. In endothelial cells, a 1.96-fold decrease in DNA-PKcs expression was observed at day 7. Moreover, the treatment decreased the level measured in unirradiated cells at day 21 in fibroblasts and at day 14 in endothelial cells.

3.3. B-Galactosidase staining and p21^{WAF1} expression

Senescence was assayed by observing morphological changes but especially by staining of senescence associated β-galactosidase (SA-β-gal) activity and by measuring p21^{WAF1}

expression by western blotting. SA-β-gal activity and $p21^{WAF1}$ expression was measured in irradiated and unirradiated fibroblasts (Fig. 5A) and endothelial cells (Fig. 5B) treated or not by PTX/Tx.

SA-β-gal activity assay showed a progressive induction of senescence in fibroblasts and endothelial cells reaching 40% of fibroblasts at day 21 after irradiation whereas the values were stronger in endothelial cells with 77% of senescent cells at day 21. The combination did not exhibit strong effects on SA-β-gal activity after irradiation except at day 14 and 21 in irradiated endothelial cells with a 2.14-fold decrease in senescent cells.

$p21^{WAF1}$ expression was strongly increased at day 1 by a factor 2.47 in fibroblasts and by a factor 1.78 in endothelial cells. Then, $p21^{WAF1}$ level decreased remaining over unirradiated cells level in both cell types at day 7 and 14 post-exposure. At day 21, $p21^{WAF1}$ expression was strongly augmented by a factor 3.23 in irradiated fibroblasts whereas this level remained at the control value in endothelial cells. The combination of PTX and Tx led to the decrease in $p21^{WAF1}$ level compared to untreated cells, especially in irradiated fibroblasts at day 14 with a 2.96-fold decrease in $p21^{WAF1}$ expression.

4. DISCUSSION

DNA damage and repair induced in dermal cells is of main relevance in the appearance of delayed skin injury participating to the radiological cutaneous syndrome. Indeed, we had previously shown that micronuclei were increased long time, 2 and 3 weeks post-exposure, after irradiation (Laurent *et al*., 2005; Laurent *et al*., 2005). The combination of pentoxifylline and trolox, an analogue of vitamin E, which was very efficient *in vivo* in reducing late cutaneous injury, provoked a decrease in ROS production and initial DNA damage, as measured by the alkaline comet assay. However it was followed by a delayed micronuclei frequency raise in 10 Gy-irradiated cells. The origin of such delayed DNA damage was unclear because treatment was shown to be non toxic on unirradiated cells. Possible origin could be either unrepaired radiation-induced double-strand breaks which would be persistent several weeks after exposure or newly DNA DSB formation as a result of chronic stress damage as described in (Laurent *et al*., 2005; Laurent *et al*., 2005) that could lead to a stress-induced premature senescence (SIPS). Therefore, the present study aimed at understanding the mechanisms involved in delayed formation of micronuclei and to investigate the possible

interference of PTX/Tx combination on such kind of damage. For this purpose, confluent primary cultures of fibroblasts and endothelial cells from adult dermis were gamma-irradiated at the high dose of 10 Gy and were treated 15 min before irradiation by the combination of pentoxifylline and trolox. DSB were measured by γ-H2AX assay at early and late times post-irradiation. DNA-PKcs protein, involved in NHEJ pathway for DSB repair, was quantified. Senescence was assayed by $p21^{WAF1}$ western blotting and SA-β-galactosidase positive cells staining.

H2AX histone is phosphorylated at double-strand breaks site. Phosphorylated H2AX, namely γ-H2AX, was stained by immunocytochemistry and quantified by mean fluorescence intensity in irradiated and unirradiated fibroblasts and endothelial cells treated or not by PTX/Tx. Histone H2AX phosphorylation occurs at DSB sites on serine 139 at the carboxy terminus by DNA-PK and ATM (Wang *et al*., 2005). This phosphorylation was shown to occur 10 minutes after 10 Gy-radiation exposure (Fig. 3 I), in skin fibroblasts (Fig. 3 II A) and endothelial cells (Fig. 3 II B). Then, repair occurred so that signal was reduced. However, in fibroblasts, a strong signal intensity was observed 3 hours after exposure. A new phosphorylation of H2AX was observed on day 7 after irradiation and signal was stronger in fibroblasts than in endothelial cells. Finally, fibroblasts presented a low γ-H2AX level increase at day 21 post exposure whereas this level returned to control values in endothelial cells. No increase in strand breaks, as measured by the alkaline comet assay, was observed later on than three hours post-irradiation. This is probably due to the fact that if this method allows detection of single- and double-strand breaks together with alkali-labile sites, it is not sensitive enough to measured DSB alone which are produced in much less amount. Moreover, strong presence of H2AX phosphorylation measured between 3hours and 7 days, indicates that newly formed DSB occurred and that delayed oxidative stress formation is produced. This was partially demonstrated in previous works where it was shown by DCHH-DA that reactive oxygen species were produced in the weeks following irradiation (Laurent *et al*., 2005). Such DNA damage could be involved in micronulei formation because increase of the latter lesion was observed to occur between 7 and 14 days in irradiated cells. However, if the relationship between DSB formation and micronuclei yield is not direct.

When PTX/Tx combination was used, a slight decrease in γ-H2AX level was measured 10 min and 21 days after onset of experiments in controls. However, this must not be significant and might be mostly artefactual because, no signal was observed at the other considered times. Surprisingly, when drugs were used, signal measured in irradiated fibroblasts was shown to be slightly reduced 10 min after irradiation. Whereas signal level was high in

absence of drugs 3 hours after irradiation, it was strongly decreased in presence of the combination. No significant changes induced by combination were observed for later times in fibroblasts. By contrast, an increase was measured in presence of PTX/Tx on days 7 and 21 in endothelial cells. The effect of the combination of drugs on DSB is not obvious because one could assume that initial DNA damage would be decreased due to its antioxidant properties. By contrast, if a small decrease was observed in case of fibroblasts, yield of DSB was shown to be either similar or increased in presence of the mixture. However, change was observed concerning the kinetic of the phenomenon. It must be reminded that caffeine, which belongs to the same family than pentoxifylline was shown to inhibit ATM protein which is one of the protein involved in phosphorylation of H2AX (Wang *et al*., 2005). Our results indicate that if ATM is inhibited by the combination PTX/Tx, DNA-PK activity might be sufficient to perform this phosphorylation. Then, DNA-PKcs protein, which constitutes in association with Ku proteins, a heterotrimer, DNA-PK involved in NHEJ process was measured by Western blotting in irradiated and unirradiated fibroblasts and endothelial cells treated or not by PTX/Tx.

DNA-PKcs expression was shown to increase on day 1 after irradiation compared to unirradiated cells. Then, DNA-PKcs expression was shown to drop in fibroblasts compared to control and remained under control level on day 14 before returning to normal value on day 21 post-irradiation. In endothelial cells, DNA-PKcs expression was still increased on day 7 before decreasing on day 14 and reaching basal level on day 21. However, DNA-PKcs expression was strongly depressed in irradiated endothelial cells on day 21. These results indicate a strong correlation between the level of DNA-PKcs and γ-H2AX phosphorylation. if we consider DNA-PKcs overexpression is involved in a stronger DSB repair and subsequent decrease in H2AX signal.

When PTX/Tx treatment was used, a decrease in DNA-PKcs level was measured in fibroblasts on day 21 after irradiation. In endothelial cells, a decline in DNA-PKcs expression was observed on day 7. Moreover, the treatment was shown to decrease the level measured in unirradiated fibroblasts on day 21 in endothelial cells on day 14.

A good correlation is found again between phosphorylated γ-H2AX level and DNA-PKcs expression. Our results are in accordance with previous works which indicated that a late hyperphosphorylation of H2AX could be connected to a decrease in DNA-PKcs level.

Senescence was assayed by observing morphological changes and by immunostaining of senescence associated β-galactosidase (SA-β-gal) activity together with measure of $p21^{WAF1}$ expression by western blotting. SA-β-gal activity and $p21^{WAF1}$ expression were measured in

irradiated and unirradiated fibroblasts (Fig. 5A) and endothelial cells (Fig. 5B) treated or not by PTX/Tx as described previously. SA-β-gal activity assay showed a progressive induction of senescence in fibroblasts and endothelial cells so that the proportion of senescent fibroblasts and endothelial cells reached 40% and 77%, respectively, on day 21. No major modifications in this ratio were observed for fibroblasts when combination was used. By contrast, a decrease in the percentage of senescent endothelial cells was measured as soon as day 5 after drugs were added. The protein $p21^{WAF1}$ expression was strongly increased on day 1 in fibroblasts and in endothelial cells. Then, its level decreased in both cell types but remained above control values until day 21. On day 21, $p21^{WAF1}$ expression was strongly augmented in irradiated fibroblasts whereas this level remained about the control level in endothelial cells. When drugs were used, a strong decrease in the level of the latter protein was observed in fibroblasts while no modifications were observed in endothelial cells. Interestingly, the raise in $p21^{WAF1}$ expression is in favour of a stress-induced premature senescence (SIPS) induction in both type of cells and is corroborated by increased SA-β-gal activity. The marked increase measured the first day after irradiation is in agreement with previous works which indicate that G1 arrest is a pre-requisite for SIPS. Considering fibroblasts, this arrest is also observed and indicates induction of stress-induced premature senescence (SIPS) but it is followed by increased level on days 7, 14 and 21. Such increase in $p21^{WAF1}$ expression might be due to DSB-induced p53 induction, which in turn participates to $p21^{WAF1}$ expression. It was in this respect observed a strong γ-phosphorylated H2AX signal until day 7 post-irradiation and on day 21. These characteristics of SIPS were already observed in young human diploid fibroblasts treated with prolonged low doses of hydrogen peroxide (Duan et al., 2005) and also in normal diploid fibroblasts exposed to ionizing radiations (Naka et al., 2004). If senescence is observed in both types of irradiated cells, drugs were shown to act in different ways on (SA-β-gal) activity and on $p21^{WAF1}$ expression.

This work allowed to define time course of DSB formation and subsequent signalling pathways after ionizing radiation exposure of skin fibroblasts and endothelial cells. After an immediate production of DSB after irradiation, a late increase was observed one week post-exposure. This increase was associated to a delayed decrease in DNA-PKcs expression and the late hyperphosphorylation of H2AX which was associated to a decrease in DNA-PKcs level. However, PTX/Tx decreased SIPS suggesting a possible role on signalling pathways leading to premature senescence. Naka *et al.* and Toussaint *et al.* proposed two different pathways leading to SIPS: one pathway via ATM, p53 and $p21^{WAF1}$ and the other pathway via

$p38^{MAPK}$ and $p16^{INK4A}$ (Naka *et al*., 2004; Toussaint *et al*., 2000). It would be of major interest to determine how irradiation and treatment modulate these pathways.

Acknowledgements

This work was supported by Electricité de France-Service de Radioprotection and Région Ile-de-France.

References

Ader, I., C. Muller, et al. (2002). "The radioprotective effect of the 24 kDa FGF-2 isoform in HeLa cells is related to an increased expression and activity of the DNA dependent protein kinase (DNA-PK) catalytic subunit." Oncogene **21**(42): 6471-9.

Cadet, J., M. Berger, et al. (1997). "Oxidative damage to DNA: formation, measurement and biological significance." Rev Physiol Biochem Pharmacol **31**: 1-87.

Chainiaux, F., J. P. Magalhaes, et al. (2002). "UVB-induced premature senescence of human diploid skin fibroblasts." Int J Biochem Cell Biol **34**(11): 1331-9.

Chiao, T. B. and A. J. Lee (2005). "Role of pentoxifylline and vitamin E in attenuation of radiation-induced fibrosis." Ann Pharmacother **39**(3): 516-22.

Debacq-Chainiaux, F., C. Borlon, et al. (2005). "Repeated exposure of human skin fibroblasts to UVB at subcytotoxic level triggers premature senescence through the TGF-beta1 signaling pathway." J Cell Sci **118**(Pt 4): 743-58.

Delanian, S., R. Porcher, et al. (2003). "Randomized, placebo-controlled trial of combined pentoxifylline and tocopherol for regression of superficial radiation-induced fibrosis." J Clin Oncol **21**(13): 2545-50.

Devik, F. (1955). "Study of the local roentgen reaction on the skin of mice, with specific reference to the vascular effects." Acta Radiol Suppl **119**.

Duan, J., J. Duan, et al. (2005). "Irreversible cellular senescence induced by prolonged exposure to H(2)O(2) involves DNA-damage-and-repair genes and telomere shortening." Int J Biochem Cell Biol **37**(7): 1407-1420.

Epstein, W. L. and H. I. Maibach (1965). "Cell renewal in human epidermis." Arch Dermatol **92**(4): 462-8.

Gorbunova, V., A. Seluanov, et al. (2002). "Expression of human telomerase (hTERT) does not prevent stress-induced senescence in normal human fibroblasts but protects the cells from stress-induced apoptosis and necrosis." J Biol Chem **277**(41): 38540-9.

Laemmli, U. K. (1970). "Cleavage of structural proteins during the assembly of the head of bacteriophage T4." Nature **227**(5259): 680-5.

Laurent, C., J. P. Pouget, et al. (2005). "Modulation of DNA damage by pentoxifylline and a-tocopherol in skin fibroblasts exposed to gamma-rays." Radiat Res **Under Press**.

Laurent, C., P. Voisin, et al. (2005). "DNA damage in cultured skin microvascular endothelial cells exposed to gamma-rays treated by the combination of pentoxifylline and alpha-tocopherol." **Submitted**.

Naka, K., A. Tachibana, et al. (2004). "Stress-induced premature senescence in hTERT-expressing ataxia telangiectasia fibroblasts." J Biol Chem **279**(3): 2030-7.

Ortiz, T., S. Lopez, et al. (2004). "Radiosensitizer effect of wortmannin in radioresistant bladder tumoral cell lines." Int J Oncol **24**(1): 169-75.

Rudolph, R., J. Vande Berg, et al. (1988). "Slowed growth of cultured fibroblasts from human radiation wounds." Plast Reconstr Surg **82**(4): 669-77.

Toussaint, O., E. E. Medrano, et al. (2000). "Cellular and molecular mechanisms of stress-induced premature senescence (SIPS) of human diploid fibroblasts and melanocytes." Exp Gerontol **35**(8): 927-45.

Towbin, J. A., T. Staehelin, et al. (1979). "Electrophoretic transfer of proteins from polyacrylamide gels to nitrocellulose sheets: procedure and some applications." Proc Natl Acad Sci U S A **76**: 4350-4354.

Wang, H., M. Wang, et al. (2005). "Complex H2AX phosphorylation patterns by multiple kinases including ATM and DNA-PK in human cells exposed to ionizing radiation and treated with kinase inhibitors." J Cell Physiol **202**(2): 492-502.

Withers, H. R. (1967). "Recovery and repopulation in vivo by mouse skin epithelial cells during fractionated irradiation." Radiat Res **32**(2): 227-39.

Withers, H. R., L. J. Peters, et al. (1980). The pathology of late effects of irradiation. Radiation Biology in Cancer Research. R. E. M. a. H. R. Withers. New York, Raven Press**:** 439-448.

Figure legends

Figure 1. DNA damage in irradiated skin fibroblasts (A) and endothelial cells (B) treated by PTX/Tx.

Figure 2. Micronuclei frequency in irradiated skin fibroblasts (A) and endothelial cells (B) treated by PTX/Tx.

Figure 3. γ-H2AX formation in irradiated skin fibroblasts (A) and endothelial cells (B) treated by PTX/Tx. Phosphorylated H2AX was assayed by immunocytochemistry. Panel I presents γ-H2AX staining after 10 Gy- radiation exposure at 10 minutes after irradiation and the dose-effect curve of γ-H2AX. Panel II presents the results obtained with (+) corresponding to a positive stainin whereas (0) corresponds to no staining.

Figure 4. DNA-PKcs expression in irradiated skin fibroblasts (A) and endothelial cells (B) treated by PTX/Tx. DNA-PKcs expression was assayed by Western blotting.

Figure 5. Senescence in irradiated skin fibroblasts (A) and endothelial cells (B) treated by PTX/Tx. SA-β-galactosidase activity (right panel) and p21WAF1 expression (left panel) were assayed.

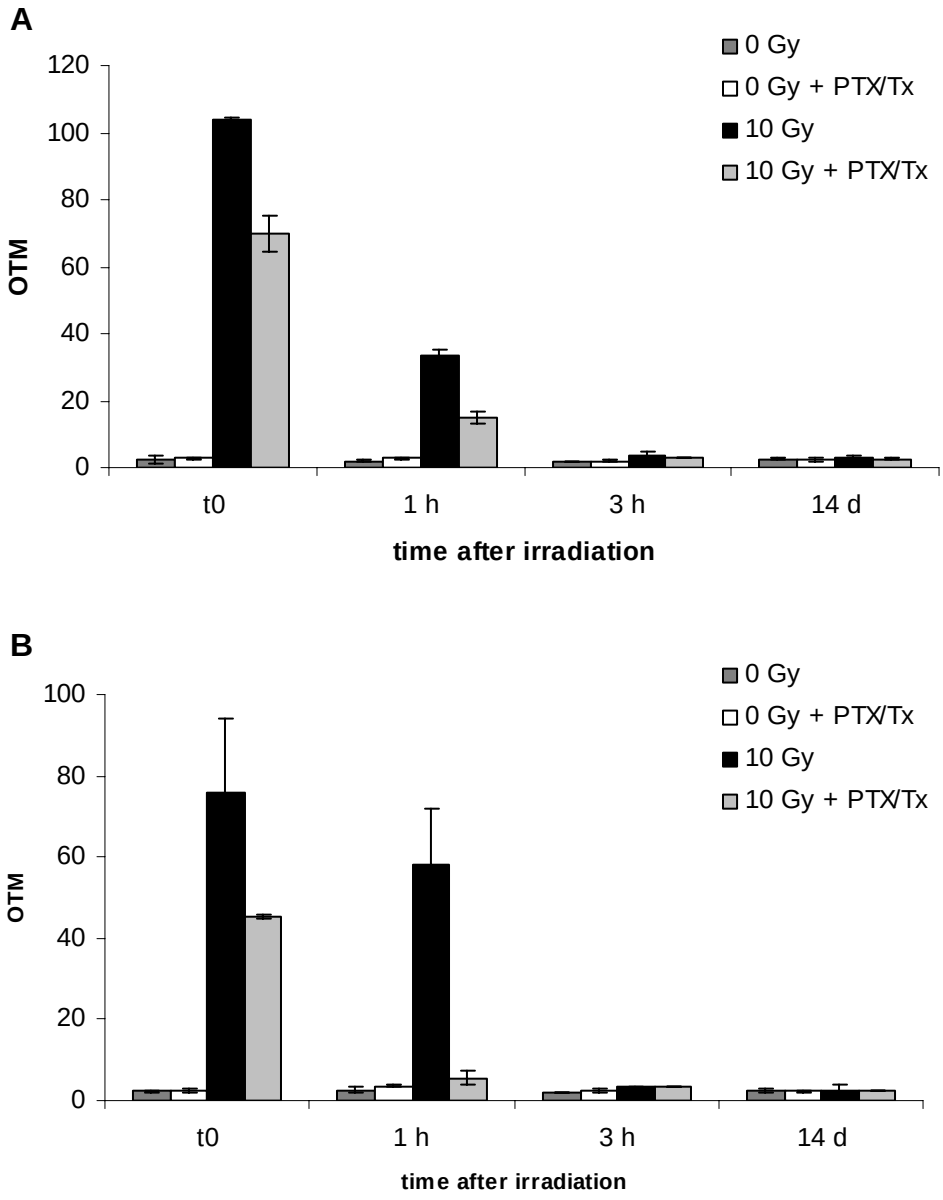
A
0 Gy
0 Gy + PTX/Tx
10 Gy
10 Gy + PTX/Tx
OTM
120
100
80
60
40
20
0
t0
1 h
3 h
14 d
time after irradiation
B
0 Gy
0 Gy + PTX/Tx
10 Gy
10 Gy + PTX/Tx
OTM
100
80
60
40
20
0
t0
1 h
3 h
14 d
time after irradiation

Figure 1

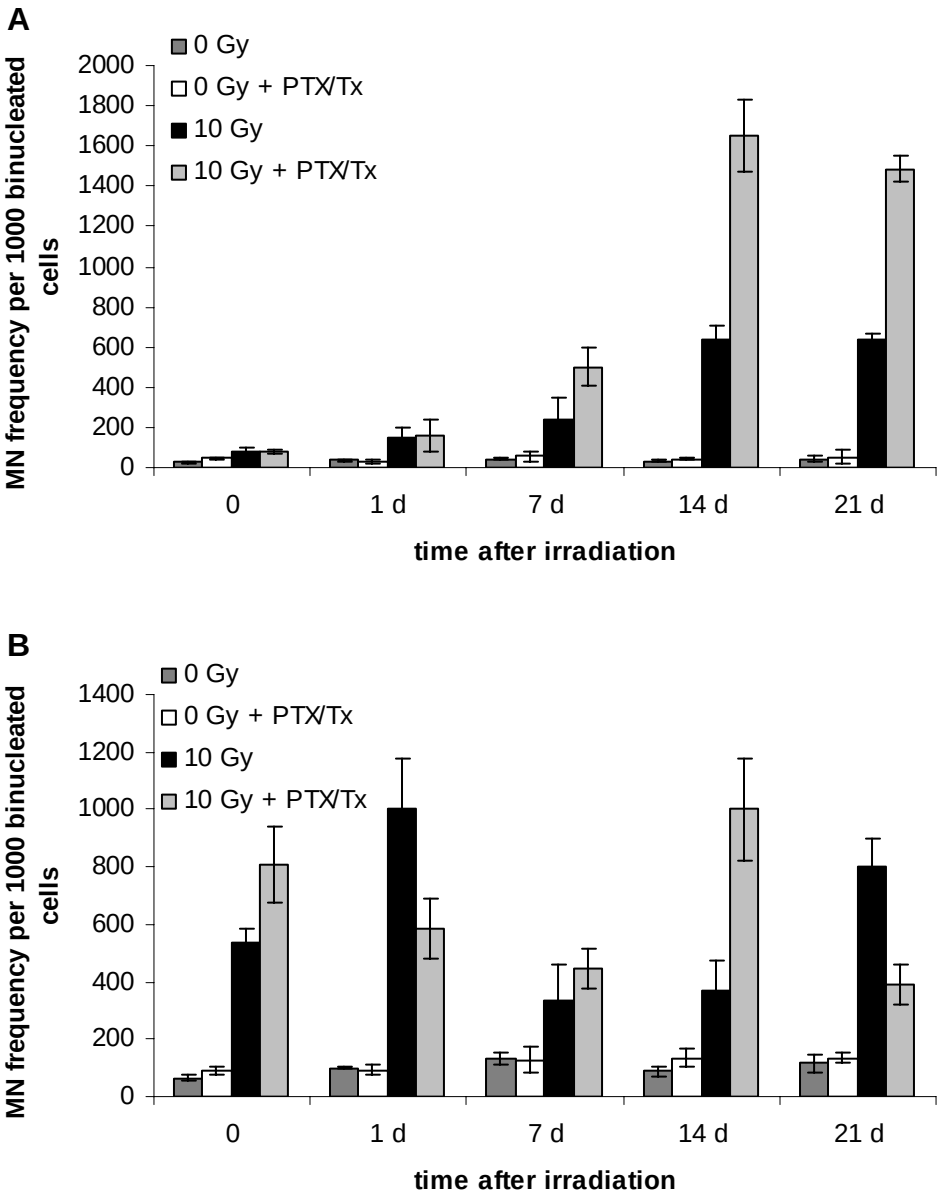
A
0 Gy
0 Gy + PTX/Tx
10 Gy
10 Gy + PTX/Tx
MN frequency per 1000 binucleated cells
2000
1800
1600
1400
1200
1000
800
600
400
200
0
0
1 d
7 d
14 d
21 d
time after irradiation
B
0 Gy
0 Gy + PTX/Tx
10 Gy
10 Gy + PTX/Tx
MN frequency per 1000 binucleated cells
1400
1200
1000
800
600
400
200
0
0
1 d
7 d
14 d
21 d
time after irradiation

Figure 2

I

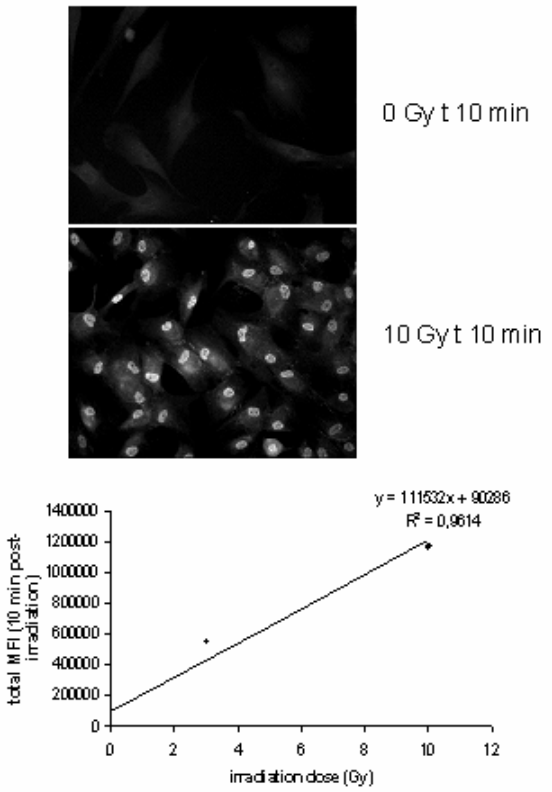

II

A

time after irradiation	0 Gy	0 Gy + PTX/Tx	10 Gy	10 Gy + PTX/Tx
10 min	0	+	+++	++
1 h	0	0	+	++
3 h	0	0	+++	+
7 d	0	0	++	++
14 d	0	0	0	0
21 d	0	+	+	+

B

time after irradiation	0 Gy	0 Gy + PTX/Tx	10 Gy	10 Gy + PTX/Tx
10 min	0	0	+++	+++
1 h	0	0	0	0
3 h	0	0	0	0
7 d	0	0	+	++
14 d	0	0	0	0
21 d	0	0	0	+

Figure 3

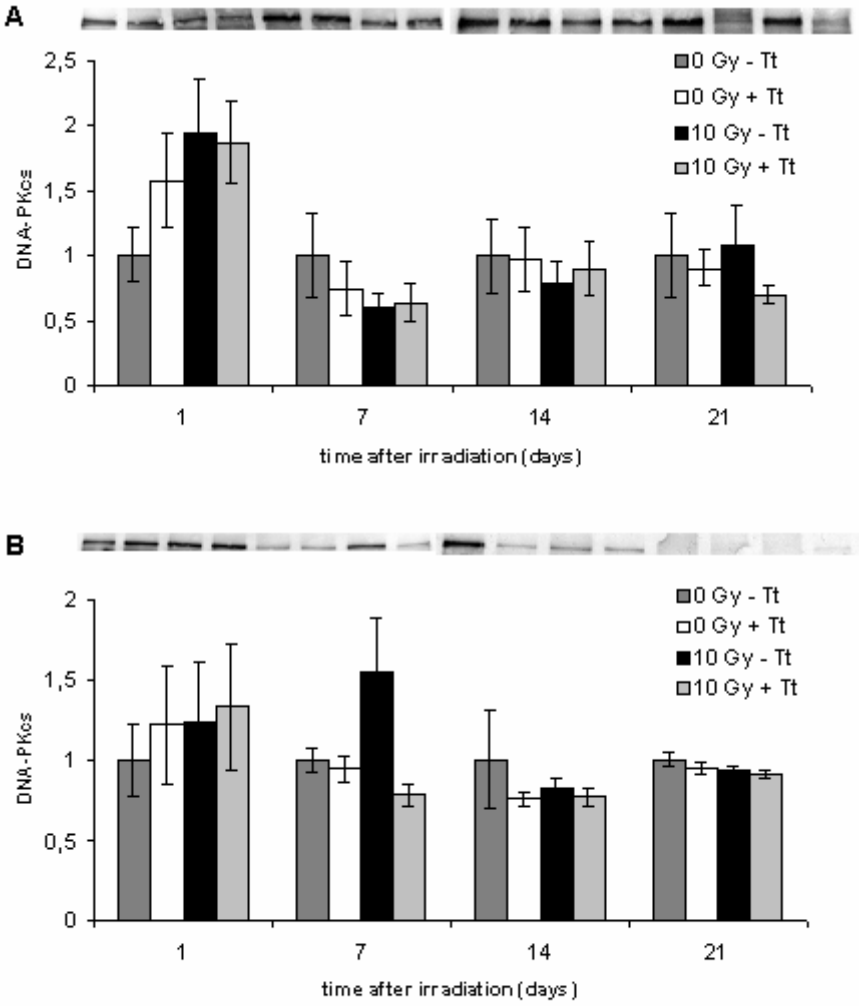
A
2,5
2
1,5
1
0,5
0
DNA-PKcs
0 Gy - Tt
0 Gy + Tt
10 Gy - Tt
10 Gy + Tt
1
7
14
21
time after irradiation (days)
B
2
1,5
1
0,5
0
DNA-PKcs
0 Gy - Tt
0 Gy + Tt
10 Gy - Tt
10 Gy + Tt
1
7
14
21
time after irradiation (days)

Figure 4

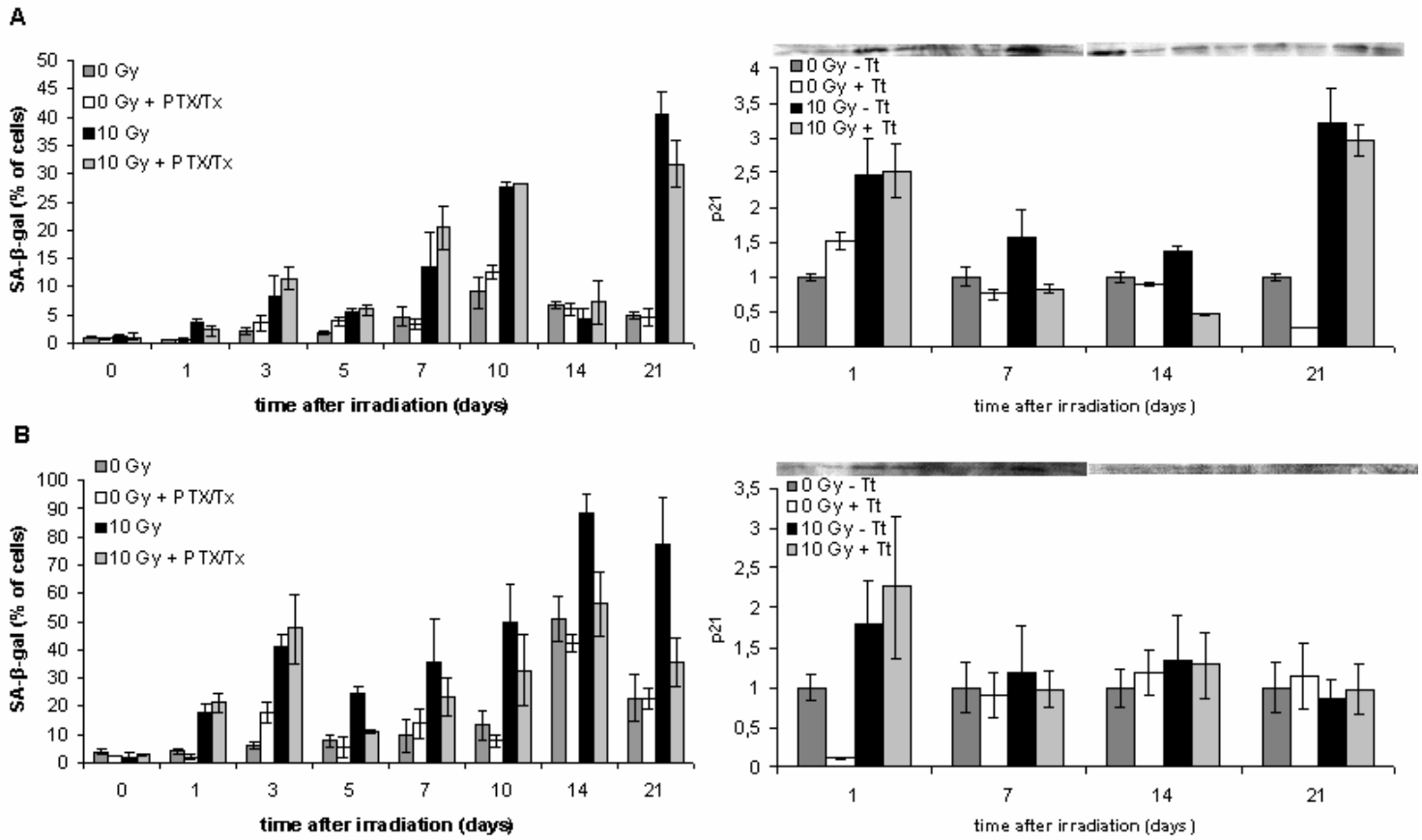
A
SA-β-gal (% of cells)
0 Gy
0 Gy + PTX/Tx
10 Gy
10 Gy + PTX/Tx
time after irradiation (days)
p21
0 Gy - Tt
0 Gy + Tt
10 Gy - Tt
10 Gy + Tt
time after irradiation (days)
B
SA-β-gal (% of cells)
0 Gy
0 Gy + PTX/Tx
10 Gy
10 Gy + PTX/Tx
time after irradiation (days)
p21
0 Gy - Tt
0 Gy + Tt
10 Gy - Tt
10 Gy + Tt
time after irradiation (days)

Figure 5

DISCUSSION GENERALE

Les irradiations d'origine accidentelle sont, pour la plupart, localisées ou hétérogènes, c'est à dire qu'elles ne concernent l'exposition que d'une partie de l'organisme. En effet, sur les quelques 560 accidents d'irradiation qui se sont produits durant les cinquante dernières années et qui ont impliqué environ 15 000 personnes et fait pas moins de 180 victimes, 54% étaient des irradiations localisées. Ces irradiations constituent un problème délicat pour l'équipe médicale car bien souvent de très fortes doses, par ailleurs difficiles à estimer, peuvent être délivrées. La peau constitue alors dans tous les cas l'organe cible commun à toutes les situations du fait de sa localisation anatomique, et de la forte radiosensibilité de l'épiderme. L'ensemble des symptômes qui caractérise la réponse du tissu cutané à une irradiation aigüe à fortes doses est regroupé au sein du syndrome cutané radio-induit (SCRI). C'est dans bien des situations accidentelles la prise en charge des symptomes associés à ce type de lésions qui conditionne le pronostic vital de la victime.

Le SCRI se décompose en deux phases caractérisées par des symptomes cliniques dont la gravité et le délai d'apparition après exposition sont fonctions de la dose d'irradiation. Les lésions aiguës précoces regroupent l'érythème, la desquamation sèche et la desquamation humide alors que les lésions tardives comportent les télangiectasies, la nécrose et la fibrose. Les effets précoces apparaissent dans les jours ou les semaines suivant l'irradiation et les effets tardifs dans les mois ou les années qui font suite. C'est essentiellement sur le problème des lésions tardives que les médecins radiothérapeutes et les médecins prenant en charge les victimes d'accidents d'irradiations se retrouvent. En effet, si les médecins radiothérapeutes savent depuis longtemps s'affranchir des lésions précoces en se plaçant au dessous des doses seuil d'apparition des lésions en fractionnant la dose délivrée et en bénéficiant des progrès techniques associés aux dispositifs d'irradiation, la prévention des effets tradifs tels que la fibrose restent plus problématique car fortement dépendant de la radiosensiblité individuelle.
Trois théories ont été avancées pour expliquer l'apparition de ces lésions tardives : la théorie épithéliale, la théorie vasculaire et la théorie stromale. La théorie épithéliale donne un rôle prépondérant à l'épiderme. L'épiderme est un tissu constitué essentiellement de kératinocytes qui sont des cellules à renouvellement rapide, et dont la perte serait à l'origine des effets précoces mais qui pourrait aussi influer sur l'apparition des effets tardifs. La théorie vasculaire implique une fibrose progressive contribuant à l'hypoplasie retardée du

parenchyme. Enfin, la théorie stromale explique l'apparition des lésions tardives par la mort mitotique des fibroblastes et cellules endothéliales du derme. Ces cellules porteuses de lésions de l'ADN incompatibles avec le bon déroulement de la mitose mourraient au cours de la première division cellulaire, généralement longtemps après l'exposition, du fait de leur faible index mitotique.

Un point commun à toutes ces théories semble être le rôle joué par le stress oxydatif. Celui-ci peut être induit par l'irradiation elle même, soit généré au cours des processus inflammatoires chroniques ou des processus de réparation tissulaire. Or, ces phénomènes conduisent, via la perte ou le dysfonctionnement des cellules vasculaires et du parenchyme, à l'apparition de la fibrose ou de la nécrose (Denham et Hauer-Jensen, 2002). Même si l'origine exacte des effets tardifs est encore matière à débat, le rôle du stress oxydatif dans leur génèse semble être prépondérant (pour revue, Robbins et Zhao, 2004) : au niveau du rein (Massy et Nguyen-Khoa, 2002 ; Locatelli *et al*., 2003), au niveau du poumon (Kinnula et Crapo, 2003), au niveau du système nerveux central (Castagne *et al*., 1999). Toutefois, au niveau de la peau irradiée à fortes doses, il n'y a pas de preuve directe de présence du stress oxydatif. Des preuves indirectes existent au travers de résultats obtenus par l'utilisation de traitement anti-oxydants et qui ont montré une restauration de l'intégrité tissulaire. Ainsi, la forme liposomale administrée chez le porc et chez l'homme de la CuZnSOD/MnSOD, enzyme anti-oxydante, a permis la réversion de la fibrose et la restauration du tissu lésé après irradiation (Baillet *et al*., 1986; Delanian *et al*., 1994; Lefaix *et al*., 1996). D'autre part, l'association pentoxifylline et α-tocophérol, appartenant au groupe le plus important des anti-oxydants liposolubles, a aussi conduit à la réversion des effets tardifs (Delanian *et al*., 1999; Lefaix *et al*., 1999; Delanian *et al.*, 2003; Chiao et Lee, 2005).

Qu'il soit directement lié à l'irradiation elle même où à la réponse physiologique du tissu à l'agression que constitue l'irradiation, le stress oxydatif peut conduire à la formation d'espèces radicalaires telles que °OH ou H°. En présence d'oxygène, de nouvelles espèces radicalaires plus stables sont formées : l'anion superoxyde $O_2°^-$ et le radical hydroxyle $HO_2°$. Ces espèces réactives sont aussi appelées espèces réactives de l'oxygène (ERO). Des molécules issues de processus de recombinaison radicalaires sont aussi produites, H_2 et H_2O_2 en font partie. Si les systèmes de défenses antioxydantes des cellules (enzymatiques ou non-enzymatiques) sont dépassés, il y aura alors un déséquilibre en faveur des espèces réactives (conduisant à un état de stress oxydatif) qui vont pouvoir interagir avec les macromolécules biologiques.

Nos premiers travaux ont consisté à développer une méthode de dosimétrie biologique basée sur le dénombrement des aberrations chromosomiques stables dans les fibroblastes de peau irradiée. Cette approche, d'abord mise au point sur des explants de peau humaine irradiée *ex vivo*, a été appliquée à l'accident radiologique survenu en Géorgie en 2001 (**article 1**).

Au cours de cet accident, trois victimes ont été exposées au niveau du dos à une source de ^{90}Sr. Une des victimes a été traitée environ 3 mois après l'exposition au Centre de Traitement des Brûlés de l'Hôpital Percy de Clamart afin d'y subir une exérèse du tissu lésé suivie de greffes successives de peau. Le tissu excisé a été divisé en secteurs et les fibroblastes du derme isolés afin d'être mis en culture. Après plusieurs jours, le dénombrement des fragments excédentaires de chromosome par métaphase a été effectué par la technique de PCC-FISH. En utilisant une courbe de calibration établie *ex vivo*, il a été possible de déterminer la dose d'irradiation reçue par chacun des secteurs et d'établir une cartographie du territoire irradié. Il a été montré une bonne corrélation entre les doses ainsi calculées et les estimations établies à partir des données cliniques, physiques (Résonance Paramagnétique Electronique) ou de dosimétrie biologique appliquée aux lymphocytes. Par ailleurs, nous avons observé la présence de cellules fortement lésées comportant un grand nombre d'aberrations chromosomiques. Un marquage de la protéine Ki67 a montré que ces cellules étaient quiescentes. Une des hypothèses pouvant expliquer la présence de cellules aussi fortement endommagées et quiescentes plusieurs semaines après irradiation peut être un phénomène de sénescence prématurée des fibroblastes induit par l'instauration d'un stress chronique.

Afin de démontrer *in vivo* la présence de phénomènes oxydatifs dans le tissu cutané après irradiation, nous avons exposé des rats hairless irradiés localement au niveau des pattes postérieures à l'aide d'une source de rayonnements X (**article 2**). Des doses de 10, 20 et 30 Gy ont été délivrées et la période d'observation a porté sur un mois. Nous avons mesuré le niveau des défenses anti-oxydantes, de marqueurs de l'inflammation et de dommages des macromolécules biologiques à la fois dans l'épiderme et le derme. L'existence d'une « corrélation » entre la modification des paramètres cités ci-dessus et les signes cliniques (pathologie du tissu cutané, formule sanguine, masse des rats, état général) a été recherchée. Nous avons constaté qu'en moins de deux semaines après irradiation l'érythème observé chez les rats irradiés à 20 Gy et 30 Gy évoluait respectivement vers une desquamation sèche et humide. Deux semaines plus tard, la desquamation sèche avait totalement régressé et les

lésions observées chez les rats les plus fortement irradiés étaient en cours de cicatrisation. Ces signes cliniques précoces étaient parfaitement corrélés aux variations du taux de lymphocytes et à une forte chute de l'activité SOD dans le derme maximale vers le 12ème jour post-irradiation avant un retour au niveau du contrôle à un mois. L'activité catalase présentait une diminution moins marquée et l'activité GPx semblait peu affectée. Nous avons également pu observer une atteinte des lipides (MDA) et de l'ADN (8-oxodGuo) maximales deux jours après irradiation ainsi qu'un niveau élevé de myéloperoxydase (MPO) et une forte augmentation du niveau de TNF-α le 12ème jour post-irradiation chez les rats irradiés à 30 Gy et chez tous les rats irradiés à J30. Ces résultats démontrent l'induction d'un stress oxydatif en particulier lié à des phénomènes inflammatoires dès le 2ème jour après irradiation. Le stress oxydatif qui en découle évolue par phases successives et dépend de la dose d'irradiation. Par ailleurs, nos résultats suggèrent un rôle prépondérant de l'activité SOD dont la chute est l'événement le plus caractéristique de perte des défenses antioxydantes.

Devant la complexité du modèle *in vivo* et la difficulté d'interprétation des résultats, liée à la l'enchevêtrement de paramètres physiologiques (inflammation, réparation tissulaire, relation épiderme-derme etc.) et ceux liés à l'irradiation elle-même (lésions initiales du tissu), nous avons restreint nos travaux suivants à l'étude du stress oxydatif radio-induit au niveau du derme et en particulier des deux principaux types cellulaires que sont les cellules endothéliales et les fibroblastes. En outre, une approche utilisant des modèles *in vitro* nous a semblé plus adaptée à l'étude des mécanismes d'action impliquée dans l'association de la pentoxifylline et de l'α-tocophérol. Compte tenu des résultats cliniques remarquables obtenus par l'utilisation de cette association dans la restauration des tissus lésés, il nous paraissait essentiel d'en comprendre le mode d'action.

L'objectif de notre étude était de répondre aux questions suivantes :

- *Le stress oxydatif initial radio-induit conduit-il à l'accumulation de lésions de l'ADN dans les cellules à renouvellement lent (fibroblastes, cellules endothéliales) qui serait responsable des effets tardifs ?*

- *Existe-il des phénomènes oxydatifs tardifs et sont-ils impliqués dans l'apparition d'effets tardifs ?*

- *Existe-t-il un phénomène de sénescence prématurée qui conduirait à une accumulation des lésions avant la mort cellulaire ?*

- *Quel sont les mécanismes d'action de l'association pentoxifylline/α-tocophérol ?*

Pour répondre à ces questions, des cultures primaires de fibroblastes et de cellules endothéliales de microvascularisation du derme ont été utilisées. Une caractérisation des modèles cellulaires a été effectuée. Les fibroblastes et les cellules endothéliales ont été irradiées à 3 ou 10 Gy à confluence afin de se rapprocher de la configuration tissulaire réelle. Pour cela, le rayonnement γ d'une source de césium 137 délivré à 1 Gy par minute a été utilisé. Ces doses d'irradiation ont été choisies d'après les données de la littérature qui donnaient les valeurs des D_0 pour chaque type cellulaire et des courbes de survie clonogénique que nous avons préalablement établies. La période d'observation des effets de cette irradiation a porté sur 21 jours après irradiation. Le traitement associant pentoxifylline (PTX) et trolox (Tx), l'analogue hydrosoluble de l'α-tocophérol, a été administré 15 minutes avant l'irradiation, 30 minutes après l'irradiation, *i.e.* lorsque les phénomènes oxydatifs initiaux se sont déjà produits, ou 24 heures après, ce qui évitait en principe toute interférence avec les mécanismes de réparation de l'ADN. Le traitement a été maintenu tout au long de l'expérimentation par dilution extemporanée dans le milieu. La concentration choisie pour chacune des drogues est de 0,5 mM. Nous avons préalablement montré par différents tests cytotoxiques ou génotoxiques qu'à cette concentration, les drogues ne présentaient aucune toxicité sur des cellules contrôles tout en possédant la plus forte capacité anti-oxydante comme démontré par le test ORAC.

L'**article 3** et l'**article 4** présentent la production d'espèces réactives de l'oxygène (ERO), mesurée par le test du DCFH-DA, pour chacun des types cellulaires et en fonction du temps, de la dose d'irradiation et de l'administration ou non du traitement. Le niveau des dommages de l'ADN est aussi mesuré par la technique des comètes en milieu alcalin, et par la mesure de la fréquence des micronoyaux. Les effets sur la distribution des cellules dans les différentes phases du cycle cellulaire a également été mesurée. L'**article 5** présente, en utilisant la même approche, les effets séparés des deux drogues.

Les propriétés anti-oxydantes des deux drogues ont conduit à une modification de la production d'ERO, ou plus précisément de la production cytoplasmique de peroxyde d'hydrogène et d'oxydants issus de la réduction du peroxyde d'hydrogène par les peroxydases. Nous avons observé, une première vague de production d'ERO immédiatement après irradiation mais aussi d'autres plus tardives dans les deux types cellulaires, les fibroblastes et les cellules endothéliales. L'association PTX/Tx diminue le niveau d'ERO produites aux différents temps considérés et ceci même lorsque le traitement est administré

après irradiation, démontrant ainsi que les phases secondaires et initiales de production d'ERO sont indépendantes. Par ailleurs, PTX/Tx a également fortement diminué le niveau de base de production de radicaux.

Le radical hydroxyle et l'anion superoxyde, particulièrement délétère, ne faisaient pas partie des espèces radicalaires détectées par le test du DCFH-DA. Néanmoins, des études récentes ont montré que l'association PTX et vitamine E inhibait la libération des radicaux superoxydes et hydroxyles dans le tissu ovarien après ischémie-reperfusion (Uguralp et al., 2005).

Ces espèces étant très impliquées dans la formation des lésions de l'ADN, nous nous sommes intéressés à l'effet du traitement PTX/Tx sur la production de ce type de dommages. La technique des comètes en milieu alcalin permet de mesurer simultanément les cassures simple- et double-brins ainsi que les sites alcali-labiles. Nous avons mis en évidence une production maximale de dommages de l'ADN immédiatement après irradiation, de manière dose-dépendante et dans des proportions identiques dans les deux types cellulaires. L'association PTX/Tx a conduit à une réduction du niveau de ces dommages sans doute par ses propriétés anti-oxydantes. D'autre part, on peut exclure une fragmentation totale de l'ADN pour la plus forte dose d'irradiation, c'est-à-dire 10 Gy, puisque la viabilité des cellules irradiées à 10 Gy était d'environ 80% dans les premières heures et que le marquage des cellules par l'acridine orange et le Bromure d'Ethydium n'a pas révélé de phénomène de nécrose ou d'apoptose. De plus, une relation dose-effet linéaire a été observée avec des valeurs de 5, 35 et 105 unités arbitraires du moment de la queue de la comète (selon Olive *et al.*) respectivement à 0 Gy, 3 Gy et 10 Gy. Nous avons ensuite observé une diminution du moment de la queue de la comète reflétant les phénomènes de réparation de l'ADN. Celle-ci s'effectue plus rapidement dans les fibroblastes que dans les cellules endothéliales. Une heure après irradiation, la valeur du moment de la queue de la comète mesurée en présence du traitement PTX/Tx reste inférieure à celle mesurée en son absence. Enfin, trois heures après irradiation, le niveau de dommages de l'ADN dans les cellules irradiées est retourné au niveau de base suggérant une réparation complète des coupures mesurées par la méthode des comètes. Nous n'avons ensuite observé aucune formation de dommages, y compris à des temps plus tardifs (14 jours et 21 jours post-irradiation).

Lorsque le traitement a été administré 30 min après irradiation, une diminution du niveau de dommages de l'ADN, du même ordre de grandeur que celle mesurée lorsque le traitement était administré avant, a été mesurée une heure après exposition. Plusieurs hypothèses pourraient expliquer ce phénomène :

i) Une part importante des coupures mesurées dans l'heure consécutive à l'irradiation est due à la génération d'une deuxième vague d'espèces réactives de l'oxygène. Cette hypothèse semble peu probable car d'une part, aucune augmentation majeur de peroxydes n'a été mise en évidence par la méthode du DCFH-DA mais surtout, la diminution est forte et suggèrerait que la plupart des coupures seraient dues à des événements secondaires et non à l'effet direct de l'irradiation elle même, ce qui est peu probable.

ii) Une part des coupures mesurées dans l'heure suivant l'irradiation serait des coupures secondaires produites comme intermédiaires dans les processus de réparation. Le traitement agirait soit en accélérant leur réparation soit en en inhibant leur formation. Cette hypothèse, suppose une interférence du traitement avec les systèmes de réparation de l'ADN. En effet, de nombreux travaux ont souligné l'effet de PTX sur la réparation. Il a été démontré que PTX inhibait la réparation des cassures double brins (Theron *et al*., 2000; Binder *et al*., 2002), induisait des aberrations chromosomiques, des échanges de chromatides soeurs et conduisait à la formation de micronoyaux (Bozsakyova *et al*., 2001). Quant à l'αT, il a été montré qu'outre ses propriétés anti-oxydantes, ce composé protégeait des cellules lymphoblastiques des dommages à l'ADN (Sweetman *et al*., 1997) et qu'un composé relativement proche, le D-alpha-tocopheryl succinate (αTS) réduisait le taux de formation des aberrations chromosomiques dans les cellules normales (Kumar *et al*., 2002). De même, il a enfin été souligné *in vivo* que la vitamine E réduisait le nombre de métaphases aberrantes ainsi que le taux de micronoyaux mesurés dans la moelle osseuse de souris irradiées (Sarma et Kesavan, 1993; Satyamitra *et al*., 2003).

Ces données de littérature suggèrent l'interférence des deux drogues utilisées séparément avec les mécanismes de réparation des cassures double-brins. Or, si la méthode des comètes en milieu alcalin permet simultanément la détection des cassures simple-brins (CSB), des cassures double-brins (CDB) et des sites alcali-labiles (SAL), il n'est pas possible de déterminer de façon catégorique quelle classe de lésions est impliquée dans la diminution du moment de la queue de la comète observée dans les heures consécutives à l'irradiation en présence du traitement. Néanmoins, il a été montré que la proportion des CDB par rapport à celle des (CSB) était environ de 40 CDB pour 1000 CSB par cellule et par Gy de rayonnement gamma. On peut donc supposer que la majeure partie des lésions mesurées par la méthode des comètes après irradiation gamma correspond à des CSB et des SAL.

De même, en dépit de sa grande sensibilité, et pour les mêmes raisons, on ne peut pas exclure que certaines CDB ne soient toujours pas réparées au bout de 3 heures après irradiation. En effet, leur présence pourrait être englobée dans le bruit de fond de la méthode ou dans le niveau basal correspondant à une production endogène (métabolisme cellulaire) de coupures.

Afin d'établir le rôle du traitement sur la formation/réparation des CDB, une mesure indirecte a été effectuée par marquage de l'histone phosphorylé H2AX, appelé γ-H2AX (article 6). Cette technique est considérée comme très sensible et a été décrite comme marqueur des CDB (Rothkamm et Lobrich, 2003). Il a en effet été montré que la protéine histone était phosphorylée au niveau du site des CDB par la protéine DNA-PK ou ATM.
Nous avons observé un marquage maximal de γ-H2AX 10 min après l'irradiation dans les deux types cellulaires étudiés. A la dose d'irradiation de 10 Gy, le nombre de CDB attendu par cellule est de 400. Etant donné l'intensité du marquage, nous n'avons pas pu dénombrer les foci présents dans les noyaux comme cela était décrit dans la littérature. De plus, la mesure de la fluorescence ne pouvait convenir pour comparer les différents temps entre eux puisque le nombre de cellules par lame variait selon le temps. Le marquage a donc été estimé visuellement sur la base de critères qualitatifs. Aucun signal n'a été mesuré dans les cellules non irradiées en absence de traitement. En présence de PTX/Tx, un léger signal a été mis en évidence au début (10 min) et en fin (J21) de l'expérimentation dans les fibroblastes contrôles. Néanmoins, le traitement n'a pas d'effets sur la formation des CDB pendant les 3 semaines suivantes, ce qui est en accord avec le caractère non toxique du traitement démontré par les autres tests cytotoxiques ou génotoxiques. Le fort marquage observé 10 min après irradiation traduisant la formation initiale des CDB diminue plus rapidement dans les cellules endothéliales que dans les fibroblastes suggérant une formation des CDB plus faible ou bien une réparation plus rapide. Une heure après la réparation des CDB semble achevée dans les cellules endothéliales alors qu'elle n'est jamais totale dans les fibroblastes. Une cinétique inverse de la réparation avait été soulignée par la méthode des comètes. De façon plus surprenante, une forte augmentation de signal a été mise en évidence 3 heures après irradiation dans les fibrobalstes. Elle traduit une production de CDB qui n'a pas été détectée par la méthode des comètes en milieu alcalin. Le signal est aussi mesuré les $7^{ème}$ et $21^{ème}$ jour après irradiation dans les deux types cellulaires. L'origine de cette production reste indéterminée mais indique l'existence de phénomènes génotoxiques actifs puisque le signal mesuré est d'ampleur équivalente à celle du marquage obtenu immédiatement après irradiation.

Lorsque le traitement PTX/Tx a été utilisé, des effets parfois contradictoires ont été mesurés entre les deux types cellulaires. On observe néanmoins très peu ou pas du tout d'effet sur le niveau initial de signal mesuré. Par contre, une augmentation suivie d'une forte diminution de signal est mesurée respectivement 1 heure et 3 heures après irradiation dans les fibroblastes. Ces résultats semblent indiquer que le traitement n'agit pas sur la formation des CDB via son activité anti-oxydante, puisque le niveau initial devrait être largement plus faible dans les deux types cellulaires mais pourrait interférer comme la littérature le suggère avec les processus de réparation qui interviennent dans les premières heures après irradiation. Entre le $7^{ème}$ et $21^{ème}$ jour, le traitement soit augmente soit ne modifie pas le signal H2AX.

Comme une des conséquences d'une mauvaise réparation des CDB est la formation d'aberrations chromosomiques, nous avons recherché la présence de micronoyaux dans les cellules irradiées et traitées. Nous avons constaté dans les deux modèles cellulaires que le traitement accentuait de façon significative l'augmentation du nombre de micronoyaux mesurée 14 et 21 jours après exposition. Cet effet du traitement n'est pas dû à une toxicité propre de celui-ci puisqu'il ne conduit à aucun effet cytotoxique ou génotoxique dans les cellules non-irradiées.

Nous avons montré que, contrairement à un traitement par PTX, l'utilisation de Tx seul s'accompagnait d'une diminution des cassures de l'ADN mesurées par la méthode des comètes en milieu alcalin, mais d'une augmentation de la fréquence des micronoyaux (article 5). Or d'après la littérature, PTX est décrit comme un agent inducteur d'aberrations chromosomiques et inhibiteurs de la réparation des CDB de l'ADN (Theron *et al*., 2000; Bozsakyova *et al*., 2001; Sarkaria et Eshleman, 2001; Binder *et al*., 2002) et Tx serait plutôt radioprotecteur (Sweetman *et al*., 1997; Kumar *et al*., 2002). Les résultats que nous avons obtenus sont en partie contradictoires à ceux-ci puisque Tx serait responsable, au sein de l'association de la formation des micronoyaux.

Dans le but de comprendre le possible rôle du traitement sur l'induction des CDB, nous avons mesuré par la technique de « Western blot » l'expression de la protéine DNA-PK dans les lysats totaux de fibroblastes et de cellules endothéliales irradiés et/ou traités.

La phosphorylation de l'histone H2AX peut en effet s'effectuer par DNA-PK ou ATM (Wang *et al*., 2005). DNA-PKcs est la sous-unité catalytique du complexe DNA-PK qui comprend les protéines Ku 70 et 80 et qui est impliquée dans la voie du système de réparation fautif des CDB de l'ADN appelé « Non Homologous End Joinning » (NHEJ). Ce système est le mécanisme prépondérant de réparation des CDB chez les eucaryotes supérieurs et en phase

G1 du cycle cellulaire, phase dans laquelle se trouvent les fibroblastes et les cellules endothéliales arrêtés après irradiation. Des travaux précédents ont montré qu'une surexpression de DNA-PKcs était associée à une augmentation de l'activité du complexe DNA-PK (Ader *et al*., 2002) et qu'une chute de l'expression de DNA-PKcs était, au contraire, liée à une baisse de la réparation des CDB (Ortiz *et al*., 2004). De plus, l'inhibition de DNA-PKcs conduit à la radiosensibilisation des cellules (Daido *et al*., 2005).

Nous avons, dans notre étude, observé une expression plus faible de DNA-PKcs à 7 jours dans les fibroblastes irradiés alors qu'une augmentation était mesurée dans les cellules endothéliales. Ces résultats sont à rapprocher du niveau de phosphorylation élevé de la protéine H2AX, dans les deux types cellulaires, observé à 7 jours. L'association PTX/Tx n'a pas modifié le niveau de DNA-PKcs mesuré 7 jours post-irradiation dans les fibroblastes irradiés. Ce résultat est en accord avec le signal H2AX qui est identique en présence ou non du traitement. Par contre, dans le cas des cellules endothéliales, si la diminution du niveau de DNA-PKcs induite par le traitement est bien corrélée avec la diminution de signal H2AX observé, le traitement par PTX/Tx augmente le niveau de CDB associé à une diminution du niveau de DNA-PKcs.

Nous avons conduit une étude préliminaire visant à mesurer l'expression des protéines ATM et PARP par la technique de Western blot. ATM est une protéine-clé dans la signalisation des lésions de l'ADN conduisant à l'arrêt en phase G1 du cycle cellulaire (Naka *et al*., 2004). Les résultats préliminaires que nous avons obtenus semblent indiquer une augmentation de l'expression d'ATM, principalement à 14 jours dans les cellules endothéliales. En présence du traitement, cette expression est diminuée ce qui est en accord avec la littérature puisqu'il a été démontré les propriétés d'inhibition d'ATM par PTX (Sarkaria *et al*., 1999; Sarkaria et Eshleman, 2001). Par ailleurs, il a été aussi montré que Tx diminuait l'augmentation de p53 induite par ATM après irradiation (Inanami *et al*., 1999). Concernant la protéine PARP, nos résultats préliminaires indiquent que le traitement PTX/Tx diminue son niveau à 7 et 14 jours dans les deux types cellulaires. A 21 jours, PTX/Tx diminue l'expression de PARP dans les fibroblastes alors qu'il l'augmente dans les cellules endothéliales. Ces variations du niveau de ces deux protéines sont à rapprocher de l'augmentation de signal γ-H2AX ou de l'expression de DNA-PKcs puisque PARP et ATM sont impliquées dans la reconnaissance des CDB et dans le recrutement des protéines de réparation.

De nombreux travaux ont décrit l'action de la pentoxifylline sur l'arrêt radio-induit du cycle en G2 (Russell *et al*., 1996; Eley *et al*., 2002; Strunz *et al*., 2002). Afin de déterminer si l'augmentation de la fréquence des micronoyaux pouvait être due à un défaut des points de

contrôle de la progression dans le cycle cellulaire, nous avons étudié l'influence du traitement sur la distribution des cellules dans chacune des phases du cycle. Cependant, aucune modification significative de la distribution des cellules dans les phases du cycle cellulaire n'a été mise en évidence et aucune inhibition de l'arrêt en phase G1 du cycle cellulaire n'a été observée. Les effets sur la survie clonogénique ont montré une radiosensibilisation des fibroblastes par le traitement pour des doses d'irradiation au moins égales à 6 Gy. Aucune radiosensibilisation n'a été observée dans le cas des cellules endothéliales, mais leur plus grande sensibilité aux radiations nous a limité à une gamme de doses inférieures à 4 Gy. Les courbes de survie présentées dans l'article 5 montrent que Tx radioprotège les fibroblastes alors que PTX les radiosensibilise. Un effet contraire aurait pu être attendu compte tenu de l'effet de Tx et PTX sur la formation des micronoyaux. Nos résultats indiquent donc que pour la dose d'irradiation de 3 Gy, le traitement semble diminuer le niveau des cassures simple-brins ainsi que le niveau des micronoyaux alors qu'à la dose plus élevée de 10 Gy, si le niveau des lésions mesuré par la méthode des comètes (CSB+CDB+SAL) est diminué, celui des CDB et des micronoyaux tendrait à être sinon augmenté au moins maintenu (à l'exception du temps 3 h dans les fibroblastes). Par conséquent, le traitement PTX/Tx pourrait être néfaste lorsque les dommages radio-induits de l'ADN sont produits en grande quantité.

De plus, l'association a les mêmes effets, même lorsqu'elle est administrée jusqu'à 24 heures après l'irradiation montrant que les processus de réparation sur lesquels le traitement pourrait agir interviennent encore longtemps après l'irradiation. Ce résultat suggère que des lésions non réparées même après 24 heures pourraient être impliquées. Les fibroblastes en particulier sont connus pour entrer dans un processus les conduisant à une sénescence prématurée (SIPS, stress-induced premature senescence) (Chainiaux *et al.*, 2002; Gorbunova *et al.*, 2002; Debacq-Chainiaux *et al.*, 2005; Duan *et al.*, 2005; Naka *et al.*, 2004).

La SIPS est associée à des changements morphologiques, à un arrêt irréversible en phase G1 du cycle cellulaire, à l'apparition de l'activité β-galactosidase, et à l'augmentation d'expression de $p21^{WAF1}$. Plus récemment, l'apparition de ce phénotype a aussi été montré comme lié à l'augmentation de l'expression de gadd45 et de l'activité de p53 et à la baisse de capacité de réparation (Duan *et al.*, 2005). Les travaux de Naka *et al.* et Toussaint *et al.* ont proposé une voie de signalisation prépondérante impliquée dans le phénomène de SIPS (Toussaint *et al.*, 2000; Naka *et al.*, 2004). Cette voie impliquerait les proteines $p38^{MAPK}$ et $p16^{INK4A}$.

Après irradiation, nous avons observé, l'induction d'un phénomène de sénescence prématurée dans les fibroblastes et les cellules endothéliales caractérisé par une augmentation du

pourcentage de cellules positives pour l'activité SA-β-gal et par une augmentation de l'expression de $p21^{WAF1}$ et de l'expression de $p16^{INK4A}$.

L'utilisation de l'association PTX/Tx a contribué à diminuer la proportion de cellules endothéliales positives pour l'activité SA-β-gal dès le $5^{ème}$ jour alors que cette diminution n'est observée que dès le $21^{ème}$ jour dans les fibroblastes. L'utilisation de l'association PTX/Tx, qui diminuait la SIPS, a baissé le niveau d'expression de $p16^{INK4A}$ montrant l'implication du traitement dans la modulation de la voie conduisant à la SIPS.

Par conséquent, le traitement PTX/Tx pourrait interférer avec les voies de signalisation conduisant à la SIPS et conduire à l'expression de dommages de l'ADN qui seraient restés silencieux si la cellule était entrée en sénescence prématurée.

CONCLUSIONS ET PERSPECTIVES

Ce travail a permis de mettre en évidence une cinétique des phénomènes oxydatifs, soit *in vivo* chez le rat hairless, soit *in vitro* dans les fibroblastes et les cellules endothéliales après irradiation. Les études *in vivo* ont souligné la persistance de cellules très fortement endommagées au sein du tissu cutané plusieurs mois après irradiation suggérant un phénomène de sénescence prématurée alors qu'une diminution de l'activité SOD dans le derme associée à des poussées inflammatoires importantes étaient observées dans le mois consécutif à l'irradiation. Les études *in vitro* ont permis de suivre la formation des lésions de l'ADN induites soit par l'irradiation elle-même, soit par les phénomènes oxydatifs « secondaires » qui se mettent en place dans les semaines suivantes. Elles ont permis de caractériser l'entrée en sénescence des deux types cellulaires. Enfin, les mécanismes d'action de l'association PTX/Tx ont été étudiés selon que ces deux substances étaient ajoutées avant ou après irradiation. L'effet génotoxique et radiosensibilisateur du traitement, utilisé dans le cas d'exposition à de fortes doses d'irradiation, semble en partie lié à une inhibition d'entrée en sénescence des cellules et à une interférence des deux drogues avec les mécanismes de réparation des cassures de l'ADN.

Nos travaux ont permis de répondre à plusieurs questions :

- **Le stress oxydatif initial lié à l'irradiation conduit-il à l'accumulation de lésions de l'ADN radioinduites dans les cellules à renouvellement lent (fibroblastes, cellules endothéliales) ?**

REPONSE : Nous avons observé la présence de fibroblastes très endommagés dans le tissu après irradiation (article 1). Par ailleurs, les études *in vitro* ont montré la présence de dommages de l'ADN longtemps après irradiation (article 3 et article 4). En particulier, la formation de CDB a été observée une semaine après irradiation (article 6) et pourrait être à l'origine de l'augmentation du niveau de micronoyaux observée entre le $7^{ème}$ et $21^{ème}$ jour post-irradiation. L'origine de cette production tardive de lésions de l'ADN pourraient être liée à des vagues de production tardives d'espèces radicalaires. Nous avons également montré l'entrée en sénescence des cellules après irradiation ce qui suggère que certaines des cellules porteuses de dommages à l'ADN ne sont pas éliminées par un processus de mort mitotique.

- **Existe-il des phénomènes oxydatifs tardifs et sont-ils impliqués dans l'apparition d'effets tardifs**

REPONSE : Nous avons mis en évidence, après irradiation, à la fois *in vivo* chez le rat mais aussi *in vitro* dans les fibroblastes et cellules endothéliales, la production d'espèces réactives de l'oxygène à l'origine de stress oxydatif.

- **Existe-t-il un phénomène de sénescence prématurée qui conduirait à une accumulation des lésions avant la mort cellulaire ?**

REPONSE : Un phénomène de sénescence prématurée (SIPS) a été observé aux temps tardifs après irradiation dans les fibroblastes et les cellules endothéliales. Cette SIPS a été montrée comme liée aux lésions de l'ADN et à leur réparation qui ont, d'ailleurs, été proposées comme marqueur de sénescence (Duan *et al*., 2005).

- **Quel est le rôle de l'association pentoxifylline et α-tocophérol ? Quels sont ses mécanismes d'action sur les voies étudiées ?**

REPONSE : L'association PTX et Trolox a montré des propriétés anti-oxydantes conduisant à des effets bénéfiques lorsque le niveau de lésions de l'ADN est modéré. Pour des niveaux de lésions plus élevés, une augmentation du niveau des micronoyaux et, dans certains cas, des CDB a été observée. Cet effet a été observé même lorsque les drogues ont été administrées après irradiation suggérant une interférence avec les mécanismes de réparation. En revanche, l'entrée des cellules en sénescence prématurée est diminuée par la présence de PTX/Tx impliquant un effet de l'association sur les voies de signalisation conduisant à la réparation ou à la SIPS décrites par Naka *et al*. (Naka *et al*., 2004) et par conséquent à l'expression de dommages de l'ADN.

Ces résultats suggèrent un rôle primordial du stress oxydatif dans l'apparition des lésions de l'ADN. L'utilisation du traitement PTX/Tx dans le cas des victimes d'accidents radiologiques a montré son intérêt en clinique dans la restauration de l'intégrité des tissus lésés. Toutefois, nos études *in vitro* suggèrent une toxicité associée au traitement lorsque le niveau de dommages à l'ADN, résultant lui même d'un fort stress oxydatif tel que celui produit par une irradiation à fortes doses, est élevé. Le recours à l'association PTX/Tx nécessite donc la prise en considération du caractère potentiellement toxique de cette association.

Nos résultats sont en accord avec plusieurs études soulignant l'interférence des deux substances avec les mécanismes de réparation de l'ADN. Nous avons également montré son effet sur l'entrée des cellules en sénescence prématurée. Défaut de réparation et/ou non entrée des cellules en SIPS pourraient expliquer le caractère potentiellement génotoxique de cette association.

Il apparaît ainsi primordial d'étudier plus amplement les voies de signalisation conduisant à la réparation de l'ADN, comme déjà entrepris par Western blotting d'ATM et de PARP. Ceci pourrait nous permettre de mieux comprendre l'effet des drogues à long terme, notamment par l'observation de la qualité de la réparation par FISH (Fluorescence *In-Situ* Hybridization).

D'autre part, il semble particulièrement intéressant de comprendre comment l'irradiation et le traitement peuvent moduler les deux voies conduisant à la sénescence prématurée (Naka *et al.*, 2004; Toussaint *et al.*, 2000). L'étude du niveau d'expression de $p38^{MAPK}$ et de $p16^{INK4A}$ donnera une indication des voies préférentiellement empruntées après irradiation et en présence du traitement.

Enfin, l'effet de chacune des drogues utilisées séparément est à vérifier sur les voies de réparation et de sénescence.

Outre une poursuite de l'étude des voies de signalisation conduisant à la réparation et à la sénescence prématurée et au rôle de PTX/Tx sur ces paramètres, il serait particulièrement intéressant d'étudier chez l'animal l'effet du traitement, à des temps relativement précoces (< 1 mois) mais aussi plus tardifs, permettant l'expression des lésions tardives telles que la nécrose ou la fibrose. En particulier, son effet sur le niveau d'activité de la SOD ou du niveau de marqueurs de l'inflammation tels que le TNFα retient toute notre attention. Il serait également très intéressant d'étudier l'expression de marqueurs de la sénescence.

REFERENCES BIBLIOGRAPHIQUES

Adamson, I. Y., and D. H. Bowden, 1983, Endothelial injury and repair in radiation-induced pulmonary fibrosis: Am J Pathol, v. 112, p. 224-30.

Ader, I., C. Muller, J. Bonnet, G. Favre, E. Cohen-Jonathan, B. Salles, and C. Toulas, 2002, The radioprotective effect of the 24 kDa FGF-2 isoform in HeLa cells is related to an increased expression and activity of the DNA dependent protein kinase (DNA-PK) catalytic subunit.: Oncogene, v. 21, p. 6471-9.

Aebi, H., 1984, Catalase in vitro: Methods Enzymol, v. 105, p. 121-6.

Agarwal, M. L., A. Agarwal, W. R. Taylor, and G. R. Stark, 1995, p53 controls both the G2/M and the G1 cell cycle checkpoints and mediates reversible growth arrest in human fibroblasts: Proc Natl Acad Sci U S A, v. 92, p. 8493-7.

Ahnström, G., and K. Erixon, 1981, Measurement of strand breaks by alkaline denaturation and hydroxyapatite chromatography, *in* E. C. F. P. C. H. Eds, ed., DNA repair: A Laboratory Manuel Research Procedures: New York, Marcel Dekker, p. 403-418.

Akashi, M., M. Hachiya, R. L. Paquette, Y. Osawa, S. Shimizu, and G. Suzuki, 1995, Irradiation increases manganese superoxide dismutase mRNA levels in human fibroblasts. Possible mechanisms for its accumulation: J Biol Chem, v. 270, p. 15864-9.

Allen, R., 1991, Oxygen reactive species and anti-oxidant responses during development: the metabolic paradox of cellular differentiation: Proc Soc Exp Biol Med, v. 196, p. 117-29.

Amundson, S. A., T. G. Myers, and A. J. Fornace, Jr., 1998, Roles for p53 in growth arrest and apoptosis: putting on the brakes after genotoxic stress: Oncogene, v. 17, p. 3287-99.

Annane, D., J. Depondt, P. Aubert, M. Villart, P. Géhanno, P. Gajdos, and S. Chevret, 2004, Hyperbaric oxygen therapy for radionecrosis of the jaw: a randomized, placebo-controlled, double-bind trial from the ORN96 study group: J Clin Oncol, v. 22, p. 4893-900.

Archambeau, J. O., 1987, Relative radiation sensitivity of the integumentary system: dose response of the epidermal, microvascular, and dermal populations: Adv. Radiat. Biol., v. 12, p. 147-203.

Archambeau, J. O., A. Ines, and L. F. Fajardo, 1984, Response of swine skin microvasculature to acute single exposures of X rays: quantification of endothelial changes: Radiat Res, v. 98, p. 37-51.

Archambeau, J. O., A. Ines, and L. F. Fajardo, 1985, Correlation of the dermal microvasculature morphology with the epidermal and the endothelial population changes produced by single X ray fractions of 1649, 2231 and 2619 rad in swine: Int J Radiat Oncol Biol Phys, v. 11, p. 1639-46.

Archambeau, J. O., R. Pezner, and T. Wasserman, 1995, Pathophysiology of irradiated skin and breast: Int J Radiat Oncol Biol Phys, v. 31, p. 1171-85.

Archambeau, J. O., R. Pezner, and T. Wasserman, 1995, Pathophysiology of irradiated skin and breast: Int J Radiat Oncol Biol Phys, v. 31, p. 1171-85.

Azzam, E. I., S. M. de Toledo, M. J. Pykett, H. Nagasawa, and J. B. Little, 1997, CDC2 is down-regulated by ionizing radiation in a p53-dependent manner: Cell Growth Differ, v. 8, p. 1161-9.

Baillet, F., M. Housset, A. M. Michelson, and K. Puget, 1986, Treatment of radiofibrosis with liposomal superoxide dismutase. Preliminary results of 50 cases: Free Radic Res Commun, v. 1, p. 387-94.

Banin, S., L. Moyal, S. Shieh, Y. Taya, C. W. Anderson, L. Chessa, N. I. Smorodinsky, C. Prives, Y. Reiss, Y. Shiloh, and Y. Ziv, 1998, Enhanced phosphorylation of p53 by ATM in response to DNA damage: Science, v. 281, p. 1674-7.

Barton, S. P., D. R. Black, S. A. Gaskell, R. Marks, J. R. Sathyanarayana, and I. Paterson, 1985, Detection of the effects of low dose ionising irradiation on epidermal function: Br J Radiol, v. 58, p. 73-6.

Beesk, F., M. Dizdaroglu, D. Schutle-Frohlinde, and C. Von Sonntag, 1979, Radiation-induced strand breaks in deoxygenated aqueous solution. The formation of altered sugars as end groups.: Int J Radiat Biol, v. 36, p. 565-576.

Bensasson, R. V., E. J. Land, and T. G. Truscott, 1993, Light and ionizing radiation: generation of excited states and radicals, Excited States and Free Radicals in Biology and Medicine: New York, Oxford University Press, p. 249-289.

Binder, A., T. Theron, H. Donninger, M. Parker, and L. Bohm, 2002, Radiosensitization and DNA repair inhibition by pentoxifylline in NIH3T3 p53 transfectants: Int J Radiat Biol, v. 78, p. 991-1000.

Black, A. R., and J. Azizkhan-Clifford, 1999, Regulation of E2F: a family of transcription factors involved in proliferation control: Gene, v. 237, p. 281-302.

Bonnefont-Rousselot, D., 1994, Irradiation des membranes cellulaires: J Chim Phys, v. 91, p. 968-983.

Border, W. A., and N. A. Noble, 1994, Transforming growth factor beta in tissue fibrosis: N Engl J Med, v. 331, p. 1286-92.

Bozsakyova, E., I. Chalupa, L. Sebova, and D. Slamenova, 2001, Chromosomal aberrations, sister chromatid exchanges and micronuclei induced by pentoxifylline in in vitro cultivated Chinese hamster cells (V79) and human blood lymphocytes: Mutat Res, v. 497, p. 63-70.

Briggaman, R. A., 1982, Biochemical composition of the epidermal-dermal junction and other basement membrane: J Invest Dermatol, v. 78, p. 1-6.

Burger, A., H. Loffler, M. Bamberg, and H. Rodemann, 1998, Molecular and cellular basis of radiation fibrosis: Int J Radiat Biol, v. 73, p. 401-8.

Burkitt, M. J., 2001, A critical overview of the chemistry of copper-dependent low density lipoprotein oxidation: roles of lipid hydroperoxides, alpha-tocopherol, thiols, and ceruloplasmin: Arch Biochem Biophys, v. 394, p. 117-35.

Burton, G. W., D. O. Foster, B. Perly, T. F. Slater, I. C. Smith, and K. U. Ingold, 1985, Biological antioxidants: Philos Trans R Soc Lond B Biol Sci, v. 311, p. 565-78.

Cadet, J., M. Bardet, M. Berger, T. Berthod, T. Delatour, C. D'Ham, T. Douki, D. Gasparutto, A. Grand, A. Guy, F. Jolibois, D. Molko, M. Polverelli, J.-L. Ravanat, A. Romieu, N. Signorini, and S. Sauvaigo, 1997, Oxidative base damage to DNA: recent mechanistic aspects, measurement and repair., *in* M. Dizdaroglu, and A. E. Karakaya, eds., Advances in DNA Damage and Repair: Oxygen Radical effects, Cellular Protection and Biological Consequences, v. 302, NATO ASI Series, p. 47-58.

Cadet, J., S. Bellon, T. Douki, S. Frelon, D. Gasparutto, E. Muller, J.-P. Pouget, J.-L. Ravanat, A. Romieu, and S. Sauvaigo, 2004, Radiation-induced DNA damage: formation, measurement, and biochemical features: J Environ Pathol Toxicol Oncol, v. 23, p. 33-43.

Cadet, J., M. Berger, T. Douki, and J.-L. Ravanat, 1997, Oxidative damage to DNA: formation, measurement and biological significance: Rev Physiol Biochem Pharmacol, v. 31, p. 1-87.

Cadet, J., T. Delatour, T. Douki, D. Gasparutto, J. P. Pouget, J. L. Ravanat, and S. Sauvaigo, 1999, Hydroxyl radicals and DNA base damage: Mutat Res, v. 424, p. 9-21.

Cadet, J., T. Douki, D. Gasparutto, and J.-L. Ravanat, 2003, Oxidative damage to DNA: formation, measurement and biochemival features: Mutat Res, v. 531, p. 5-23.

Cadet, J., and R. Treoule, 1978, Comparative study of oxidation of nucleic acid components by hydroxyl radicals, singlet oxygen and superoxide anion radicals: Photochem Photobiol, v. 28, p. 661-7.

Canman, C. E., and D. S. Lim, 1998, The role of ATM in DNA damage responses and cancer: Oncogene, v. 17, p. 3301-8.

Canman, C. E., D. S. Lim, K. A. Cimprich, Y. Taya, K. Tamai, K. Sakaguchi, E. Appella, M. B. Kastan, and J. D. Siliciano, 1998, Activation of the ATM kinase by ionizing radiation and phosphorylation of p53: Science, v. 281, p. 1677-9.

Cao, G., H. M. Alessio, and R. G. Cutler, 1993, Oxygen-radical absorbance capacity assay for antioxidants: Free Radic Biol Med, v. 14, p. 303-11.

Casarett, G. W., 1964, Similarities and contrasts between radiation and time pathology, *in* B. Strehler, ed., Advances in Gerontological Research: New York, Academic Press, p. 109-163.

Castagne, V., M. Gautschi, K. Lefevre, A. Posada, and P. G. Clarke, 1999, Relationships between neuronal death and the cellular redox status. Focus on the developing nervous system: Prog Neurobiol, v. 59, p. 397-423.

Chainiaux, F., J. P. Magalhaes, F. Eliaers, J. Remacle, and O. Toussaint, 2002, UVB-induced premature senescence of human diploid skin fibroblasts: Int J Biochem Cell Biol, v. 34, p. 1331-9.

Chan, T. A., H. Hermeking, C. Lengauer, K. W. Kinzler, and B. Vogelstein, 1999, 14-3-3Sigma is required to prevent mitotic catastrophe after DNA damage: Nature, v. 401, p. 616-20.

Chaudhary, A. K., G. R. Reddy, I. A. Blair, and L. J. Marnett, 1996, Characterization of an N6-oxopropenyl-2'-deoxyadenosine adduct in malondialdehyde-modified DNA using liquid chromatography/electrospray ionization tandem mass spectrometry: Carcinogenesis, v. 17, p. 1167-70.

Chaudiere, J., and R. Ferrari-Iliou, 1999, Intracellular antioxidants: from chemical to biochemical mechanisms: Food Chem Toxicol, v. 37, p. 949-62.

Chen, H. J., and F. L. Chung, 1996, Epoxidation of trans-4-hydroxy-2-nonenal by fatty acid hydroperoxides and hydrogen peroxide: Chem Res Toxicol, v. 9, p. 306-12.

Chiao, T. B., and A. J. Lee, 2005, Role of pentoxifylline and vitamin E in attenuation of radiation-induced fibrosis: Ann Pharmacother, v. 39, p. 516-22.

Critchlow, S. E., R. P. Bowater, and S. P. Jackson, 1997, Mammalian DNA double-strand break repair protein XRCC4 interacts with DNA ligase IV: Curr Biol, v. 7, p. 588-98.

Daburon, F., 1997, Irradiations aiguës localisées.

Daburon, F., J. L. Lefaix, J. Remy, D. Bolnot, and J. Guilbaud, 1986, Development of lesions resulting from acute localised irradiation in the pig: trials for medical and surgical management: Br J Radiol Suppl, v. 19, p. 128-31.

Daido, S., A. Yamamoto, K. Fujiwara, R. Sawaya, S. Kondo, and Y. Kondo, 2005, Inhibition of the DNA-dependent protein kinase catalytic subunit radiosensitizes malignant glioma cells by inducing autophagy: Cancer Res, v. 65, p. 4368-75.

Darley-Usmar, V., and B. Halliwell, 1996, Blood radicals: reactive nitrogen species, reactive oxygen species, transition metal ions, and the vascular system: Pharm Res, v. 13, p. 649-62.

Davies, K. J. A., B. C. Gilbert, and R. M. Haywood, 1991, Radical-induced damage to proteins: ESR spin-trapping studies: Free Radical Research Communications, v. 15, p. 111-127.

Debacq-Chainiaux, F., C. Borlon, T. Pascal, V. Royer, F. Eliaers, N. Ninane, G. Carrard, B. Friguet, F. de Longueville, S. Boffe, J. Remacle, and O. Toussaint, 2005, Repeated exposure of human skin fibroblasts to UVB at subcytotoxic level triggers premature senescence through the TGF-beta1 signaling pathway.: J Cell Sci, v. 118, p. 743-58.

Deby, C., 1991, La biochimie de l'oxygène: La Recherche, v. 22, p. 56-64.

Decarroz, C., J. R. Wagner, J. E. van Lier, C. M. Krishna, P. Riesz, and J. Cadet, 1986, Sensitized photo-oxidation of thymidine by 2-methyl-1,4-naphthoquinone. Characterization of the stable photoproducts: Int J Radiat Biol Relat Stud Phys Chem Med, v. 50, p. 491-505.

Delanian, S., F. Baillet, J. Huart, J. L. Lefaix, C. Maulard, and M. Housset, 1994, Successful treatment of radiation-induced fibrosis using liposomal Cu/Zn superoxide dismutase: clinical trial: Radiother Oncol, v. 32, p. 12-20.

Delanian, S., S. Balla-Mekias, and J. L. Lefaix, 1999, Striking regression of chronic radiotherapy damage in a clinical trial of combined pentoxifylline and tocopherol: J Clin Oncol, v. 17, p. 3283-90.

Delanian, S., A. Bravard, M. Martin, C. Luccioni, and J.-L. Lefaix, 2001, In vitro modulation by liposomal superoxide dismutase of the fibroblast phenotype in human skin with chronic radiotherapy damage: Radiother Oncol, v. 58, p. 325-31.

Delanian, S., J. Depondt, and J. L. Lefaix, 2005, Major healing of refractory mandible osteoradionecrosis after treatment combining pentoxifylline and tocopherol: a phase II trial: Head Neck, v. 27, p. 114-23.

Delanian, S., and J.-L. Lefaix, 2004, The radiation-induced fibroatrophic process: therapeutic perspective via the antioxidant pathway: Radiother Oncol, v. 73, p. 119-131.

Delanian, S., and J. L. Lefaix, 2002, Complete healing of severe osteoradionecrosis with treatment combining pentoxifylline, tocopherol and clodronate: Br J Radiol, v. 75, p. 467-9.

Delanian, S., J. L. Lefaix, and M. Housset, 1993, [Iatrogenic fibrosis in cancerology (2): main etiologies and therapeutic possibilities]: Bull Cancer, v. 80, p. 202-12.

Delanian, S., M. Martin, A. Bravard, C. Luccioni, and J.-L. Lefaix, 1998, Abnormal phenotype of human cultures fibroblasts from cutaneous fibrosis induced by therapeutic irradiation: Radiother Oncol, v. 3, p. 255-61.

Delanian, S., R. Porcher, S. Balla-Mekias, and J. L. Lefaix, 2003, Randomized, placebo-controlled trial of combined pentoxifylline and tocopherol for regression of superficial radiation-induced fibrosis: J Clin Oncol, v. 21, p. 2545-50.

Denham, J. W., and M. Hauer-Jensen, 2002, The radiotherapeutic injury--a complex 'wound': Radiother Oncol, v. 63, p. 129-45.

Devik, F., 1955, Study of the local roentgen reaction on the skin of mice, with specific reference to the vascular effects: Acta Radiol Suppl, v. 119.

Dion, M. W., D. H. Hussey, J. F. Doornbos, A. P. Vigliotti, B. C. Wen, and B. Anderson, 1990, Preliminary results of a pilot study of pentoxifylline in the treatment of late radiation soft tissue necrosis: Int J Radiat Oncol Biol Phys, v. 19, p. 401-7.

Dion, M. W., D. H. Hussey, and J. W. Osborne, 1989, The effect of pentoxifylline on early and late radiation injury following fractionated irradiation in C3H mice: Int J Radiat Oncol Biol Phys, v. 17, p. 101-7.

Diplock, A. T., 1993, Indexes of selenium status in human populations: Am J Clin Nutr, v. 57, p. 256S-258S.

Dizdaroglu, M., 1992, Oxidative damage to DNA in mammalian chromatin: Mutat Res, v. 275, p. 331-42.

Dizdaroglu, M., and E. Gajewski, 1989, Structure and mechanism of hydroxyl radical-induced formation of a DNA-protein cross-link involving thymine and lysinein nucleohistone: Cancer Res, v. 49, p. 3463-3467.

Dorr, W., and J. H. Hendry, 2001, Consequential late effects in normal tissues: Radiother Oncol, v. 61, p. 223-31.
Duan, J., J. Duan, Z. Zhang, and T. Tong, 2005, Irreversible cellular senescence induced by prolonged exposure to H(2)O(2) involves DNA-damage-and-repair genes and telomere shortening.: Int J Biochem Cell Biol, v. 37, p. 1407-1420.
Dubray, B., S. Delanian, and J. L. Lefaix, 1997, [Late effects of mammary radiotherapy on skin and subcutaneous tissues]: Cancer Radiother, v. 1, p. 744-52.
Dutreix, J., 1986, Human skin: early and late reactions in relation to dose and its time distribution: Br J Radiol Suppl, v. 19, p. 22-8.
Ehrly, A. M., 1979, The effect of pentoxifylline on the deformability of erythrocytes and on the muscular oxygen pressure in patients with chronic arterial disease: J Med, v. 10, p. 331-8.
Ehrly, A. M., and W. Schroeder, 1977, Oxygen pressure values in the ischemic muscle tissue of patients with chronic occlusive arterial disease: Adv Exp Med Biol, v. 94, p. 401-5.
el-Deiry, W. S., J. W. Harper, P. M. O'Connor, V. E. Velculescu, C. E. Canman, J. Jackman, J. A. Pietenpol, M. Burrell, D. E. Hill, Y. Wang, and et al., 1994, WAF1/CIP1 is induced in p53-mediated G1 arrest and apoptosis: Cancer Res, v. 54, p. 1169-74.
Eley, K. W., S. H. Benedict, T. D. Chung, B. D. Kavanagh, W. C. Broaddus, R. K. Schmidt-Ullrich, and P. S. Lin, 2002, The effects of pentoxifylline on the survival of human glioma cells with continuous and intermittent stereotactic radiosurgery irradiation: Int J Radiat Oncol Biol Phys, v. 54, p. 542-50.
Emerit, J., A. M. Michelson, H. G. Robert, G. Chomette, R. A. Guerin, J. Blondon, and M. Bertrand, 1983, [Superoxide dismutase treatment of 2 cases of radiation-induced sclerosis]: Sem Hop, v. 59, p. 277-81.
Epperly, M., J. Bray, S. Kraeger, R. Zwacka, J. Engelhardt, E. Travis, and J. Greenberger, 1998, Prevention of late effects of irradiation lung damage by manganese superoxide dismutase gene therapy: Gene Ther, v. 5, p. 196-208.
Epstein, W. L., and H. I. Maibach, 1965, Cell renewal in human epidermis: Arch Dermatol, v. 92, p. 462-8.
Evans, P., and B. Halliwell, 1999, Free radicals and hearing. Cause, consequence, and criteria: Ann NY Acad Sci, v. 884, p. 19-40.
Favaudon, V., 2000, [Regulation of cell cycle and radiation-induced cell death]: Cancer Radiother, v. 4, p. 355-68.
Flohe, L., and F. Otting, 1984, Superoxide dismutase assays: Methods Enzymol, v. 105, p. 93-104.
Frankenberg-Schwager, M., and D. Frankenberg, 1990, DNA double-strand breaks: their repair and relationship to cell killing in yeast: Int J Radiat Biol, v. 58, p. 569-575.
Freitas, J. P., P. Filipe, and F. Guerra Rodrigo, 1995, [Potential antioxidative effects of pentoxifylline]: C R Seances Soc Biol Fil, v. 189, p. 401-5.
Fridovich, I., 1975, Superoxide dismutases: Annu Rev Biochem, v. 44, p. 147-59.
Fubini, B., and A. Hubbard, 2003, Reactive oxygen species and reactive nitrogen species generation by silica in inflammation and fibrosis: Free Radic Biol Med, v. 34, p. 1507-16.
Fuller, G. C., 1981, Perspectives for the use of collagen synthesis inhibitors as antifibrotic agents: J Med Chem, v. 24, p. 651-8.
Gabbiani, G., G. B. Ryan, and G. Majne, 1971, Presence of modified fibroblasts in granulation tissue and their possible role in wound contraction: Experientia, v. 27, p. 549-50.
Gailit, J., M. Pierschbacher, and R. A. Clark, 1993, Expression of functional alpha 4 beta 1 integrin by human dermal fibroblasts: J Invest Dermatol, v. 100, p. 323-8.

Gajewski, G. E., A. F. Fuciarelli, and M. Dizdaroglu, 1988, Structure of hydroxyl radical-induced DNA-protein cross-links in calf thymus nucleohistone *in vitro*: Int J Radiat Biol, v. 54, p. 445-459.

Gallo, R., C. Kim, R. Kokenyesi, N. S. Adzick, and M. Bernfield, 1996, Syndecans-1 and -4 are induced during wound repair of neonatal but not fetal skin: J Invest Dermatol, v. 107, p. 676-683.

Golstein, P., D. M. Ojcius, and J. D. Young, 1991, Cell death mechanisms and the immune system: Immunol Rev, v. 121, p. 29-65.

Gongora, R., and H. Magdelenat, 1986, Accidental acute local irradiations in France and their pathology: Br J Radiol Suppl, v. 19, p. 12-5.

Goodhead, D. T., 1989, The initial physical damage produced by ionizing radiations: Int J Radiat Biol, v. 56, p. 623-34.

Goodhead, D. T., 1994, Initial events in the cellular effects of ionizing radiations: clustered damage in DNA: Int J Radiat Biol, v. 65, p. 7-17.

Gorbunova, V., A. Seluanov, and O. M. Pereira-Smith, 2002, Expression of human telomerase (hTERT) does not prevent stress-induced senescence in normal human fibroblasts but protects the cells from stress-induced apoptosis and necrosis: J Biol Chem, v. 277, p. 38540-9.

Grawunder, U., D. Zimmer, S. Fugmann, K. Schwarz, and M. R. Lieber, 1998, DNA ligase IV is essential for V(D)J recombination and DNA double-strand break repair in human precursor lymphocytes: Mol Cell, v. 2, p. 477-84.

Grosshans, E., 1997, Histologie de la peau normale, *in* Fasc, ed., Encycl. Med. Chir., Dermatologie: Paris, p. 12220 A-12210.

Guo, H., J. A. Seixas-Silva, Jr., M. W. Epperly, J. E. Gretton, D. M. Shin, D. Bar-Sagi, H. Archer, and J. S. Greenberger, 2003, Prevention of radiation-induced oral cavity mucositis by plasmid/liposome delivery of the human manganese superoxide dismutase (SOD2) transgene: Radiat Res, v. 159, p. 361-70.

Gutteridge, J. M., and B. Halliwell, 1990, The measurement and mechanism of lipid peroxidation in biological systems: Trends Biochem Sci, v. 15, p. 129-35.

Haber, J. E., 1999, DNA recombination: the replication connection: Trends Biochem Sci, v. 24, p. 271-5.

Halliwell, B., and J. M. Gutteridge, 1995, The definition and measurement of antioxidants in biological systems: Free Radic Biol Med, v. 18, p. 125-6.

Harris, S. L., and A. J. Levine, 2005, The p53 pathway: positive and negative feedback loops: Oncogene, v. 24, p. 2899-908.

Harrison, L., Z. Hatahet, and S. S. Wallace, 1999, In vitro repair of synthetic ionizing radiation-induced multiply damaged DNA sites: J Mol Biol, v. 290, p. 667-84.

Helbock, H. J., K. B. Beckman, M. K. Shigenaga, P. B. Walter, A. A. Woodall, H. C. Yeo, and B. N. Ames, 1998, DNA oxidation matters: the HPLC-electrochemical detection assay of 8-oxo-deoxyguanosine and 8-oxo-guanine: Proc Natl Acad Sci U S A, v. 95, p. 288-93.

Hendry, J. H., 1994, Biological Response Modifiers and Normal Tissue Injury After Irradiation: Semin Radiat Oncol, v. 4, p. 123-132.

Hill, R. P., H. P. Rodemann, J. H. Hendry, S. A. Roberts, and M. S. Anscher, 2001, Normal tissue radiobiology: from the laboratory to the clinic: Int J Radiat Oncol Biol Phys, v. 49, p. 353-65.

Holley, W. R., and A. Chatterjee, 1996, Clusters of DNA induced by ionizing radiation: formation of short DNA fragments. I. Theoretical modeling: Radiat Res, v. 145, p. 188-99.

Hopewell, J. W., 1974, Letter: The late vascular effects of radiation: Br J Radiol, v. 47, p. 157-8.

Hopewell, J. W., 1980, The importance of vascular damage in the development of late radiation effects in normal tissues, *in* R. E. M. a. H. R. Withers, ed., Radiation Biology in Cancer Research: New York, Raven Press, p. 449-459.

Horvath, B., Z. Marton, R. Halmosi, T. Alexy, L. Szapary, J. Vekasi, Z. Biro, T. Habon, G. Kesmarky, and K. Toth, 2002, In vitro antioxidant properties of pentoxifylline, piracetam, and vinpocetine: Clin Neuropharmacol, v. 25, p. 37-42.

Huttner, I., and G. Gabbiani, 1982, Vascular endothelium: recent advances and unanswered questions: Lab Invest, v. 47, p. 409-11.

Iliakis, G., 1991, The role of DNA double strand breaks in ionizing radiation-induced killing of eukaryotic cells: BioEssays, v. 13, p. 641-648.

Inanami, O., K. Takahashi, and M. Kuwabara, 1999, Attenuation of caspase-3-dependent apoptosis by Trolox post-treatment of X-irradiated MOLT-4 cells: Int J Radiat Biol, v. 75, p. 155-63.

Innocente, S. A., J. L. Abrahamson, J. P. Cogswell, and J. M. Lee, 1999, p53 regulates a G2 checkpoint through cyclin B1: Proc Natl Acad Sci U S A, v. 96, p. 2147-52.

Jayaraman, J., and C. Prives, 1995, Activation of p53 sequence-specific DNA binding by short single strands of DNA requires the p53 C-terminus: Cell, v. 81, p. 1021-9.

Johansson, S., 1996, Non-collagenous matrix proteins, *in* W. Comper, ed., Extracellular matrix, molecular components and interactions: Amsterdam, Harwood, p. 68-94.

Joksic, G., S. B. Pajovic, M. Stankovic, S. Pejic, J. Kasapovic, G. Cuttone, N. Calonghi, L. Masotti, and D. T. Kanazir, 2000, Chromosome aberrations, micronuclei, and activity of superoxide dismutases in human lymphocytes after irradiation in vitro: Cell Mol Life Sci, v. 57, p. 842-50.

Kabotyanski, E. B., L. Gomelsky, J. O. Han, T. D. Stamato, and D. B. Roth, 1998, Double-strand break repair in Ku86- and XRCC4-deficient cells: Nucleic Acids Res, v. 26, p. 5333-42.

Kanatinakis, J., 1995, Structure histologique de la peau humaine, *in* I. D. Schmitt Paris, ed., Biologie de la peau humaine, p. 1-25.

Kastan, M. B., O. Onyekwere, D. Sidransky, B. Vogelstein, and R. W. Craig, 1991, Participation of p53 protein in the cellular response to DNA damage: Cancer Res, v. 51, p. 6304-11.

Kastan, M. B., Q. Zhan, W. S. el-Deiry, F. Carrier, T. Jacks, W. V. Walsh, B. S. Plunkett, B. Vogelstein, and A. J. Fornace, Jr., 1992, A mammalian cell cycle checkpoint pathway utilizing p53 and GADD45 is defective in ataxia-telangiectasia: Cell, v. 71, p. 587-97.

Kehrer, J. P., 1993, Free radicals as mediators of tissue injury and disease: Crit Rev Toxicol, v. 23, p. 21-48.

Kinnula, V. L., and D. Crapo, 2003, Superoxide dismutases in the lung and human lung diseases: Am J Respir Crit Care Med, v. 167, p. 1600-19.

Kobayashi, T., S. Ruan, J. R. Jabbur, U. Consoli, K. Clodi, H. Shiku, L. B. Owen-Schaub, M. Andreeff, J. C. Reed, and W. Zhang, 1998, Differential p53 phosphorylation and activation of apoptosis-promoting genes Bax and Fas/APO-1 by irradiation and ara-C treatment: Cell Death Differ, v. 5, p. 584-91.

Koh, W. J., K. J. Stelzer, L. M. Peterson, B. L. Staker, W. F. Ward, K. J. Russell, and T. W. Griffin, 1995, Effect of pentoxifylline on radiation-induced lung and skin toxicity in rats: Int J Radiat Oncol Biol Phys, v. 31, p. 71-7.

Kubbutat, M. H., S. N. Jones, and K. H. Vousden, 1997, Regulation of p53 stability by Mdm2: Nature, v. 387, p. 299-303.

Kuerbitz, S. J., B. S. Plunkett, W. V. Walsh, and M. B. Kastan, 1992, Wild-type p53 is a cell cycle checkpoint determinant following irradiation: Proc Natl Acad Sci U S A, v. 89, p. 7491-5.

Kumar, B., M. N. Jha, W. C. Cole, J. S. Bedford, and K. N. Prasad, 2002, D-alpha-tocopheryl succinate (vitamin E) enhances radiation-induced chromosomal damage levels in human cancer cells, but reduces it in normal cells: J Am Coll Nutr, v. 21, p. 339-43.

Kumar, S. S., R. C. Chaubey, T. P. Devasagayam, K. I. Priyadarsini, and P. S. Chauhan, 1999, Inhibition of radiation-induced DNA damage in plasmid pBR322 by chlorophyllin and possible mechanism(s) of action: Mutat Res, v. 425, p. 71-9.

Kurz, E. U., and S. P. Lees-Miller, 2004, DNA damage-induced activation of ATM and ATM-dependent signaling pathways: DNA Repair (Amst), v. 3, p. 889-900.

Laemmli, U. K., 1970, Cleavage of structural proteins during the assembly of the head of bacteriophage T4: Nature, v. 227, p. 680-5.

Laurent, C., J. P. Pouget, and P. Voisin, 2005, Modulation of DNA damage by pentoxifylline and a-tocopherol in skin fibroblasts exposed to gamma-rays: Radiat Res, v. 164, p. 63-72.

Laurent, C., P. Voisin, and J.-P. Pouget, 2005, DNA damage in cultured skin microvascular endothelial cells exposed to gamma-rays treated by the combination of pentoxifylline and alpha-tocopherol, v. Submitted.

Law, M. P., 1981, Radiation-induced vascular injury and its relation to late effects in normal tissue: Adv Radiat Biol, v. 9, p. 37.

LeBel, C. P., H. Ischiropoulos, and S. C. Bondy, 1992, Evaluation of the probe 2',7'-dichlorofluorescin as an indicator of reactive oxygen species formation and oxidative stress: Chem Res Toxicol, v. 5, p. 227-31.

Lefaix, J. L., and F. Daburon, 1998, Diagnosis of acute localized irradiation lesions: review of the French experimental experience: Health Phys, v. 75, p. 375-84.

Lefaix, J. L., F. Daburon, and Y. Tricaud, 1992, Evolution radiopathologique spontanée et après traitement médical dans deux modèles d'accident d'irradiation localisée: Bull Cancer Radiother, v. 79, p. 189-198.

Lefaix, J. L., S. Delanian, and B. Dubray, 1997, [Physiopathology of human superficial radiation-induced fibrosis]: C R Seances Soc Biol Fil, v. 191, p. 777-95.

Lefaix, J. L., S. Delanian, J. J. Leplat, Y. Tricaud, M. Martin, A. Nimrod, F. Baillet, and F. Daburon, 1996, Successful treatment of radiation-induced fibrosis using Cu/Zn-SOD and Mn-SOD: an experimental study: Int J Radiat Oncol Biol Phys, v. 35, p. 305-12.

Lefaix, J. L., S. Delanian, M. C. Vozenin, J. J. Leplat, Y. Tricaud, and M. Martin, 1999, Striking regression of subcutaneous fibrosis induced by high doses of gamma rays using a combination of pentoxifylline and alpha-tocopherol: an experimental study: Int J Radiat Oncol Biol Phys, v. 43, p. 839-47.

Letur-Konirsch, H., F. Guis, and S. Delanian, 2002, Uterine restoration by radiation sequelae regression with combined pentoxifylline-tocopherol: a phase II study: Fertil Steril, v. 77, p. 1219-26.

Li, R., S. Waga, G. J. Hannon, D. Beach, and B. Stillman, 1994, Differential effects by the p21 CDK inhibitor on PCNA-dependent DNA replication and repair: Nature, v. 371, p. 534-7.

Li, Y. X., K. Weber-Johnson, L. Q. Sun, N. Paschoud, R. O. Mirimanoff, and P. A. Coucke, 1998, Effect of pentoxifylline on radiation-induced G2-phase delay and radiosensitivity of human colon and cervical cancer cells: Radiat Res, v. 149, p. 338-42.

Liang, F., and M. Jasin, 1996, Ku80-deficient cells exhibit excess degradation of extrachromosomal DNA: J Biol Chem, v. 271, p. 14405-11.

Locatelli, F., B. Canaud, K. U. Eckardt, P. Stenvinkel, C. Wanner, and C. Zoccali, 2003, Oxidative stress in end-stage renal disease: an emerging threat to patient outcome: Nephrol Dial Transplant, v. 18, p. 1272-80.

Lord-Fontaine, S., and D. A. Averill-Bates, 2002, Heat shock inactivates cellular antioxidant defenses against hydrogen peroxide: protection by glucose: Free Radic Biol Med, v. 32, p. 752-65.

Lorenzen, I., 1981, Pharmacological control of inflammatory connective tissue diseases: Prog Clin Biol Res, v. 54, p. 209-18.

Martin, M., 1991, Activation et régulation myofibroblastiques dans un modèle de fibrose radio-induite, Université Pierre et Marie Curie.

Mason, R. M., J. Thacker, and M. P. Fairman, 1996, The joining of non-complementary DNA double-strand breaks by mammalian extracts: Nucleic Acids Res, v. 24, p. 4946-53.

Massy, Z. A., and T. Nguyen-Khoa, 2002, Oxidative stress and chronic renal failure: markers and management: J Nephrol, v. 15, p. 336-41.

Maurisse, R., 2003, Etude des triple-hélices et de leur utilisation pour développer une nouvelle approche de ciblage de gène, Université Paris VII.

Mayo, L. D., Y. Rok Seo, M. W. Jackson, M. L. Smith, J. R. Rivera Guzman, C. K. Korgaonkar, and D. B. Donner, 2005, Phosphorylation of human p53 at serine 46 determines promoter selection and whether apoptosis is attenuated or amplified: J Biol Chem.

Mayo, L. D., J. J. Turchi, and S. J. Berberich, 1997, Mdm-2 phosphorylation by DNA-dependent protein kinase prevents interaction with p53: Cancer Res, v. 57, p. 5013-6.

Meyn, M. S., 1995, Ataxia-telangiectasia and cellular responses to DNA damage: Cancer Res, v. 55, p. 5991-6001.

Mikkelsen, R. B., and P. Wardman, 2003, Biological chemistry of reactive oxygen and nitrogen and radiation-induced signal transduction mechanisms: Oncogene, v. 22, p. 5734-54.

Molteni, A., J. E. Moulder, E. P. Cohen, B. L. Fish, J. M. Taylor, P. A. Veno, L. F. Wolfe, and W. F. Ward, 2001, Prevention of radiation-induced nephropathy and fibrosis in a model of bone marrow transplant by an angiotensin II receptor blocker: Exp Biol Med (Maywood), v. 226, p. 1016-23.

Moulder, J. E., B. L. Fish, K. R. Regner, and E. P. Cohen, 2002, Angiotensin II blockade reduces radiation-induced proliferation in experimental radiation nephropathy: Radiat Res, v. 157, p. 393-401.

Moulin, V., G. Castilloux, F. A. Auger, D. Garrel, M. D. O'Connor-McCourt, and L. Germain, 1998, Modulated response to cytokines of human wound healing myofibroblasts compared to dermal fibroblasts: Exp Cell Res, v. 238, p. 283-93.

Moussard, A. M., 1963, Sur 6 observations de radiolésions cutanées d'origine thérapeutique traitées par chirurgie plastique, Thèse Faculté de Médecine de Paris.

Moustafa, H. F., and J. W. Hopewell, 1979, Blood flow clearance changes in pig skin after single doses of X rays: Br J Radiol, v. 52, p. 138-44.

Murrell, G., M. Francis, and L. Bromley, 1990, Modulation of fibroblast proliferation by oxygen free radicals: Biochem J, v. 265, p. 659-65.

Nackerdien, Z., G. Rao, M. A. Cacciuttolo, G. E. Gajewski, and M. Dizdaroglu, 1991, Chemical nature of DNA-protein cross-links produced in mammalian chromatin by hydrogen peroxide in the presence of iron or copper ions: Biochemistry, v. 30, p. 4873-4879.

Naka, K., A. Tachibana, K. Ikeda, and N. Motoyama, 2004, Stress-induced premature senescence in hTERT-expressing ataxia telangiectasia fibroblasts: J Biol Chem, v. 279, p. 2030-7.

O'Keefe, E. J., R. E. Payne, Jr., N. Russell, and D. T. Woodley, 1985, Spreading and enhanced motility of human keratinocytes on fibronectin: J Invest Dermatol, v. 85, p. 125-30.

Okada, K., Y. Takahashi, K. Ohnishi, O. Ishikawa, and Y. Miyachi, 1994, Time-dependent effect of chronic UV irradiation on superoxide dismutase and catalase activity in hairless mice skin: J Dermatol Sci, v. 8, p. 183-6.

Okunieff, P., E. Augustine, J. E. Hicks, T. L. Correlison, R. M. Altemus, B. G. Naydich, I. Ding, A. K. Huser, E. H. Abraham, J. J. Smith, N. Coleman, and L. H. Gerber, 2004, Pentoxifylline in the treatment of radiation-induced fibrosis: J Clin Oncol, v. 22, p. 2207-13.

Oleinick, N. L., S. Chiu, N. Ramakrishnan, and L. Xue, 1987, The formation, identification, and significance of DNA-protein cross-links in mammalian cells: Br J Cancer, v. 55 (Suppl. VIII), p. 135-140.

Oliver, F. J., J. Menissier-de Murcia, and G. de Murcia, 1999, Poly(ADP-ribose) polymerase in the cellular response to DNA damage, apoptosis, and disease: Am J Hum Genet, v. 64, p. 1282-8.

Ortiz, T., S. Lopez, M. A. Burguillos, A. Edreira, and J. Pinero, 2004, Radiosensitizer effect of wortmannin in radioresistant bladder tumoral cell lines.: Int J Oncol, v. 24, p. 169-75.

Ozturk, B., I. Egehan, S. Atavci, and M. Kitapci, 2004, Pentoxifylline in prevention of radiation-induced lung toxicity in patients with breast and lung cancer: a double-blind randomized trial: Int J Radiat Oncol Biol Phys, v. 58, p. 213-9.

Paillard, S., and F. Strauss, 1991, Analysis of the mechanism of interaction of simian Ku protein with DNA: Nucleic Acids Res, v. 19, p. 5619-24.

Pajovic, S. B., G. Joksic, J. Kasapovic, S. Pejic, and D. T. Kanazir, 2000, Role of antioxidant enzymes in radiosensitivity of human blood cells: J Environ Pathol Toxicol Oncol, v. 19, p. 325-31.

Pang, D., S. Yoo, W. S. Dynan, M. Jung, and A. Dritschilo, 1997, Ku proteins join DNA fragments as shown by atomic force microscopy: Cancer Res, v. 57, p. 1412-5.

Paris, F., Z. Fuks, A. Kang, P. Capodieci, G. Juan, D. Ehleiter, A. Haimovitz-Friedman, C. Cordon-Cardo, and R. Kolesnick, 2001, Endothelial apoptosis as the primary lesion initiating intestinal radiation damage in mice: Science, v. 293, p. 293-7.

Pasquier, D., T. Hoelscher, J. Schmutz, S. Dische, D. Mathieu, M. Baumann, and E. Lartigau, 2004, Hyperbaric oxygen therapy in the treatment of radio-induced lesions in normal tissues: a literature review: Radiother Oncol, v. 72, p. 1-13.

Patterson, T. J. S., and G. Wiernik, 1976, Pig skin as a model for the effect of X-irradiation on skin grafts: Biorheol, v. 13, p. 259-260.

Paula, E. M., D. C. Mathangi, and A. Namasivayam, 2003, Free radical changes in methanol toxicity: Indian J Physiol Pharmacol, v. 47, p. 207-11.

Pellegata, N. S., R. J. Antoniono, J. L. Redpath, and E. J. Stanbridge, 1996, DNA damage and p53-mediated cell cycle arrest: a reevaluation: Proc Natl Acad Sci U S A, v. 93, p. 15209-14.

Pence, B. C., and M. F. Naylor, 1990, Effects of single-dose ultraviolet radiation on skin superoxide dismutase, catalase, and xanthine oxidase in hairless mice: J Invest Dermatol, v. 95, p. 213-6.

Perdereau, B., F. Campana, J. R. Vilcoq, A. de la Rochefordiere, C. Barbaroux, A. Fourquet, and H. Magdelenat, 1994, [Superoxide dismutase (Cu/Zn) in cutaneous application in the treatment of radiation-induced fibrosis]: Bull Cancer, v. 81, p. 659-69.

Peter, R. U., 1996, Cutaneous radiation syndromes: clinical and therapeutical aspects: Radiol Prot Bul, v. 183, p. 19-25.

Peter, R. U., and P. Gottlober, 2002, Management of cutaneous radiation injuries: diagnostic and therapeutic principles of the cutaneous radiation syndrome: Mil Med, v. 167, p. 110-2.

Peters, L. J., and H. R. Withers, 1982, Critique of "Radiobiological basis of total body irradiation with different dose rate and fractionation: repair capacity of hemopoietic cells": Int J Radiat Oncol Biol Phys, v. 8, p. 1819-20.

Phillips, T. L., 1966, An ultrastructural study of the development of radiation injury in the lung: Radiology, v. 87, p. 49-54.

Piwnica-Worms, H., 1999, Cell cycle. Fools rush in: Nature, v. 401, p. 535, 537.

Pleschke, J. M., H. E. Kleczkowska, M. Strohm, and F. R. Althaus, 2000, Poly(ADP-ribose) binds to specific domains in DNA damage checkpoint proteins: J Biol Chem, v. 275, p. 40974-80.

Poli, G., 2000, Pathogenesis of liver fibrosis: role of oxidative stress: Mol Aspects Med, v. 21, p. 49-98.

Pouget, J.-P., 2000, Effet du rayonnement ionisant sur l'ADN cellulaire: mesure des bases puriques et pyrimidiques modifiées.

Pouget, J. P., T. Douki, M. J. Richard, and J. Cadet, 2000, DNA damage induced in cells by gamma and UVA radiation as measured by HPLC/GC-MS and HPLC-EC and Comet assay: Chem Res Toxicol, v. 13, p. 541-9.

Pouget, J. P., S. Frelon, J. L. Ravanat, I. Testard, F. Odin, and J. Cadet, 2002, Formation of modified DNA bases in cells exposed either to gamma radiation or to high-LET particles: Radiat Res, v. 157, p. 589-95.

Pouget, J. P., C. Laurent, M. Delbos, M. Benderitter, I. Clairand, F. Trompier, J. Stephanazzi, H. Carsin, F. Lambert, P. Voisin, and P. Gourmelon, 2004, PCC-FISH in skin fibroblasts for local dose assessment: biodosimetric analysis of a victim of the Georgian radiological accident: Radiat Res, v. 162, p. 365-76.

Prise, K. M., M. Folkard, H. C. Newman, and B. D. Michael, 1994, Effect of radiation quality on lesion complexity in cellular DNA: Int J Radiat Biol, v. 66, p. 537-42.

Puck, T. T., P. I. Marcus, and S. J. Cieciura, 1956, Clonal growth of mammalian cells in vitro; growth characteristics of colonies from single HeLa cells with and without a feeder layer: J Exp Med, v. 103, p. 273-83.

Pugliese, P. T., 1998, The skin's antioxidant systems: Dermatol Nurs, v. 10, p. 401-16; quiz 417-8.

Radford, I. R., 1986, Evidence for a general relationship between the induced level of DNA double-strand breakage and cell-killing after X-irradiation of mammalian cells: Int J Radiat Biol, v. 49, p. 611-620.

Ramakrishnan, N., D. E. McClain, and G. N. Catravas, 1993, Membranes as sensitive targets in thymocyte apoptosis: Int J Radiat Biol, v. 63, p. 693-701.

Ramsden, D. A., and M. Gellert, 1998, Ku protein stimulates DNA end joining by mammalian DNA ligases: a direct role for Ku in repair of DNA double-strand breaks: Embo J, v. 17, p. 609-14.

Remacle, J., M. Raes, O. Toussaint, P. Renard, and G. Rao, 1995, Low levels of reactive oxygen species as modulators of cell function: Mutat Res, v. 316, p. 103-22.

Riley, P., 1994, Free radicals in biology: oxidative stress and the effects of ionizing irradiation: Int J Radiat Biol, v. 65, p. 27-33.

Rimbach, G., A. M. Minihane, J. Majewicz, A. Fischer, J. Pallauf, F. Virgli, and P. D. Weinberg, 2002, Regulation of cell signalling by vitamin E: Proc Nutr Soc, v. 61, p. 415-25.

Robbins, M. E., and W. Zhao, 2004, Chronic oxidative stress and radiation-induced late normal tissue injury: a review: Int J Radiat Biol, v. 80, p. 251-9.

Robbins, M. E., and W. Zhao, 2004, Chronic oxidative stress and radiation-induced late normal tissue injury: a review.: Int J Radiat Biol, v. 80, p. 251-9.

Ross, G. M., J. J. Eady, N. P. Mithal, C. Bush, G. Steel, and P. A. Jeggo, 1995, DNA strand break rejoining defect in *xrs*-6 is complemented by transfection with the human *Ku*80 gene: Cancer Res, v. 55, p. 1235-1238.

Rothkamm, K., and M. Lobrich, 2003, Evidence for a lack of DNA double-strand break repair in human cells exposed to very low x-ray doses: Proc Natl Acad Sci U S A, v. 100, p. 5057-62.

Rube, C. E., F. Wilfert, D. Uthe, K. W. Schmid, R. Knoop, N. Willich, A. Schuck, and C. Rube, 2002, Modulation of radiation-induced tumour necrosis factor alpha (TNF-alpha) expression in the lung tissue by pentoxifylline: Radiother Oncol, v. 64, p. 177-87.

Rubin, P., 1984, The Franz Buschke lecture: late effects of chemotherapy and radiation therapy: a new hypothesis: Int J Radiat Oncol Biol Phys, v. 10, p. 5-34.

Rubin, P., and G. W. Casarett, 1968, Clinical radiation pathology as applied to curative radiotherapy: Cancer, v. 22, p. 767-78.

Rubin, P., and G. W. Casarett, 1968, Clinical Radiation Pathology, Vols. I and II: Philadelphia, London and Toronto, W. B. Saunders Company.

Rubin, P., C. Johnston, J. Williams, S. McDonald, and J. Finkelstein, 1995, A perpetual cascade of cytokines post-irradiation leads to pulmonary fibrosis: Int J Radiat Oncol Biol Phys, v. 33, p. 99-109.

Rudolph, R., J. Vande Berg, J. A. Schneider, J. C. Fisher, and W. L. Poolman, 1988, Slowed growth of cultured fibroblasts from human radiation wounds: Plast Reconstr Surg, v. 82, p. 669-77.

Russell, K. J., L. W. Wiens, G. W. Demers, D. A. Galloway, T. Le, G. C. Rice, J. A. Bianco, J. W. Singer, and M. Groudine, 1996, Preferential radiosensitization of G1 checkpoint-deficient cells by methylxanthines: Int J Radiat Oncol Biol Phys, v. 36, p. 1099-106.

Sarkaria, J. N., E. C. Busby, R. S. Tibbetts, P. Roos, Y. Taya, L. M. Karnitz, and R. T. Abraham, 1999, Inhibition of ATM and ATR kinase activities by the radiosensitizing agent, caffeine: Cancer Res, v. 59, p. 4375-82.

Sarkaria, J. N., and J. S. Eshleman, 2001, ATM as a target for novel radiosensitizers: Semin Radiat Oncol, v. 11, p. 316-27.

Sarma, L., and P. C. Kesavan, 1993, Protective effects of vitamins C and E against gamma-ray-induced chromosomal damage in mouse: Int J Radiat Biol, v. 63, p. 759-64.

Satyamitra, M., P. Uma Devi, H. Murase, and V. T. Kagiya, 2003, In vivo postirradiation protection by a vitamin E analog, alpha-TMG: Radiat Res, v. 160, p. 655-61.

Savio, M., L. A. Stivala, A. I. Scovassi, L. Bianchi, and E. Prosperi, 1996, p21waf1/cip1 protein associates with the detergent-insoluble form of PCNA concomitantly with disassembly of PCNA at nucleotide excision repair sites: Oncogene, v. 13, p. 1591-8.

Shindo, Y., and T. Hashimoto, 1997, Time course of changes in antioxidant enzymes in human skin fibroblasts after UVA irradiation: J Dermatol Sci, v. 14, p. 225-32.

Siddiqi, M. A., and E. Bothe, 1987, Single and double strand break formation in DNA irradiated in aqueous solution: dependence on dose and °OH radical scavenger concentration: Radiat Res, v. 112, p. 449-463.

Siliciano, J. D., C. E. Canman, Y. Taya, K. Sakaguchi, E. Appella, and M. B. Kastan, 1997, DNA damage induces phosphorylation of the amino terminus of p53: Genes Dev, v. 11, p. 3471-81.

Slupphaug, G., B. Kavli, and H. E. Krokan, 2003, The interacting pathways for prevention and repair of oxidative DNA damage: Mutat Res, v. 531, p. 231-51.

Stanley, J. R., D. T. Woodley, S. I. Katz, and G. R. Martin, 1982, Structure and function of basement membrane: J Invest Dermatol, v. 79 Suppl 1, p. 69s-72s.

Steiner, D. R., N. C. Gonzalez, and J. G. Wood, 2002, Interaction between reactive oxygen species and nitric oxide in the microvascular response to systemic hypoxia: J Appl Physiol, v. 93, p. 1411-8.

Strunz, A. M., P. Peschke, W. Waldeck, V. Ehemann, M. Kissel, and J. Debus, 2002, Preferential radiosensitization in p53-mutated human tumour cell lines by pentoxifylline-mediated disruption of the G2/M checkpoint control: Int J Radiat Biol, v. 78, p. 721-32.

Suzuki, K., S. Kodama, and M. Watanabe, 1999, Recruitment of ATM protein to double strand DNA irradiated with ionizing radiation: J Biol Chem, v. 274, p. 25571-5.

Swain, I. D., and L. J. Grant, 1989, Methods of measuring skin blood flow: Phys Med Biol, v. 34, p. 151-75.

Sweetman, S. F., J. J. Strain, and V. J. McKelvey-Martin, 1997, Effect of antioxidant vitamin supplementation on DNA damage and repair in human lymphoblastoid cells: Nutr Cancer, v. 27, p. 122-30.

Taipale, J., and J. Keski-Oja, 1997, Growth factors in the extracellular matrix: Fed Am Soc Exp Biol J, v. 11, p. 51-9.

Takata, M., M. S. Sasaki, E. Sonoda, C. Morrison, M. Hashimoto, H. Utsumi, Y. Yamaguchi-Iwai, A. Shinohara, and S. Takeda, 1998, Homologous recombination and non-homologous end-joining pathways of DNA double-strand break repair have overlapping roles in the maintenance of chromosomal integrity in vertebrate cells: Embo J, v. 17, p. 5497-508.

Teoule, R., 1987, Radiation-induced DNA damage and its repair: Int J Radiat Biol Relat Stud Phys Chem Med, v. 51, p. 573-89.

Teyssier, F., J. O. Bay, C. Dionet, and P. Verrelle, 1999, [Cell cycle regulation after exposure to ionizing radiation]: Bull Cancer, v. 86, p. 345-57.

Theron, T., A. Binder, F. Verheye-Dua, and L. Bohm, 2000, The role of G2-block abrogation, DNA double-strand break repair and apoptosis in the radiosensitization of melanoma and squamous cell carcinoma cell lines by pentoxifylline: Int J Radiat Biol, v. 76, p. 1197-208.

Tibbetts, R. S., K. M. Brumbaugh, J. M. Williams, J. N. Sarkaria, W. A. Cliby, S. Y. Shieh, Y. Taya, C. Prives, and R. T. Abraham, 1999, A role for ATR in the DNA damage-induced phosphorylation of p53: Genes Dev, v. 13, p. 152-7.

Tibbles, P. M., and J. S. Edelsberg, 1996, Hyperbaric-oxygen therapy: N Engl J Med, v. 334, p. 1642-8.

Toussaint, O., P. Dumont, J. Dierick, and e. al., 2000, Stress-induced premature senescence. Essence of life, evolution, stress, and aging: Proc Natl Acad Sci (NY), v. 908, p. 85-98.

Toussaint, O., E. E. Medrano, and T. von Zglinicki, 2000, Cellular and molecular mechanisms of stress-induced premature senescence (SIPS) of human diploid fibroblasts and melanocytes.: Exp Gerontol, v. 35, p. 927-45.

Toussaint, O., J. Remacle, J. Dierick, and e. al., 2002, Approach of evolutionary theories of ageing, stress, senescence-like phenotypes, calorie restriction and hormesis from the view point of far-from-equilibrium thermodynamics: Mech Ageing Dev, v. 123, p. 937-46.

Towbin, J. A., T. Staehelin, and J. Gordon, 1979, Electrophoretic transfer of proteins from polyacrylamide gels to nitrocellulose sheets: procedure and some applications: Proc Natl Acad Sci U S A, v. 76, p. 4350-4354.

Ts'ao, C. H., W. F. Ward, and C. D. Port, 1983, Radiation injury in rat lung. III. Plasminogen activator and fibrinolytic inhibitor activities: Radiat Res, v. 96, p. 301-8.

Tubiana, M., M. Dutreix, and A. Wambersie, 1986, Effets des rayonnements sur les molécules d'ADN et les chromosomes, *in* P. Hermann, ed., Radiobiologie, p. 33-71.

Uguralp, S., A. Bay Karabulut, and B. Mizrak, 2005, Effects of pentoxifylline and vitamin E on the bilateral ovary after experimental ovarian ischemia: Eur J Pediatr Surg, v. 15, p. 107-13.

Uitto, J., and L. Pulkkinen, 1996, Molecular complexity of the cutaneous basement membrane zone: Mol Biol Rep, v. 23, p. 35-46.

Uitto, J., E. M. Tan, and L. Ryhanen, 1982, Inhibition of collagen accumulation in fibrotic processes: review of pharmacologic agents and new approaches with amino acids and their analogues: J Invest Dermatol, v. 79 Suppl 1, p. 113s-120s.

Valk, E. E., and G. Hornstra, 2000, Relationship between vitamin E requirement and polyunsaturated fatty acid intake in man: a review: Int J Vitam Nutr Res, v. 70, p. 31-42.

Van der Rest, M., 1993, Les collagènes, une famille de protéines très diversifiée: Reg Bioch, v. 4, p. 33-34.

von Essen, C. F., 1969, Radiation tolerance of the skin: Acta Radiol Ther Phys Biol, v. 8, p. 311-30.

von Essen, C. F., 1972, Clinical radiation tolerance of the skin and upper aerodigestive tract: Front Radiat Ther Oncol, v. 6, p. 148-159.

von Sonntag, C., 1987, The chemical basis of radiation biology: New York, Taylor & Francis, p. 117-166, 221-294.

Vozenin-Brotons, M. C., V. Sivan, N. Gault, C. Renard, C. Geffrotin, S. Delanian, J. L. Lefaix, and M. Martin, 2001, Antifibrotic action of Cu/Zn SOD is mediated by TGF-beta1 repression and phenotypic reversion of myofibroblasts: Free Radic Biol Med, v. 30, p. 30-42.

Wang, H., M. Wang, H. Wang, W. Bocker, and G. Iliakis, 2005, Complex H2AX phosphorylation patterns by multiple kinases including ATM and DNA-PK in human cells exposed to ionizing radiation and treated with kinase inhibitors.: J Cell Physiol, v. 202, p. 492-502.

Ward, J. F., 1985, Biochemistry of DNA lesions: Radiat Res, v. 104, p. S103-S111.

Ward, J. F., 1988, DNA damage produced by ionizing radiation in mammalian cells: identities, mechanisms of formation, and reparability: Prog Nucleic Acid Res Mol Biol, v. 35, p. 95-125.

Ward, W. F., Y. T. Kim, A. Molteni, C. Ts'ao, and J. M. Hinz, 1992, Pentoxifylline does not spare acute radiation reactions in rat lung and skin: Radiat Res, v. 129, p. 107-11.

Ward, W. F., P. J. Lin, P. S. Wong, R. Behnia, and N. Jalali, 1993, Radiation pneumonitis in rats and its modification by the angiotensin-converting enzyme inhibitor captopril evaluated by high-resolution computed tomography: Radiat Res, v. 135, p. 81-7.

Ward, W. F., A. Shih-Hoellwarth, and R. D. Tuttle, 1983, Collagen accumulation in irradiated rat lung: modification by D-penicillamine: Radiology, v. 146, p. 533-7.

Weiss, J. F., and M. R. Landauer, 2003, Protection against ionizing radiation by antioxidant nutrients and phytochemicals: Toxicology, v. 189, p. 1-20.

Withers, H. R., 1967, Recovery and repopulation in vivo by mouse skin epithelial cells during fractionated irradiation: Radiat Res, v. 32, p. 227-39.

Withers, H. R., L. J. Peters, and H. D. Kogelnik, 1980, The pathology of late effects of irradiation, *in* R. E. M. a. H. R. Withers, ed., Radiation Biology in Cancer Research: New York, Raven Press, p. 439-448.

Worthington, H. V., J. E. Clarkson, and O. B. Eden, 2002, Interventions for treating oral mucositis for patients with cancer receiving treatment: Cochrane Database Syst Rev, p. CD001973.

Wurm, R., N. G. Burnet, N. Duggal, J. R. Yarnold, and J. H. Peacock, 1994, Cellular radiosensitivity and DNA damage in primary human fibroblasts: Int J Radiat Oncol Biol Phys, v. 30, p. 625-33.

Xiong, Y., G. J. Hannon, H. Zhang, D. Casso, R. Kobayashi, and D. Beach, 1993, p21 is a universal inhibitor of cyclin kinases: Nature, v. 366, p. 701-4.

Yarom, R., I. S. Harper, S. Wynchank, D. van Schalkwyk, J. Madhoo, K. Williams, R. Salie, S. Genade, and A. Lochner, 1993, Effect of captopril on changes in rats' hearts induced by long-term irradiation: Radiat Res, v. 133, p. 187-97.

Yohn, J. J., D. A. Norris, D. G. Yrastorza, I. J. Buno, J. A. Leff, S. S. Hake, and J. E. Repine, 1991, Disparate antioxidant enzyme activities in cultured human cutaneous fibroblasts, keratinocytes, and melanocytes: J Invest Dermatol, v. 97, p. 405-9.

Yoshida, Y., E. Niki, and N. Noguchi, 2003, Comparative study on the action of tocopherols and tocotrienols as antioxidant: chemical and physical effects: Chem Phys Lipids, v. 123, p. 63-75.

Zang, H.-Y., M. Gharaee-Kermani, and S. H. Phan, 1997, Regulation of lung fibroblasts a-sm actin expression, contractile phenotype, and apoptosis by IL-1β: J of Immunol, v. 158, p. 1392-1399.

Zhang, K., and R. H. Kramer, 1996, Laminin 5 deposition promotes keratinocyte motility: Exp Cell Res, v. 227, p. 309-22.

PUBLICATIONS – COMMUNICATIONS

Publications :

- Modulation of DNA damage by pentoxifylline and α-tocopherol in skin fibroblasts exposed to gamma-rays. C. Laurent, J.-P. Pouget and P. Voisin. *Radiat Res.* 2005, v. 164, p. 63-72.

- Modulation of radio-induced oxidative damage by the combination of pentoxifylline and α-tocopherol in skin fibroblasts and microvascular endothelial cells. C. Laurent, P. Voisin, L. Roy and J.-P. Pouget. *IJRR*. 2004, v. 1, p. 13-14. ISSN 0973-0168. Abstract.

- PCC-FISH in skin fibroblasts for local dose assessment: biodosimetric analysis of a victim of the Georgian radiological accident. J.-P. Pouget, C. Laurent, M. Delbos, M. Benderitter, I. Clairand, F. Trompier, J. Stephanazzi, H. Carsin, F. Lambert, P. Voisin and P. Gourmelon. *Radiat Res*. 2004, v. 162, p. 365-76.

- DNA damage in skin microvascular endothelial cells exposed to gamma-rays treated by the combination of pentoxifylline and α-tocopherol. C Laurent, P Voisin and J-P Pouget. Révisée.

- Differential effects of pentoxifylline, α-tocopherol and the combination on radiation-induced DNA damage in skin fibroblasts. C Laurent, P Voisin and J.-P. Pouget. En cours de rédaction.

- Oxidative stress-associated clinical symptoms in locally X-irradiated skin of hairless rats: role of superoxide dismutase? J-P Pouget, J-L Ravanat and C Laurent. En cours de rédaction.

- Late H2AX hyperphosphorylation associated to decreased DNA-PKcs expression and SIPS in irradiated skin fibroblasts and endothelial cells and modulation by pentoxifylline and trolox. C Laurent, M Delbos, Pa Voisin, Ph Voisin and J-P Pouget. En cours de rédaction.

Communications :

- Modulation of radio-induced oxidative damage by the combination of pentoxifylline and α-tocopherol in skin fibroblasts and microvascular endothelial cells. C Laurent, P Voisin, L Roy and J-P Pouget. International Conference on Recent Trends in Radiation Biology, Bombay (Inde), 2004 (**communication orale**).

- Rôle du stress oxydatif dans le développement des effets cellulaires radio-induits au niveau cutané. C Laurent. Journées des thèses IRSN, Aussois, 2004 (**communication orale**).

- Radio-induced DNA damage in skin fibroblasts treated by the combination of pentoxifylline and α-tocopherol. C Laurent, P Voisin and J-P Pouget. 33rd Annual Meeting of the European Society for Radiation Biology, Budapest (Hongrie), 2004 (**communication orale**).

- Dommages à l'ADN induits par les rayonnements ionisants dans les fibroblastes du derme, effets du traitement pentoxifylline et α-tocophérol. C Laurent. 7ème Congrès des Jeunes Chercheurs d'Ile-de-France, Paris, 2004 (**communication orale**).

- Evaluation of DNA damage on comet assay using computerized image analysis and visual scoring. E Grégoire, O Garcia, V Buard, C Laurent, L Roy, P Voisin. ISAC XXII International Congress, Montpellier, 2004 (communication affichée).

- Stress oxydatif radio-induit dans les fibroblastes et les cellules endothéliales du derme traités par la combinaison pentoxifylline et alpha-tocophérol. C Laurent et J-P Pouget. 8ème reunion de la Société de Biologie du Vieillissement, Limeil-Brévannes, 2003 (**communications orale** et affichée).

- Rôle du stress oxydatif dans le développement des effets cellulaires radio-induits au niveau cutané. C Laurent. Journées des thèses IRSN, Paris, 2003 (**communication orale**).

- DNA damage in dermal fibroblasts and endothelial cells exposed to gamma rays treated by the combination of pentoxifylline and α-tocopherol. C Laurent, J-P Pouget and P Voisin. International Comet Assay Workshop No. 5, Aberdeen (Ecosse), 2003 (communication affichée).

- Nouvelle estimation de la dose à la peau par dosimétrie biologique : Application à l'accident de Géorgie. J-P Pouget, C Laurent, M Delbos, M Benderitter, F Trompier, J Stéphanazzi, H Carsin, Lambert and P Gourmelon. 6ème colloque International de Radiobiologie Fondamentale et Appliquée, Batz-sur-Mer, 2003 (communication orale).

- Skin biodosimetry on PCC-FISH analysis in primary fibroblasts and keratinocytes: application to an accidental overexposure. J-P Pouget, M Benderitter, M Delbos, C Laurent, P Voisin, J Stéphanazzi, H Carsin, and P Gourmelon. 32nd Annual meeting of the European Society for Radiation Biology, Liège, 2002 (communication affichée).